IL
NUOVO CIMENTO
ORGANO DELLA SOCIETÀ ITALIANA DI FISICA
SOTTO GLI AUSPICI DEL CONSIGLIO NAZIONALE DELLE RICERCHE

VOL. VIII, N. 6 | *Serie decima* | 16 Giugno 1958

On Spherically Symmetric Solutions in Moffat's Unified Field Theory.

R. P. KERR
Trinity College - Cambridge

(ricevuto il 12 Dicembre 1957)

Summary — In this paper, the complete spherically symmetric solution for Moffat's complex-symmetric field theory is calculated. It is found that the solution is not a unique function of the boundary conditions, even when four co-ordinate conditions are adjoined to the field equations. Consequently, it is necessary to add four more field equations to those that Moffat assumed. The solution is found when these are generalised De Donder conditions.

1. – Introduction.

We shall associate with the four-dimensional space-time, with real co-ordinates x_μ ($\mu = 0, 1, 2, 3$), a complex-symmetric tensor $g_{\mu\nu}$ [1,2]. Let us consider the spherically symmetric form of $g_{\mu\nu}$ in polar co-ordinates $x_1 = r$, $x_2 = \theta$, $x_3 = \varphi$, and $x_4 = t$ (*):

$$g_{\mu\nu} = \left\| \begin{array}{cccc} -e^{\nu} & \cdot & \cdot & -e^{\mu} \\ \cdot & -e^{\alpha} & \cdot & \cdot \\ \cdot & \cdot & -e^{\alpha}\sin^2\theta & \cdot \\ -e^{\mu} & \cdot & \cdot & e^{\nu} \end{array} \right\|, \tag{1.1}$$

(*) Relativistic units are chosen so that $c = k = 1$, where k is the Newtonian gravitational constant.

(1) J. MOFFAT: *Proc. Camb. Phil. Soc.*, **52**, 623 (1956).

(2) J. MOFFAT: *Proc. Camb. Phil. Soc.*, **53**, 473 (1957).

where α, λ, μ, and ν are functions of r and t. The only transformations which preserve the spherically symmetric form (1.1) are the scale transformations

$$r^* = f(r, t)\,, \qquad t^* = h(r, t)\,, \tag{1.2}$$

and the trivial rotations of the co-ordinate axes.

It has been proved [3] that there exists a transformation of type (1.2) reducing a real $g_{\mu\nu}$, which satisfies the field equations $R_{\mu\nu} = 0$, to a diagonal and static form. If $g_{\mu\nu}$ is a complex-symmetric tensor satisfying the equivalent equations, it is not possible, in general, to reduce it to either a static or a diagonal form. This could only be done by a *complex* co-ordinate transformation, which is not allowed in real space.

In the complex-symmetric theory, the following field equations may be derived from a variational principle [1,2],

$$R_{\mu\nu} = -\lambda g_{\mu\nu}\,, \tag{1.3}$$

where (*)

$$R_{\mu\nu} = -\Gamma^{\lambda}_{\mu\nu,\lambda} + \log\sqrt{-g}_{,\mu,\nu} + \Gamma^{\lambda}_{\varrho\mu}\Gamma^{\varrho}_{\lambda\mu} - \Gamma^{\lambda}_{\mu\nu}\log\sqrt{-g}_{,\lambda}\,, \tag{1.4}$$

λ is the cosmological constant, and $g = \operatorname{Det}(g_{\mu\nu})$. $\Gamma^{\lambda}_{\mu\nu}$ is defined by the equations,

$$\Gamma^{\lambda}_{\mu\nu} = \tfrac{1}{2} g^{\lambda\sigma}(g_{\mu\sigma,\nu} + g_{\nu\sigma,\mu} - g_{\mu\nu,\sigma})\,. \tag{1.5}$$

In the following, the general static spherically symmetric solution for $g_{\mu\nu}$ will be found; that is, we shall consider $g_{\mu\nu}$ as a function of r and θ only.

2. – Derivation of solution.

The $\Gamma^{\lambda}_{\mu\nu}$ may be calculated in terms of the $g_{\mu\nu}$ by using (1.5). We shall use ($'$) to denote differentiation with respect to r.

(*) Here, a comma denotes ordinary differentiation, while a semicolon denotes covariant differentiation.

(3) L. LANDAU and E. LIFSCHITZ: *The Classical Theory of Fields* (Cambridge, Mass. 1951).

$$
(2.1)\quad \left\{\begin{array}{ll}
\Gamma^1_{11} = \frac{1}{A}\left(\frac{1}{2}p' \exp[p+\nu] + \mu' \exp[2\nu]\right) & \Gamma^4_{14} = \left(\frac{1}{2}p' - \mu'\right)\frac{\exp[p+\mu]}{A} \\
\Gamma^1_{44} = \frac{1}{2}\nu' \frac{\exp[2\nu]}{A}, & \Gamma^4_{44} = \frac{1}{2}\nu' \frac{\exp[\mu+\nu]}{A}, \\
\Gamma^4_{14} = \frac{1}{2}\nu' \frac{\exp[p+\nu]}{A}, & \Gamma^1_{41} = -\frac{1}{2}\nu' \frac{\exp[\mu+\nu]}{A}, \\
\Gamma^1_{22} = -\frac{1}{2}\alpha' \frac{\exp[\alpha+\nu]}{A}, & \Gamma^4_{22} = -\frac{1}{2}\alpha' \frac{\exp[\mu+\alpha]}{A}, \\
\Gamma^1_{33} = \sin^2\theta \cdot \Gamma^1_{22}, & \Gamma^4_{33} = \sin^2\theta \cdot \Gamma^4_{22}, \\
\Gamma^2_{12} = \frac{1}{2}\alpha', & \Gamma^3_{13} = \frac{1}{2}\alpha', \\
\Gamma^2_{33} = -\sin\theta\cdot\cos\theta, & \Gamma^3_{23} = \operatorname{ctg}\theta .
\end{array}\right.
$$

Here, A and g are given by

$$
(2.2)\quad \left\{\begin{array}{l}
A = \exp[p+\nu] + \exp[2\mu], \\
g = -A\exp[2\chi]\sin^2\theta .
\end{array}\right.
$$

Substituting these values for $\Gamma^\lambda_{\mu\nu}$ into eq. (1.4) we get,

$$
(2.3)\quad R_{11} = \alpha'' + \frac{1}{2}\alpha'^2 - \frac{1}{2}\alpha'\left(\frac{A'}{A}\right) + \frac{1}{2}\frac{\exp[p+\nu]}{A}\left[\nu'' + \nu'(\nu'+\alpha') - \frac{\nu'}{2}\left(\frac{A'}{A}\right)\right],
$$

$$
(2.4)\quad R_{22} = \frac{1}{2}\frac{\exp[\alpha+\nu]}{A}\cdot\left[\alpha'' + \alpha'(\alpha'+\nu') - \frac{1}{2}\alpha'\left(\frac{A'}{A}\right)\right] - 1,
$$

$$
(2.5)\quad R_{33} = \sin^2\theta\cdot R_{22},
$$

$$
(2.6)\quad R_{44} = -\frac{1}{2}\frac{\exp[2\nu]}{A}\cdot\left[\nu'' + \nu'(\nu'+\alpha') - \frac{1}{2}\nu'\left(\frac{A'}{A}\right)\right],
$$

$$
(2.7)\quad R_{41} = -\exp[\mu-\nu]R_{44} .
$$

There are only two independent field equations,

$$
(2.8)\quad \frac{1}{2}\frac{\exp[2\nu]}{A}\cdot\left[\nu'' + \nu'(\nu'+\alpha') - \frac{1}{2}\nu'\left(\frac{A'}{A}\right)\right] = \lambda\exp[\nu],
$$

$$
(2.9)\quad \alpha'' + \frac{1}{2}\alpha'^2 - \frac{1}{2}\alpha'\left(\frac{A'}{A}\right) = 0,
$$

We infer from (2.9) that

$$A = \tfrac{1}{4} a^2 \alpha'^2 e^\alpha . \tag{2.10}$$

Substituting this into (2.8), we obtain

$$\left(\frac{\nu'}{\alpha'} \cdot \exp\left[\nu + \frac{1}{2}\alpha\right]\right)' = \frac{1}{2} a^2 \lambda \alpha' \exp[3\alpha/2] , \tag{2.11}$$

$$\nu' \exp[\nu] = b\alpha' \exp\left[-\frac{1}{2}\alpha\right] + \frac{1}{3} a^2 \lambda \alpha' \exp[\alpha] , \tag{2.12}$$

$$\exp[\nu] = c - 2b \exp[-\alpha/2] + \frac{a^2}{3} \lambda \exp[\alpha] . \tag{2.13}$$

Finally, the general static spherically symmetric solution is

$$g_{\mu\nu} = \left\{\begin{matrix} -\dfrac{a^2(1-v^2)u'^2}{c - 2b/u + (\lambda/3)a^2u^2} & \cdot & \cdot & -au'v \\ \cdot & -u^2 & \cdot & \cdot \\ \cdot & \cdot & -u^2 \sin^2\theta & \cdot \\ -au'v & \cdot & \cdot & c - \dfrac{2b}{u} + \dfrac{\lambda}{3} a^2 u^2 \end{matrix}\right\} . \tag{2.14}$$

We have written $\alpha = 2 \cdot \log(u)$ and $\exp[\mu] = -au'v$. u and v are arbitrary complex functions.

Because $g \neq 0$, we see from (2.10) that u' is also non-zero. Consequently, if u is real we can deduce that it is a monotonic function of r, and hence there exists a proper co-ordinate transformation, $^*r = u(r)$, which transforms g_{22} into the form $^*r^2$. On the other hand, if u is a complex function, neither $\mathrm{Rl}(u)$ nor mod (u) need be monotonic, and so it is not generally possible to transform either into $^*r$ by a *non-singular* transformation.

3. – Particle solutions in Moffat's theory.

In future, we shall only consider solutions in which $\lambda = 0$, and the field $g_{\mu\nu} \to \eta_{\mu\nu}$ at infinity (*). The latter condition implies that

$$\left.\begin{matrix} \dfrac{u(r)}{r} \to 1 \\ v(r) \to 0 \end{matrix}\right\} \text{ as } \quad r \to \infty . \tag{3.1}$$

(*) $\eta_{\mu\nu}$ is the Galilean metric with signature $(-, -, -, +)$.

1720

Since g_{11} tends to -1 and g_{00} to $+1$ as r rends to ∞, we have

$$\left\{\begin{aligned} a &= 1\,,\\ c &= 1\,. \end{aligned}\right. \tag{3.2}$$

Moreover, as r tends to ∞ we see that

$$u'(r) \to 1\,. \tag{3.3}$$

In the real-symmetric theory, (3.3) is implied by (3.1), because u is a monotonic function, but, in the complex-symmetric theory this is not so, as may be seen from the following example; $u = r + (i/r)\sin(r)$.

The complete particle solution is

$$g_{\mu\nu} = \left\{\begin{array}{cccc} -\dfrac{u'^2(1-v^2)}{1-2b/u} & \cdot & \cdot & -u'v \\ \cdot & -u^2 & \cdot & \cdot \\ \cdot & \cdot & -u^2\sin^2\theta & \cdot \\ -u'v & \cdot & \cdot & 1-2b/u \end{array}\right| \tag{3.4}$$

where u and v satisfy conditions (3.1)–(3.3) (*). In Einstein's real-symmetric theory g_{01} can be eliminated by the following transformation,

$$\left|\begin{aligned} t^* &= t - \int \frac{v\,\mathrm{d}u}{1-(2b/u)},\\ r^* &= r\,, \end{aligned}\right. \tag{3.5}$$

but if $g_{\mu\nu}$ is complex the transformation (3.5) is not in general real, and so g_{01} cannot be removed.

In general relativity, the particle solution may be written in Schwarzschild's canonical form, which only involves one arbitrary constant m. In the complex-symmetric theory there are two arbitrary *complex* functions as well as the complex constant b. This is equivalent to four *real* functions and two real constants. Only two of these functions can be eliminated by a real co-ordinate transformation of the type (1.2), and so the canonical form for (3.4) will involve two arbitrary real functions.

(*) If we put $u = r$, $v = 0$, in $g_{\mu\nu}$ we obtain Moffat's particular solution ([4]).

([4]) J. MOFFAT: *Proc. Camb. Phil. Soc.*, **53**, 489 (1957).

This indeterminacy of the particle solutions is a consequence of the fact that the field equations satisfy four *complex* identities, which are equivalent to eight real identities in all. These are

$$[R^{\mu\nu} - \tfrac{1}{2} g^{\mu\nu} R^{\sigma}{}_{\sigma}]_{;\nu} = 0 \,. \tag{3.6}$$

In Moffat's theory, because of the identities (3.6), there are only six independent complex field equations to determine the ten unknown $g_{\mu\nu}$. Even when four real co-ordinate conditions are added, there are still four real equations too few to determine the field. In fact, it is possible to have solutions which are regular everywhere, including at infinity, but do not correspond to a flat space. As an example of this we can choose

$$\begin{cases} b = v = 0 \,, \\ u = r + i r^2 e^{-r} \,, \end{cases} \tag{3.7}$$

in (3.4).

Before the *physical field* is uniquely determined by the boundary conditions and the singularities, if any, four extra real conditions have to be postulated. This same problem exists in Maxwell's Theory, where the potential is only unique if the gauge condition,

$$A^{\mu}{}_{,\mu} = 0 \,, \tag{3.8}$$

is adjoined to the field equations. Any general four potential A^{μ} is physically equivalent to a four potential $^*A^{\mu}$ which satisfies (3.8). We could generalize this to the complex-symmetric theory by postulating the existence of an equivalence relation on the set of complex $g_{\mu\nu}$

$$g_{\mu\nu} \sim {}^*g_{\mu\nu} \,. \tag{3.9}$$

If this equivalence relation were invariant under general co-ordinate transformations, then (3.9) would imply that

$$\frac{\partial f^{\varrho}(x)}{\partial x^{\mu}} \cdot \frac{\partial f^{\sigma}(x)}{\partial x^{\nu}} \cdot g_{\varrho\sigma}(f(x)) \sim \frac{\partial f^{\varrho}}{\partial x^{\mu}} \cdot \frac{\partial f^{\sigma}}{\partial x^{\nu}} \cdot {}^*g_{\varrho\sigma}(f(x)) \,, \tag{3.10}$$

for all functions $f^{\varrho}(x_0, x_1, x_2, x_3)$ whose Jacobian is non-vanishing. Then the field equations could be made determinate by choosing a representative from each equivalence set in a relativistically invariant way.

The other solution to the indeterminacy is to postulate four more real

equations to be satisfied by the field variables. This is essentially what Moffat did [2] in order to deduce the equations of motion for charged particles. He assumed that it was possible to choose a co-ordinate system in which $g_{\mu\nu}$ satisfied four complex equations which were the natural generalization of the co-ordinate conditions in [5]. For a general complex-symmetric field such a co-ordinate system will not exist as there are eight real equations to be satisfied, but only four co-ordinate conditions at our disposal. Consequently, there were really four more non-covariant field equations postulated in Moffat's eight co-ordinate conditions.

It has been suggested by FOCK [6] and ROSEN [7] that general relativity should be considered as a potential theory in a special relativistic space. They gave physical significance to the De Donder co-ordinate conditions,

$$\mathfrak{g}^{\mu\nu}{}_{,\nu} = 0\,, \tag{3.11}$$ (*)

and said that co-ordinate systems in which equations (3.11) were satisfied were physically more important than other co-ordinate systems. In the complex-symmetric theory we could postulate that (3.11) is satisfied by the complex $g_{\mu\nu}$ in the *physical* frames of reference, and then the $g_{\mu\nu}$ would be completely determined by the boundary conditions. As these conditions are similar to those that MOFFAT assumed in [2] we shall find the spherically symmetric solution of (1.3) (+) and (3.11). First, it is necessary to notice that (3.11) cannot be satisfied in spherical polar co-ordinates so we have to transform to « rectangular » co-ordinates,

$$ {}^*x_1 = r\cdot\sin\theta\cdot\cos\varphi\,, \qquad {}^*x_2 = r\cdot\sin\theta\cdot\sin\varphi\,, \qquad {}^*x_3 = r\cos\theta\,, \tag{3.12}$$

then

$$\left\{\begin{aligned} {}^*\mathfrak{g}^{00} &= \frac{(1-v^2)}{1-2b/u}\cdot\frac{u'u^2}{r^2}\,,\\ {}^*\mathfrak{g}^{0n} &= -u^2 v\left(\frac{{}^*x_n}{r^3}\right),\\ {}^*\mathfrak{g}^{mn} &= -\delta_{mn}\cdot u' - \left(\frac{1-2b/u}{u'^2} - \frac{r^2}{u^2}\right)\frac{u'u^2}{r^2}\cdot\frac{{}^*x^m\,{}^*x^n}{r^2}\,. \end{aligned}\right. \tag{3.13}$$

---

(5) A. EINSTEIN and L. INFELD: *Can. Journ. Math.*, **1**, 209 (1949).
(6) W. A. FOCK: *Journ. Exp. Theor. Phys.*, **7**, 81 (1939).
(7) N. ROSEN: *Phys. Rev.*, **57**, 147 (1940).
(*) $\mathfrak{g}^{\mu\nu}$ is a tensor density: $\mathfrak{g}^{\mu\nu} = \sqrt{-g}\, g^{\mu\nu}$.
(+) As before we shall take $\lambda = 0$.

The De Donder conditions (3.11) give

$$(3.14)\qquad \begin{cases} v = \alpha\, u^{-2}\,, \\ u = r + b\,, \end{cases}$$

so that the complete solution is a function of two complex constants α and b. When it is expressed in the *non-physical* spherical polar co-ordinates

$$(3.15)\qquad g_{\mu\nu} = \begin{Vmatrix} -\dfrac{1-\alpha^2/(r+b)^4}{1-2b/(r+b)} & \cdot & \cdot & -\dfrac{\alpha}{(r+b)^2} \\ \cdot & -(r+b)^2 & \cdot & \cdot \\ \cdot & \cdot & -(r+b)^2\sin^2\theta & \cdot \\ -\dfrac{\alpha}{(r+b)^2} & \cdot & \cdot & \left(1-\dfrac{2b}{r+b}\right) \end{Vmatrix}.$$

Here, $b = m + i\cdot e$, where m and e behave like the mass and charge respectively in the equations of motion, as we shall deduce in a later paper. α, which is an arbitrary complex constant, plays no part in the first order equations of motion. It can be seen that in general the only transformations that preserve (3.11) and the boundary conditions are Lorentz transformations. This is not true if $g_{\mu\nu}$ is real (i.e. if α and b are real).

4. – Conclusions.

We have seen that the complex-symmetric equations (1.3) are not sufficient to determine the ten complex $g_{\mu\nu}$, even when four co-ordinate conditions are added. There are two ways out of this impasse. One of these is to find a « 4-dimensional » equivalence relation on the $g_{\mu\nu}$ and then choose a representative from each equivalence set. This is done in Maxwell's theory where the equivalence relation is

$$(4.1)\qquad A_\mu \sim A_\mu + \partial_\mu \varphi \quad (*)$$

and the representative satisfies equation (3.8).

The other possibility is to adjoin an extra four real equations (or two complex equations) to the field equations (1.3). These may be either covariant or, if Fock and Rosen's view of general relativity is taken, non-covariant.

(*) φ is an arbitrary scalar.

As an example we have taken generalized De Donder equations (3.11) and found that then the spherically symmetric solutions are functions of two arbitrary, physically invariant, complex constants. In a later paper we shall calculate the equations of motion for such particles in the quasi-static approximation.

* * *

The author wishes to express his sincere thanks to Sir ARTHUR SIMS, who enabled this work to be undertaken, and to Dr. EDEN, Dr. CANDLIN and Mr. J. R. MOFFAT, for many stimulating discussions.

RIASSUNTO (*)

Nel presente lavoro si calcola la soluzione a simmetria sferica completa della teoria di campo a simmetria complessa di Moffat. Si trova che la soluzione, anche aggiungendo alle equazioni del campo quattro condizioni dipendenti dalle coordinate, non è una funzione unica delle condizioni al contorno. È pertanto necessario aggiungere altre quattro equazioni di campo a quelle proposte da Moffat. La soluzione si trova se queste quattro equazioni corrispondono a condizioni di De Donder generalizzate.

(*) *Traduzione a cura della Redazione.*

Some Aspects of the Covariant Functional Formalism of Field Theory - II.

R. S. LIOTTA

Istituto di Fisica dell'Università - Roma
Istituto Nazionale di Fisica Nucleare - Sezione di Roma

(ricevuto il 9 Gennaio 1958)

Summary. — Hamilton's covariant equations for an electromagnetic field in the presence of a given current are written based on a previous work. The Jacobi equation is written such that it defines a class of canonical trasformations which conserve the true covariance of the scheme. By means of a proper introduction of covariant functional operators, the Tomonaga equation is written such that it is covariant independently of the particular choice of canonical variables, and, hence, is covariant even in the Schrödinger representation. It is shown by means of a generalization of the W.K.B. method that under certain assumptions the Tomonaga equation reduces to the classical Jacobi equation.

1. – Introduction.

The covariant Hamiltonian formalism for field theory, both classical and quantum mechanical, has been studied by various authors. With regard to the classical argument, BORN (1), WEYL (2), DIRAC (3) and GOOD (4) have made contributions in which they developed formalisms of indefinite Eulerian character without giving an explicit form to the general integral of the equations of motion; and, hence, without referring to the initial conditions of the dynamic

(1) M. BORN: *Proc. Roy. Soc.*, A **143**, 410 (1934).
(2) H. WEYL: *Phys. Rev.*, **46**, 505 (1934).
(3) P. A. M. DIRAC: *Phys. Rev.*, **73**, 1092 (1948); *Rev. Mod. Phys.*, **21**, 392 (1949); *Ann. Inst. Poincaré*, **13**, 1 (1952).
(4) R. H. GOOD: *Phys. Rev.*, **93**, 239 (1954).

problem. WEISS ([5]), instead, considers the problem of giving in an explicit manner not only the differential equation, but also the initial and boundary conditions. From a general mathematical point of view, he gives correctly the so called « mixed data ».

WEISS considers the cylinder generated in the space-time by allowing an element of space-like surface σ_0 to be displaced to the configuration σ_1; the « mixed data » then consist of assigning the field variables and conjugate momenta to σ_0, and the field variables to the lateral area of the said cylinder. Moreover, the equations of motion determine the value of the field variables and the conjugate momenta on σ_1.

WEISS uses a definition of the Hamiltonian function which is different from the one we have used in a preceding work ([6]), as well as different definitions for the conjugate momenta. Moreover, WEISS does not consider the problem of the interaction of fields.

We note that, in general, there result further conditions for the integrability of the equations of motion. In fact, by a knowledge of the initial conditions on σ_0, we pass, in effect, to values upon σ_1 by means of a succession of canonical transformations (induced by the equations of motion) which make use of a generic family of space-like surfaces which fill the space between σ_0 and σ; therefore, in general, the hamiltonian of the system will contain additive terms dependent upon the family of space-like surfaces chosen to study the motion. In particular, these terms were found by TOMONAGA and KANESAWA ([7]) in a study of the interaction of a scalar meson field with an electromagnetic field, making use of Tomonaga's equation. With regard to the formulation of the covariant quantum mechanical Hamiltonian, the cited works of BORN, WEYL, DIRAC and WEISS introduce quantum mechanical commutators in a formal manner without giving explicit form to the field operators.

Other papers on the covariant Hamiltonian formalism, which must be considered, are the papers of TOMONAGA and his co-workers; in these papers, however, there results a covariant formulation in the interaction representation, but the field operators are not given in explicit form ([8]).

The purpose of the present paper is the following:

1) to give a formulation for interacting fields, which is valid in the Schrödinger representation and which is truly covariant;

2) to give an explicit functional form to the field operators such that the true covariance of the scheme is always conserved.

([5]) P. WEISS: *Proc. Roy. Soc.*, A **166**, 192 (1936); A **169**, 102 (1938-39).
([6]) R. S. LIOTTA: *Nuovo Cimento*, **3**, 438 (1956); hereinafter referred to as I.
([7]) S. KANESAWA and S. TOMONAGA: *Progr. Theor. Phys.*, **3**, 9 (1948).
([8]) See also P. BOCCHIERI and A. LOINGER: *Nuovo Cimento*, **2**, 1058 (1955).

To realize point 1), it is clearly necessary to demonstrate how the integration of the equations of motion can be carried out when the initial conditions on σ_0 are known even for the case of interacting fields. It is then possible to pass to the quantum mechanical case by substituting operators, which become « time independent », into the initial Lagrangian variables and the initial conjugate momenta, and thereby obtain the Schrödinger representation.

It should be noted that the conditions on the lateral surface of the cylinder with bases σ_0 and σ_1 can be readily neglected. As already pointed out by WEISS, these correspond to the properties of the walls of the receptacle containing the radiation, provided that it is in a finite space. And, if it is in an infinite space, the elimination of the condition upon the lateral surface is equivalent to the condition that fields are, suitably infinitesimal at infinity and that no radiation comes from infinity. Hence the expressions (I.24) and (I.25) given for the integrals of the equations of motion can be considered justified.

Assumption 2) is realized by introducing functional covariant operators which satisfy the commutation relations for boson fields, and by showing (with certain hypotheses for the state vector being assumed satisfied) that the approximation $h \to 0$ permits us to go from the equation of Tomonaga to the classical Jacobi equations, and to a supplementary condition on the amplitude of the state vector. The case of spinor fields will be treated in another paper.

Moreover, it must be stated that the functional form for the quantum mechanical equations of motion has already been made use of, in a non-covariant form, by many authors [9], and that the deduction of the W.K.B. method is only a particular application of one of such formulations.

2. – Electromagnetic field in the presence of a given current distribution.

We repeat briefly the classical considerations developed in I in order to introduce some quantities necessary in the quantum mechanical formulation.

For an electromagnetic field in the presence of a given current distribution $J_\mu(x)$, we assume the Lagrangian:

$$L = -\frac{1}{2}\frac{\partial A_\mu}{\partial x_\nu}\frac{\partial A_\mu}{\partial x_\nu} + \frac{1}{c} J_\mu A_\mu \,, \tag{1}$$

in which we have suppressed the summation symbol, and have used the notation employed in I.

[9] K. GOTÔ: *Nuovo Cimento*, **3**, 533 (1956).

From the Lagrangian (1), we obtain the equation of motion

$$\square A_\mu = -\frac{1}{c} J_\mu , \tag{2}$$

where the Lorentz condition must be added separately.

Even in this case, as for that of the free electromagnetic field, the conjugate momenta are given by

$$P_{\mu\nu} = -4 \frac{\partial A_\mu}{\partial x_\nu} , \tag{3}$$

while the spur of the canonical tensor is

$$H = H(P_{\mu\nu}, A_\mu, J_\mu) = T_{\mu\mu} = -\tfrac{1}{8} P_{\mu\nu} P_{\mu\nu} - \frac{4}{c} J_\mu A_\mu , \tag{4}$$

which is composed of two terms: the first is the Hamiltonian H^0 of the free field already written in I, and the second is the interaction Hamiltonian H_1 proportional to the interaction energy density.

Following a procedure similar to that described in I, and using the same significance for the symbols, we arrive at Hamilton's equations

$$\frac{\partial P_{\mu\nu}}{\partial x_\nu} = -\frac{\partial H}{\partial A_\mu} = +\frac{4}{c} J_\mu , \tag{5}$$

$$\frac{\partial A_\mu}{\partial x_\nu} = \frac{\partial H}{\partial P_{\mu\nu}} = -\frac{1}{4} P_{\mu\nu} , \tag{6}$$

for which the solutions are written in the forms:

$$A_\mu = A_\mu(A^0_\mu, P^0_{\mu\nu}, J^0_\mu, J_\mu(x), x) , \tag{7}$$

$$P_{\mu\nu} = P_{\mu\nu}(A^0_\mu, P^0_{\mu\nu}, J^0_\mu, J_\mu(x), x) , \tag{8}$$

where the preceding expressions are functionals dependent upon the values A^0_μ, $P^0_{\mu\nu}$, J^0_μ which these quantities assume at the points of the space-like surface σ_0 from which the motion is studied, upon the values which $J_\mu(x)$ assumes at the points x of the generic space-like surface σ, and upon the point x explicitly.

The Jacobi equation for this case is written in the forms

$$\frac{\partial V_\nu}{\partial x_\nu} + H\left(A_\mu, J_\mu, \frac{\partial V_\nu}{\partial A_\mu}\right) = 0 , \quad \frac{\delta V(\sigma)}{\delta\sigma(x)} + H\left(A_\mu, J_\mu, \frac{\partial V_\nu}{\partial A_\mu}\right) = 0 , \tag{9}$$

where the function H is that given by (4), and where it is assumed that the function and the functional

$$(10)\qquad V_\nu = V_\nu(A_\mu(x), J_\mu(x), x)\,; \qquad V(A_\mu, J_\mu, \sigma) = \int_\sigma V_\nu(A_\mu(x'), J_\mu(x'), x')\, d\sigma'_\nu\,,$$

(where the convention and symbols are those used in I), have been introduced.

The equations of motion can be resolved when an integral of the type

$$(11)\qquad V_\nu = V_\nu(A^0_\mu, A_\mu, J^0_\mu, J_\mu, x)$$

is given, provided that

$$P^0_{\mu\nu} = \frac{\partial V_\nu}{\partial A^0_\mu}, \qquad P_{\mu\nu} = \frac{\partial V_\nu}{\partial A_\mu},$$

are substituted.

The procedure upon which the demonstration is based is that analogous to the one followed in I. We note finally that a canonical transformation can be used such that the transformed Hamiltonian is only the interaction part $-(4/c)\,J_\mu A_\mu$. In this case, it can be said that the classical equations of motion are written in the interaction representation.

3. – Covariant functional form of the field equation; W.K.B. approximation.

On the basis of the forgoing premises, a covariant quantum mechanical Hamiltonian formulation for field theory is permissible independently of the particular choice of canonical variables. In fact, we limit ourselves to a group of canonical transformations which keep the system covariant in order to obtain a covariant Hamiltonian formulation upon which we can apply the development to follow.

Here we limit ourselves to the case of an electromagnetic field in interaction with a given distribution of currents giving a covariant functional formulation to the Schrödinger representation; the Lorentz condition will be considered separately in a succeeding paper; therefore the development contained in this section can be considered as referring to an arbitrary tensor field for which the classical Hamiltonian is expressed in quadratic form in the Lagrangian variables and in the conjugate momenta.

Fixing the family of the space-like surface with which we study the evolution of the system, we indicate with $n_\nu(x)$ the unit vector normal to a space-like surface, such that it is directed towards the future, and is located at the in its generic point of the surface.

Then

$$n_\nu \mathrm{d}\sigma = \mathrm{d}\sigma_\nu \,, \tag{12}$$

where $\mathrm{d}\sigma$ represents the extension of the element of area considered.

In order to write the quantum mechanical equation of motion, we suppose that the states of the system are represented by functionals which depend upon the Lagrangian variables and on the space-like surface σ upon which they are defined.

We shall write the state vector in the form:

$$\Phi(A, \sigma) = \Phi[A_\varrho(x)] \,, \tag{13}$$

where x is a generic point of the space-like surface σ, and $\Phi(A, \sigma)$ is a c number, for which we assume there exists a functional derivative $\delta\Phi(\sigma)/\delta\sigma(x)$. If $\gamma(x)$ is an arbitrary function of the point x in σ, we have [10]

$$\int_\sigma n_\nu \frac{\delta}{\delta A_\mu(x)} [A_\lambda(x')\Phi(A)\gamma(x)] \mathrm{d}\sigma = \\ -\int_\sigma A_\lambda(x') n_\nu \frac{\delta}{\delta A_\mu(x)} [\Phi(A)\gamma(x)] \mathrm{d}\sigma + \delta_{\lambda\mu}\, \gamma(x')\Phi(A) \,, \tag{14}$$

where $\delta/\delta A_\mu(x)$ is the functional derivative with respect to $A_\mu(x)$.

The relation (14) is equivalent to

$$n_\nu \frac{\delta}{\delta A_\mu(x)} A_\lambda(x')\Phi(A) = A_\lambda(x') n_\nu \frac{\delta}{\delta A_\mu(x)} \Phi(A) + \delta_{\lambda\mu}\delta_\nu(x - x')\Phi(A) \,, \tag{15}$$

where $\delta_\nu(x - x')$ is the Dirac δ-function relative to the space-like surface σ.

Further there results

$$\delta_\nu(x - x') = \frac{\partial}{\partial x_\nu} D(x - x') \,, \tag{16}$$

where $D(x - x')$ is the invariant function of Pauli and Jordan relative to the field under consideration. Therefore, equation (15) can be written in the form:

$$\left[n_\nu \frac{\delta}{\delta A_\mu(x)} , A_\lambda(x')\right]_- = \delta_{\lambda\mu} \frac{\partial}{\partial x_\nu} D(x - x') \,. \tag{17}$$

([10]) K. O. Friedrichs: *Mathematical Aspects of the Quantum Theory of Fields*, (New York, 1953).

Hence, we can let the quantum mechanical operator

$$\mathcal{P}_{\mu\nu}(x) = -\hbar n_\nu \frac{\delta}{\delta A_\mu(x)}, \tag{18}$$

correspond to the classical conjugate momentum $P_{\mu\nu}(x)$ while all the Lagrangian variables $A_\varrho(x)$ correspond to the multiplicative operators $\mathcal{A}_\varrho(x)$.

Then, by substitution of (18) into (17), we obtain the commutation relations,

$$[\mathcal{P}_{\mu\nu}(x), \mathcal{A}_\lambda(x')]_- = -\hbar\delta_{\lambda\mu}\frac{\partial}{\partial x_\nu} D(x-x'), \tag{19}$$

while all the other dynamical quantities commute according to the usual formulation.

In the particular case that the space-like surface reduces to a surface $t = \text{const}$, then the usual non-covariant conjugate momenta $\mathcal{P}_{\mu 4}$ intervene, the unit vector is of the type

$$n_\nu = (0, 0, 0, i)$$

and there results as is noted [10]:

$$\mathcal{P}_{\mu 4}(x) = -i\hbar\frac{\delta}{\delta A_\mu(x)}, \tag{20}$$

$$[\mathcal{P}_{\mu 4}(x), \mathcal{A}_\lambda(x')]_{x_4'=x_4} = -\hbar\delta_{\lambda\mu}\left(\frac{\partial}{\partial x_4} D(x-x')\right)_{x_4=x_4'} = -\hbar\delta_{\lambda\mu}\delta(r-r'),$$

where r and r' represent the points x and x' respectively when $x_4 = x_4'$.

Consider now the invariant Hamiltonian (4). If we substitute equation (18) into it, we obtain an operator, and we can, therefore, write the Tomonaga equation in the form:

$$\mathcal{H}\Phi(A, \sigma) = i\hbar\frac{\delta\Phi(A, \sigma)}{\delta\sigma(x)}, \tag{21}$$

and if we define the operator $\mathcal{H}$ at the points of the furface σ_0, we then obtain a representation in which $\mathcal{H}$ is « time-independent » while $\Phi(A, \sigma)$ is « time dependent ».

This, by definition, is the Schrödinger representation; it is obviously clearly covariant.

Following the method of Wentzel, Kramers and Brillouin, we now want to show that, under certain conditions, the preceding equation reduces to the Jacobi equation (9).

We suppose that the state vector $\Phi(A, \sigma)$ can be written, as for systems with a finite number of degrees of freedom, in the general form:

$$\Phi(A, \sigma) = B(A, \sigma) \exp \left[\frac{i}{\hbar} V(A, \sigma)\right], \tag{22}$$

where σ is the generic space-like surface and B and V are real functionals depending also upon the function J_μ.

Since equation (21) is written explicitly as

$$\left[-\frac{1}{8}\hbar^2 \left(n_\nu \frac{\delta}{\delta A_\mu(x)}\right)^2 - \frac{4}{c} J_\mu \mathcal{A}_\mu\right] \Phi(A, \sigma) = i\hbar \frac{\delta\Phi(A, \sigma)}{\delta\sigma(x)}, \tag{23}$$

by virtue of the function (22), we obtain, after separating the real and imaginary parts, the two equations

$$\begin{aligned} -\frac{1}{8} n_\nu^2 \left[\hbar^2 \frac{\delta^2 B(A, \sigma)}{\delta A_\mu^2(x)} - B(A, \sigma) \left(\frac{\delta V(A, \sigma)}{\delta A_\mu(x)}\right)^2\right] - \\ -\frac{4}{c} J_\mu A_\mu B(A, \sigma) = -B(A, \sigma) \frac{\delta V(A, \sigma)}{\delta\sigma(x)}, \end{aligned} \tag{24}$$

$$-\frac{1}{4} n_\nu^2 \frac{\delta B(A, \sigma)}{\delta A_\mu(x)} \frac{\delta V(A, \sigma)}{\delta A_\mu(x)} - \frac{1}{8} n_\nu^2 B(A, \sigma) \frac{\delta^2 V(A, \sigma)}{\delta A_\mu^2(x)} = \frac{\delta B(A, \sigma)}{\delta\sigma(x)}. \tag{25}$$

From the first equation, we obtain for $\hbar \to 0$:

$$\frac{\delta V(A, \sigma)}{\delta\sigma(x)} + \frac{1}{8} n_\nu^2 \left(\frac{\delta V(A, \sigma)}{\delta A_\mu(x)}\right)^2 - \frac{4}{c} J_\mu A_\mu = 0. \tag{26}$$

When we take into account the second equation of (10), equation (26) is identified with the Jacobi equation (9), provided that the classical function V_ν is of the type:

$$V_\nu[A_\mu(x),\ J_\mu(x),\ x] = n_\nu(x) V[A_\mu(x),\ J_\mu(x)], \tag{27}$$

where the tensor character is contained only in $n_\nu(x)$, and $V[A_\mu(x), J_\mu(x)]$ is a point invariant function. The relation (27) expresses the fact that the functional $V(A, \sigma)$, which gives the phase of the state vector, is defined, point by point on the space-like surface σ from the normal component of the Jacobi function $V[A_\mu(x), J_\mu(x)]$.

Hence the second term — of (26) which is paired with $-\frac{1}{8}(\delta V(A, \sigma)/\delta A_\mu(x))^2$ represents the trace of the canonical tensor of the free field and it can be thought of as the product $-\frac{1}{8}(P_{\mu\nu} n_\nu)(P_{\mu\lambda} n_\lambda)$.

1733

That is, we again find the condition already examined in I° that the conjugate momenta which effectively determine the motion of the field are the components of the tensor $P_{\mu\nu}$ normal to the space-like surface.

The approximation which is made for $\hbar \to 0$ is lawful when:

$$\left| \frac{1}{B(A,\sigma)} \frac{\delta^2 B(A,\sigma)}{\delta A_\mu^2(x)} \right| \ll \frac{1}{\hbar^2} \left| \frac{\delta V(A,\sigma)}{\delta A_\mu(x)} \right|^2 , \tag{28}$$

results, i.e. for fields in which the spur of the canonical tensor is high and the amplitude $B(A, \sigma)$ of the state vector can be thought of as being concentrated about a given value $A_\mu(x)$ for any x.

Equation (25) can also be written as

$$\frac{1}{4} \frac{\delta}{\delta A_\mu(x)} \left(B^2(A,\sigma) \frac{\delta V(A,\sigma)}{\delta A_\mu(x)} \right) = \frac{\delta B^2(A,\sigma)}{\delta \sigma(x)} . \tag{29}$$

If we consider $B^2(A, \sigma)(\delta V(A, \sigma)/\delta A_\mu(x))$ as a « current density » four vector of the field $\Phi(A, \sigma)$, equation (29) can be interpreted as the divergence of the « current density » (with respect to $A_\mu(x)$) which is proportional to the derivative of the probability density with respect to the space-like surface.

The Lorentz conditions and other aspects of the state vector will be discussed in another paper.

* * *

The author wishes to thank Professor B. FERRETTI for many stimulating discussions and Professor P. CALDIROLA for suggesting many references.

RIASSUNTO

Quale ulteriore sviluppo di un precedente lavoro si scrivono le equazioni di Hamilton covarianti per il campo elettromagnetico in presenza di correnti note. Si scrive l'equazione di Jacobi e viene definita una classe di trasformazioni canoniche che conserva la covarianza a vista dello schema. Mediante una opportuna introduzione di operatori funzionali covarianti, si scrive l'equazione di Tomonaga che risulta essere covariante indipendentemente dalla particolare scelta delle variabili canoniche, e quindi anche nella rappresentazione di Schrödinger. Si dimostra, mediante una generalizzazione del metodo di W.K.B., che sotto certe ipotesi l'equazione di Tomonaga si riduce all'equazione di Jacobi classica.

IL NUOVO CIMENTO Vol. VIII, N. 6 16 Giugno 1958

Identification of Fast Heavy Nuclei of the Cosmic Radiation Using Nuclear Emulsion Techniques.

B. J. O'Brien (*) and J. H. Noon (+)

The F.B.S. Falkiner Nuclear Research and Adolph Basser Computing Laboratories, School of Physics, (×) *The University of Sydney - Sydney, N.S.W.*

(ricevuto il 3 Febbraio 1958)

Summary. — Various workers disagree in their measured charge spectra of the heavy nuclei of the primary cosmic radiation. This disagreement could be due to unreliable charge identification. Since there is inadequate information on comparison of measurement techniques, we have made measurements of six parameters of tracks of nuclei with $4 \leqslant Z \leqslant 9$ in a stack of G-5 stripped emulsion flown at 41 °N geomagnetic latitude. The δ-ray, blob, and isolated-grain densities, the Fowler-Perkins coefficient, integral gap length, and probability of development have been found for each track. Estimates have been made of the effect of various sources of error in these measurements, including a study of the change in each measured parameter with a 20% change in minimum grain density of the emulsion. From the comparison and analysis of these measurements, recommendations are given on the use of the above techniques in the identification of fast heavy nuclei in nuclear emulsion.

(*) Now at Antarctic Division, Department of External Affairs, Melbourne.

(+) Now at Physics Department, University of Queensland.

(×) Also supported by the Nuclear Research Foundation within the University of Sydney.

1. – Introduction.

In recent years various techniques have been used in about twenty nuclear-emulsion [1-10] and counter measurements [11-14] of the charge spectrum of the primary cosmic radiation, but there still is disagreement on the relative abundances of the light ($3 \leqslant Z \leqslant 5$) and medium ($6 \leqslant Z \leqslant 9$) groups and on the relative abundances of the individual elements within these groups. WADDINGTON [8] has summarized most of the recent results and shown that the discrepancies cannot be explained on the basis of the statistical fluctuations in the numbers of particles arriving at the detectors. Neither does there seem to be any possible explanation in terms of the different altitudes and geomagnetic latitudes of the flights. And, since conflicting results have come from stacks flown with the same balloon [6,7], variations in the charge spectrum with time cannot explain the discrepancies. Accordingly, the discrepancies must be due to errors associated with at least some of the identification techniques used in these experiments.

Most work on the charge spectrum has been done using nuclear emulsions and many identification techniques have been used in these studies. To our knowledge, there has been little detailed comparison of the use of these techniques in identification of fast heavy nuclei, although in some experiments two or more techniques have been used. For example, WADDINGTON [8] made Fowler-Perkins-coefficient measurements as well as δ-ray counts on all his tracks of L and M nuclei.

We therefore decided to measure a number of tracks of L and M nuclei by various emulsion techniques both to compare the techniques themselves and to gain information on the cosmic-ray charge spectrum.

---

(1) H. L. BRADT and B. PETERS: *Phys. Rev.*, **80**, 943 (1950).

(2) A. D. DAINTON, P. H. FOWLER and D. W. KENT: *Phil. Mag.*, **43**, 729 (1952).

(3) M. F. KAPLON, J. H. NOON and G. W. RACETTE: *Phys. Rev.*, **96**, 1408 (1954).

(4) H. FAY: *Zeits. f. Naturfor.*, **10a**, 572 (1955).

(5) R. E. DANIELSON, P. S. FREIER, J. E. NAUGLE and E. P. NEY: *Phys. Rev.*, **103**, 1075 (1956).

(6) J. H. NOON, A. J. HERZ and B. J. O'BRIEN: *Nuovo Cimento*, **5**, 854 (1957).

(7) Reported by B. PETERS: *Varenna Conference* (1957); also R. R. DANIEL: private communication (1957).

(8) C. J. WADDINGTON: *Phil. Mag.*, **2**, 1059 (1957).

(9) Reported by C. M. GARELLI: *Varenna Conference* (1957).

(10) M. KOSHIBA, G. SCHULTZ and M. SCHEIN: reported by M. SCHEIN at *Varenna Conference* (1957).

(11) J. LINSLEY: *Phys. Rev.*, **101**, 826 (1956).

(12) T. H. STIX: *Phys. Rev.*, **95**, 782 (1954).

(13) W. R. WEBBER: *Nuovo Cimento*, **4**, 1285 (1956).

(14) B. J. O'BRIEN, A. J. HERZ and J. H. NOON: *Varenna Conference* (1957).

A preliminary report [14] on most of these measurement was given at the Varenna Conference in June 1957. Here we consider only comparison of the measurement techniques used by us. We do not consider photometric techniques [15-17] or the use of emulsions of various low sensitivities.

Since the minimum grain density in our G5 emulsion was low we were able to measure 86 tracks with $4 \leqslant Z \leqslant 9$ by six different methods. The six parameters, not altogether independent, are:

1) δ-ray density N_δ (δ rays/100 μm) [18-21].

2) Blob density N_b (blobs/100 μm) [21,22].

3) Integral gap length L_g (%) [22].

4) Fowler-Perkins coefficient G (/mm) [23].

5) Probability of development p [23-28].

6) Density of isolated grains N_s (/100 μm) [29]

In this way we obtained frequency distributions for the six parameters. We correlated the peaks of these distributions with the charge of the nuclei by calibrating the emulsion, using methods we describe below.

Such « charge spectra » derived from measurement of a single parameter for many tracks may be in error because of:

1) inadequate or incorrect charge calibration or extrapolation;

2) inadequate charge resolution;

3) systematic errors in the measurements.

We examine here these causes of error, and make recommendations designed to minimize these errors. For completeness we include several recommen-

---

(15) S. von Friesen and K. Kristianson: *Ark. f. fys.*, **4**, 505 (1952).
(16) M. Artom and C. Gentile: *Suppl. Nuovo Cimento*, **4**, 254 (1956).
(17) M. Della Corte and M. Ramat: *Nuovo Cimento*, **9**, 605 (1952).
(18) P. Freier, E. J. Lofgren, E. P. Ney and F. Oppenheimer: *Phys. Rev.*, **74**, 1818 (1948).
(19) H. L. Bradt and B. Peters: *Phys. Rev.*, **74**, 1828 (1948).
(20) J. Crussard: *Thesis* (Université de Paris, 1952).
(21) L. Voyvodic: *Progress in Cosmic Ray Physics*, II (1954).
(22) C. Castagnoli, G. Cortini and A. Manfredini: *Nuovo Cimento*, **2**, 301 (1955).
(23) P. H. Fowler and D. Perkins: *Phil. Mag.*, **46**, 587 (1955).
(24) W. W. Happ, T. E. Hull and A. H. Morrish: *Can. Journ. Phys.*, **30**, 699 (1952).
(25) C. O'Ceallaigh: CERN Document BS 11 (1954).
(26) A. J. Herz and G. Davis: *Austral. Journ. Phys.*, **8**, 129 (1955).
(27) M. Della Corte, M. Ramat and L. Ronchi jr.: *Nuovo Cimento*, **10**, 509 (1953).
(28) J. M. Blatt: *Austral. Journ. Phys.*, **8**, 248 (1955).
(29) B. J. O'Brien: *Nuovo Cimento*, **7**, 314 (1958).

dations which are already well known but which we believe to be sufficiently important to be mentioned again.

2. – Stack details.

2·1. *Flight latitude and energy cut-off.* – The flight was made at 41° N geomagnetic latitude and consequently all particles had energies greater than 1.3 GeV/nucleon [30]. This energy corresponds to the trough in the curve of energy-loss rate versus primary energy, and the rate of restricted energy loss of a particle at this energy is about 12% less than that of a particle of the same charge but at plateau ionization [31].

Using an integral energy spectrum with exponent 1.5, one can show that 75% of particles with charge Z will lose energy at a rate differing by less than 4% from Z^2I_0, where I_0 is the minimum rate of energy loss. Thus the majority of the observed particles will have an energy loss corresponding to the minimum rather than the plateau value.

2·2. *Details of emulsion stack.* – The stack [6] consisted of fifteen sheets of 600-μm G5 stripped emulsion, all in contact.

It was developed in three batches, each of five consecutive sheets. The first batch, containing the scanning sheet, was the one in which all heavy-primary measurements were made, except those relating to development studies. The minimum grain density in our emulsion was much lower than that of « normal » G5 of about 20 to 25 grains/100 μm; plateau grain density in the scanning sheet was found to be (8 ± 0.5) grains per 100 μm from counting grains in tracks of electrons from π-μ-e decays. Fifty α particles with length per plate more than 7.5 mm were found in the scanning sheet and traced from it. These had a mean grain density [32] of (32.6 ± 0.7) grains per 100 μm in the scanning sheet. The spread in grain counts is consistent with a zero variation in the sensitivity (*) over the scanning plate when allowance is made for the extra spread imposed by the energy spectrum. No variation of development with depth was found over the central 500 μm of the 600 μm sheet.

Further counts were made on the α particles throughout the first batch of plates. From the measured variation of grain density, the variation of sensitivity within this batch is less than 2%.

---

(30) R. A. Alpher: *Journ. Geophys. Res.*, **55**, 37 (1950); see also J. A. Simpson, K. B. Fenton, J. Katzman and D. C. Rose: *Phys. Rev.*, **102**, 1648 (1956).

(31) W. H. Barkas and D. M. Young: University of California Rad. Lab. Report UCRL-2579 (1954).

(32) B. J. O'Brien and J. H. Noon: *Nuovo Cimento*, **5**, 1463 (1957).

(*) We mean by variations in emulsion sensitivity, variations in minimum grain density and probability of development for singly-charged minimum-ionizing particles.

Eleven α particles in the first and second batches of plates had mean grain densities of (32.3 ± 0.7) and (26.1 ± 0.6) grains per 100 μm respectively. Thus there was a decrease of $(19 \pm 3)\%$ in the minimum grain density from the first batch to the second. The measured grain diameter however was the same in both batches. The effects of change in emulsion sensitivity on the different measurement techniques are examined in Sect. **8**·5.

3. – Measurement details.

The 4-grain δ-ray criterion ([19]) was used in counts of 106 tracks which had grain density greater than ten times minimum and had lengths per plate greater than 3 mm. Details have been gives elsewhere ([6]).

Eighty-six of these tracks, with δ-ray densities between 0.3 and 2.3 per 100 μm, were selected for further measurements in the first batch of five plates. δ-ray recounts were made by two of the previous four observers. No standard tracks were measured during these recounts.

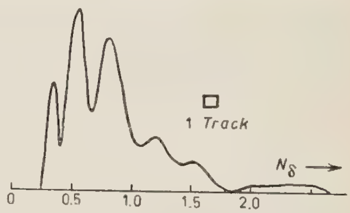

Fig. 1. – δ-ray-density distribution.

Along-the-track parameters were all measured by one observer over a 500-μm length of each track in the central 300 μm of the scanning sheet. A Koristka microscope with ×1600 magnification was used, and for blob-density and integral-gap-length measurements a gap counter ([25,33-36]), was used with the stage moved automatically by a small motor. For isolated-grain and Fowler-Perkins-coefficient measurements, the stage was moved by hand. A filar eyepiece was used in counting gaps longer than 0.94 μm.

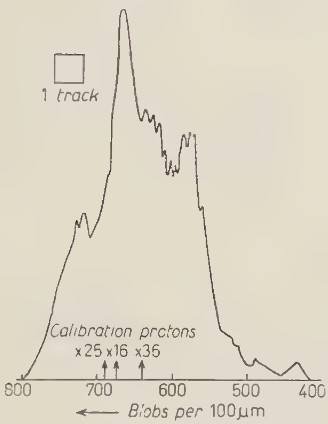

Fig. 2. – Blob-density distribution.

The results of all these measurements are shown in Figs. 1-6. Here a form of triangle plotting which is helpful in obtaining the peaks of each distribution has been used. Each measured parameter is plotted as a triangle of unit area, with a base width of twice the standard deviation of the measurement. In Fig. 1 the

(33) D. M. Ritson: *Phys. Rev.*, **91**, 1572 (1953).
(34) M. Della Corte: *Nuovo Cimento*, **12**, 28 (1954).
(35) G. Baroni and C. Castagnoli: *Suppl. Nuovo Cimento*, **12**, 364 (1954).
(36) J. E. Hooper and M. Scharff: CERN no. 12 (1954).

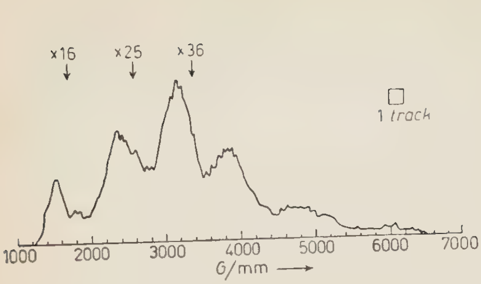

Fig. 3. – Integral-gap-length distribution.

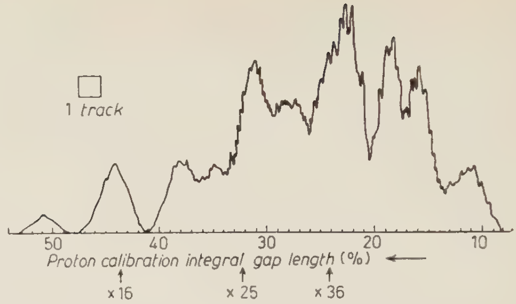

Fig. 4. – Fowler-Perkins-coefficient distribution.

standard deviation was taken as the Poissonian one. In the other figures the standard deviation was derived from the BLATT ([28]) theory. (See Sect. 8·2).

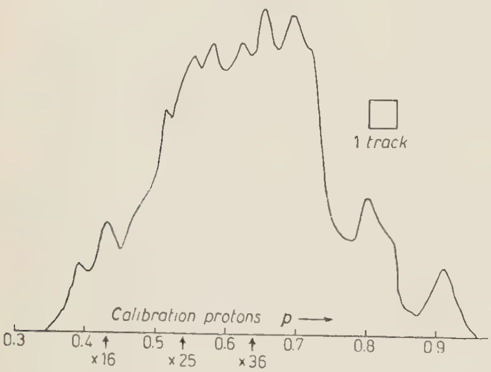

Fig. 5. – Probability-of-development distribution.

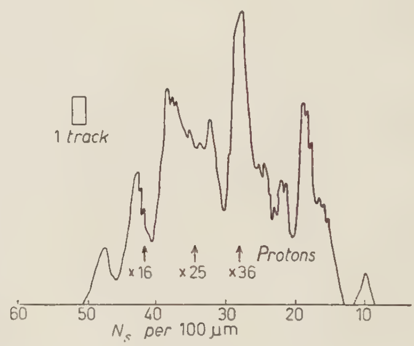

Fig. 6. – Isolated-grain-density distribution.

4. – Charge calibration.

To calibrate the emulsion one must establish the correlation between values of track parameters which correspond to various rates of energy loss and those of fast heavy nuclei of various charges. The rate of energy loss of a relativistic nucleus of charge Z is proportional to Z^2, but very few track parameters are directly proportional to Z^2. The methods by which we calibrated our emulsion ([6]) are conventional, and we merely summarize them here.

4·1. *Calibration with stopping known tracks*, – It has been assumed for some time (see, for example, reference ([17])) that the along-the-track characteristics of a proton at a residual range corresponding to a restricted energy-

loss rate of say twenty-five times minimum will be the same as those of a nucleus of charge five which is at minimum ionization. There seems no significant theoretical or experimental evidence against this assumption provided restricted energy loss [31,37,38] not total energy loss, is considered.

The δ-ray density along the tracks of stopping protons is not proportional to the restricted rate of energy loss because the maximum energy transferred to the δ-ray electrons decreases as the proton slows down. As a result, the density of acceptable δ-rays drops rapidly when the proton comes to the end of its range, and very slow protons have no visible δ-rays at all. Stopping tracks cannot, therefore, be used in the charge calibration of δ-ray densities; details of suitable calibration methods have been given by DAINTON *et al.* [2,39], KAPLOON *et al.* [3] and VOYVODIC [21].

We measured along-the-track parameters of nine stopping protons which were flat, at least 5 mm long, and which had been identified by scattering measurements. Values obtained at residual ranges of 220 μm, 500 μm, and 1.3 mm were taken as corresponding to rates of restricted energy loss which are respectively 36, 25 and 16 times the minimum rate [31,38]. There was consistent agreement between values obtained from the proton measurements and peaks of the distributions of the heavy-nuclei measurements (see Figs. 2-4, 6).

Because the majority of the 86 tracks were too heavy to have their grain densities measured reliably, no attempt was made to measure N_g for all the tracks. However the graind ensities of protons measured at residual ranges of 1.3 mm and 500 μm agreed [6] with the grain densities of tracks classified as Be an B nuclei from the above absolute charge calibration.

4·2. *Calibration check.* – Calibration-type interactions are an accepted means of charge calibration. A suitable interaction has no visible excitation star, and has a narrow cone of secondary fragments of charge 2 or greater. Recent discussions of calibration interactions have been given by KOSHIBA *et al.* [10] and by WADDINGTON [8].

In our stack we found only one such calibration interaction. This gave as secondaries two α particles identified by grain counts over a range of 3 cm of emulsion. The characteristics of the primary nucleus were in agreement with those of the group classified as beryllium nuclei by the above calibration.

5. – Charge extrapolation.

Calibration by means of stopping tracks is only possible, in general, for $Z \leqslant 6$. If no calibration interactions occur with heavier primary nuclei, one must extrapolate from the $Z \leqslant 6$ region to higher charges. Theoretically the

(37) G. ALEXANDER and R. H. W. JOHNSTON: *Nuovo Cimento*, 5, 363 (1957).
(38) A. J. HERZ: private communication (1957).

δ-ray density (N_δ) of a relativistic nucleus of charge Z is given [18,19,39,40] by

$$N_\delta = aZ^2 + b\,,$$

where a and b are constants, b being the background correction. If this relation held experimentally over wide ranges of Z, one could reliably predict the δ-ray density up to $Z = 26$. Extrapolation based on this relationship is, however, only reliable over limited ranges.

In practice, b depends on Z, and it is only constant for small ranges of Z. Further, when making δ-ray counts over a wide range of charges, subjective effects may cause an observer to unknowingly adopt different counting criteria. The heaviest δ-ray densities measured in our stack are of order 22% less than that predicted for $Z = 26$ on the basis of extrapolation from our absolute charge calibration and are consistent with $Z \sim 23$.

Random subjective variations in repeat measurements of several tracks were found to be less than 5% (see Sect. **8**·2). However, it is possible that we systematically under-estimated the δ-ray densities of very heavy nuclei because of the low minimum grain density of our emulsion. This could only be checked by suitable calibration interactions caused by very heavy primary nuclei, and we observed no such interactions. Accordingly, even though our flight was at less than 12 g cm^{-2}, our heaviest tracks cannot be reliably classified as iron nuclei.

Charge extrapolation using parameters other than N_δ is also subject to error because no other parameter varies in a simple manner with Z^2 over a wide range of Z. All along-the-track parameters are subject to saturation. Recently KOSHIBA *et al.* [10] reported that N_b varied as Z for $Z > 5$ in a G5 emulsion of normal sensitivity. If this relation is found to be generally applicable it will prove very useful. We have not been able to test it satisfactorily because we have no calibration interactions with primary nuclei of the heavy group.

Some along-the-track parameters are proportional to Z^2 where no saturation effects occur, and vary smoothly with Z^2 thereafter. However extrapolation on this basis is liable to considerable error.

6. – Charge resolution.

We consider that satisfactory charge resolution occurs when the difference in the mean parameters for neighbouring charges Z and $(Z-1)$ equals at least two standard deviations in the measured parameter for tracks of charge Z.

---

(39) A. D. DAINTON, P. H. FOWLER and D. W. KENT: *Phil. Mag.*, **42**, 317 (1951).
(40) D. TIDMAN, E. P. GEORGE and A. J. HERZ: *Proc. Phys. Soc.*, A **66**, 1019 (1953).

The number of δ-rays which must be counted to resolve neighbouring charges is a function of the charge Z.

The Poissonian standard deviation in number of δ rays in a track length t is given by $N^{\frac{1}{2}}$. To resolve two neighbouring charges Z and $(Z-1)$, the number of δ rays counted must be such that

$$2N^{\frac{1}{2}} > |Z^2-(Z-1)^2|\,at$$

$$> 2N/Z$$

$$\text{i.e.}\quad N > Z^2\,.$$

If counting is done over short track lengths so that $N < Z^2$, the resolution between neighbouring charges is affected. This is true irrespective of the value of a, or of the emulsion sensitivity. Fifty δ-rays are obviously not enough to give good resolution between charges 7, 8 and 9 (see Fig. 1).

Since saturation affects along-the-track characteristics these will not always be proportional to Z^2 and then the relative separation in measured parameters for neighbouring charges Z and $(Z-1)$ is $< 2/Z$. However since these parameters vary in a complex fashion with Z^2 and the emulsion characteristics, it is not possible to give simple general expressions applicable to any emulsion for charge resolution obtainable from these parameters. Our results obtained from 500-μm track lengths show resolution between charges 5 and 6 of 30% for L_g and G (Figs. 3 and 4) and 20% for N_s (Fig. 6) but very little resolution for N_b and p (Figs. 2 and 5). None of the measured parameters gives adequate resolution for charges 7, 8 and 9, but measurements over track-lengths of 1 mm or more should give better resolution. However in some cases, for example Fowler-Perkins coefficients for very heavy tracks, or blob density in the region of maximum blob density, the parameters will be very insensitive to changes in the rates of energy loss and the statistical accuracy of measurement necessary to give charge resolution could only be obtained from very long track lengths. Over such lengths, emulsion variations

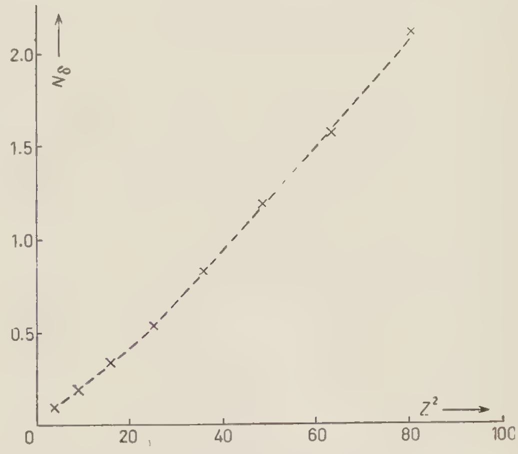

Fig. 7. – Charge extrapolation based on δ-ray density.

may be important (see Sect. 8·5). Moreover small effects such as person-to-person variations could obscure the separation between charges.

In Sect. **9** we indicate which track parameters give best resolution in different regions of ionization.

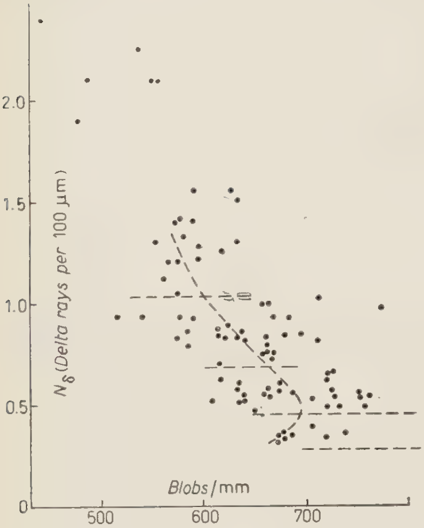

Fig. 8. – Correlation of δ-ray density with blob density.

7. – Correlation of measurements.

The correlation diagrams of the δ-ray density with each of the other measurements are given in Figs. 8-12. Lines are drawn in these diagrams through the mean values of each parameter for the different charges. For the blob density and the probability of development, the proton calibration points are used to estimate these means, and for the other parameters the peaks of the distributions (Figs. 3, 4, 6) are used.

Also shown in all except Fig. 8 are dashed lines which correspond to half-integral charges, derived from peaks of the distributions in each parameter. The half-width of the measured distributions in many cases is greater than

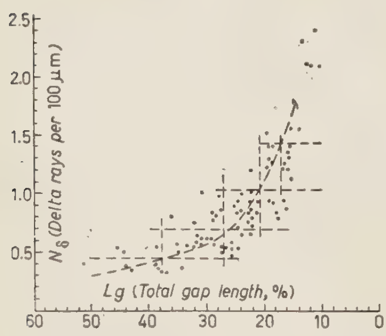

Fig. 9. – Correlation of δ-ray density with integral gap length.

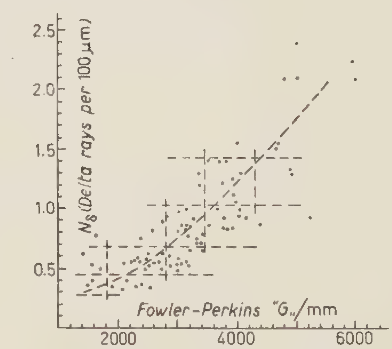

Fig. 10. – Correlation of δ-ray density with Fowler-Perkins coefficient.

the difference between the mean and the dashed lines which make up « boxes » around each charge. Points outside the boxes due to spread in the measure-

ments of each parameter indicate incomplete resolution between charges for some tracks.

The usefulness of each type of measurement in different charge regions is discussed in Sect. **9**. We first consider how measurements of all these track parameters are affected by experimental conditions.

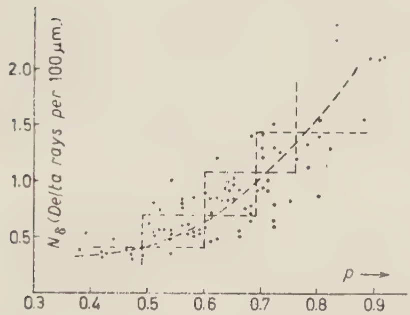

Fig. 11. – Correlation of δ-ray density with probability of development.

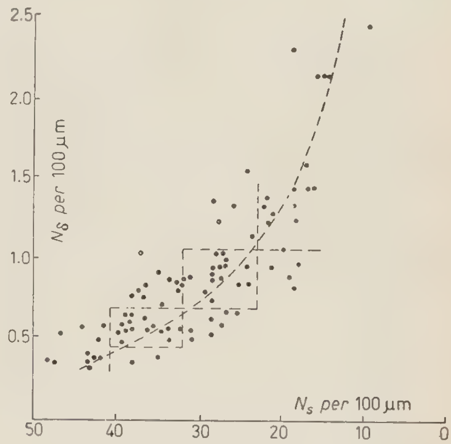

Fig. 12. – Correlation of δ-ray density with density of isolated grains.

8. – Sources of error in measured parameters.

8·1. *Intrinsic errors.* – These arise because of the statistical nature of the occurrence of δ rays and of the process of track formation.

The intrinsic errors in δ-ray density are Poissonian. However for along-the-track parameters the finite grain size and the influence of saturation give rise to intrinsic errors which vary with the density of the track but which are always less than Poissonian ([23,25,28,41]).

The intrinsic errors may be calculated ([41]) by use of the Blatt fluctuation theory ([28]).

8·2. *Subjective errors.* – The magnitude of subjective variations can only be estimated by a significant number of remeasurements over fixed sections of one or more tracks during the same period of time as the experimental measurements.

δ-ray measurements are known ([42]) to be liable to subjective errors of 5% or more. We measured the random subjective error as 5% when three observers made repeat counts on three tracks with widely different values of

([41]) B. J. O'Brien: *Nuovo Cimento*, **7**, 147 (1958).

([42]) N. Norlind: *Kungl. Fysiografiska Sallskapets. - I. Lund Forhandlinghar*, **24**, no. 12 (1954).

δ-ray density. This figure applies for both the 4-grain and the range counting criteria.

However larger systematic subjective errors may occur if one counts successively tracks of very different densities. A method such as that used by WADDINGTON [3] may serve to minimize such errors.

Measurements of along-the-track characteristics are in general less subjective than δ-ray counts, and in favourable circumstances subjective variations may be neglected [37,41]. However, since the separation between neighbouring charges is sometimes small with along-the-track parameters, small subjective variations can be important. For example, when four observers measured G for 1-mm lengths of our 86 tracks, person-to-person variations obscured the resolution of charges 5 and 6. However, as shown in Fig. 10, one observer measuring over 500-μm lengths obtained good resolution.

8·3. *Variation of track characteristics with dip.* – The corrections to δ-ray densities of dipping tracks will have a complex dependence on the dip and the counting criterion used. If short tracks with dip of order 1 in 2 are counted the measured δ-ray density may be as much as 20% less than that of longer tracks with dip of order 1 in 4. Such a variation has been found [43] for two stacks of comparable minimum grain density, where in one stack the emulsion sheets were horizontal and in the other they were vertical when the balloon flights were made. No corrections were necessary in our case since the maximum dip was 1 in 5.

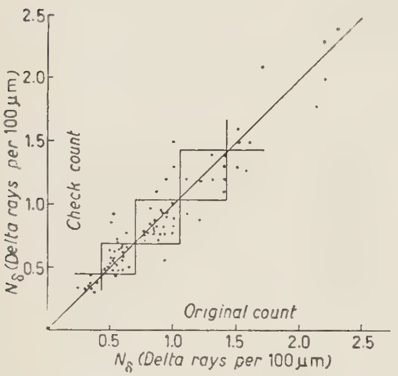

Fig. 13. – Plot of initial versus check δ-ray counts.

Besides the foreshortening of a dipping track in an emulsion, the thickness of the grains in the track will result in shortening the apparent lengths of the gaps and, in extreme cases, will block out completely the smaller gaps.

Simple geometric corrections for dip have been given by O'CEALLAIGH [25] and by WINZELER [44]. All our along-the-track measurements were corrected for dip.

8·4. *Variation of track characteristics with quality of illumination.* – The effect of reduced illumination on δ-ray densities is small in general, and, espe-

---

[43] J. H. NOON: *University of Rochester Ph. D. Thesis* (1954).

[44] H. WINZELER: *Suppl. Nuovo Cimento*, **4**, 258 (1956).

cially for the range criterion, appears to be negligible over a reasonable range of illumination.

A reduction in illumination was made to approximately one third in power from our normal working conditions and it was found that the measured grain diameter was ten percent larger than under our normal working illumination.

This increase in apparent grain size means that gaps smaller than about 0.05 μm are no longer visible, and each measurement of a gap length is reduced by this amount.

A very quick way of estimating the effect of this upon every measurement of along-the-track characteristics comes from the gap length distribution of Fig. 14. In this figure, the density of gaps $\geqslant l$ is plotted against the gap length (l) for heavy nuclei of various charges. It can be seen, for example, that the 10-percent change in apparent grain diameter given above will reduce the blob density and integral gap length by about 30% for $Z \sim 23$, and about 11% for $Z = 5$. In theory, the Fowler-Perkins coefficient remains unchanged, though reduced illumination may increase subjective effects.

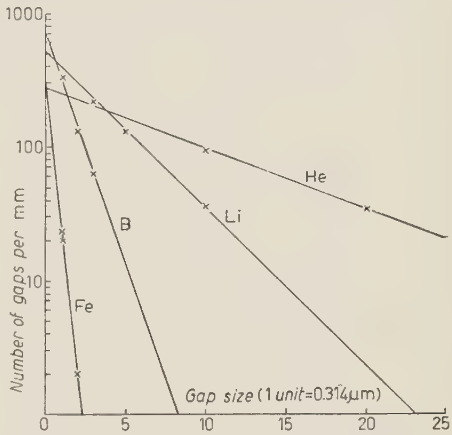

Fig. 14. – Number of gaps of length $> l$ versus gap size l plotted for several tracks of fast heavy nuclei.

8·5. *Variation of characteristics with changes in emulsion sensitivity.* – We consider the dependence of track characteristics on the minimum grain density of the emulsion in two separate phases:

1) Where small-scale variations (of order 1%) in the emulsion are evident from very detailed analysis of measurements.

2) Where variation (of order 10%) of the emulsion is apparent after a few measurements on the same track in different regions of the emulsion.

We have studied these phases in this stack of low minimum grain density.

In Sect. 2 we showed using measurements on fast α particles over the 9 in. by 10 in. sheet that variations in the minimum grain density were less than 2%. The above statements, and all measurements in this stack, refer to regions of the emulsion at least 100 μm from either the surface or the glass.

More detailed analysis was carried out on several long tracks of different charges. In each case it was found ([41]) that there was definite evidence for variations of order 1% in minimum grain density over lengths of order 1 mm, these variations introducing a spread of about 25% of the Poissonian error in blob counts. Recently other workers ([37]) have also indicated some evidence of a similar effect. Our work showed that such small variations in an otherwise uniform emulsion do not greatly affect charge identification or resolution between charges.

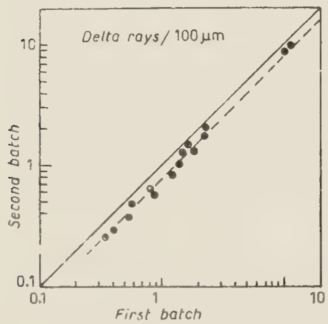

Fig. 15. – Comparison of δ-ray counts in first and second emulsion batches.

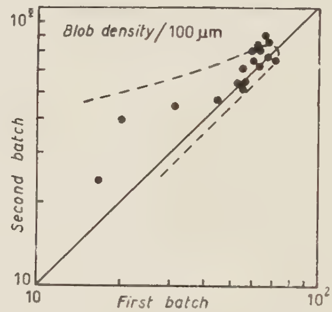

Fig. 16. – Comparison of blob density in first and second emulsion batches.

It must be emphasized that we are here concerned only with changes in minimum grain density, since the grain diameter was the same in each batch. We have found in another stack for two batches with the same minimum grain density but different mean grain diameter, that the along-the-track characteristics of heavy nuclei were very different. Thus it is not sufficient to measure only the minimum grain density in checking uniformity of the emulsion characteristics.

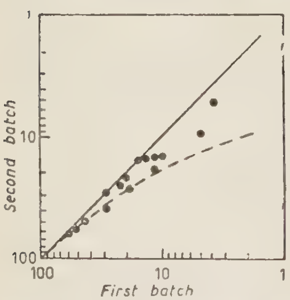

Fig. 17. – Comparison of integral gap length in first and second emulsion batches.

The effects of larger variations in emulsion sensitivity are important even when the mean grain diameter is constant. Grain counts on 11 fast α particles show that there is a decrease of $(19\pm3)\%$ in their grain density from one batch to the next. Sixteen heavy-primary tracks ranging in δ-ray density from 0.2 to 13.0 per 100 μm were measured in each batch in the same way that the 86 tracks were measured in the first batch. The correlation diagrams of measured parameters in both batches are shown in Figs. 15-19.

Fig. 15 shows that all δ-ray densities in the second batch are approximately

1748

20% lower than in the first batch. Although the number of δ-rays produced in a given energy interval depends only on the primary particle and the emulsion composition, with a lower emulsion sensitivity not all tracks of electrons

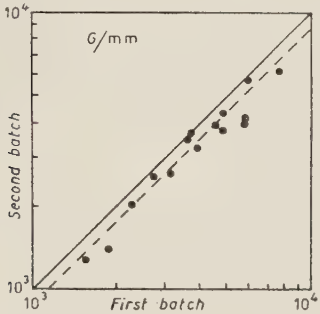

Fig. 18. – Comparison of Fowler-Perkins coefficients in first and second emulsion batches.

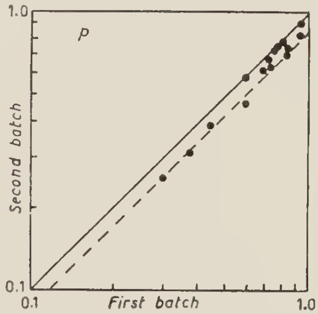

Fig. 19. – Comparison of probability of development in first and second emulsion batches.

in this energy interval satisfy the criteria originally adopted for counting δ rays. Low-energy electrons must have higher initial energy on the average to produce 4 grains, and high-energy electron tracks will have fewer grains near the primary causing the δ rays. Thus the effective value of the constant a in the relation

$$N_\delta = aZ^2 + b$$

is decreased. We have tested this explanation experimentally by measuring the projected-range distribution of acceptable δ rays over 8-mm track lengths of one track in two different emulsion batches and the results are shown in Fig. 20. We see that δ-ray densities in emulsions of low minimum grain density are strongly affected by variations in the emulsion sensitivity.

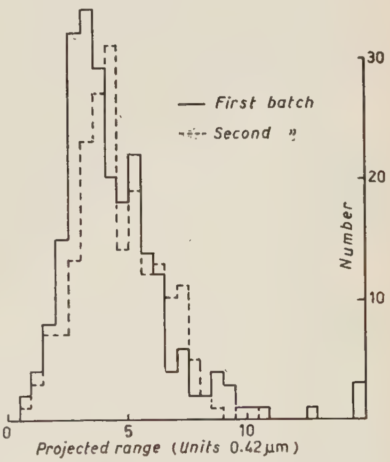

Fig. 20. – Projected range distributions of 4-grain δ rays measured over 8-mm lengths of the same track in first and second emulsion batches.

A number of workers ([3,5,7,39]) using the 4-grain criterion, have found values of a very close to 0.1 in G5 emulsions of normal minimum grain density. Our value for a in G5 emulsion of minimum grain density about 8/100 μm is about one quarter this value. Clearly, the value of a is not linearly related to the

minimum grain-density over a wide range. However it should be feasible to construct a curve of a versus minimum grain density for G5 emulsion if more values were available. Such a curve might be used in any emulsion, as a calibration check in low-charge regions, although extrapolation to higher charge regions would still require careful calibration of individual emulsions.

The effect of differences in development upon along-the-track characteristics is shown in Figs. 16-19. Only the Fowler-Perkins coefficient G, shown in Fig. 18, varies in a simple manner with development, and as found by FOWLER and PERKINS [23], the normalized value of G is independent of development for $G < 3000$ mm.

For discussion of other along-the-track characteristics, it is convenient to invoke the probability of development p which is used in several models of track formation. We consider here only the Herz-Davis model [26] since this has been found to give good fit to along-the-track characteristics both for singly-charged particles and in our emulsion for tracks of heavy nuclei.

In general, after the emulsion is calibrated, the value of p for any track is estimated from the measured value of w, the mean gap width. However, if one is dealing with dense tracks, we recommend estimating p from the integral gap length L_g, as p varies more rapidly with L_g for $p \to 1$, and also as the error in $\overline{w}$ comes from errors in both L_g and in N_b.

It has recently been shown [45] that the normalized value of p is independent of development up to $p \sim 0.5$ (*).

Accordingly in Figs. 16-19 we have drawn dotted lines showing the change in track parameters which was calculated on the assumption that the value of p of each track changed by 19% from the first emulsion batch to the second.

Clearly the above assumption must break down for $p \to 1$, but it can be seen that a rough fit is obtained for $p \leqslant 0.4$.

9. – Conclusions and recommendations.

As a result of the comparison of measurements outlined in this paper, we make some general recommendations regarding the use of the identification techniques which we have employed.

All tracks should be measured by at least two methods so that the correlation can be used as a check on the reliability of the measurements. δ-ray density which can be extrapolated over a wide range of energy-loss rates. should be measured in conjunction with one or more along-the-track cha-

---

[45] N. SOLNTSEFF: private communication.

(*) This quoted value of p is for emulsions where the integral part Γ of the crystal growth factor is 1. For other values of Γ one can calculate the corresponding p.

racteristics. If measurements are made over a wide range of Z, then extrapolation should be checked with calibration interactions.

Identification of the charge of a track can be made on the basis of an established δ-ray calibration by counting over a fixed track-length provided that a number of δ-rays $N > Z^2$ is counted. However it is necessary that along-the-track parameters should be measured not over a fixed track-length independent of charge but over a track length sufficient in each case to give adequate charge resolution.

The most suitable along-the-track parameters for different regions of ionization are listed below. If the emulsion is calibrated in a manner based on the Herz-Davis model, the recommendations we make regarding choice of a track parameter should be valid irrespective of the type or sensitivity of the emulsion. However, since the choice of the growth factor is somewhat arbitrary it must be borne in mind that in calculating p we have taken the integral part Γ of the growth factor as 1.

For tracks with p less than 0.35, the blob density will be the most rapid and reliable measurement, since it is less subjective than grain counting for these tracks, and moderate variations in illumination will have negligible effect.

In the region $0.35 < p < 0.65$, blob density will be unreliable because it changes slowly with rate of energy loss. The density of isolated grains changes more rapidly, and measurement of isolated grains does not require use of a filar eyepiece or alignment of the microscope stage along the direction of each track.

The Fowler-Perkins coefficient and integral gap length are also sensitive to ionization changes over this region, and they are more sensitive than isolated grain density for $p \sim 0.35$. However they involve slightly greater experimental difficulties in measurement.

For very clogged tracks where $p > 0.65$, the integral gap length and the blob density give best charge resolution. The quality and constancy of the illumination are particularly important for these tracks.

To reduce subjective variations it is necessary to select certain « standard » tracks of different densities and count them at regular intervals throughout the course of the experiment.

Variations of the order of ten percent in minimum grain density of the emulsion will affect charge identification and charge resolution no matter which parameter is used, although in emulsions of minimum grain density greater than about 20 per 100 μm, δ-ray density is probably affected least. Charge assignments must be made only from measurements in regions of the emulsion which have been calibrated.

The presentation of results of limited statistical weight should be made using the triangle-plot method rather than the block-histogram method. This

is helpful for obtaining the values of peaks of distributions where these are required accurately to establish a charge calibration which can be extrapolated to higher charges, and also for estimating relative abundances of different heavy nuclei.

Our overall results for relative abundances of different charges are shown in Table I. The statistical accuracy is sufficient in the case of charges 5 and 6 to show that for all methods of identification the observed ratio of charges 5 and 6 is not 1.0 as originally reported, but certainly is not less than 0.75. Although our observed ratio of charges 6 : 7 : 8 is about 3 : 2 : 1, our resolution is poor in this region and the number of tracks is not large enough for a definite figure to be quoted.

TABLE I.

Method \ Charge	4	5	6	7	8	9
N_δ	9	25	31	12	4	5
L_g	6	26	28	11	9	6
G	7	22	29	16	10	2
N_s	8	29	29	12	7	1
Overall Ratio	26	83	100	44	26	12

Relative numbers of individual heavy nucleai based on different identification techniques applied to 86 tracks.

Comparison of our results with those of WADDINGTON ([8]) shows that the use of several identification techniques, and the longer track lengths available in stripped emulsion stacks, have resulted in better agreement than previously existed on the relative abundances of different heavy cosmic-ray nuclei. The value of the boron-carbon ratio however is still not clearly established. We cannot explain this continued disagreement.

* * *

The scanners who have taken part in this experiment are Mrs. M. CHARTRES, Mrs. M. DOCHERTY, Mrs. I. THOW, Mrs. M. WOODGER, and Miss M. WOODWARD. We have had many helpful discussions with Drs. A. J. HERZ and N. SOLNTSEFF. The balloon exposure was arranged through the U.S. Office of

Naval Research. One of us (B.J. O'B.) is indebted to the Australian Atomic Energy Commission for a research studentship. Professor H. MESSEL and the Nuclear Research Foundation of the University of Sydney have helped to make this work possible.

RIASSUNTO (*)

Vari autori sono in disaccordo per quanto riguarda le misure da loro eseguite sugl spettri della carica dei nuclei pesanti della radiazione cosmica primaria. Il disaccordo potrebbe essere causato da identificazioni inattendibili delle cariche. Poichè non si hanno dati adeguati sui confronti delle varie tecniche di misura, abbiamo eseguito le misure di 6 parametri di tracce di nuclei con $4 \leqslant Z \leqslant 9$ in un pacco di emulsioni G-5 strappate fatte ascendere a 41° di latitudine geomagnetica. Per ogni traccia sono state trovate le densità di raggi δ, di blob e di granuli isolati, il coefficiente di Fowler-Perkins, la lunghezza integrale delle lacune e la probabilità di sviluppo. Si sono valutati gli effetti su tali misure di varie cause di errore, incluso lo studio delle variazioni di ogni singolo parametro misurato, con una variazione del 20% sulla densità minima dei granuli dell'emulsione. Dal confronto e l'analisi di tali misure scaturiscono avvertenze sull'impiego delle tecniche suddette per l'identificazione dei nuclei pesanti veloci nelle emulsioni nucleari.

(*) *Traduzione a cura della Redazione.*

1753

IL NUOVO CIMENTO Vol. VIII, N. 6 16 Giugno 1958

On the Solutions of the Low Scattering Equation in a Simple Model.

F. Duimio

Istituto di Scienze Fisiche dell' Università - Milano
Istituto Nazionale di Fisica Nucleare - Sezione di Milano

(ricevuto il 12 Febbraio 1958)

Summary. — It is shown that for the Low scattering equation associated to a simple model proposed by Dyson, a unique solution can be found, when a complete set of physical parameters is known. These parameters consist of the energy levels and of the « renormalized coupling constants » of the true bound states which explicitly appear in the Low equation, supplemented by the analogous quantities for the possible unstable states (the Glaser-Källén states, in the framework of the Lee model).

1. – Introduction.

Castillejo, Dalitz and Dyson (1), showed, in an accurate mathematical analysis, that the Low scattering equation, for the case of the charged and neutral scalar meson theories with fixed sources, in the one-meson approximation, admits an infinity of solutions. The solution given by Chew and Low (2), for the p-wave scattering in the Chew static model, would also follow to be non-unique.

Some objections have been raised against this conclusion, and some arguments have also been put forward in order to substantiate the hypothesis that the redundant solutions have no physical meaning (3).

In a successive paper (4), Dyson discussed on the same lines a very simple

(1) L. Castillejo, R. H. Dalitz and F. J. Dyson: *Phys. Rev.*, **101**, 453 (1956).
(2) G. F. Chew and F. E. Low: *Phys. Rev.*, **101**, 1570 (1956).
(3) R. Haag: *Nuovo Cimento*, **5**, 203 (1957).
(4) F. J. Dyson: *Phys. Rev.*, **106**, 157 (1957).

and resoluble model. A comparison between the exact solution and the solution of the Low scattering equation derived from such a model showed clearly that, at least in this case, each of the infinite solutions of the Low equation corresponds to a different model (*i.e.* to a different choice of the parameters which characterize it): a great variety of models give the same Low equation.

In this paper we shall examine closely the solutions of the Low equations for the Dyson model and we shall find that it is possible to establish a one-to-one correspondence between a given specification of the model and a solution of the Low equation with peculiar analytical properties.

2. – The Dyson model. Exact solution.

Let's write the Hamiltonian of the Dyson model in the following simplified form:

$$(1)\qquad \left\{\begin{aligned} H\; &= H_0 + H_I\,, \\ H_0 &= \sum_1^N{}_n E_n|n\rangle\langle n| + \int (E_0+\omega)|\omega\rangle\langle\omega|\,\mathrm{d}\omega\,, \\ H_I &= -\int f(\omega)\sum{}_n g_n\big\{|n\rangle\langle\omega| + |\omega\rangle\langle n|\big\}\mathrm{d}\omega\,, \end{aligned}\right.$$

where $|\omega\rangle$ describe a state of a meson with energy $\omega=\sqrt{\mu^2+k^2}$, in presence of a scatterer in its ground state (with energy E_0). The states $|n\rangle$ ($n=1\,...,\,N$) are excited states of the scatterer, with energies $E_n>E_0$. The transitions between the two kinds of states take place through N coupling constants g_n. $f(\omega)$ is a cut-off function.

The solutions of the eigenvalue equation

$$(2)\qquad H|\alpha\rangle = \varepsilon_\alpha|\alpha\rangle$$

will be of the general form

$$(3)\qquad |\alpha\rangle = \sum_1^N{}_n c_n^{(\alpha)}|n\rangle + \int \psi^{(\alpha)}(\omega)\,|\omega\rangle\,\mathrm{d}\omega\,.$$

Substitution of (3) into (2), gives

$$(4)\qquad \left\{\begin{aligned} &(E_n-\varepsilon_\alpha)c_n^{(\alpha)} - g_n\int\psi^{(\alpha)}(\omega)f(\omega)\,\mathrm{d}\omega = 0\,. \\ &(E_0+\omega-\varepsilon_\alpha)\psi^{(\alpha)}(\omega) - \sum_1^N{}_n g_n c_n^{(\alpha)}\cdot f(\omega) = 0\,. \end{aligned}\right.$$

The solutions of the system (4) fall into two classes:

a) The bound state solutions, with $\varepsilon_\alpha < E_0+\mu$, which will be denoted by

$$|\boldsymbol{m}\rangle = \sum_1^N {}_n\, c_n^{(m)}|n\rangle + \int \psi^{(m)}(\omega)\,|\omega\rangle\,\mathrm{d}\omega\,, \qquad m = 1\,\ldots,\, N' \leqslant N. \tag{5}$$

b) The scattering solutions, with $\varepsilon_\alpha \geqslant E_0+\mu$, denoted by

$$|\boldsymbol{\omega}\rangle = \sum_1^N {}_n\, c_n(\omega)\,|n\rangle + \int \psi(\omega;\,\omega')\,|\omega'\rangle\,\mathrm{d}\omega'\,. \tag{6}$$

In the case *a*) we obtain (with $\varepsilon_m = E_0+\omega_m$ and $c^{(m)} = \sum_1^N {}_n\, g_n c_n^{(m)}$)

$$\left\{\begin{aligned} \psi^{(m)}(\omega) &= c^{(m)}\,\frac{f(\omega)}{\omega-\omega_m}\,,\\ c_n^{(m)} &= c^{(m)}\,\frac{g_n}{E_n-E_0-\omega_m}\int\frac{f^2(\omega)}{\omega-\omega_m}\,\mathrm{d}\omega\,. \end{aligned}\right. \tag{7}$$

The ω_m are given by the eigenvalue equation

$$R(\omega_m)J(\omega_m) = 1 \tag{8}$$

$$R(\omega_m) = \sum_1^N {}_n\,\frac{g_n^2}{E_n-E_0-\omega_m}\,, \tag{8a}$$

$$J(\omega_m) = \int\frac{f^2(\omega)}{\omega-\omega_m}\,\mathrm{d}\omega\,, \tag{8b}$$

and the normalization condition gives for $c^{(m)}$

$$c^{(m)} = \left\{\sum_1^N {}_n\,\frac{g_n^2}{(E_n-E_0-\omega_m)^2}\,J^2(\omega_m) + \int\frac{f^2(\omega)}{(\omega-\omega_m)^2}\,\mathrm{d}\omega\right\}^{-\frac{1}{2}} = \tag{9}$$

$$= \left\{R'(\omega_m)\,R^{-2}(\omega_m) + J'(\omega_m)\right\}^{-\frac{1}{2}}.$$

The case *b*) gives (for outgoing waves)

$$\left\{\begin{aligned} \psi(\overline{\omega};\,\omega) &= \delta(\omega-\overline{\omega}) + c(\overline{\omega})\,\frac{f(\omega)}{\omega-\overline{\omega}-i\varepsilon}\,,\\ c_n(\overline{\omega}) &= \frac{g_n}{E_n-E_0-\overline{\omega}}\left\{f(\overline{\omega}) + c(\overline{\omega})\int\frac{f^2(\omega)}{\omega-\overline{\omega}-i\varepsilon}\,\mathrm{d}\omega\right\}, \end{aligned}\right. \tag{10}$$

with

$$c(\overline{\omega}) = R(\overline{\omega})f(\overline{\omega})\{1-J(\overline{\omega}+i\varepsilon)R(\overline{\omega})\}^{-1}\,. \tag{11}$$

In such a way we obtain a *complete* system of eigenstates of H, given by the continuous set of the scattering states (6) (with (10), (11)), and N' bound states (5) (with (7), (8), (9)). The completeness of such a system can be

established extending to our case arguments used by GLASER and KÄLLÉN [5].

If $\bar{N}$ is the number of states $|n\rangle$, with $E_n < E_0 + \mu$, N' can be equal either to $\bar{N}$ or to $\bar{N}+1$ [6], *i.e.* the system admits $\bar{N}$ or $\bar{N}+1$ true bound states whose energies are determined by the solutions of the eq. (8), obviously with $\omega_m < \mu$ the integral (8*b*) having a meaning only in that case.

If, however, we assume that $J(\omega_m)$, in the case $\omega_m > \mu$ is defined by its principal value, other solutions of (8) may appear. Evidently they are in number $N - N'$, that is $N - \bar{N}$ or $N - \bar{N} - 1$. For the Lee model, which is closely connected with the present model, when $N = 1$, this type of solution has been discussed in the mentioned paper of GLASER and KÄLLÉN [5]. Their physical meaning is clear: they describe unstable states, which decay into the ground state plus a meson.

From the mathematical point of view we are faced with a problem of the spectral theory of hermitian operators, in the case when the discrete spectrum may partially overlap the continuous spectrum.

It is easy to see that one can introduce in a formal way renormalized coupling constants by the definition:

$$g^r_m = c^{(m)} \tag{12}$$

between the ground state and both the true bound states and the unstable states. (For the latter case, $J'(\omega_m)$ in (9) will have the meaning of derivative of the principal part of $J(\omega_m)$).

In such a way the model is completely defined either by the g_n and the E_n ($n = 1, ..., N$), or by the g^r_m and the $\varepsilon_m = E_0 + \omega_m$ ($m = 1, ..., N$) with ω_m solutions of (8), with the convention of taking the principal value for $J(\omega_m)$, when $\omega_m > \mu$.

Scattering amplitudes, phase shifts etc., can be computed in the usual way.

Furthermore we assume that the cut-off function is such that no ghost complications appear.

3. – The Low equation.

The Low scattering equation for the model we are treating, with the standard procedure [2,6,7] turns out to be

$$r(\omega) = \sum_1^{N'}{}_m \frac{(g^r_m)^2}{\omega_m - \omega} + \int_\mu^\infty \frac{f^2(\omega')\,|r(\omega')|^2}{\omega' - \omega - i\varepsilon}\,\mathrm{d}\omega' \,, \tag{13}$$

([5]) V. GLASER and G. KÄLLÉN: *Nucl. Phys.*, **2**, 706 (1957); see also H. ARAKI, Y. MUNEKATA, M. KAWAGUCHI and T. GOTÖ: *Progr. Theor. Phys.*, **17**, 419 (1957); T. OKABAYASHI and S. SATO: *Progr. Theor. Phys.*, **17**, 30 (1957); K. NAITO: *Progr. Theor. Phys.*, **18**, 200 (1957).

([6]) G. C. WICK: *Rev. Mod. Phys.*, **27**. 339 (1955).

([7]) K. W. FORD: *Phys. Rev.*, **105**, 320 (1957).

where

$$-f(\omega)f(\omega')r(\omega') = \langle \boldsymbol{\omega}' | V_\omega | 0 \rangle ,$$

i.e., since $V_\omega = -f(\omega) \sum_{1}^{N}{}_n g_n |n\rangle\langle 0|$,

$$f(\omega')r(\omega') = \sum_{1}^{N}{}_n g_n \langle \boldsymbol{\omega}' | n \rangle . \tag{14}$$

$|0\rangle$ is the state consisting of the scatterer alone in its ground state.

The function of the complex variable z, $H(z)$, defined as

$$H(z) = \sum_{1}^{N'}{}_m \frac{(g_m^r)^2}{\omega_m - z} + \int_{\mu}^{\infty} \frac{f^2(\omega')|r(\omega')|^2}{\omega' - z} \, \mathrm{d}\omega' , \tag{15}$$

obviously satisfies

$$\lim_{z \to \omega + i\varepsilon} H(z) = r(\omega) \qquad \omega \text{ real}$$

and is a generalized R-function [1], in the complex plane, cut on the real axis for $\omega \geqslant \mu$, *i.e.* it has the property

$$\operatorname{Im} H(z) \geqslant 0 \qquad \text{for } \operatorname{Im} z > 0$$

in the cut plane.

The function $h(z) = -1/H(z)$ is a generalized R-function too, with the properties:

$$h(z^*) = h^*(z) , \tag{16}$$

$$h(\omega) = 0 \qquad \text{for real } \omega < \mu \text{ in the } N' \text{ points } \omega_m, \tag{17}$$

$$\left[\frac{\mathrm{d}h(\omega)}{\mathrm{d}\omega}\right]_{\omega=\omega_m} = (g_m^r)^{-2} , \tag{18}$$

$$\lim_{z \to \omega + i\varepsilon} \operatorname{Im} h(z) = \pi f^2(\omega) \qquad \text{for real } \omega > \mu \text{ except at points at which } H(\omega) = 0. \tag{19}$$

$$\operatorname{Im} h(z) \geqslant 0 \qquad \text{for } \operatorname{Im} z > 0. \tag{20}$$

An application of the Herglotz theorem [1,8,9] (taking into account the properties (16), (19), (20)) states that the function $h(z)$ must have the follow-

(8) J. A. SHOHAT, J. D. TAMARKIN: *The problem of Moments* (New York, 1943). Chap. 2.

(9) M. H. STONE: *Linear Transformations in Hilbert Space* (New York, 1932), p. 593.

ing form:

$$h(z) = Az + B + \int_{\mu}^{\infty} \frac{f^2(\omega)}{\omega - z}\, \mathrm{d}\omega + \sum_{1}^{M}{}_i \frac{R_i}{\omega_i - z}\,, \tag{21}$$

with A, B, R_i and ω_i $(i = 1, \ldots, M)$, undetermined constants.

The conditions (17), (18), as stressed by DYSON, are not sufficient to determine these constants, because the number M is *a priori* arbitrary.

4. – Comparison of the solutions.

In order to establish a correspondence between the solutions of the Low equation

$$r(\omega) = \lim_{z \to \omega + i\varepsilon} \left(- \frac{1}{h(z)} \right)$$

and the exact solutions, from (14) and (6), (11) we derive

$$\lim_{z \to \omega + i\varepsilon} h(z) = - R^{-1}(\omega) + J(\omega + i\varepsilon)\,. \tag{22}$$

The vanishing of the real part of the r.h.s. of (22) reproduces eq. (8), also in the extension we had assumed for it, in the case $\omega_m > \mu$, as the real part of $J(\omega + i\varepsilon)$ is equal to the principal value of $J(\omega)$.

This means that, if we want the solution of the Low equation to coincide with the exact solution of the given model, the real part of the function $h(z)$ must have zeros at the points ω_m which are the solutions of eq. (8), both for $\omega_m < \mu$ and $\omega_m > \mu$:

$$\lim_{z \to \omega + i\varepsilon} \operatorname{Re} h(z) = 0 \qquad \text{at the points } \omega_m \ (m = 1, \ldots, N). \tag{23}$$

Furthermore, with $\tilde{J}(\omega) = J(\omega)$ for $\omega < \mu$, and equal to the principal part of it for $\omega > \mu$:

$$\left[\frac{\mathrm{d}}{\mathrm{d}\omega} \left(\lim_{z \to \omega + i\varepsilon} \operatorname{Re} h(z) \right) \right]_{\omega = \omega_m} = \left[\frac{\mathrm{d}}{\mathrm{d}\omega} \left[- R^{-1}(\omega) + \tilde{J}(\omega) \right] \right]_{\omega = \omega_m} = (c^{(m)})^{-2} - (g^r_m)^{-2}\,. \tag{24}$$

for all $m = 1, \ldots, N$.

It is clear that the conditions (23), (24) coincide with conditions (17), (18) for $\omega_m < \mu$. For $\omega_m > \mu$ they impose supplementary conditions to $h(z)$, expressing that the unstable states must have given energies, and given renormalized coupling constants. (23) and (24) are sufficient to determine comple-

tely the constants A, B, R_i, ω_i in (21) and so to give a unique solution to the Low equation (13). The number M appearing in (21) will be $N-1$.

We want to stress that this is a consequence of the fact that the true bound states and the scattering states form a complete set of eigenstates of H. In deriving the Low equation essential use is made of completeness. It follows that the characteristic quantities (ω_m and g^r_m) of the unstable states do not appear explicitly in it. They must be used, *a posteriori*, to choose among the solutions the one which correctly expresses the number and the properties of those unstable states, *i.e.* which fixes their energies (which obviously will be resonance energies for the scattering) and their coupling strengths (connected with their mean life).

5. – The Lee-Glaser-Källén case.

As an example let us consider the case with $N=1$ ($M=0$). Eq. (23) and (24) assume the form

$$\left\{\begin{aligned} & A\omega + B + \tilde{J}(\omega) = 0\,, \\ & A + \tilde{J}'(\omega_1) = (g_1^r)^{-2}\,, \end{aligned}\right. \tag{25}$$

ω_1 and g_1^r are supposed to be known.

One obtains:

$$\lim_{z\to\omega+i\varepsilon} h(z) = (\omega-\omega_1)[(g_1^r)^{-2} + \tilde{J}'(\omega_1)] + J(\omega+i\varepsilon) - \tilde{J}(\omega_1)\,. \tag{26}$$

From the exact solution we have

$$\lim_{z\to\omega+i\varepsilon} h(z) = -R^{-1}(\omega) + J(\omega+i\varepsilon) = -\frac{E_1-E_0-\omega}{g_1^2} + J(\omega+i\varepsilon)\,. \tag{27}$$

From (26), (27) it follows:

$$g_1^2/(g_1^r)^2 = 1 + g_1^2\tilde{J}'(\omega_1)\,,$$

which coincides for $\omega_1<\mu$ and $\omega_1>\mu$ respectively with the relations between the unrenormalized and the renormalized coupling constants for the case of the stable particle [10] and of the instable one [5] of the Lee model.

---

[10] G. Källén and W. Pauli: *Dan. Mat. Fys. Medd.*, **30**, No. 7 (1955).

Concluding we observe that the conventional static meson theories, treated by the Low equation method, in the one meson approximation, present some analogies with the Dyson model. So it seems likely that arguments similar to the ones used in this note could apply also to them.

* * *

Thanks are due to Prof. P. CALDIROLA for his interest and to Dr. S. ALBERTONI whose advices and suggestions on the mathematical aspects of the present work have been precious.

RIASSUNTO

Si mostra come sia possibile determinare un'unica soluzione per l'equazione di Low associata a un semplice modello proposto da DYSON, quando siano noti tutti i parametri fisici del sistema. Questi ultimi consistono dei livelli energetici e delle costanti d'accoppiamento rinormalizzate per gli stati legati veri che appaiono esplicitamente nell'equazione di Low insieme alle analoghe quantità per gli eventuali stati instabili (i cosiddetti stati di Glaser-Källén, nell'ambito del modello di Lee).

IL NUOVO CIMENTO VOL. VIII, N. 6 16 Giugno 1958

A Note on an Acausality Test - (I).

D. ITO, S. MINAMI (*) and H. TANAKA (+)

Institute of Physics, Tokyo University of Education - Tokyo, Japan
(*) *Department of Physics, Osaka City University - Osaka, Japan*
(+) *Istituto di Fisica dell'Università - Bologna, Italy*
Istituto Nazionale di Fisica Nucleare - Sezione di Bologna

(ricevuto il 24 Febbraio 1958)

Summary. — When the microcausality does not hold the error of the dispersion relations is shown to be two times the forward scattering amplitude in the acausal region. Then, the order of magnitude of this acausal region is discussed concerning the discrepancy in π^--p scattering found by PUPPI and STANGHELLINI.

1. – Introduction.

Since the experimental discovery of the nucleon core in the electron-proton scattering there have been often discussed the effects of the core on the phenomena involving mesons, nucleons and antinucleons. However, from the field theoretical point of view, one may be interested mostly in the question if the nucleon core be of causal character or not. That is, in the core of the nucleon the signal velocity might be faster than the light velocity. As an example of the extreme case, one may imagine the nucleon core as a classical rigid body.

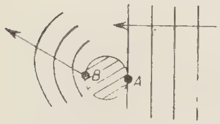

Fig. 1. – In the case of the rigid body the signal velocity is greater than the light velocity.

Then, the moment it receives the incident pulse at an end point A, it emits, from another end point B, the scattered wave with energy. This means that, the signal is transmitted with a velocity greater than that of light (Fig. 1). In terms of the field theory, the propagator $[J_\mu(A), J_\nu(B)]$ which connects the incident wave's sink $J_\mu(A)$ and the scattered wave's source $J_\nu(B)$ should be spread evenly over the space-like inter-

vals $(A-B)^2>0$, violating the so-called microcausality. Now that some kind of finite extension of the charge-current density $J_\mu(x)$ is recognized experimentally, the relations $[J_\mu(A), J_\nu(B)]=0$ $((A-B)^2>0)$ are no more self-evident as hitherto has been supposed generally, but should be worth a reconsideration in a phenomenological way.

What was found in the electron-proton scattering is a non-local distribution of the charge-current, $J_\mu = i\bar{\psi}\gamma_\mu\psi$, and not the core of the proton itself. But if one could interpret it most naively as an evidence of the same distribution of the « nucleon matter », it might have a core of the same order also as the meson source function $i\bar{\psi}\gamma_5\psi$. If so, concerning γ-π production and π-nucleon scattering the propagators $[J_\mu(A), J_5(B)]$, $[J_5(A), J_5(B)]$ should be an interesting subject in the consideration of the microcausality.

According to PUPPI-STANGHELLINI (1), in the low energy region the dispersion relations do not agree with the π^--p scattering data if the coupling constant $f^2=0.08$ of the π^+-p scattering is used. And even the corrections (2) by the electromagnetic field or K-particle field seem to be far from a successful result. In fact, as they concluded, in the frame of the standard meson theory it would be difficult to find out an explanation of the observed effects.

Recently it was shown (3) that the S waves in the π-nucleon scattering should be appreciably influenced by the nucleon's internal structure. It is why the ordinary cut-off meson theory ignoring the internal structure of the nucleon has failed at all to explain the S wave behaviour in spite of its large success in interpreting the P wave phenomena. In view of this, the large discrepancy of the dispersion relations for the π^--p scattering contributed largely from the S wave would shed a doubt about the validity of the microcausality supposed in the formula.

However, in the sense of the special relativity, the existence of the rigid body propagator must be denied evidently. But one has no sufficient reason to believe that even in the nucleon core relativity should hold without any doubt. In reality, the relativity theory of macroscopic origin has survived even in the subatomic system, probably by the reason that the point particle system interacting through the d'Alembert waves was a good model for the structure of matter. But in the space of the elementary particles one might have encountered, the first time, the real rigid substance which is essentially of acausal character. If so, the phenomenological analysis of the nucleon core would be really of physical importance.

---

(1) G. PUPPI and A. STANGHELLINI: *Nuovo Cimento*, **5**, 1307 (1957).
(2) A. AGODI, M. CINI and S. VITALE: *Phys. Rev.*, **107**, 630 (1957).
(3) D. ITO, S. MINAMI and H. TANAKA: *Nuovo Cimento* in the press.

2. – Errors of dispersion relations.

The dispersion relations being an important clue for the acausality test, we shall begin to rearrange the formula in a convenient form for our analysis of the problem.

The causal amplitude in π-nucleon scattering is given in general by [4]

$$M(\omega) = \int \mathrm{d}^4 x \eta(x_0) \exp[-ikx] \langle p\lambda | [J(x), J(0)] | p\lambda' \rangle . \tag{2.1}$$

Its Fourier transform is easily integrated, if one observes the independence of the propagator matrix $\langle p\lambda | [J(x), J(0) | p\lambda' \rangle$ on the $\boldsymbol{x}$ direction, resulting

$$M(z) = \int_{-\infty}^{\infty} \mathrm{d}\omega M(\omega) \exp[-i\omega z] = \tag{2.2}$$

$$= (2\pi)^2 \int_0^\infty r\,\mathrm{d}r \int_0^\infty \mathrm{d}t R(r, t-z) \langle p\lambda | [J(\boldsymbol{r}, t), J(0, 0)] | p\lambda' \rangle ,$$

where

$$\left\{\begin{aligned} R(r, t-z) &\equiv \frac{1}{\pi} \int_{-\infty}^{\infty} \frac{\sin(\sqrt{\omega^2 - \mu^2 r})}{\sqrt{\omega^2 - \mu^2}} \exp[i\omega(t-z)]\,\mathrm{d}\omega , \\ &= \begin{cases} 0 & |t-z| > r , \\ J_0(\mu\sqrt{r^2 - (t-z)^2}) & |t-z| < r . \end{cases} \end{aligned}\right. \tag{2.3}$$

In the above expression (2.3), the integral region where $R(r, t-z$ has non vanishing contributions is illustrated in the Fig. 2 by the vertical hatching, for the case $z > 0$ in (a), for the case $z < 0$ in (b). If the causality really holds, the commutator $[J(\boldsymbol{r}, t), J(0, 0)|$ is always zero in the space-like interval of (r, t), and not zero only inside the light cone as shown by the

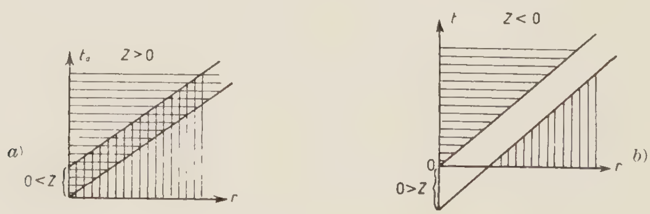

Fig. 2. – $R(r, t-z)$ does not vanish in the vertically hatched region, while non-zero contribution of $[J(x), J(0)]$ comes only from the inside of the light cone hatched horizontally.

---

[4] M. GOLDBERGER: *Phys. Rev.*, **99**, 979 (1955).

1764

horizontal hatching in the Fig. 2. Then, in the case $z \leqslant 0$ (Fig. 2 (*b*)), where $R(r, t-z)$ and $[J(\boldsymbol{r}, t), J(0, 0)]$ have no common region for their non-vanishing contributions, the integral (2.2) over these two functions becomes identically zero. Accordingly, the causal condition should be expressed by

$$M(z) = 0 \qquad \text{for } z \leqslant 0 . \tag{2.4}$$

From this condition, the relation

$$\lim_{z \to 0^-} M(z) = \lim_{z \to 0^-} \int_{-\infty}^{\infty} M(\omega) \exp\left[-i\omega z\right] d\omega = 0 ,$$

is derived, that is, the regularity of $M(\omega)$ on the upper surface of the ω-space. Thus, the eq. (2.4) is the fundamental base of the dispersion relations.

However, in the acausal case where the commutator $[J(\boldsymbol{r}, t), J(0, 0)]$ is spread over the space-like region (see the Fig. 3), $M(z)$ is no more zero if z approaches to zero crossing the critical value $-l_0$. At that time, all one can say is only

$$M(-l_0) = \int_{-\infty}^{\infty} M(\omega) \exp\left[i\omega l_0\right] d\omega = 0 ,$$

and in place of $M(\omega)$ the quantity $M(\omega)\exp\left[i\omega l_0\right]$ is now regular on the upper surface of ω. The non-vanishing value of $M(z)$ is determined, as is seen in the Fig. 3, by the overlapping of $R(r, t-z)$ with the spread of the commutator over the acausal region. Therefore, the values of $M(z)$ in the region $z \leqslant 0$ would supply the important information on the acausal smearing of the commutation relations. From the error of the dispersion relations we shall estimate the amplitude $M(z)$ in the acausal region.

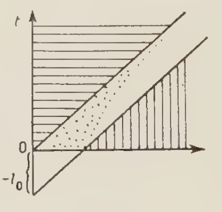

Fig. 3. – If there is an acausal smearing (dotted curve) of the commutator, it gives a non-zero contribution to the forward amplitude $M(z)$ when z becomes $z > -l_0$.

The dispersion relations are obtained from the Cauchy relation on the regularity of $M(\omega)$,

$$M(\omega) + \frac{i}{\pi} P \int_{-\infty}^{\infty} \frac{M(\omega')}{\omega' - \omega} d\omega' = 0 , \tag{2.5}$$

with the well known crossing symmetry

$$M(-\omega) = M^*(\omega) . \tag{2.6}$$

The meaning of the dispersion relations is easily seen in the z-space, where

the Cauchy relation takes the following form

$$(2.7)\qquad M(z) + \frac{i}{\pi} P\int_{-\infty}^{\infty} \mathrm{d}\omega\,\mathrm{d}\omega' \,\frac{\exp\,[i(\omega'-\omega)z]}{\omega'-\omega}\, M(\omega')\exp\,[-i\omega' z] = 0\,.$$

There, remarking that

$$(2.8)\qquad \frac{i}{\pi} P\int_{-\infty}^{\infty} \frac{\exp\,[i(\omega'-\omega)z]}{\omega'-\omega}\,\mathrm{d}\omega = -\frac{z}{|z|}\,,$$

one obtains the final expression

$$(2.9)\qquad \left(1-\frac{z}{|z|}\right) M(z) = 0\,.$$

This relation (2.9) really indicates that $M(z)$ must be zero for all $z<0$. In such way, the dispersion formula is proved to be the guaranty of the non-existence of the acausal smearing in the commutation relations.

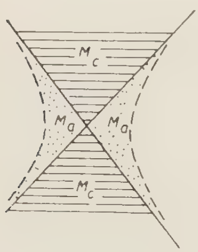

Fig. 4. – M_c: Causal amplitude coming from the inside of the light cone. M_a: Acausal amplitude coming from the outside of the light cone.

After the above preparation, we shall enter into the main problem. If in the eq. (2.1) the commutator $[J(x), J(0)]$ is spread over the outside of the light cone, as in the Fig. 4, the contributions to $M(\omega)$ from the outside and inside of the cone are written $M_a(\omega)$ and $M_c(\omega)$ respectively,

$$(2.10)\qquad M(\omega) = M_c(\omega) + M_a(\omega)\,.$$

Then, $M(\omega)$ is no more regular on the upper ω surface, but $M_c(\omega) = M(\omega) - M_a(\omega)$, free from the acausal smearing by definition, is still regular on the upper surface. Accordingly, for this $M_c(\omega)$ the Cauchy relation holds,

$$(2.11)\qquad M(\omega) - M_a(\omega) = \frac{1}{\pi i} P\int_{-\infty}^{\infty} \mathrm{d}\omega'\,\frac{M(\omega') - M_a(\omega')}{\omega'-\omega}\,.$$

Writing explicitly the real and the imaginary parts of $M(\omega)$ and $M_a(\omega)$,

$$(2.12)\qquad M\ (\omega) = D\ (\omega) + iA(\omega)$$

$$(2.13)\qquad M_a(\omega) = D_a(\omega) + iA(\omega)$$

one gets finally the relations

$$(2.14)\qquad D(\omega)-\frac{1}{\pi}P\int\limits_0^\infty d\omega'\left(\frac{1}{\omega'-\omega}+\frac{1}{\omega'+\omega}\right)A(\omega') = \\ = D_a(\omega)-\frac{1}{\pi}P\int\limits_0^\infty d\omega'\left(\frac{A_a(\omega')}{\omega'-\omega}-\frac{A_a(-\omega')}{\omega'+\omega}\right),$$

$$(2.15)\qquad A(\omega)+\frac{1}{\pi}P\int\limits_0^\infty d\omega'\left(\frac{1}{\omega'-\omega}-\frac{1}{\omega'+\omega}\right)D(\omega') = \\ = A_a(\omega)+\frac{1}{\pi}P\int\limits_0^\infty d\omega'\left(\frac{D_a(\omega')}{\omega'-\omega}-\frac{D_a(-\omega')}{\omega'+\omega}\right),$$

where the crossing symmetry was used only for $M(\omega)$. If one sets the right sides of the eqs. (2.14) and (2.15) equal to zero, just the ordinary dispersion relations are obtained. Therefore, the right sides of the above equations represent the contributions from the acausal scattering.

In such acausal case, the use of the optical theorem for the cross-section

$$(2.16)\qquad A(\omega)=\frac{k}{4\pi}\,\sigma(\omega)\,,$$

may be rather doubtful because of its derivation from the conservation of the probability. Anyway however, the non-vanishing values of the eqs. (2.14) and (2.15) with $A(\omega)$ replaced by $(k/4\pi)\sigma(\omega)$ and $D(\omega)$ by the experimental values are just the error calculated by PUPPI-STANGHELLINI. Therefore, for the moment, one may consider such errors $\varrho(\omega)$ and $\lambda(\omega)$ in the eqs. (2.14) and (2.15) respectively as the known quantities found by them. Then, if the errors came only from the acausal reason, the acausal amplitudes are obtained by the following inhomogeneous equations

$$(2.17)\,(^*)\qquad \left|\begin{aligned} & D_a(\omega)-\frac{1}{\pi}P\int\limits_0^\infty d\omega'\left(\frac{A_a(\omega')}{\omega'-\omega}-\frac{A_a(-\omega')}{\omega'+\omega}\right)=\varrho(\omega)\,,\\ & A_a(\omega)+\frac{1}{\pi}P\int\limits_0^\infty d\omega'\left(\frac{D_a(\omega')}{\omega'-\omega}-\frac{D_a(-\omega')}{\omega'+\omega}\right)=\lambda(\omega)\,. \end{aligned}\right.$$

(*) $\varrho(\omega)$, $\lambda(\omega)$ are estimated only in the region $\omega\geqslant\mu$, but for the region $\omega<\mu$ putting

$$S(\omega)=M(\omega)+\frac{i}{\pi}\int\frac{M(\omega')}{\omega'-\omega}\,d\omega'\,,$$

one may take the analytical continuation for this region. Then, for $\omega\leqslant 0$, $S(\omega)$ must

1767

The equations are easily solved. Multiplying the second equation by i and summing each side of the two equations, one gets (*)

$$M_a(\omega) + \frac{i}{\pi}\int_{-\infty}^{\infty} d\omega' \frac{M_a(\omega')}{\omega' - \omega} = \varrho(\omega) + i\lambda(\omega) = S(\omega) \,. \tag{2.18}$$

The transformation to the z-space is done by multiplying $\exp[-i\omega z]$ on each side and integrating over ω. There, following the same procedure as for the previous deduction of the eqs. (2.5)–(2.9), one obtains the final result

$$\left(1 - \frac{z}{|z|}\right) M_a(z) = S(z) \,, \tag{2.19}$$

where the error $S(z)$ in z space is defined by

$$S(z) = \int_{-\infty}^{\infty} d\omega \exp[-i\omega z](\varrho(\omega) + i\lambda(\omega)) \,. \tag{2.20 (*)}$$

Consequently one has the relation for $z < 0$

$$2M_a(z) = S(z) \qquad (z < 0). \tag{2.21}$$

As the causal part $M_c(z)$ is always zero in the region $z < 0$, $M_a(z)$ is equal to $M(z)$. Thus, one arrives at the following important conclusion.

The error of the dispersion relations $S(z)$ is twice the forward scattering amplitude $M(z)$ spread over the acausal region $z < 0$. Therefore, from the discrepancy of the dispersion relations one could get the information about the spread of the commutator $[J(x), J(0)]$ over the space-like intervals.

3. – Discussion.

The practical application of this method to the analysis of the π^--p scattering will be given in another occasion, but even without entering into details one can estimate, from the above conclusion, the order of the acausal region inside the nucleon.

---

be defined in a manner that $S(\omega)$ satisfies the same crossing symmetry as $M(\omega)$ does. Strictly speaking however, $M(z)$ is not determined uniquely from the errors $\varrho(\omega)$ and $\lambda(\omega)$ of the $\omega \geqslant \mu$ region only. But if $M(z)$ is given, $\varrho(\omega)$ and $\lambda(\omega)$ are determined completely.

(*) What one knows from the work of PUPPI-STANGHELLINI are the values of $\varrho(\omega)$ and $\lambda(\omega)$ for $\omega \geqslant \mu$ region. Then, in the integral of the eq. (2.20), lacking the knowledge on the region $\mu > \omega \geqslant 0$ (therefore also for $0 \geqslant \omega > -\mu$), one cannot determine the exact value of $S(z)$ only from the estimated errors of Puppi-Stanghellini.

In the Fig. 5. the results of Puppi-Stanghellini are given schematically, where the dotted line may be said to be the experimental value of $D(\omega)$. On the other hand, the real line was calculated by the dispersion relations in which the amplitude $A(\omega)$ was estimated from the cross-section by the optical theorem. (See the eq. (2.17)). Therefore, the difference of the real and dotted lines is what we call the error of the dispersion relations.

In the present experimental precision the behaviour of $\varrho(\omega)$ as a function of ω is rather ambiguous. But $|D(\omega)|$ is known to be small in the high energy region, and $\int \sigma(\omega')/(\omega'^2 - \omega^2)$ also will be small owing to the tendency $\sigma(\omega) \to \text{const}$. Then, $\varrho(\omega)$ must not be so relevant in the high energy region. Although one cannot know, from the result of Puppi-Stanghellini, the important features of $\varrho(\omega)$ in the high energy region and for our purpose we need to know $\varrho(\omega)$ in a higher energy region than taken by them, one might guess somehow the tendency of the error as in the Fig. 5. In such very rough estimate the spread of $\varrho(\omega)$ in the ω scale will be $\langle\omega\rangle \gtrsim 2\mu$.

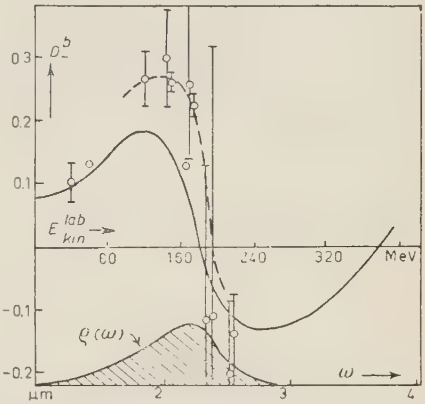

Fig. 5. – The dotted line represents the experimental data, while the continuous curve is calculated by Puppi-Stanghellini for the coupling constant $f^2 = 0.08$. The difference of these two curves is what we call the error $\varrho(\omega)$ of the dispersion relations and given tentatively, as an example, by the hatched zone.

According to our above conclusion, $M(z)$ which gives the spread of the commutator in the acausal region is

$$\mathrm{Re}\, M(z) = \frac{1}{2}\int \varrho(\omega) \exp\left[-i\omega z\right] \mathrm{d}\omega\,.$$

Then, the spread of $\varrho(z)$ in the z-scale would be, (not exactly because of the ignorance of $\varrho(\omega)$ in the $\mu > \omega \geqslant 0$ region),

$$\langle -z\rangle \sim \frac{1}{\langle\omega\rangle} \lesssim \frac{1}{2\mu}\,. \tag{3.1}$$

Therefore, if one supposes that the discrepancy of the dispersion relations for π^--p scattering arises only from the acausal spread of the nucleon, such acausal extension would be of the order of

$$\sim \frac{1}{2}\langle -z\rangle \lesssim \frac{1}{4\mu}\,. \tag{3.2}$$

The conjectured value is smaller than the ascribed proton core radius $a \sim 1/2\mu$, and our presumption would be not unreasonable. (If the error of the dispersion relations is spread to a higher energy than considered above, the acausal region becomes smaller) (*).

Another test of the acausality is to use the regularity of $M(\omega)\exp[i\omega l_0]$ in place of $M(\omega)$, if $M(z)$ is spread out in the region $0 \geqslant z > -l_0$. In this case, the real and imaginary parts of $M(\omega)\exp[i\omega l_0]$, are connected by the dispersion relations in the following way (5),

$$\begin{aligned}(3.3)\quad D(\omega)\cos\omega l_0 - \frac{2}{\pi}\int_0^\infty \frac{\omega' \mathrm{d}\omega'}{\omega'^2-\omega^2}\, D(\omega')\sin\omega' l_0 = \\ = A(\omega)\sin\omega l_0 + \frac{2}{\pi}\int_0^\infty \frac{\omega' \mathrm{d}\omega'}{\omega'^2-\omega^2}\, A(\omega')\cos\omega' l_0 \,.\end{aligned}$$

For the given value of l_0 the right hand side of the equation is a known function of ω calculated from the experimental cross-section. This integral equation for $D(\omega)$ is solved in the approximation that $D(\omega)$ in the integral is replaced by the value of $D(\omega)$ at $l_0 = 0$ (causal case). According to the preliminary calculation of HOSHIZAKI (6), $l_0 = 1/4\mu$ gives an agreement with the data of PUPPI-STANGHELLINI. This value is consistent with our estimation.

(*) Puppi-Stanghellini curves are based on rather earlier data and have been recently recalculated by SALZMAN with the data of Anderson-Piccioni, yielding, however, a discrepancy essentially like the previous one but more remarkable in the high energy region. That is, the spread of the error $\langle\omega\rangle$ in the ω scale will be larger than 2μ as supposed above. On the other hand, according to the latest data at 41.5 MeV (California) and 98 MeV (Liverpool) the discrepancy in the low energy may be remarkably reduced.

(5) R. OEHME: *Phys. Rev.*, **100**, 1503 (1955).

(6) Private communication. We thank Mr. HOSHIZAKI for his kind discussion on this subject.

RIASSUNTO (*)

Si dimostra che quando cessa la validità della microcasualità le relazioni di dispersione sono il doppio dell'ampiezza di scattering in avanti nella regione acasuale. Si discute poi l'ordine di grandezza di tale regione acasuale con riferimento alla discrepanza nello scattering π^+-p trovata da PUPPI e STANGHELLINI.

(*) *Traduzione a cura della Redazione.*

Grundgleichungen der relativistischen Mechanik eines materiellen Punktes mit veränderlicher Masse.

N. S. Kalitzin

Physikalisches Institut der Bulgarischen Akademie der Wissenschaften - Sofia (Bulgarien)

(ricevuto l'11 Marzo 1958)

Zusammenfassung. — Es werden die Gleichungen der Mechanik eines materiellen Punktes mit veränderlicher Masse für relativistische Geschwindigkeiten verallgemeinert, wobei man den allgemeinsten Fall betrachtet, nämlich wenn der Massendefekt des Punktes von Null verschieden ist. Es werden einige Anwendungen der Grundgleichungen gegeben, insbesondere wird für den Fall der «reinen» Rakete eine allgemeine Formel gegeben.

Die Grundgleichung der nichtrelativistischen Mechanik eines materiellen Punktes mit veränderlicher Masse wurde zum ersten Mal im Jahre 1897 von I. W. Meschtcherski angegeben. Die Gleichung von Meschtcherski führt zu der Formel von Tziolkovski, auf Grund von welcher die Bewegung der einstufigen und der mehrstufigen Raketen berechnet wird.

In unserer Arbeit (1) haben wir eine Verallgemeinerung der Formel von Meschterski für relativistische Geschwindigkeiten des Massenpunktes und seines Massenzuwachses gegeben. Diese Verallgemeinerung aber, wie wir es hier auch zeigen werden, hat sich mit der Einschränkung verbunden erwiesen, daß der Massendefekt des Punktes mit veränderlicher Masse gleich Null sein soll, d.h. die Energie im Koordinatensystem des Massenpunktes, die dem Massenzuwachs übertragen wird, soll aus dem Außenraum genommen werden.

Im vorliegenden Artikel betrachten wir den allgemeineren Fall einer relativistischen Verallgemeinerung der Formel von Meschtcherski, nämlich den Fall, wenn der Massendefekt des Punktes mit veränderlicher Masse von Null

(1) N. S. Kalitzin: *Žurn. Èkxper. Theor. Fiz.*, **28**, 631 (1955), ins Englische übersetzt in *JETP* (New-York).

verschieden ist, d.h. wenn ein Teil der Energie des Massenzuwachses vom Punkte mit veränderlicher Masse geschöpft wird.

Wir benutzen den vierdimensionalen Raum von Minkowski. Es seien x_1, x_2, x_3 die Koordinaten unserer physikalischen Welt. Die vierte Koordinate ist $x_4 = ict$, wobei c die Lichtgeschwindigkeit in Vakuum bedeutet, t ist die relative Zeit von Einstein. Den Raum x_i von Minkowski bezeichnen wir mit R_4, den Raum (x_1, x_2, x_3) mit R_3.

Jeder materielle Punkt beschreibt eine Weltlinie in R_4. Das unendlich kleine Intervall auf einer Weltlinie wird uns durch den Ausdruck

$$\mathrm{d}s^2 = - \mathrm{d}x_i \mathrm{d}x_i \tag{1}$$

gegeben. Der Vektor der Vierergeschwindigkeit lautet

$$u_i = dx_i/\mathrm{d}s \,. \tag{2}$$

Wir wollen seine Komponenten in R_3 ausdrücken. Zu diesem Zweck bemerken wir, daß nach (1)

$$\mathrm{d}s = c\,\mathrm{d}t\sqrt{1 - (v^2/c^2)}\,, \tag{3}$$

wobei v die gewöhnliche dreidimensionale Geschwindigkeit in R_3 bedeutet. Auf diese Weise

$$\left\{\begin{aligned} u_\alpha &= v_\alpha/c\sqrt{1 - (v^2/c^2)}\,, \qquad \alpha = 1, 2, 3, \\ u_4 &= i/\sqrt{1 - (v^2/c^2)}\,. \end{aligned}\right. \tag{4}$$

Die Komponenten der 4-Geschwindigkeit sind voneinander nicht unabhängig. Indem wir merken, daß $dx_i^2 = - \mathrm{d}s^2$ ist, haben wir

$$u_i^2 = -1\,. \tag{5}$$

In einem Koordinatensystem, welches wir als ruhend denken, betrachten wir, in einem gegebenen Zeitpunkt (die Zeit wird in demselben System gemessen), zwei Punkte: einen mit der Masse m, welcher die Geschwindigkeit u_i in Bezug auf das gegebene Koordinatensystem besitzt, und einen anderen mit der Masse $\mathrm{d}m'$ und mit Geschwindigkeit a_i. Im Zeitpunkt $t + \mathrm{d}t$ bilden diese zwei Punkte einen Punkt mit der Masse $m + \mathrm{d}m$, dessen Geschwindigkeit gleich $u_i + \mathrm{d}u_i$ ist. Im Zeitpunkt t ist die Bewegungsgröße des Systems gleich

$$cmu_i + c\,\mathrm{d}m'a_i$$

und im Zeitpunkt $t + \mathrm{d}t$

$$c(m + \mathrm{d}m)(u_i + \mathrm{d}u_i)\,.$$

1772

Der Zuwachs der Bewegungsgröße ist

$$\mathrm{d}p_i = \mathrm{d}(cmu_i) - c\,\mathrm{d}m' a_i \,. \tag{6}$$

Der Fall $\mathrm{d}m' > 0$ entspricht einer sich anschliessenden Masse, $\mathrm{d}m' < 0$ einer sich abscheidenden Masse.

Den Massenzuwachs $\mathrm{d}m'$ erhalten wir indem wir Gleichung (6) skalar mit u_i multiplizieren. Mit Hilfe von (5) ergibt sich

$$\mathrm{d}p_i u_i = -c\,\mathrm{d}m - c\,\mathrm{d}m' a_i u_i \tag{7}$$

oder

$$\mathrm{d}m' = -\frac{c\,\mathrm{d}m + \mathrm{d}p_i u_i}{c a_i u_i} \,. \tag{8}$$

Aus (6) und (8) erhalten wir

$$\mathrm{d}p_i = \mathrm{d}(cmu_i) + \frac{c\,\mathrm{d}m + \mathrm{d}p_j u_j}{a_j u_j}\, a_i \,. \tag{9}$$

Wir führen den 4-Vektor der Kraft durch die Ableitung

$$f_i = \frac{\mathrm{d}p_i}{\mathrm{d}s} = \frac{\mathrm{d}}{\mathrm{d}s}(cmu_i) + \frac{c\,\mathrm{d}m/\mathrm{d}s + (\mathrm{d}p_j/\mathrm{d}s)u_j}{a_j u_j}\, a_i \,. \tag{10}$$

ein.

Gleichung (10) wollen wir im Raume R_3 ausdrücken. Der Vektor der Kraft wird in R_3 durch den Ausdruck

$$\boldsymbol{F} = c(f_1, f_2, f_3)\sqrt{1 - (v^2/c^2)}$$

bestimmt. Der Zuwachs der Bewegungsgröße wird uns in R_3 durch

$$\mathrm{d}\boldsymbol{p} = (\mathrm{d}p_1, \mathrm{d}p_2, \mathrm{d}p_3) = \boldsymbol{F}\,\mathrm{d}t$$

und der zu Energiezuwachs durch $\mathrm{d}E = c\,\mathrm{d}p_4/i$ gegeben. Dann läßt sich Gl. (10) in der Form schreiben

$$\boldsymbol{F} = \frac{\mathrm{d}}{\mathrm{d}t}\left(\frac{m\boldsymbol{v}}{\sqrt{1-(v^2/c^2)}}\right) + \frac{(\mathrm{d}m/\mathrm{d}t)c^2\sqrt{1-(v^2/c^2)} + \boldsymbol{F}\boldsymbol{v} - (\mathrm{d}E/\mathrm{d}t)}{\boldsymbol{a}\boldsymbol{v} - c^2}\,\boldsymbol{a}\,, \tag{11}$$

$$\frac{\mathrm{d}E}{\mathrm{d}t} = \frac{\mathrm{d}}{\mathrm{d}t}\left(\frac{mc^2}{\sqrt{1-(v^2/c^2)}}\right) + \frac{(\mathrm{d}m/\mathrm{d}t)c^2\sqrt{1-(v^2/c^2)} + \boldsymbol{F}\boldsymbol{v} - (\mathrm{d}E/\mathrm{d}t)}{\boldsymbol{a}\boldsymbol{v} - c^2}\, c^2 \,. \tag{12}$$

Gleichung (12) ergibt sich aus Gl. (11) indem wir die letzte skalar mit $\boldsymbol{v}$ multiplizieren und die Identität benutzen

$$(13)\qquad \mathrm{d}\left(\frac{m\boldsymbol{v}}{\sqrt{1-(v^2/c^2)}}\right)\boldsymbol{v}-\mathrm{d}\left(\frac{mc^2}{\sqrt{1-(v^2/c^2)}}\right)=-\,\mathrm{d}m\,c^2\sqrt{1-(v^2/c^2)}\,.$$

Der Massendefekt ist Null wenn

$$(14)\qquad \mathrm{d}m'=\mathrm{d}m\,.$$

In diesem Falle bekommen wir aus (8)

$$(15)\qquad c(1+a_iu_i)\,dm=-\,\mathrm{d}p_iu_i$$

oder

$$(16)\qquad \mathrm{d}\boldsymbol{p}\boldsymbol{v}=\mathrm{d}E-\mathrm{d}m\left(c^2\sqrt{1-(v^2/c^2)}+\frac{\boldsymbol{a}\boldsymbol{v}}{\sqrt{1-(a^2/c^2)}}-\frac{c^2}{\sqrt{1-(a^2/c^2)}}\right)$$

oder nach (6) und (14)

$$(17)\qquad \boldsymbol{F}\boldsymbol{v}=\frac{\mathrm{d}}{\mathrm{d}t}\left(\frac{mc^2}{\sqrt{1-(v^2/c^2)}}\right)-\frac{\mathrm{d}m}{\mathrm{d}t}\left(c^2\sqrt{1-(v^2/c^2)}+\frac{\boldsymbol{a}\boldsymbol{v}}{\sqrt{1-(a^2/c^2)}}\right).$$

Gleichungen (15), (16) und (17) haben wir in unseren Arbeiten (1) und (2) abgeleitet. Aus (11) und (16) ergibt sich

$$(18)\qquad \boldsymbol{F}=\frac{\mathrm{d}}{\mathrm{d}t}\left(\frac{m\boldsymbol{v}}{\sqrt{1-(v^2/c^2)}}\right)-\frac{(\mathrm{d}m/\mathrm{d}t)\cdot\boldsymbol{a}}{\sqrt{1-(a^2/c^2)}}=0\,.$$

Das ist die Grundformel unserer Arbeit (1), womit erwiesen ist, daß diese nur für den Fall, wenn der Massendefekt des Punktes mit veränderlicher Masse gleich Null ist, gültig ist.

Wir betrachten jetzt den anderen Grenzfall, wenn $\mathrm{d}p_i=0$, d.h. $\boldsymbol{F}=0$; $\mathrm{d}E/\mathrm{d}t=0$. Gleichung (11) ergibt in diesem Fall

$$(19)\qquad \frac{\mathrm{d}}{\mathrm{d}t}\left(\frac{m\boldsymbol{v}}{\sqrt{1-(v^2/c^2)}}\right)+\frac{(\mathrm{d}m/\mathrm{d}t)c^2\sqrt{1-(v^2/c^2)}}{\boldsymbol{a}\boldsymbol{v}-c^2}\,\boldsymbol{a}=0\,.$$

Gleichung (19) gilt für die «reine» Rakete, d.h. eine solche, welche sich in einem Raum frei von Gravitation, Energie und Materie bewegt.

---

(2) N. S. Kalitzin: *Verallgemeinerung der Grundgleichungen der Raketendynamik für relativistische Geschwindigkeiten*, im Druck.

Es sei $\boldsymbol{q}$ die Geschwindigkeit der weggeschleuderten Teilchen in Bezug auf die Rakete. Nach der speziellen Relativitätstheorie haben wir (vergl [3], S. 286)

$$\boldsymbol{a} = \frac{1}{1 + (\boldsymbol{qv}/c^2)}\left[\boldsymbol{q}\sqrt{1-(v^2/c^2)} + \frac{\boldsymbol{v}(\boldsymbol{qv})}{v^2}\left(1-\sqrt{1-(v^2/c^2)}\right) + \boldsymbol{v}\right]. \tag{20}$$

Aus (20) erhalten wir

$$\boldsymbol{av} - c^2 = \frac{v^2 - c^2}{1 + (\boldsymbol{qv}/c^2)} \tag{21}$$

und

$$\sqrt{1-(a^2/c^2)} = \frac{\sqrt{(1-(q^2/c^2))(1-(v^2/c^2))}}{1 + (\boldsymbol{qv}/c^2)}. \tag{22}$$

Aus (19) und (21) ergibt sich

$$\mathrm{d}\left(\frac{m\boldsymbol{v}}{\sqrt{1-(v^2/c^2)}}\right) - \mathrm{d}m\,\frac{1 + (\boldsymbol{qv}/c^2)}{\sqrt{1-(v^2/c^2)}}\,\boldsymbol{a} = 0\,, \tag{23}$$

und indem wir noch (22) benutzen

$$\mathrm{d}\left(\frac{m\boldsymbol{v}}{\sqrt{1-(v^2/c^2)}}\right) - \mathrm{d}m\,\frac{\sqrt{1-(q^2/c^2)}}{\sqrt{1-(a^2/c^2)}}\,\boldsymbol{a} = 0\,. \tag{24}$$

Die Gleichung (6) gibt uns in demselben Fall ($dp_i = 0$)

$$\mathrm{d}\left(\frac{m\boldsymbol{v}}{\sqrt{1-(v^2/c^2)}}\right) - \mathrm{d}m'\,\frac{1}{\sqrt{1-(a^2/c^2)}}\,\boldsymbol{a} = 0\,. \tag{25}$$

Aus dem Vergleich von (24) und (25) erhalten wir

$$\mathrm{d}m' = \mathrm{d}m\sqrt{1-(q^2/c^2)}\,. \tag{26}$$

Die gleiche Beziehung ergibt sich auch direkt aus (8) indem wir $\mathrm{d}p_i = 0$ ansetzen und (21) und (22) benutzen. Die Beziehung (26) zeigt, daß der Massendefekt $c^2(\mathrm{d}m - \mathrm{d}m')$ von $\boldsymbol{v}$ und von dem Winkel zwischen $\boldsymbol{v}$ und $\boldsymbol{q}$ unabhängig ist, wie es sein muß.

Wir setzen (20) in (23) ein und erhalten die Differentialgleichung

$$\mathrm{d}\left(\frac{m\boldsymbol{v}}{\sqrt{1-(v^2/c^2)}}\right) - \mathrm{d}m\left[\boldsymbol{q} + \frac{\boldsymbol{v}(\boldsymbol{qv})}{v^2}\left(\frac{1}{\sqrt{1-(v^2/c^2)}} - 1\right) + \frac{\boldsymbol{v}}{\sqrt{1-(v^2/c^2)}}\right] = 0\,. \tag{27}$$

[3] R. Becker: *Theorie der Elektrizität* (Leipzig, 1933), II Bd.

Gleichung (27) skalar mit $\boldsymbol{v}$ multipliziert ergibt

$$m\boldsymbol{v}\,\mathrm{d}\boldsymbol{v} = \mathrm{d}m\,\boldsymbol{q}\boldsymbol{v}\left(1-\frac{v^2}{c^2}\right).$$

Das Integral dieser Gleichung für $m=m_0$ bei $\boldsymbol{v}=\boldsymbol{v}_0$ lautet

$$\ln\frac{m}{m_0} = \int\limits_{\boldsymbol{v}_0}^{\boldsymbol{v}} \frac{\boldsymbol{v}\,\mathrm{d}\boldsymbol{v}}{\boldsymbol{q}\boldsymbol{v}(1-(v^2/c^2))}\,. \tag{28}$$

Im Falle wenn $\boldsymbol{v}$ und $\boldsymbol{q}$ auf einer Geraden liegen, $\boldsymbol{q}\boldsymbol{v} = -qv$, $\boldsymbol{v}_0 = 0$, dann erhalten wir aus (28)

$$\frac{m_0}{m} = \left(\frac{1+(v/c)}{1-(v/c)}\right)^{c/2q}. \tag{29}$$

Das gleiche Integral ist von SÄNGER in seiner Arbeit ([4]) gegeben. Unser Kurvenintegral (28) behandelt den allgemeineren Fall wenn $\boldsymbol{v}$ und $\boldsymbol{q}$ einen Winkel miteinander bilden, der eine beliebige Funktion von der Geschwindigkeit $\boldsymbol{v}$, $(\boldsymbol{q}-\boldsymbol{q}(\boldsymbol{v}))$, sein kann. Dieser Fall wird von Bedeutung für die zukünftige Astronautik sein.

Für nichtrelativistische Geschwindigkeiten $\boldsymbol{v}$ der Rakete ergibt sich aus (18)

$$\frac{\mathrm{d}}{\mathrm{d}t}(m\boldsymbol{v}) - \frac{\boldsymbol{a}}{\sqrt{1-(a^2/c^2)}}\frac{\mathrm{d}m}{\mathrm{d}t} = \boldsymbol{F}\,. \tag{30}$$

Wir wollen den Fall untersuchen, wenn

$$\mathrm{d}\boldsymbol{p}/\mathrm{d}t = \boldsymbol{F} = 0 \tag{31}$$

ist. Dieser Ansatz ist für nichtrelativistische Geschwindigkeiten $\boldsymbol{v}$ kovariant. Das ist der Fall, wenn die Rakete von allen Seiten des Raumes Energie ansaugt, sodaß $\mathrm{d}\boldsymbol{p}=0$ ist. Aus (16) ergibt sich in diesem Falle

$$\mathrm{d}E = \mathrm{d}m\,c^2\left(1-\frac{1}{\sqrt{1-(q^2/c^2)}}\right) \tag{32}$$

wie es auch sein muß. Wenn $\boldsymbol{v}$ und $\boldsymbol{a}$ auf einer Geraden liegen, dann haben wir

$$a = v - q\,. \tag{33}$$

([4]) E. SÄNGER: *VDI-Forschungsheft*, **19**, 437 (1953).

Aus (30), (31) und (33) erbgit sich

$$\frac{\mathrm{d}v\sqrt{1-(q^2/c^2)}}{v\sqrt{1-(q^2/c^2)}-v+q}=-\frac{\mathrm{d}m}{m}\,. \tag{34}$$

Das Integral von (34) für $m=m_0$ bei $v=0$ lautet

$$\ln\left(1+\frac{v(\beta-1)}{q}\right)=\frac{\beta-1}{\beta}\ln\frac{m_0}{m}\,,\qquad \beta=\sqrt{1-(q^2/c^2)}\,. \tag{35}$$

Wir entwickeln $\ln\left\{1+(v(\beta-1)/q)\right\}$ in einer Potenzreihe, welche sicher konvergent ist, da $v\ll q$ und behalten nur das erste Glied. So erhalten wir

$$v=\frac{q}{\beta}\ln\frac{m_0}{m}\,. \tag{36}$$

Für den gleichen Grenzfall ergibt die Formel (29) von Sänger

$$v=q\ln\frac{m_0}{m}\,. \tag{37}$$

Das ist die klassiche Formel von Tziolkovski, welche also bei Antrieb der Rakete durch eigene Energie auch für relativistische Geschwindigkeiten der zurückgeschleuderten Massen gilt.

* * *

Für die wertvolle Kritik bin ich Herrn Prof. CHR. CHRISTOV zu großem Dank verpflichtet.

RIASSUNTO (*)

Si generalizzano, per il caso di velocità relativistiche, le equazioni della meccanica di un punto materiale di massa variabile, considerando il caso più generale, cioè quello nel quale il difetto di massa del punto è diverso da zero. Si danno alcune applicazioni delle equazioni fondamentali, dando particolarmente una formula generale per il caso del razzo « puro ».

(*) *Traduzione a cura della Redazione.*

IL NUOVO CIMENTO Vol. VIII, N. 6 16 Giugno 1958

Remarks on a Model for S-Wave Meson-Nucleon Scattering (*).

T. Kobayashi and A. Klein

University of Pennsylvania - Philadelphia, Pennsylvania

(ricevuto il 15 Marzo 1958)

Summary. — In a recent paper by Lomon, an attempt was made to produce an exact solution of the field theoretic model for S-wave meson-nucleon scattering in which the interaction is the sum of a scalar pair term and of an isotopic spin-orbit coupling. The solution in question is shown to be exact only in the classical limit, *i.e.*, to correspond to the linear or one-meson approximation. It is also shown that the attempt to take the point source limit of the renormalization encounters difficulties similar to those found in the Lee model and in the simple pair theory.

1. – Introduction and summary.

Because their study has been so instructive, it continues to be of interest to search for simplified, albeit unrealistic, models of field theories whose consequences can as far as possible be obtained without approximation.

In a recent paper, Lomon (1) suggested that a popular model for S-wave meson-nucleon scattering be added to the very select list of such theories. By means of an elaborate technique involving « double operators », *i.e.*, bilinear forms in the meson and nucleon field operators, a diagonalization of the Hamiltonian was achieved which was claimed to be exact.

In this note, we first investigate the same model by a more familiar calculational technique and demonstrate that the solution in question is exact only in the classical limit.

It is nevertheless of interest to investigate the renormalization of our re-

(*) Supported in part by a Frederick Gardner Cottrell grant of the Research Corporation.

(1) E. L. Lomon: *Nuovo Cimento*, 4, 106 (1956).

sults. Using the prescription of DESER, THIRRING and GOLDBERGER ([2]), it is indicated that we may anticipate the occurrence of « ghost states » ([3]) with the attendant difficulties of physical interpretation.

Sect. 2 describes our method of calculation for the Hamiltonian which describes the S-wave coupling of the meson to the nucleon by means of both a pair term and an isotopic spin-orbit coupling term. The phase shifts for isotopic spin $\frac{3}{2}$ and $\frac{1}{2}$, obtained in an approximation which is clearly the classical or one-meson approximation, are exactly those of LOMON.

The problem of renormalization is discussed in Sect. 3. For the sake of concreteness, a Yukawa cut-off function is adopted. Adjusting our coupling constants to the Orear phase shifts ([4]) for S-wave scattering, the conditions for the occurrence of the « ghost states » appear for a cut-off momentum larger than 5μ, μ the meson rest mass. These results are discussed in the last section.

2. – Derivation of phase shifts.

The Hamiltonian is written as the sum of two parts:

$$H = H_0 + H_1 \,, \tag{1}$$

where

$$H_0 = \frac{1}{2}\int \mathrm{d}^3\boldsymbol{x}\,[\pi_i^2 + (\nabla\varphi_i)^2 + \mu^2\varphi_i^2] \tag{2}$$

is the Hamiltonian of the free meson field, and H_1 describes the interaction between S-wave mesons and a fixed nucleon. We take a specific interaction for H_1 guided by the form which is obtained upon application of the Tani-Foldy ([5]) transformations to the relativistic theory,

$$H_1 = \lambda_1\left(\int \varrho\varphi_i \mathrm{d}^3\boldsymbol{x}\right)^2 + \lambda_2\psi^\dagger\boldsymbol{\tau}\psi\cdot\left(\int\varrho\boldsymbol{\varphi}\mathrm{d}^3\boldsymbol{x}\right)\times\left(\int\varrho\boldsymbol{\pi}\mathrm{d}^3\boldsymbol{x}\right), \tag{3}$$

with $\boldsymbol{\pi}$ the canonical momentum of the meson field and ϱ the source density. λ_1 and λ_2 are coupling constants which, before renormalization, can be related to the pseudoscalar coupling constant g^2:

$$\lambda_1 = \frac{g^2}{2M}\,, \qquad \lambda_2 = \left(\frac{g^2}{2M}\right)^2 . \tag{4}$$

([2]) S. DESER, W. E. THIRRING and M. L. GOLDBERGER: *Phys. Rev.*, **94**, 711 (1954).
([3]) G. KÄLLÉN and W. PAULI: *Mat. Fys. Medd. Dan. Vid. Selsk.*, **30**, No. 7 (1955).
([4]) J. OREAR: *Phys. Rev.*, **100**, 288 (1955).
([5]) S. TANI: *Prog. Theor. Phys.*, **6**, 267 (1950); L. L. FOLDY: *Phys. Rev.*, **84**, 168 (1951); S. D. DRELL and E. M. HENLEY: *Phys. Rev.*, **88**, 1053 (1952).

From this Hamiltonian there follow the equations of motion for φ_i and π_i:

$$\dot{\varphi}_i = i[H, \varphi_i] = \pi_i + \lambda_2 \varepsilon_{ijk} \psi^\dagger \tau_j \psi \left(\int \varrho \varphi_k \, \mathrm{d}^3\boldsymbol{x} \right) \varrho \,, \tag{5}$$

$$\dot{\pi}_i = i[H, \pi_i] = (\nabla^2 - \mu^2)\varphi_i - 2\lambda_1 \left(\int \varrho \varphi_i \, \mathrm{d}^3\boldsymbol{x} \right) \varrho + \lambda_2 \varepsilon_{ij} \, \psi^\dagger \tau_j \psi \left(\int \varrho \pi \, \mathrm{d}^3\boldsymbol{x} \right) \varrho \,, \tag{6}$$

where ε_{ijk} represents the three dimensional Levi-Civita tensor density in isotopic spin space. Eliminating π_i from (5) and (6) we obtain the equation of motion for φ_i,

$$\begin{aligned} (-\Box^2 + \mu^2)\varphi_i(\boldsymbol{x}, t) = &-2\lambda_1 \left(\int \varrho \varphi_i \, \mathrm{d}^3\boldsymbol{x} \right) \varrho + 2\lambda_2 \varepsilon_{ijk} (\psi^\dagger \tau_j \psi)_{in} \left(\int \varrho \dot{\varphi}_k \, \mathrm{d}^3\boldsymbol{x} \right) \varrho + \\ &+ 2\lambda_2^2 \left(\int \varrho \varphi_i \, \mathrm{d}^3\boldsymbol{x} \right) \left(\int |\varrho|^2 \, \mathrm{d}^3\boldsymbol{x} \right) \varrho - i\lambda_2^2 \varepsilon_{ijk} (\psi^\dagger \tau_j \psi)_{in} \left(\int \varrho \varphi_k \, \mathrm{d}^3\boldsymbol{x} \right) \left(\int |\varrho|^2 \, \mathrm{d}^3\boldsymbol{x} \right) \varrho \,. \end{aligned} \tag{7}$$

In passing from (5) and (6) to (7) we have made an essential approximation. We have neglected the time derivative of $\psi^\dagger \boldsymbol{\tau} \psi$. Consistent with this we have repladed $\psi^\dagger \boldsymbol{\tau} \psi$ by $\psi^\dagger_{in} \boldsymbol{\tau} \psi_{in}$, where ψ_{in} means ψ in the remote past satisfying the free field equation.

It is convenient to introduce the wave function in co-ordinate space defined by [6]

$$T_{ii'}(\boldsymbol{k}, \mu) = \langle \text{one nucleon} | \varphi_i(\boldsymbol{x}, t) | \boldsymbol{k}, i' \rangle \,, \tag{8}$$

where $|\boldsymbol{k}, i'\rangle$ represents the scattering state of a meson with momentum $\boldsymbol{k}$ and isotopic spin i'. Then we can rewrite Eq. (7) as the equation for $T_{ii'}$ as follows:

$$\begin{aligned} [-\nabla^2 + \mu^2 - \omega^2(k)] T_{ii'}(\boldsymbol{k}, \boldsymbol{x}) = &-2 \left(\lambda_1 - \lambda_2^2 \int |\varrho|^2 \, \mathrm{d}^3\boldsymbol{x} \right) \varrho \left(\int \varrho T_{ii'} \, \mathrm{d}^3\boldsymbol{x} \right) - \\ &- i\lambda_2 \left(2\omega(k) + \lambda_2 \int |\varrho|^2 \, \mathrm{d}^3\boldsymbol{x} \right) \varepsilon_{ijk} \tau_j \varrho \left(\int \varrho T_{ki'} \, \mathrm{d}^3\boldsymbol{x} \right), \end{aligned} \tag{9}$$

where $\omega^2(k) = k^2 + \mu^2$.

We now decompose $T_{ii'}$ into the eigenstates of total isotopic spin $\frac{1}{2}$ and $\frac{3}{2}$ by means of projection operators,

$$T_{ii'} = \sum_{\alpha = 1,3} T_{ii'} P_{ii'}(\alpha) \,. \tag{10}$$

$$\begin{aligned} P_{ii'}(3) &= \tfrac{1}{3}[2\delta_{ii'} - i\varepsilon_{ii'k}\tau_k] \,, \\ P_{ii'}(1) &= \tfrac{1}{3}[\delta_{ii'} + i\varepsilon_{ii'k}\tau_k] \,. \end{aligned} \tag{11}$$

([6]) A similar approach to the *P*-wave problem has been carried out by S. F. EDWARDS and P. T. MATHEWS: *Phil. Mag.*, **2**, 176 (1957).

Thus equation (9) can be rewritten

$$(12)\quad [-\nabla^2+\mu^2-\omega^2(k)]T^{\alpha}_{ii'} = -2\left(\lambda_1-\lambda_2^2\int|\varrho|^2\,\mathrm{d}^3\boldsymbol{x}\right)\varrho\left(\int\varrho T^{\alpha}_{ii'}\,\mathrm{d}^3\boldsymbol{x}\right)+ \\ +\Gamma_\alpha\left[2\omega(k)\lambda_2+\lambda_2^2\int|\varrho|^2\,\mathrm{d}^3\boldsymbol{x}\right]\varrho\left(\int\varrho T^{\alpha}_{ii'}\,\mathrm{d}^3\boldsymbol{x}\right),$$

where

$$(13)\qquad \Gamma_\alpha=\begin{cases}+2\,, & \alpha=1\,,\\ -1\,, & \alpha=3\,.\end{cases}$$

Equation (12) represents a Schrödinger-like equation with separable potential and the solution under the boundary condition that there is an incoming wave with momentum $\boldsymbol{k}$ can be obtained in a straightforward manner. We obtain immediately for the scattering phase shift,

$$(14)\qquad \operatorname{tg}\delta_\alpha(k) = -\frac{2\pi^2k\,|\varrho(k)|^2[2\lambda_1-\lambda_2^2V(2+\Gamma_\alpha)-2\Gamma_\alpha\,\lambda_2\omega(k)]}{1-[2\lambda_1-\lambda_2^2V(2+\Gamma_\alpha)-2\Gamma_\alpha\,\lambda_2\omega(k)]\int\left(\dfrac{|\varrho(k')|^2}{k^2-k'^2}\right)\mathrm{d}^3k'}\,,$$

where

$$(15)\qquad \varrho(k)=\frac{1}{(2\pi)^3}\int\varrho(|\boldsymbol{x}|)\exp\,[\boldsymbol{k}\cdot\boldsymbol{x}]\,\mathrm{d}^3\boldsymbol{x}\,,$$

$$(16)\qquad V=\frac{1}{(2\pi)^3}\int|\varrho(k)|^2\,\mathrm{d}^3\boldsymbol{k}$$

and we have assumed the spherical symmetry of the source function.

We see that (14) agrees essentially with Lomon's result (see Lomon's Eqs. (26) and (28)). In his method, it is the algebra of the « double operators » which is approximate. The neglect in this algebra of contributions from « single operators » corresponds precisely to the classical or linear approximation stated below Eq. (7).

3. – Renormalization of the coupling constants.

In order to renormalize the coupling constants λ_1 and λ_2 we adopt the prescription of DESER, THIRRING and GOLDBERGER [2]. We define the scattering length at zero energy and vanishing meson mass as

$$(17)\qquad a_\alpha=\lim_{k\to 0}\left(\frac{\operatorname{tg}\delta_\alpha(k)}{k}\right)_{\mu=0}\,,\qquad \alpha=1,\,3.$$

By means of Eq. (14), λ_1 and λ_2^2 can be expressed in terms of a_1 and a_3 which are essentially observable quantities. It is worthy of remark that there is no linear term in λ_2 in this renormalization prescription [7].

We find that

$$\lambda_1 = \frac{3I(0)a_1a_3 + 2\pi^2(a_1 - 4a_3)}{6\Delta_1\Delta_3}, \tag{18}$$

$$\lambda_2^2 = \frac{2\pi^2(a_1 - a_3)}{3V\Delta_1\Delta_3}, \tag{19}$$

where

$$\Delta_\alpha = I(0)a_\alpha - 2\pi^2, \qquad \alpha = 1, 3, \tag{20}$$

and

$$I(0) = \left[\int \frac{|\varrho(k')|^2}{k^2 - k'^2}\,\mathrm{d}^3\boldsymbol{k}\right] = \int \frac{|\varrho(k')|^2}{-k'^2}\,\mathrm{d}^3\boldsymbol{k}. \tag{21}$$

For a square cut-off at momentum k_c, λ_2^2 turns out to be

$$\lambda_2^2 = \frac{1}{\pi}\left(\frac{1}{2k_c}\right)^5 \frac{a_1 - a_3}{(a_1 + (1/2k_c))(a_3 + (1/2k_c))}. \tag{22}$$

According to the experiment on S-wave meson-nucleon scattering a_1 is positive whereas a_3 is negative. It follows from (22) that λ_2^2 may become negative for sufficiently large k_c. In the same way λ_1 becomes

$$\lambda_1 = \left(\frac{1}{2\pi}\right)^2\left(\frac{1}{2k_c}\right)^2 \frac{3I(0)a_1a_3 + 2\pi^2(a_1 - 4a_3)}{6(a_1 + (1/2k_c))(a_3 + (1/2k_c))}, \tag{23}$$

which also can reverse sign as k_c increases.

The situation here is quite analogous to that which occurs in the Lee model [8] and in meson pair theory [9]. To be more specific let us choose a Yukawa cut-off function and Orear's phase shifts to determine a_1 and a_3,

$$\begin{cases} \varrho(k) = \dfrac{k_c^2}{k^2 + k_c^2}, \\ a_1 \sim 0.167/\mu, \\ a_3 \sim -0.105/\mu. \end{cases} \tag{24}$$

λ_1 and λ_2^2 then become negative for $k > k_c$, where $k_c \sim 5\,\mu$.

(7) This is true only in the limit of vanishing meson mass. Otherwise the situation is rather more complicated, but our qualitative considerations should remain unaltered.

(8) T. D. Lee: *Phys. Rev.*, **95**, 1329 (1954).

(9) A. Klein and B. H. McCormick: *Phys. Rev.*, **98**, 1428 (1955).

4. – Concluding remarks.

We have considered a theory with two coupling constants, λ_1 and λ_2 the first of which can become negative as in meson pair theory (leading to a breakdown of the vacuum state) and the other of which can become imaginary, reminiscent of behaviour of the Lee model ([10]). Though we have not demonstrated this in detail here, the implication is the physical unacceptability of the resulting theory. However, HEISENBERG ([11]) has recently demonstrated that this is not a forgone conclusion even for the Lee model. We aim to return to the discussion of these matters for the present model on a later occasion.

([10]) The general situation has been summarized by W. PAULI: *Suppl. Nuovo Cimento*, **4** 703 (1956).
([11]) W. HEISENBERG: *Nuclear Physics*, **4**, 532 (1957).

Note added in proof.

It should be remarked that the occurence of the « ghost states » is assured only if we assign the experimental signs to the scattering lenght as LOMON pointed out in his paper. A point source limit without « ghost states » is possible for the special case $a_2 > 0$ and $a_3 = 0$.

RIASSUNTO (*)

In un recente lavoro di LOMON è stato fatto il tentativo di trovare una soluzione esatta di una teoria di campo per lo scattering mesone-nucleon in onde S in cui l'interazione è rappresentata dalla somma di un termine corrispondente a una coppia scalare con un accoppiamento spin-orbita isotopico. Si dimostra che la soluzione in questione è esatta soltanto nel limite classico, corrisponde, cioè, alla approssimazione lineare o di un mesone. Si dimostra anche che il tentativo di spingere la rinormalizzazione fino al limite della sorgente puntiforme incontra difficoltà simili a quelle offerte dal modello di Lee e dalla teoria delle coppie semplici.

(*) *Traduzione a cura della Redazione.*

IL NUOVO CIMENTO Vol. VIII, N. 6 16 Giugno 1958

A Further Example of an Anomalous K^+-decay (*).

D. J. Prowse (+)

University of California, Los Angeles, California

D. Evans

University of Bristol - Bristol, England

(ricevuto il 28 Marzo 1958)

Summary. – In a systematic study of K^+-meson secondaries, one example has been found in which the charged product is a π-meson of 61.7 MeV. This must be compared with the example published by the Columbia group in which the π-meson energy was 60 MeV. Both are probably due to the decay mode: $K^+ \to \pi^+ + \pi^0 + \gamma$ although the possibility that they belong to a two body decay mode: $K^+ \to \pi^+ + X^0$, where X^0 is a neutral boson and has a mass of $(500 \pm 5)\, m_e$, should not be overlooked. A description of the event is given and the interpretation discussed.

1. – Introduction.

Recently the Columbia emulsion group (1) has published details of an event which they propose as the first observed case of the possible decay $K^+ \to \pi^+ + \pi^0 + \gamma$. The purpose of this note is to describe a similar event found in Bristol and analysed in Los Angeles.

During a systematic search for K-mesons decaying in τ' or $\varkappa$-modes, 353 K^+-meson decays in good geometry have been examined in detail by the Bristol and Dublin groups in a stack exposed to the unseparated K^+-beam of the Berkeley bevatron. The results of this investigation have recently been sent to press (2). In that communication the scanning and analysis procedure

(*) Was partially supported by the U. S. Atomic Energy Commission.

(+) On leave from the H. H. Wills Physical Laboratory, University of Bristol.

(1) G. Harris, J. Lee, J. Orear and S. Taylor: *Phys. Rev.*, **108**, 1561 (1957).

(2) B. Bhowmik, D. Evans, D. J. Prowse, F. Anderson, A. Kernan and D. Keefe: submitted to *Nuovo Cimento* (January 1958).

have been fully described: measurements were made on the secondary tracks if they had a projected length of greater than 1 mm per plate and if the initial grain-density measurement (a count of 400 grains) indicated that $g^+ > 1.4$ (the measured grain density divided by that of the beam π-mesons which were $1.01 \cdot g_{min}$), the secondary track was followed to rest or sufficiently far to exclude the possibility of its being due to a π-meson of energy < 53 MeV (the maximum energy to be expected from the decay of a τ'-meson) or a μ-meson of < 50 MeV (the chosen cut-off for the $\varkappa$-secondary spectrum). In this way 11 τ'-mesons and 9 $\varkappa$-mesons were detected in an unbiased fashion. During this work one secondary event having a $g^+ = 1.5$ was followed for > 4.2 cm, thus effectively excluding the possibility of it being due to a π-meson or μ-meson of < 50 MeV from the τ' or $\varkappa$-modes of decay. It was hence provisionally classified as a χ-meson whose initial ionization measurement was anomalously high or a $\varkappa$ having a high energy secondary μ-meson. The secondary has now been followed to rest and its corrected true range is 5.03 cm and it exhibits a typical π-μ decay at its end, the μ-meson being 604 μm long. The upper limit for the range of a π-meson from the τ'-mode of decay is 3.95 cm.

2. – Description of the event.

The K-meson which has been identified by the $\Delta g^+/\Delta R$ method decays at a depth of 64 μm in the emulsion sheet. The angle between the final K-meson direction and the emitted π-meson is $(120 \pm 3)°$, the relatively large uncertainty arising from the difficulty of measuring the exact direction of the K-meson due to multiple scattering at the end of its range. The fact that this angle is $> 90°$ effectively excludes the possibility that the event is a decay in flight of a τ'-meson. In the Columbia event the angle is 49° and although the τ'-explanation is unlikely they could not rigidly exclude it. The upper limit on the possible K-meson energy at decay is 5 MeV. This rigidly excludes the possibility of a χ-meson decay in flight. The secondary is flat —4.6 mm/plate—and it scatters through an angle of 11° in its second emulsion sheet. It then continues at ~ 1.1 cm/plate until it comes to rest in its seventh pellicle, 137 μm from the emulsion surface. The range of the μ-meson 604 μm, is in excellent agreement with that expected for normal π-μ-decay. The angle between the π and μ-mesons is 97°. Measurements of the integral gap length from the end of the μ-meson track gave an abrupt discontinuity at 604 μm residual range indicating that it is not a single scatter of a μ-meson at this point but a true decay.

One possibility that has to be excluded if our interpretation is correct is that the scatter of 11° in the second pellicle is an inelastic scatter of a π-meson from the normal χ-decay mode. If this were the case the loss of energy would

be ~ 56 MeV and the grain density should show a change of 25%. Counting 1000 grains before and after the scatter, we obtain a ratio of $1.01 \pm .05$ for the grain density before and after. In addition the value of g^+ at the emission of the π-meson is 1.51 which is 6 standard deviations from that expected from a π-meson from the χ-mode. As the interpretation of the event is critically dependent on the grain counting measurement before this single scatter, great attention has been paid to determining the correct value of the minimum ionization in the two plates in question, 153 and 154. In Fig. 1 is shown the calibration figures of these plates compared with the others in the stack. 1000 blobs were counted on each of 5 tracks supposedly π-mesons in the beam in the regions of the two plates where the K-decay event is situated. It can be seen that the values of the ionization in plates 153 and 154 are not anomalously low and agree very well with the values from the other plates of the same processing batch. The probability of a combination of these most unlikely circumstances—a high grain count in plates 153 and 154 before the single scatter, six standard deviation from that expected, which immediately becomes normal after the scattering event coupled with an inelasticity in the scatter of 56 MeV—can therefore be assumed to be negligible.

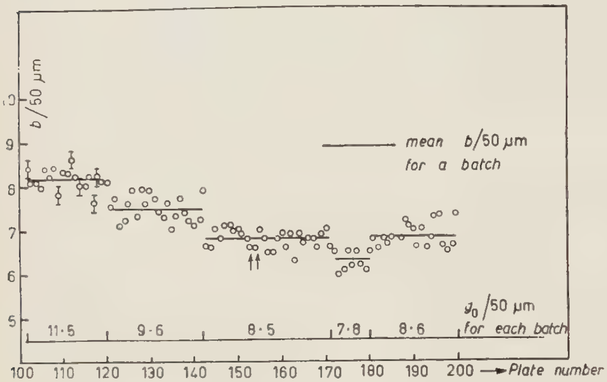

Fig. 1.

3. – Discussion.

The π-meson energy corresponding to the observed range of $(5.03 \pm .05$ cm) is 61.7 MeV (using the Barkas-Range-Energy relation ([3])). After allowing for the fact that the density of the stack was not exactly known and we might expect up to a 1% variation from 3.185 g/cm^3, the density of « standard emulsion », for which the range-energy relation is known to a high degree of precision, the total probable error including the straggling error is likely to be ± 1.5 MeV. The energy of the π-meson in the Columbia event is quoted by

([3]) W. H. BARKAS: privately circulated preprint.

HARRIS, LEE, OREAR and TAYLOR as (60 ± 1) MeV. The equality of these two energies might be taken to indicate that the decay process is a 2-body one. If one assumes a mode: $K^+ \rightarrow \pi^+ + X^0$, the mass of particle X^0 must be $(500 \pm 5)\, m_e$. Whether or not this should be identified with a neutral « 500 mass particle », the charged counterpart of which has been reported by ALIKHANIAN (4) is a matter of conjecture and must await further work to confirm the unique π-energy in the 60 MeV region. A more probable explanation is that put forward by HARRIS *et al.* to explain their event. They consider the decay modes,

$$\text{(A)} \qquad K^+ \rightarrow \pi^+ + \pi^0 + \gamma\,,$$

$$\text{(B)} \qquad \rightarrow \pi^+ + 2\gamma\,,$$

$$\text{(C)} \qquad \rightarrow \pi^+ + \nu + \bar{\nu}\,.$$

Assuming mode (A), the photon energy in both events would be between 55 and 158 MeV. They exclude mode (B) on an order of magnitude evaluation of the matrix element and mode (C) is excluded because all interactions involving neutrinos have previously been accompanied by a charged lepton. ONEDA (5) (*) has calculated the energy spectrum expected for this mode if $\nu \neq \bar{\nu}$ and if $\nu = \bar{\nu}$. In the $\nu \neq \bar{\nu}$ case the relative probability of a π-meson energy of 60 MeV is small (+). HARRIS *et al.* calculate the π^+-meson energy spectrum to be expected from a direct electric or magnetic dipole transition from the K^+-state to the (π^+, π^0) state ((mode (A)) using the matrix element given by DALITZ (6). The spectrum has a broad peak at $(50 \div 60)$ MeV and it is not too unreasonable to have the first two events observed in this energy region. It would be premature to take these events as good evidence for the existence of a 500 mass particle, therefore, as there does exist a certain experimental bias favoring the detection of π-mesons in the energy range 55 MeV to 80 MeV from decaying K-particles because this is the region where distinction from the τ'-mode is possible and distinction from the χ-mode can be made on the basis of a fairly rough grain-count; if the π-energy exceeds 80 MeV it is difficult to distinguish such cases from the normal π-meson for the χ-decay.

An alternative explanation is of course that both examples are merely cases in which the charged π-meson has lost energy in the initial acceleration

(4) A. I. ALIKHANIAN *et al.*: *Žu. Ėksp. i Teoret. Fiz.*, **31**, 955 (1956).

(5) S. ONEDA: *Nucl. Phys.*, **3**, 598 (1957).

(*) We thank Dr. R. H. W. JOHNSTON for bringing this reference to our attention.

(+) S. ONEDA: private communication.

(6) R. DALITZ: *Phys. Rev.*, **99**, 915 (1955).

process by « bremsstrahlung ». An order of magnitude calculation by DALITZ (7) gives a probability for this process which is not too far from that observed (which is 2 anomalous in about 1400 normal $K_{\pi 2}$ decays).

* * *

We would like to thank the scanners at Bristol for their work in the large investigation of K^+-meson secondaries. D. J. PROWSE is grateful to Professor C. F. POWELL for the loan of the relevant plates to the Department of Physics, University of California at Los Angeles. We thank Dr. D. H. STORK, Dr. S. GOLDHABER, Dr. W. H. BARKAS, and Professor R. H. DALITZ for discussion. D. J. PROWSE is greatly indebted to Professor J. R. RICHARDSON for the kind hospitality of his laboratory and we thank Drs. E. J. LOFGREN and R. W. BIRGE for the exposure at the Bevatron.

---

(7) R. H. DALITZ, private communication.

RIASSUNTO (*)

In uno studio sistematico di secondari dei mesoni K^+ si è trovato un esempio nel quale il prodotto carico è un meson π di 61.7 MeV. Questo deve essere confrontato con l'esempio pubblicato dal gruppo di Columbia in cui l'energia del mesone π era di 60 MeV. Ambedue sono probabilmente dovuti a un decadimento di modo $K^+ \to \pi^+ + \pi^0 + \gamma$; non si deve, tuttavia, perdere di vista la possibilità che siano dovuti a un decadimento in due corpi di modo $K^+ \to \pi^+ + X^0$, dove X^0 è un bosone neutro ed ha massa $(500 \pm 5)\, m_e$. Si dà una descrizione dell'evento e se ne discute l'interpretazione.

(*) *Traduzione a cura della Redazione.*

IL NUOVO CIMENTO Vol. VIII, N. 6 16 Giugno 1958

Limits on Coupling Constants in Field Theories with Finite Sources.

M. A. Ruderman (*)

Istituto di Fisica dell'Università - Roma

S. Gasiorowicz (+)

Institute of Theoretical Physics, University of Copenhagen - Copenhagen

(ricevuto il 28 Marzo 1958)

Summary. — The interaction of a boson field with a source is assumed to vanish outside of a radius a; no special properties are assumed for this source within the radius. It is shown that with such a model for the interaction of pions or K-mesons with nucleons and hyperons, rigorous upper limits, depending only upon a and the particle masses, can be established for the renormalized coupling constants $g^2_{\Lambda\Sigma\pi}$, $g^2_{p\Sigma K}$, and $g^2_{p\Lambda K}$ corresponding to the matrix elements for the processes $\pi+\Lambda^0\leftrightarrow\Sigma$, $\overline{K}+p\leftrightarrow\Sigma$ and $K^-+p\leftrightarrow\Lambda^0$. For the pion-nucleon interaction a maximum $g^2_{np\pi}$ is found, above which there must exist a doubly charged state of the system π^++p. If $g^2_{np\pi}$ does approach infinity or if a approaches zero, it is proved that the neutron-proton mass difference goes to zero independently of other interactions or whether the bare masses are identical. Similar results hold for the mass difference of any baryon pair if they transform into each other by single boson emission or absorption. Finally a general class of field theory models, which will always have « ghosts », is described.

(*) John Simon Guggenheim Fellow. Permanent address: Department of Physics, University of California, Berkeley.

(+) National Science Foundation Fellow on leave of absence from the Radiation Laboratory, University of California, Berkeley.

1. – Introduction.

For a particle bound by a potential, the asymptotic wave function is $c \exp[-\alpha r]/r$ with, in general, no limitation on the constant c. If the potential vanishes outside the radius $r = a$ then the asymptotic wave function can be continued to this radius, and the statement that the probability for the particle being anywhere in the region $r > a$ is less than one puts an upper limit on $|c|^2$.

The system $\pi^- + p$ possesses a bound state, the neutron, and in many formal relations the coupling constant $g^2_{np\pi^-}$ plays a role analogous to $|c|^2$ in the potential problem. The formal similarities and differences between various coupling constants $g^2_{np\pi}$, $g^2_{\Lambda\Sigma\pi}$, $g^2_{p\Sigma K}$, etc., and the quantity $|c|^2$ are conveniently studied in terms of dispersion type relations in which the g^2 or $|c|^2$ appear explicitly in the inhomogeneous terms. Indeed, in the case of an interaction which vanishes outside of some finite radius, it is found that many of the g^2 possess upper bounds which cannot be exceeded unless « ghosts » (1) are present.

For a causal interaction the scattering amplitude satisfies a dispersion relation which relates its real and imaginary parts and some properties of the bound states of the system (2). Such dispersion relations have been examined and applied in great detail during the past few years. Whether the interaction is causal or not the scattering amplitude is restricted by the spatial dependence of the interaction as the distance between the particle and the scatterer approaches infinity. These restrictions are particularly clear when the interaction vanishes for r greater than some radius a. Then the completeness of the wave functions for $r > a$ relates the real and imaginary parts of the scattering amplitude to the bound states. These connections can also be simply expressed by a dispersion relation which, however, explicitly involves the range a, but which, unlike the usual causal dispersion relations, is valid not only for the total scattering amplitude but also for the amplitude for a single partial wave.

In this paper we study and exploit such single partial wave dispersion relations and especially the connection between the bound state constants and the scattering amplitude. In Sect. **2** the consequence of the remark that the probability of a state is not larger than one is developed for a finite range potential (not necessarily local). Sect. **3** and **4** develop similar results from the regularity properties of functions related to such amplitudes, in a form useful for field theory. In Sect. **5** the appropriate dispersion type relations are found

---

(1) G. KÄLLÉN and W. PAULI: *Dan. Mat. Fys. Medd.*, **30**, no. 7 (1955).
(2) M. L. GOLDBERGER: *Phys. Rev.*, **99**, 979 (1955).

for field theory with an interaction confined to a region $r < a$. Sect. 6 contains the application of these results to various theories and coupling constants, and contains the main results of this paper.

2. – Potential scattering.

The properties of the scattering amplitude from an interaction of finite range in field theory are, in part, analogous to those of a single partial wave amplitude interacting with a non-local potential of the same range. We consider a spherically symmetric interaction which vanishes for $r > a$, and which has a bound state of energy $E_B = -\alpha^2/2m$. We shall also assume only elastic scattering, although this is a restriction which is easily removed. The s-wave eigenfunctions $\varphi_k(r)$ and $\varphi_B(r)$ for the continuum and bound state are unknown except for $r > a$ where

$$\varphi_k(r) = (2\pi)^{-\frac{3}{2}} \frac{\exp[-ikr] - S(k)\exp[ikr]}{2kr}, \tag{1}$$

$$\varphi_B(r) = C\,\frac{\exp[-\alpha r]}{r}. \tag{2}$$

The S-matrix $S(k)$ is given by $\exp[2i\delta)]$, where δ is the phase shift. The functions $\varphi(r)$ are assumed to form a complete orthonormal set; therefore

$$4\pi\int_0^\infty k^2\,\mathrm{d}k\,\varphi_k(r)\varphi_k^*(r') + \varphi_B(r)\varphi_B^*(r') = \frac{\delta(r-r')}{4\pi rr'}. \tag{3}$$

The r.h.s. of eq. (3) is just the s-wave part of $\delta(\boldsymbol{r}-\boldsymbol{r}')$. Substituting (1) and (2) into eq. (3) we obtain two relations

$$S(k)S^*(k) = 1 \tag{4}$$

and

$$\frac{1}{8\pi^2}\int_0^\infty \mathrm{d}k\,\{[S(k)-1]\exp[ik(r+r')] + \text{c.c.}\} = \\ = |c|^2\exp[-\alpha(r+r')]\,. \qquad \text{for } r, r' > a\,. \tag{5}$$

Now we *define*

$$S(-k) = S^*(k) \tag{6}$$

1671

so that eq. (5) is simply

$$(7)\qquad \int_{-\infty}^{\infty} \mathrm{d}k[S(k)-1]\exp[2ika]\exp[2ik\varrho] = \\ = 8\pi^2|c|^2\exp[-2\alpha a]\exp[-2\alpha\varrho] \qquad ; \varrho > 0 .$$

From eq. (7) it follows that there exists a function $S(k)$ of a complex variable k which is equal to the S-matrix for real k, which has a pole at $k = i\alpha$ in the upper half plane of the complex variable k, and which is regular everywhere else in that half-plane except possibly at infinity. The function $\exp[2iak]\cdot S(k)$ remains regular even there ([3-7]). The scattering amplitude

$$(8)\qquad f(k) = [S(k)-1]/2ik$$

defined also for complex k, is such that the function $R(k)$ given by

$$(9)\qquad R(k) = \exp[2iak]\left[f(k) + \frac{4\pi|c|^2}{k^2+\alpha^2}\right],$$

is a regular function of k for $\mathrm{Im}\, k > 0$. The same relation also obtains for the scattering of a relativistic neutral (Klein-Gordon) particle ([7]) by a scalar potential, since the non-relativistic Schrödinger equation can always be recast into this form.

The significant point for future reference is that the magnitude of the residue of the pole of $f(k)$ at $k = i\alpha$ is given by $|c|^2$, and in turn has its magnitude limited by the wave function normalization implied in eqs. (2) and (3). Thus

$$\int_0^{\infty} 4\pi r^2\,\mathrm{d}r\,|\varphi_B(r)|^2 = 1 ,$$

so that

$$\int_a^{\infty} 4\pi\,\mathrm{d}r\,|c|^2\exp[-2\alpha r] \leqslant 1 ,$$

and therefore

$$(10)\qquad |c|^2 \leqslant \frac{\alpha}{2\pi}\exp[2\alpha a] .$$

([3]) W. Heisenberg: *Zeits. f. Naturfor.*, **1**, 608 (1946).
([4]) N. Hu: *Phys. Rev.*, **74**, 131 (1948).
([5]) E. P. Wigner: *Phys. Rev.*, **98**, 145 (1955).
([6]) N. G. Van Kampen: *Phys. Rev.*, **91**, 1267 (1953).
([7]) C. Goebel, R. Karplus and M. A. Ruderman: *Phys. Rev.*, **100**, 240 (1955).

The inequality (10) is not altered by the existence of other bound states (with positive normalization). In field theory the residue of the bound state pole corresponding to $\pi^- + \mathrm{p}$ in the state n (neutron) is proportional to the square of the renormalized coupling constant, and a relation, similar to the inequality (10) but valid under more restrictive conditions, can be derived.

For p-wave scattering eqs. (9) and (10), and the arguments leading to them, remain valid with only slight alterations. Instead of (1) and (2) we have

$$\varphi_k(r) = (2\pi)^{-\frac{3}{2}} \frac{(1 - i/kr)\exp[-ikr] + S(k)(1 + i/kr)\exp[ikr]}{2kr}, \tag{1'}$$

$$\varphi_B(r) = c_\mathrm{p}\,\frac{\exp[-\alpha r]}{r}\left(1 + \frac{1}{\alpha r}\right), \tag{2'}$$

and on the r.h.s. of eq. (3) we replaced $\delta(r - r')/rr'$ by $(\mathrm{d}/\mathrm{d}r)(\mathrm{d}/\mathrm{d}r')(\delta(r - r')/rr')$ In the absence of bound states the regularity of $\exp[2iak]\cdot S(k)$ follows as before. With a bound state, the sign of the residue is opposite to that for the s-wave amplitude, and we obtain the regularity of

$$R(k) = \exp[2iak]\left[f(k) - \frac{4\pi|c_\mathrm{p}|^2}{k^2 + \alpha^2}\right], \tag{9'}$$

and the condition

$$|c_\mathrm{p}|^2 \leqslant \frac{\alpha}{2\pi}\,\frac{\exp[2\alpha a]}{1 + 2/\alpha a}. \tag{10'}$$

For small αa the limitation on the residue is much more severe than in the s-wave case.

Inelastic scattering will not alter the results of eqs. (9) or (10), provided that $f(k)$ now refers to the elastic scattering amplitude. If particle « 1 » can produce other outgoing waves (designated by « 2 », « 3 », etc.) then the wave functions of eq. (4) must be replaced by the Fock column vectors [8]

$$\Psi_n = \begin{vmatrix} \dfrac{\exp[-ikr] - S_{11}\exp[ikr]}{r} \\[2ex] S_{12}\,\dfrac{\exp[ik'r]}{r} \\[2ex] S_{13}\,\dfrac{\exp[ik''r]}{r} \\ \cdot \\ \cdot \\ \cdot \end{vmatrix} \quad \begin{vmatrix} S_{21}\,\dfrac{\exp[ikr]}{r} \\[2ex] \dfrac{\exp[-ik'r] - S_{22}\exp[ik'r]}{r} \\[2ex] S_{23}\,\dfrac{\exp[ik''r]}{r} \\ \cdot \\ \cdot \\ \cdot \end{vmatrix} \quad \text{etc.,} \tag{11}$$

[8] V. Fock: *Zeits. f. Phys.*, **75**, 622 (1932).

and the completeness relation is

$$\underset{n}{S}\,\Psi_n(r)\widetilde{\Psi}_n^*(r') = \frac{\delta(r-r')}{4\pi rr'}\,I\,, \tag{12}$$

where I is the unit matrix and $\widetilde{\Psi}_n$ is the transposed row vector. Eq. (12) yields the unitarity of the complete S-matrix together with relations analogous to (7) for S_{11}, S_{22}, etc. and for the off-diagonal elements S_{12}, S_{13}, etc., with $|c|^2=0$.

3. – Bounds on scattering amplitude residues.

The upper bounds for the residues of the scattering amplitude $f(k)$ can be shown to follow from the analyticity property of eqs. (9) or (9′) together with some general properties of $\operatorname{Im} f(k)$ for real k. Thus for example $\operatorname{Im} f(k) > 0$ and $|\operatorname{Im} f(k)| \leqslant 1/k$ are sufficient to derive the inequalities (10) or (10′) from eqs. (9) or (9′). Since in the application to field theoretic models we shall consider combinations of sums and differences of amplitudes, upper bounds for the residues are derived below for various assumptions about the behavior of $\operatorname{Im} f(k)$ for real positive values of k.

CASE A. *$f(k)$ satisfies eq.* (9) *or* (9′).

We consider the function $F(k)$ defined by

$$F(k) = \frac{k-i\alpha}{k+i\alpha}\exp\,[2iak]f(k)\,. \tag{13}$$

The function $F(k)$ is regular in the upper half k-plane and satisfies the symmetry condition

$$F(k) = F(-k)^* \qquad \text{for real } k. \tag{14}$$

It also goes to zero as $k\to\infty$, $\operatorname{Im} k \geqslant 0$. Therefore

$$F(k) = \frac{1}{2\pi i}\int_{-\infty}^{\infty}\mathrm{d}k'\,\frac{F(k')}{k'-k}\,. \qquad \operatorname{Im} k > 0\,. \tag{15}$$

As $\operatorname{Im} k\to 0$, this is equivalent to

$$F(k) = \frac{P}{\pi i}\int_{-\infty}^{\infty}\mathrm{d}k'\,\frac{F(k')}{k'-k}\,. \tag{16}$$

1794

The real part of eq. (16) together with eq. (14) give

(17) $$\operatorname{Re} F(k) = \frac{2}{\pi} P \int_0^\infty \mathrm{d}k' \, \frac{k' \operatorname{Im} F(k')}{k'^2 - k^2} \, .$$

A function regular in the upper half k-plane which satisfies eq. (17) as a boundary condition is represented by

$$F(k) = \frac{2}{\pi} \int_0^\infty \mathrm{d}k' \, \frac{k' \operatorname{Im} F(k')}{k'^2 - k^2} \, ,$$

and in particular

(18) $$F(i\alpha) = \frac{2}{\pi} \int_0^\infty \mathrm{d}k' \, \frac{k' \operatorname{Im} F(k')}{k'^2 + \alpha^2} \, .$$

From eqs. (9) and (13) we have

(19) $$F(i\alpha) = \frac{\pi |c|^2}{\alpha^2} \exp\left[-2a\alpha\right] .$$

(For p-waves the sign is opposite). The definition of $F(k)$ is such that

(20) $$|\operatorname{Im} F(k')| \leqslant |F(k')| = |f(k')|$$

and from eqs. (18)–(20) we infer the inequality

(21) $$|c|^2 \exp\left[-2a\alpha\right] \leqslant \frac{2\alpha^2}{\pi^2} \int_0^\infty \mathrm{d}k' \, \frac{k' |f(k')|}{k'^2 + \alpha^2} \, .$$

In various applications $f(k)$ may be a scattering amplitude in which case $|f(k')| \leqslant 1/k'$ and eq. (21) gives

$$|c|^2 \leqslant \frac{\alpha}{\pi} \exp\left[2a\alpha\right] .$$

More commonly $\alpha =$ the boson mass $= \mu$,

(22) $$f(k) = \frac{\mu}{2\omega} \left[f_1(k) - f_2(k)\right] ,$$

where f_1 and f_2 are the amplitudes for a boson and its charge conjugate and therefore

(23) $$|c|^2 \leqslant \frac{4\mu}{\pi^2} \exp\left[2a\mu\right] .$$

CASE B. *$f(k)$ satisfies eq.* (9), $\operatorname{Im} f(k') \geqslant 0$ *for k' real and positive,* $|f(k')| \leqslant 1/k'$.

The function $F_1(k)$ defined by

(24) $$F_1(k) = \frac{i\alpha - k}{i\alpha + k} \exp[2iak]\left(f(k) + \frac{1}{2ik}\right) - \frac{1}{2ik},$$

is regular for $\operatorname{Im} k > 0$, finite for $k = k'$ real, and on the positive real axis satisfies the inequality

(25) $$0 \leqslant \operatorname{Im} F_1(k') \leqslant 1/k' .$$

Then $F_1(k)$ satisfies eq. (18)

(26) $$0 \leqslant F_1(i\alpha) = \frac{2}{\pi}\int_0^\infty \mathrm{d}k' \, \frac{k' \operatorname{Im} F_1(k')}{k'^2 + \alpha^2} \leqslant \frac{1}{\alpha}.$$

From eqs. (9), (24) and (26) we then obtain

(27) $$0 \leqslant -\frac{\pi |c|^2}{\alpha^2} \exp[-2\alpha a] + \frac{1}{2\alpha} \leqslant \frac{1}{\alpha},$$

or

(28) $$|c|^2 \leqslant \frac{\alpha}{2\pi} \exp[2\alpha a],$$

in agreement with eq. (10). The limit is one half of that which results from eq. (21).

CASE C. *$f(k)$ satisfies eq.* (9′) *(p-wave scattering),* $f(0) = 0$, $\operatorname{Im} f(k') \geqslant 0$ *for k' real and positive, and* $|f(k')| \leqslant 1/k'$.

We define the function

(29) $$F_2(k) = \frac{k - i\alpha}{k + i\alpha}\,\frac{k + i\beta}{k - i\beta} \exp[2ika]\left(f(k) + \frac{1}{2ik}\right) - \frac{1}{2ik}.$$

If we choose β to satisfy

(30) $$(\alpha^{-1} + a)\beta = 1$$

then

(31) $$F_2(0) = 0 .$$

Except for a pole at $k = i\beta$, this function satisfies all the conditions of

$F_1(k)$, and the dispersion relation

$$F_2(k) = \frac{K}{k^2+\beta^2} + \frac{2}{\pi}\int_0^\infty \mathrm{d}k' \, \frac{k' \, \mathrm{Im}\, F_2(k')}{k'^2 - k^2}, \tag{32}$$

with K an unknown constant (real), which depends upon the value of $f(k)$ at $k = i\beta$. But $F_2(0) = 0$, and the integral on the r.h.s. of eq. (32) is positive at $k = 0$. Therefore $K \leqslant 0$. From eq. (30) $\beta \leqslant \alpha$ so that we have finally

$$F_2(i\alpha) \geqslant 0 \, . \tag{33}$$

Thus eq. (9′), (29) and (33) give

$$-\frac{\pi |c_\mathrm{p}|^2}{\alpha^2} \exp[-2a\alpha] \left(1 + \frac{2}{a\alpha}\right) + \frac{1}{2\alpha} \geqslant 0 \, , \tag{34}$$

or

$$|c_\mathrm{p}|^2 \leqslant \frac{\alpha}{2\pi} \exp[2a\alpha] \left(1 + \frac{2}{a\alpha}\right)^{-1} . \tag{35}$$

The conditions of cases (A), (B), (C), lead to the inequalities (22) or (23), (28) and (35), which will be used later.

4. – Bound states and ghosts.

If $f(k)$ has more than one bound state, the limitations of the preceding section will either be strengthened or will disappear depending upon the relative signs of the residues at the bound states. For potential scattering and many field theory problems the signs of the bound state residues are fixed by the positive normalization implied in eq. (3). If there are two bound states at $k = i\alpha$ and $k = i\alpha'$, then eq. (9) will be replaced by

$$\exp[2iak] \left(f(k) + \frac{4\pi |c|^2}{k^2 + \alpha^2} + \frac{4\pi |c'|^2}{k^2 + \alpha'^2} \right) = R(k) \, . \tag{36}$$

The procedure which leads to eq. (21) will then give

$$\left| |c|^2 \frac{\exp[-2\alpha a]}{\alpha^2} + \frac{|c'|^2 \exp[-2\alpha' a]}{(\alpha + \alpha')^2} \right| \leqslant \frac{2}{\pi^2} \int_0^\infty \mathrm{d}k' \, \frac{k' \, |f(k')|}{k'^2 + \alpha^2} \, . \tag{37}$$

If, in a formal way $|c|^2$ is allowed to exceed the limit given by eq. (21),

then $|c'|^2$ can no longer be positive. For the potential problem this is impossible (because of the positive metric) and the bound state at $k=i\alpha'$ would then be a ghost. In the pion-nucleon system, the possibility of bound isobars for $\pi^+ + p$ can lead to expressions of the type (36) with opposite signs for the terms in $|c|^2$ and $|c'|^2$, because in this problem $f(k)$ is not a scattering amplitude but μ/ω times the difference of the elastic scattering amplitudes for $\pi^- + p$ and $\pi^+ + p$. The equality in signs for the $|c|^2$ and $|c'|^2$ terms will hold only if $f(k)$ is a scattering amplitude itself, is a sum of scattering amplitudes, or is a difference of scattering amplitudes where however only one of the amplitudes represents a particle which can have bound states. In all of these cases the residue has an upper limit which can be exceeded only by the introduction of a «ghost» state with negative normalization [1].

5. – Field theory with finite range sources.

We consider the scattering in a given angular momentum state of a boson by a source whose interaction is not necessarily causal but which is confined to a region $r<a$. The only significant complication beyond Sect. 2 is that the boson's antiparticle need not be identical with the boson itself. This gives rise to the complication that the functions $R(k)$ of eq. (9), (9') can have branch points at $k=i\mu$, where μ is the boson mass. Such branch points prevent the immediate application of eq. (15). This is the same kind of complication that exists in the usual derivation of dispersion relations for the scattering amplitude from a causal interaction, where it proves most convenient to consider separately the sum of the amplitudes for the boson and its antiparticle, and μ/ω times the difference [2]. Neither combination has a branch at $k=i\mu$. The only essential difference between the analytic properties of the usual total scattering amplitude from a causal interaction and the amplitude for a single partial wave from any interaction which vanishes beyond $r=a$ is the behavior at infinity. A necessary property of the scattering amplitude for our applications is the particular bound that can be put on the single partial wave amplitude for real momenta, and which the total amplitude does not necessarily obey.

It is well known that the coefficient of the residue of the scattering amplitude gives one definition for the square of the renormalized coupling constant, and this residue will be limited in particular cases by the arguments of Sect. 2.

The properties which we want to establish for the scattering amplitude for a single partial wave can be derived in a manner exactly analogous to the technique used to establish the dispersion relations for the total scattering amplitude. It will however not be necessary to assume the interaction to be casual.

For a boson described by a field operator $\varphi(\boldsymbol{r}, t)$ obeying the equation

$$(\square^2 - \mu^2)\varphi(\boldsymbol{r}, t) = j(\boldsymbol{r}, t) \tag{38}$$

the elastic scattering amplitudes can be conveniently obtained by use of the reduction formulae [9],

$$M^+(\omega, \boldsymbol{k}, \boldsymbol{k}') = i\int \mathrm{d}t \int \mathrm{d}\boldsymbol{r} \int \mathrm{d}\boldsymbol{r}' \exp[i\omega t] \exp[i\boldsymbol{k}\cdot\boldsymbol{r}] \exp[-i\boldsymbol{k}'\cdot\boldsymbol{r}'] \cdot \\ \cdot \langle I | \theta(t)[j^*(\boldsymbol{r}', t), j(\boldsymbol{r}, 0)] - \delta(t)[j^*(\boldsymbol{r}', t), \dot{\varphi}(\boldsymbol{r}, 0)] | I \rangle , \tag{39}$$

$$M^-(\omega, \boldsymbol{k}, \boldsymbol{k}') = -i\int \mathrm{d}t \int \mathrm{d}\boldsymbol{r} \int \mathrm{d}\boldsymbol{r}' \exp[i\omega t] \exp[i\boldsymbol{k}\cdot\boldsymbol{r}] \exp[-i\boldsymbol{k}'\cdot\boldsymbol{r}'] \cdot \\ \cdot \langle I | \theta(t)[j(\boldsymbol{r}', t), j^*(\boldsymbol{r}, 0)] - \delta(t)[j(\boldsymbol{r}', t), \dot{\varphi}^*(\boldsymbol{r}, 0)] | I \rangle . \tag{40}$$

The state $|I\rangle$ is the state of the scatterer; $\boldsymbol{k}$ and $\boldsymbol{k}'$ are the incident and final momenta of the boson; $\omega^2 - \mu^2 = k^2 = k'^2$. M^- and M^+ refer to the scattering amplitude for the boson and its antiparticle (e.g. π^- and π^+) respectively. We see from eq. (39) and (40) that if

$$j(\boldsymbol{r}, t) = 0 , \qquad |\boldsymbol{r}| > a. \tag{41}$$

Then $M^{\pm}(\omega, \boldsymbol{k}, \boldsymbol{k}') \exp[2iak]$ is a regular function of ω, $\mathrm{Im}\,\omega > 0$ [10] and fixed angle between $\boldsymbol{k}$ and $\boldsymbol{k}'$. The s-wave amplitude

$$f^{\pm}(\omega) = (4\pi)^{-2} \int \mathrm{d}\Omega_{\hat{k}} \int \mathrm{d}\Omega_{\hat{k}'} M^{\pm}(\omega, \boldsymbol{k}, \boldsymbol{k}') . \tag{42}$$

then also has the property that $f^{\pm}(\omega)\exp[2iak]$ is regular for $\mathrm{Im}\,\omega > 0$. The same statement is true for any partial wave amplitude. Also eqs. (39) and (40) contain the crossing symmetry [11] for real ω:

$$M^-(\omega, \boldsymbol{k}, \boldsymbol{k}')^* = M^+(-\omega, -\boldsymbol{k}, -\boldsymbol{k}') , \tag{43}$$

which gives

$$f^-(\omega)^* = f^+(-\omega) . \tag{44}$$

Now from eqs. (39), (40) and (42) we see that the combinations $[f^+(\omega) + f^-(\omega)]$ and $(\mu/\omega)[f^-(\omega) - f^+(\omega)]$ are real functions of k and ω^2 so that

---

[9] H. Lehmann, K. Symanzik and W. Zimmermann: *Nuovo Cimento*, **1**, 205 (1955).

[10] R. Oehme: *Phys. Rev.*, **102**, 1174 (1956); Umezawa and Kamefuchi: *Prog. Theo. Phys.* **6**, 543 (1951).

[11] M. Gell-Mann and M. L. Goldberger: *Proceedings of the Fourth Annual Rochester Conference on High Energy Nuclear Physics* (1954).

in k-space they will have no branch at $k = i\mu$. This is most apparent when the time integrations in eqs. (39) and (40) are performed and a complete set $|m\rangle$ of energy eigenfunctions is used to obtain the Low equations ([12])

$$(45)\qquad f^+(\omega) = \sum_m \left\{\frac{|\langle I|J^*(k)|m\rangle|^2}{E_m - E_I - \omega - i\varepsilon} + \frac{|\langle I|J(k)|m\rangle|^2}{E_m - E_I + \omega + i\varepsilon}\right\},$$

$$(46)\qquad f^-(\omega) = \sum_m \left\{\frac{|\langle I|J(k)|m\rangle|^2}{E_m - E_I - \omega - i\varepsilon} + \frac{|\langle I|J^*(k)|m\rangle|^2}{E_m - E_I + \omega + i\varepsilon}\right\},$$

with

$$(47)\qquad \langle I|J(k)|m\rangle = \int \mathrm{d}\boldsymbol{r}\,\frac{\sin kr}{kr}\,\langle I|j(\boldsymbol{r}, 0)|m\rangle\,.$$

The last term on the r.h.s. of eqs. (39) and (40) changes nothing, often vanishes, and has been dropped. The combinations of eqs. (45) and (46) with the condition derived from eq. (41) gives two functions of k:

$$(48)\qquad \exp[2iak]\frac{f^+(\omega) - f^-(\omega)}{2} = \\ = \sum_m (E_m - E_I)\,\frac{|\langle I|J^*(k)|m\rangle|^2 + |\langle I|J(k)|m\rangle|^2}{(E_m - E_I)^2 - \mu^2 - k^2}\exp[2iak]\,,$$

$$(49)\qquad \exp[2iak]\frac{f^-(\omega) - f^+(\omega)}{2\omega} = \sum_m \frac{|\langle I|J(k)|m\rangle|^2 - |\langle I|J^*(k)|m\rangle|^2}{(E_m - E_I)^2 - \mu^2 - k^2}\exp[2iak]\,,$$

each of which is a regular function of k in the upper half k-plane except for poles whenever there is a state $|m\rangle$ such that the numerators do not vanish and $E_m - E_I < \mu$. Thus for the scattering of scalar negative «pions» by protons, if isobars are not present, the only such state is the neutron. The operator J acting to the right increases the charge by one, J^* decreases it by one. In the approximation of equal neutron and proton mass we have

$$(50)\qquad \exp[2iak]\frac{f^+(\omega) + f^-(\omega)}{2} = R(k)\,,$$

$$(51)\qquad \exp[2iak]\left[\frac{f^-(\omega) - f^+(\omega)}{2\omega} + \frac{|\langle p|J(i\mu)|n\rangle|^2}{k^2 + \mu^2}\right] = \bar{R}(k)\,,$$

where $R(k)$ and $\bar{R}(k)$ are regular functions of k in the upper half-plane.

The fundamental results, eqs. (50) and (51), can also be obtained in a manner quite analogous to eqs. (9) or (9′) from the assumption that in the presence of the scatterer the equal time commutation rules remain valid outside

---

([12]) F. Low: *Phys. Rev.*, **97**, 1392 (1955).

of the interaction region,

$$[\varphi(\boldsymbol{r}),\, \pi^*(\boldsymbol{r}')] = i\delta(\boldsymbol{r} - \boldsymbol{r}')\,, \tag{52}$$

$$[\varphi(r),\, \varphi^*(r')] = 0\,, \tag{53}$$

$$[\pi(r),\, \pi^*(r')] = 0\,. \tag{54}$$

Then with a_n and $b_{n'}$ the usual annihilation operators for negative and positive mesons in states n and n', we may expand the wave operators φ and π in terms of exact wavefunctions analogous to eq. (1) or (11) instead of the more conventional plane waves. If the negative meson has a bound state at $\omega = 0$, the commutation rules of eqs. (52), (53) and (54) give respectively

$$\int\limits_{-\infty}^{\infty} \exp\,[ik(r + r')][S_-(k) - S_+(k)]\,\mathrm{d}k = 0\,, \tag{55}$$

$$\int\limits_{-\infty}^{\infty} \exp\,[ik(r + r')][S_-(k) - S_+(k)]\,\frac{\mathrm{d}k}{\omega} = -\,8\pi^2\,|c|^2 \exp\,[-\,\mu(r + r')]\,, \tag{56}$$

$$\int\limits_{-\infty}^{\infty} \exp\,[ik(r + r')][S_-(k) - S_+(k)]\omega\,\mathrm{d}k = 0\,. \tag{57}$$

The S-matrix elements S^- and S^+ refer to the elastic scatteringa mplitudes for negative and positive mesons. The unknown constant c normalizes the bound state as in eq. (2). The eqs. (55) and (56) express the analytic properties given for the scattering amplitudes in eqs. (50) and (51) and are a consequence of a generalization of the completeness argument of Sect. 2.

6. – Application to coupling constants.

For a Yukawa coupling of scalar mesons, in eq. (51)

$$|\langle p\,|J(i\mu)\,|\,n\rangle\,|^2 = 2g_0^2\left|\int \mathrm{d}\boldsymbol{r}\varrho(\boldsymbol{r})\,\frac{\sinh \mu r}{\mu r}\,\langle p\,|\tau_+|\,n\rangle\,\right|^2 = 2g^2\,. \tag{58}$$

Here g^2 is the renormalized and g_0^2 is the unrenormalized coupling constant squared (in unrationalized units in which $e^2 = 1/137$). Actually the renormalized coupling constant is more conventionally defined without the $\sinh \mu r/$

term of eq. (58), i.e. by the vertex operator for $\omega = 0$, $k = 0$, rather than $\omega = 0$, $k = i\mu$, but the difference is small, $\sim (\mu a)^2$. The definition $2g^2 = p|J(i\mu)|n\rangle|^2$ is also that used in dispersion relation deductions of g^2.

From eqs. (51), (58), (44) and (23) (case A, Sect. 2) we obtain

$$g^2 \leqslant \frac{8}{\pi} \exp [2a\mu] . \tag{59}$$

The coupling constant g^2 can exceed this limit while not violating the positiveness of the metric if there exists a doubly charged bound state of $\pi^+ + p$ so that the second term on the r.h.s. of eq. (49) contributes a pole. Thus g^2 exceeding the limit of eq. (59) is a sufficient condition for the appearance of a doubly charged isobar ([13]). If such isobars are not present, then ghost states of the $\pi^- + p$ system (with negative g^2) must be introduced (cf. eq. (37)). These conclusions and the inequality (59) in no way depend upon the fact that only s-wave coupling was considered in this example.

When a bound state occurs for a state $|m\rangle$ such that $E_m \neq E_I$ then we obtain poles for the sum in eq. (48). All of the residues have the same sign and so rigorous upper bounds can be given, bounds which cannot be violated so long as the metric is positive definite. Thus for example if the neutron-proton mass difference is not neglected, eqs. (48), (58) and eq. (28) (case B, Sect. 3) give

$$g^2(M_n - M_p) \leqslant \mu \exp [2a\mu] , \tag{60}$$

for an s-wave coupling, and from eq. (35) (case C, Sect. 3)

$$g^2(M_n - M_p)\left(1 + \frac{2}{a\mu}\right) \leqslant \mu \exp [2a\mu] , \tag{61}$$

for p-wave coupling. Eqs. (60) and (61) give the interesting result that as long as the meson has no interaction with the nucleon outside of some radius a the mass difference between neutron and proton must approach zero as g^2 approaches infinity, or even as a approaches zero in the case of p-wave coupling. This result does not depend upon the nature of other interactions which may simultaneously be present, or even any assumed equality of the « bare » neutron and proton masses. Similar mass equalities will exist in the nucleon-hyperon system as the K-coupling become infinitely strong.

In the notation of the previous section, the Lee model ([14]) has $f^+(\omega) = 0$,

([13]) See in this connection C. GOEBEL: *The use of the Chew-Low Equation in Strong Coupling*, to be published in the *Phys. Rev.*

([14]) T. D. LEE: *Phys. Rev.*, **95**, 1329 (1954). Cfr. also ref. ([1]) and K. FORD: *Phys. Rev.*, **105**, 320 (1957).

$f^-(\omega) \neq 0$. The crossing theorem, eq. (44), can formally be satisfied by writing $f^-(\omega) = \theta(\omega)\, f(\omega)$ and $f^+(\omega) = \theta(-\omega)\, f^*(-\omega)$ for real ω. Near $\omega = 0$, $f^-(\omega) \cong$ $\cong -\theta(\omega)\; g^2/\omega$ and $f^+(\omega) \cong \theta(-\omega) g^2/\omega$ so that $[f^-(\omega) - f^+(\omega)]/\omega \sim -g^2/\omega^2 \cdot$ $\cdot[\theta(\omega) + \theta(-\omega)] = -g^2/(k^2+\mu^2)$ has no branch point at $k = i\mu$ and satisfies eq. (51). Therefore g^2 has an upper limit which is one half that of eq. (59). Since the $\pi^+ - \mathrm{p}$ system is non-interacting and therefore can have no isobars, this limit can only be exceeded if a ghost state also appears. Actually in the particular case of the Lee model, the scattering amplitude approaches zero as the range a approaches zero. The integral which gives the r.h.s. of eq. (59) must then vanish as $a \to 0$, and a ghost state will occur for any non-zero g^2 in this limit. Generally any model in which the $\pi^+ + \mathrm{p}$ system can have no bound state will have to have a ghost as $g^2 \to \infty$. From eq. (60) and (61) we also obtain the result that a model in which the observed neutron and proton (or Λ and Σ, or proton and Σ) masses were not exactly equal in the limit of $g^2_{\mathrm{np}\pi}$ (or $g^2_{\Lambda\Sigma\pi}$ or $g^2_{\mathrm{p}\pi\mathrm{K}}$) approaching infinity would also have a ghost state.

If interactions among pions, K-mesons and strange particles are described by the kind of model which has as its property the regularity of the functions (48) and (49), i.e. a limited range interaction, an upper limit may be obtained for the renormalized coupling constants associated with many of the vertices. In the case of the vertex matrix element describing $\Sigma^- \leftrightarrow \pi^- - \Lambda^0$, the particle has isotopic spin zero and $f^-(k)$ and $f^-(k)$, for the scattering of π^- and π^- by Λ^0 are identical. Then only eq. (48) remains. The coupling constant is defined in analogy with eq. (58) so that $|\langle\Sigma^+|J(i\alpha)|\Lambda^0\rangle|^2 \equiv 2g^2_{\Lambda\Sigma\pi}$ and from eq. (48) and eq. (28) (case B in Sect. 3) we obtain

$$g^2_{\Lambda\Sigma\pi} \leqslant \frac{\alpha}{M_\Sigma - M_\Lambda} \exp\,[2a\alpha]\,, \tag{62}$$

with

$$\alpha = \sqrt{\mu^2 - (M_\Sigma - M_\Lambda)^2}\,.$$

Again as $g^2_{\Lambda\Sigma\pi} \to \infty$, $M_\Sigma \to M_\Lambda$. A stronger upper limit obtains if the pion, which contributes to the vertex, is in a p-wave, as would, for example, be necessary in a theory with a universal pion-baryon coupling. Then from case C, Sect. 3 we obtain

$$g^2_{\Lambda\Sigma\pi} \leqslant \frac{\alpha \exp\,[2a\alpha]}{(M_\Sigma - M_\Lambda)(1 + 2/a\alpha)}\,. \tag{63}$$

For a range a of one nucleon Compton wavelength this gives $g^2_{\Lambda\Sigma\pi} < \frac{1}{9}$ which is to be compared with the known $g^2_{\mathrm{np}\pi} \cong \frac{1}{12}$ For small a the max-

imum g^2 for p-wave coupling is proportional to a so that such g^2 are much more sensitive to the range than in the s-wave case.

Finally similar arguments may be applied to the strength of the coupling of K-mesons to nucleons and hyperons. For example the vertex $\Sigma^- \leftrightarrow \pi + K^-$ with a coupling constant $g_{n\Sigma K}$ can contribute a pole at $k = i\sqrt{M_K^2 - (M_\Sigma - M_n)^2}$ in both eqs. (48) and (49). Here f^- is the amplitude for elastic K^--n scattering and f^+ for elastic K^+-n scattering. In a manner analogous to that which leads to eq. (59) the analogue of eq. (51) leads to

$$g^2_{n\Sigma K} \leqslant \frac{8}{\pi} \exp[2a\alpha'] \,, \tag{64}$$

where

$$\alpha' = \sqrt{M_K^2 - (M_\Sigma - M_n)^2} \,, \tag{65}$$

and the analogues of eqs. (60) and (61) are

$$g^2_{n\Sigma K} \leqslant \frac{\alpha'}{M_\Sigma - M_n} \exp[2a\alpha'] \,, \tag{66}$$

for s-wave coupling and

$$g^2_{n\Sigma K} \leqslant \frac{\alpha'}{(M_\Sigma - M_n)(1 + 2/a\alpha')} \exp[2a\alpha'] \,. \tag{67}$$

for p-wave coupling. Because of the large K-meson mass, the restriction on $g^2_{n\Sigma K}$ is less severe that that on $g^2_{\Lambda\Sigma\pi}$. For a of the order of the nucleon Compton wavelength, the limits in eqs. (64), (66) and (67) are all greater than 0.7. A similar set of limits exists for $g^2_{n\Lambda K}$ and the appropriately weighted sum of $g^2_{n\Lambda K}$ and $g^2_{n\Sigma K}$ (cf. eq. (37)). Similar arguments and limits can be made for $g^2_{\Lambda\Xi K}$ corresponding to $\Lambda^0 + K^- \leftrightarrow \Xi^-$.

The replacement of the restriction that the interaction vanishes outside of $r = a$ by a more gradual fall-off, will in general prevent the establishment of rigorous model-independent limits on the coupling strenght. Even if the interaction falls off exponentially or with a Yukawa tail, the analytic properties of the scattering amplitude are no longer simple. For example the s-wave scattering amplitude in an exponential potential has an infinite number of poles in the upper half k-plane, none of which need correspond to a bound state [15]. Even the signs of the residues at these « redundant » poles is not fixed. We know of no reason for similar difficulties to be absent in field theory. Even the relativistic transformation to the center of mass system, in which individual partial waves may conveniently be projected, involves branch points

---

[15] S. T. MA: *Phys. Rev.*, **69**, 668 (1946).

which can make the individual partial wave scattering amplitude very complicated and exclude the simple dispersion type relations such as those of Sect. **3**, which lead to the coupling constant bounds.

* * *

It is a pleasure to thank the National Science Foundation and the John Simon Guggenheim Foundation for their generous support. We are happy to express our appreciation to Professor N. BOHR and the staff of the Institute for Theoretical Physics in Copenhagen and Professor E. AMALDI and the Istituto di Fisica in Rome for their kind hospitality.

RIASSUNTO (*)

Si assume che l'interazione di un campo bosonico con una sorgente si annulli oltre il raggio a; entro tale raggio non si postulano speciali proprietà della sorgente. Si dimostra che, con tale modello, per l'interazione di pioni o mesoni K con nucleoni e iperoni si possono porre per le costanti di accoppiamento rinormalizzate $g^2_{\Lambda\Sigma\pi}$, $g^2_{\mathrm{p}\Sigma\mathrm{K}}$ e $g^2_{\mathrm{p}\Lambda\mathrm{K}}$, corrispondenti agli elementi di matrice per i processi $\overline{\mathrm{K}}+\mathrm{p} \leftrightarrow \Sigma$ e $\mathrm{K}^-+\mathrm{p} \leftrightarrow \Lambda^0$, rigorosi limiti superiori dipendenti soltanto da a e dalle masse delle particelle. Per l'interazione pione-nucleone si trova un $g^2_{\mathrm{np}\pi}$ massimo, oltre il quale deve esistere uno stato del sistema $\pi^++\mathrm{p}$ dotato di carica doppia. Si trova che se $g^2_{\mathrm{np}\pi}$ tende all'infinito o se a tende a zero, la differenza tra le masse del neutrone e del protone si annulla indipendentemente da altre interazioni o dal fatto che le masse nude siano identiche. Risultati simili valgono per la differenza fra le masse di qualsiasi coppia di barioni se si trasformano l'una nell'altra con emissione o assorbimento di un singolo bosone. Finalmente si descrive una classe generale di modelli di teorie di campo che debbono sempre condurre a «fantasmi».

(*) *Traduzione a cura della Redazione.*

IL NUOVO CIMENTO   VOL. VIII, N. 6   16 Giugno 1958

The Intensity and Angular Distribution of Mu-Mesons 1100 Feet Underground (*).

C. A. RANDALL

Ohio University - Athens, Ohio

W. E. HAZEN

University of Michigan - Ann Arbor, Michigan

(ricevuto il 31 Marzo 1958)

Summary. — The results of the determination of the intensity and angular distribution of the μ-mesons at a depth of $8.5\cdot10^4$ g/cm² underground are $I = I_0 \cos^n \theta$ with $I_0 = (2.10 \pm 0.5)\cdot 10^{-6}\, s^{-1}\, cm^{-2}\, sr^{-1}$ and $n = 2.3 \pm 0.3$. The significance of the results in determining the parentage of the μ-mesons is discussed.

Certain features of high-energy cosmic-ray interactions can be inferred from observations of their high-energy descendants. The latter can be selected by making suitable observations underground. The review by the Cornell group [1] gives, in detail, the types of measurements, methods of analysis, and conclusions obtained from observations made underground.

In this report we give the results of a more accurate analysis of our data [2] for the intensity and angular distribution of μ-mesons at a depth of $8.5\cdot10^4$ g/cm².

The data were taken with a «telescope» consisting of two trays of counter tubes. The counter tubes were made from one inch O.D. tubing with 1/32 inch

(*) Assisted by the Office of Naval Research and the Atomic Energy Commission.

(1) P. H. BARRETT, L. M. BOLLINGER, G. COCCONI, Y. EISENBERG and K. GREISEN: *Rev. Mod. Phys.*, **24**, 133 (1952).

(2) C. A. RANDALL and W. E. HAZEN: *Phys. Rev.*, **81**, 144 (1951).

walls. The sensitive length was 28 in. The central six tubes in each bank were in contact but the outer tubes were separated by spacers, 3/16 in for the outermost spaces and 1/8 in for the next to outermost spaces. A 15 cm lead absorber between the counters reduced the number of coincidences due to vertically incident electrons to negligible proportions. Side-shower coincidences in which an electron triggered the bottom tray were negligible because of the 15 cm absorber above the tray and equivalent side shielding. Side showers in which an electron triggered the top tray are not negligible. The effect was evaluated with the aid of auxiliary experiments on the frequency and lateral distribution of electron secondaries from the mine ceiling plus the aid of a preliminary estimate of the angular distribution of the mesons. The effect was found to be small and calculable with sufficient accuracy.

Other corrections were small and calculable from data of auxiliary experiments, for example, the correction because of μ-mesons that dit not pass through counters but produced secondaries in the apparatus that did pass through counters.

As a means of determining the angular distribution and the absolute intensity, it proved more convenient to vary the tray separation (L) than to vary the telescope orientation.

The resulting gross counting rates and the rates that represent our best evaluation of the μ-meson fluxes are given in Table I. The μ-meson fluxes were obtained by subtracting the effects of side showers, etc., discussed above.

TABLE I. - *Gross counting rates and meson fluxes as a function of tray separation* (L).

L (in.)	Counting Rate (s^{-1})	Meson Flux ($s^{-1}\ cm^{-2}\ sr^{-1}$)
3 5/16	$4.06 \cdot 10^{-3}$	$4.02 \pm .13 \cdot 10^{-3}$
8	$3.17 \cdot 10^{-3}$	$3.03 \pm .11 \cdot 10^{-3}$
12	$2.28 \cdot 10^{-3}$	$2.16 \pm .06 \cdot 10^{-3}$
18	$1.51 \cdot 10^{-3}$	$1.42 \pm .06 \cdot 10^{-3}$
24	$1.08 \cdot 10^{-3}$	$0.99 \pm .04 \cdot 10^{-3}$

1. – Analysis.

The intensity of μ-mesons was approximated by the usual expression,

$$I = I_0 \cos^n \theta \tag{1}$$

and the expected fluxes through the telescope were calculated as a function of I_0, n, and L.

The calculation followed the general idea of GREISEN [3] that a twofold integration can be avoided in cases where the counter tube diameter is small compared with the separation of the tubes. The effect of the approximation was evaluated for the least favorable geometry and found to be negligible. In our case, we calculated the flux through all possible pairs of counters and formed the appropriate sums in order to find the total flux registered by the trays. The overlap of pairs involving adjacent counters was appreciable for small L. Corrections were made by calculating effective counter widths in all cases.

2. – Results.

The best fit to equation (1) corresponds to:

$$I_0 = (2.10 \pm 0.5)\cdot 10^{-6}\ \text{s}^{-1}\ \text{cm}^{-2}\ \text{sr}^{-1} \quad \text{and} \quad n = 2.3 \pm 0.3\ .$$

This value of n is significantly different from 3.1 ± 0.15, the logarithmic slope of the depth-intensity curve at this depth [1]. The Cornell group [1] have discussed in detail the implications of the difference in the two slopes in terms of the origin of the μ-mesons. Of course, the properties of the K-meson have become better known since the Cornell analysis was published and one now predicts a smaller difference between the decay effects of μ-mesons and K-mesons. At depths of 500 to 2 000 mwe, the value of m-n for K-μ decay is only 0.2 less than for π-μ decay (where m is the depth-intensity exponent and n is the zenith angle-intensity exponent). The difference $m - n$ in the present case is 0.8 ± 0.4, which slightly favors π-meson parentage.

The atmospheric temperature effect observed by SHERMAN [4] at the same depth favors the assumption of K-meson parentage (taking into account the now-known properties of K-mesons).

On the other hand, the Cornell experiments at about twice our depth favor K-parentage from the $m - n$ result and π-parentage from the temperature effect. Thus there is no indication of either a systematic discrepancy between the $m - n$ data and the temperature data or of a systematic change in parentage with depth, i.e., energy of the primaries. If one weights the measurements according to the stated uncertainties, an admixture of K-meson parents with the π-meson parents is slightly favored.

---

(3) K. I. GREISEN: *Phys. Rev.*, **61**, 212 (1942).
(4) N. SHERMAN: *Phys. Rev.*, **93**, 208 (1954).

* * *

We appreciated the assistance of the personnel of the Detroit Mine of the International Salt Company while the observations were being made and of Dr. BIBHA CHOWDHURI who aided in some of the calculations.

RIASSUNTO (*)

I risultati della determinazione dell'intensità e della distribuzione angolare dei mesoni μ alla profondità di $8.5\cdot 10^4$ g/cm^2 sotto terra sono $I = I_0 \cos^n \theta$ con $I_0 = (2.10 \pm 0.5)\cdot 10^{-6}$ s^{-1} cm^{-2} sr^{-1} e $n = 22.3 \pm 0.3$. Si discute il significato dei risultati in rapporto alla determinazione dell'origine dei mesoni μ.

(*) *Traduzione a cura della Redazione.*

IL NUOVO CIMENTO Vol. VIII, N. 6 16 Giugno 1958

Virtual Pion Effects in μ-Meson Capture.

L. Wolfenstein (*)

CERN - Genève

(ricevuto il 31 Marzo 1958)

Summary. — The μ-meson capture process contains an effective pseudoscalar interaction not present in the corresponding electron processes due to the decay of a single virtual pion emitted by the nucleon. The effect of this interaction on various possible observations is calculated for μ-meson capture in hydrogen and shown to be as large as 25%.

A number of recent papers (1-3) have discussed possible observations on the process $\mu^- + p \rightarrow n + \nu$; particular interest lies in the question whether the basic coupling responsible for this process is identical to that in β-decay. These theoretical discussions have considered the direct interaction indicated by diagram (*a*); in addition to these there are the corrections due to virtual pions, which are represented to lowest order in the pion-nucleon coupling constant by diagrams (*b*) and (*c*). The box in (*c*) represents a virtual nucleon-anti-nucleon pair. Diagram (*b*) has been considered (using fixed-source pion theory) by Finkelstein and Moszkowski (4), who show that it may result in an appreciable renormalization of the weak coupling constants and that

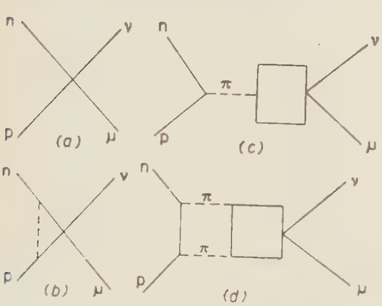

Fig. 1.

(*) On leave of absence from Carnegie Institute of Technology, Pittsburgh, Pa., USA.

(1) I. S. Shapiro, E. I. Dolinsky and L. D. Blohinčev: *Nucl. Phys.*, **4**, 273 (1957).
(2) K. Huang, C. N. Yang and T. D. Lee: *Phys. Rev.*, **108**, 1340 (1957).
(3) L. Wolfenstein: *Nuovo Cimento*, **7**, 706 (1958).
(4) R. J. Finkelstein and S. A. Moszkowski: *Phys. Rev.*, **95**, 1695 (1954).

this effect is approximately the same for μ-mesons and electrons. There is also a non-locality introduced by the virtual pion, but this is not very important because the momentum transfers involved are relatively small. In view of the unreliability of any calculation of diagram (*b*) and the higher-order corrections of this sort and in view of the possibility of additional direct weak interaction involving two (or more) pions such as those proposed by FEYNMAN and GELL-MANN (5) to cancel this diagram, it seems best to take diagram (*b*) into account by noting that renormalized coupling constants are used in (*a*).

Diagram (*c*) is of special interest for two reasons:

1) since it involves a single pion in the intermediate state, it of necessity corresponds to an effective pseudoscalar interaction between the four fields even though the direct interaction may not contain any pseudoscalar term;

2) since the diagram may be considered as involving the decay of a virtual pion, it should be of no importance for β-decay since pions are known experimentally not to decay into electrons;

thus even if diagram (*a*) were identical for electrons and μ-mesons, we should expect experimental differences due to diagram (*c*) (*). The calculation of diagram (*c*) may be performed using the fixed-source pion theory to treat the nucleon-pion vertex and using a phenomenological direct pion decay interaction to treat the transition of the virtual pion to a μ-meson and a neutrino. By using the empirical values of the renormalized pion-nucleon coupling constant and the lifetime of the free pion, one calculates the sum of all diagrams involving an intermediate state consisting of a single pion, including all possibilities, such as virtual hyperons, for the box. Since the virtual pion is off the energy shell by an amount between one and two pion masses, the use of these empirical values may be expected to introduce errors of the order of (m_π/M), (m_π = pion mass, M = nucleon mass). One obtains, of course, the same result if one assumes pion decay really occurs via a direct interaction. This calculation of diagram (*c*) has been outlined by LOPES (6); the result is equivalent to a direct pseudoscalar interaction between the four fermion fields

---

(5) R. P. FEYNMAN and M. GELL-MANN: *Phys. Rev.*, **109**, 193 (1958). More general reasons for considering direct weak pion interactions are given by S. WEINBERG: *Phys. Rev.*, **106**, 1301 (1957).

(*) The diagram could be ignored in β-decay even if the ratio of $\pi \to e + \nu$ to $\pi \to \mu + \nu$ were 10^{-4} as predicted by the universal V, A Fermi interaction. This difference between μ-meson capture and β-decay therefore is essentially due to the fact that the magnitude of this virtual pion correction depends on the lepton mass.

(6) J. L. LOPES: *Phys. Rev.*, **109**, 509 (1958).

with an effective coupling constant given by

$$|c_P'| = 9\cdot 10^{-5}\,\frac{m_\pi^2 + q_0^2}{M^2(m_\pi^2 + q^2)}\,, \tag{1}$$

where q is the four-momentum transfer and q_0^2 $(=\frac{1}{2}m_\pi^2)$ is the value of q^2 for capture in hydrogen. This is to be compared with the Fermi coupling constant (C_S or C_V) in β-decay of $1.0\cdot 10^{-5}/M^2$. While, as shown by LOPES [6], diagram (c) by itself can only explain something like 5% of the μ-meson captures in nuclei, its interference with the direct interaction (diagram (a)) cannot be ignored.

TABLE I. – *Observables for* $\mu^- + p \to n + \nu$ *calculated in various approximations. An equal mixture of Fermi* (G_F) *and Gamow-Teller* (G_G) *direct couplings is assumed.* (a) *and* (c) *refer to diagrams,* NR = *non-relativistic,* R = *relativistic.* + *and* — *refer to the sign of* (C_P'/G_G).

Observable	Direct Coupling	Diagram (a) NR	(a) NR plus (c)		(a) R plus (c)	
			+	—	+	—
I_0	$G_F = G_G$	$4G^2$	$3.28G^2$	$5.17G^2$	$3.24G^2$	$5.23G^2$
	$G_F = -G_G$	$4G^2$	$3.28G^2$	$5.17G^2$	$3.66G^2$	$5.65G^2$
A	$G_F = G_G$	0	−.22	+.23	−.11	.31
	$G_F = -G_G$	0	−.22	+.23	−.21	.22
$-a/I_0 = \langle\boldsymbol{\sigma}_n\rangle\cdot\mathbf{p}_n$	$G_F = G_G$	0	+.29	−.18	.17	−.27
	$G_F = -G_G$	1	.93	.96	.94	.96
$\frac{1}{4}(\lambda_+ - \lambda_-)/\bar{\lambda}$	$G_F = G_G$	0	.10	−.06	.13	−.02
	$G_F = -G_G$	−1	−.93	−.96	−.93	−.96

We illustrate in Table I the effect of diagram (c) for the capture in hydrogen on some of the observables discussed before [3]:

1) I_0, which is proportional to the capture rate,

2) A, the neutron asymmetry for polarized μ-mesons, and

3) $(-a)/I_0$, the longitudinal polarization of the neutron for unpolarized μ-mesons, as well as

4) $\frac{1}{4}(\lambda_+ - \lambda_-)/\bar{\lambda}$, the relative difference between the capture rates in the $F=1((\lambda_+)$ and $F=0\,(\lambda_-)$ hyperfine states of the μ-mesic atom K-shell ([7]).

If the nucleons are treated non-relativistically in diagram (a) and no direct pseudoscalar interaction is assumed, the results depend on G_F, G_G, and C'_P (assuming two-component neutrino theory) and may be calculated from the published equations ([3,7]). For Table I we have assumed $G_F = \pm G_G$ and $C'_P = 9G_F$, as suggested by Equation (1). The relativistic effects (on diagram (a)) associated with the final neutron velocity are illustrated on the further assumption that G_F is vector and G_G is axial-vector. The results depend greatly on the sign of C'_P relative to G_G; the capture rate changes by about 50% and the neutron asymmetry (of about 20%) reverses with a change of sign of C'_P. If it is assumed that $\pi \to \mu + \nu$ is primarily due to an intermediate nucleon pair which decays by means of the axial-vector coupling ($C_A = G_G$), the contribution of diagram (c) is directly proportional to G_G and the relative sign is determined in principle. Using the lowest order perturbation theory for this case, we find C'_P has the same sign as G_G; however, we cannot prove this in general. This assumption about $\pi \to \mu + \nu$ requires the introduction of some interaction to cancel out the corresponding $\pi \to e + \nu$ decay, as has been suggested by HUANG and LOW ([8]), for example. If, on the other hand, it is concluded from the absence of $\pi \to e + \nu$ that some different interaction is primarily responsible for $\pi \to \mu + \nu$, such as a direct coupling or a coupling involving virtual hyperons that does not exist for electrons ([9]), the relative sign cannot be determined in principle.

We should consider also the possibility that a direct pseudoscalar interaction contributes to diagram (a). Such an interaction present for μ-mesons and not for electrons could be assumed to be the primary mechanism for $\pi \to \mu + \nu$. Two possibilities for this coupling constant C_P must be considered:

a) C_P is considerably less than C'_P. Such a magnitude for C_P appears to be sufficient to produce the experimental rate for $\pi \to \mu + \nu$ if the calculation is made using a reasonable cut-off. In this case the direct pseudoscalar interaction is essentially unobservable because the indirect process (c), which cannot be calculated exactly, is much larger;

([7]) J. BERNSTEIN, T. D. LEE, C. N. YANG and H. PRIMAKOFF: *Phys. Rev.* (to be published).

([8]) K. HUANG and F. LOW: *Phys. Rev.*, **109**, 1400 (1958).

([9]) B. D'ESPAGNAT and J. PRENTKI: *Nucl. Phys.*, 6, 596 (1958). The interaction as explicitly assumed in this paper does include the relative sign, but it does not seem essential.

b) C_P is comparable to or bigger than C'_P. In this case the direct pseudoscalar interaction could be observed and would be expected to add constructively (*) to the indirect process (*c*). However, such a large value would seem unlikely.

The relatively large contribution of diagram (*c*) raises the question whether diagrams involving intermediate states consisting of two or more pions (such as (*d*)) can be neglected. (We are not considering here an expansion in powers of the pion-nucleon coupling constant, but rather in the number of pions appearing alone). Qualitative arguments can be given indicating that these diagrams are not important, but in view of the impossibility of the calculation, such arguments must be considered chiefly as hopes. Two general remarks about the two-meson diagrams (such as (*d*)) may be made:

1) These can contribute only to effective scalar and vector direct couplings (+). Neglecting the non-locality corresponding to the two virtual pions, these diagrams may be considered as a further renormalization of the Fermi coupling constant G_F.

2) These diagrams are important both for μ-mesons and electrons, but there appears to be no way of comparing their contributions for the two cases. The expectation that the virtual decay $\pi+\pi \rightarrow e+\nu$ should be quite as likely as $\pi+\pi \rightarrow \mu+\nu$ may be made plausible by noting that if one of the π-mesons is replaced by a K-meson, the diagrams for these virtual decays become the diagrams for the equally probable decays $K \rightarrow e+\nu+\pi$ and $K \rightarrow \mu+\nu+\pi$.

In the light of this discussion, a reasonable program for analysis of the initial data on the process $\mu^- + p \rightarrow n + \nu$ would seem to be to consider diagram (*a*) non-relativistically with G_F and G_G as unknowns and diagram (*c*) using Eq. (1) with the sign of C'_P unknown. One omits in this way the re-

(*) Assuming the π-meson interaction is of the γ_5 type, the relation between diagrams (*a*) and (*c*) is closely related to that between a free pion propagator and its self-energy corrections. From this one may conclude that C_P and C'_P have the same sign.

(+) This follows from the fact that the intermediate state of two spin-zero particles of the same parity is defined by two four-vectors, which may be chosen as P_μ and Q_μ, the sum and differences respectively, of the four-momenta of the pions. Charge independence requires that this state has isospin one and so is odd in Q_μ. The virtual decay of the two pions may thus have the forms $\bar{\psi}Q_\mu P_\mu \psi$, $\bar{\psi}Q_\mu\gamma_\mu\psi$, $\bar{\psi}Q_\mu P_\nu \gamma_\mu \gamma_\nu \psi$ where ψ is the lepton spinor. The last of these reduces to the scalar and vector forms by the use of the Dirac equation. This argument assumes parity conservation; however, the conclusion is correct if parity is conserved in the strong interactions only. It may be noted that a similar vector term associated with the exchange of two pions has been suggested as an extra direct interaction (5).

1814

latívistic effects, which are expected to be of the order of 10 % or less and the uncertainty of C'_P, which should not be more than a 5 % effect on the capture rates. Diagrams (*b*) and two-pion diagrams such as (*d*) are considered as renormalizing the coupling constants in (*a*). One should keep in mind the possibilities of a large direct pseudoscalar interaction or of cancellations between C_V and C_A or C_S and C_T that would make relativistic effects more important ([3]). All these considerations, of course, remain important for the capture process in complex nuclei. It may be noted also that the current associated with the virtual pion in diagram (*c*) should be included in the calculation of the radiative μ-meson capture ([2]).

* * *

I am indebted to Dr. S. FUBINI for some discussions.

Note added in proof.

In a paper to be published M. L. GOLDBERGER and S. B. TREIMAN, using « dispersion relation techniques », support our conclusion that the main effects of virtual pions are (*a*) a renormalization (dependent on the four-momentum transfer) of the interaction constants and (*b*) an effective pseudoscalar interaction given by our equation (1). Their discussion also yields a positive sign for (C'_P/G_G) provided $\pi \to \mu + \nu$ is due to the axial-vector coupling G_G.

RIASSUNTO (*)

Il processo di cattura del mesone μ contiene un'interazione pseudoscalare effettiva che non è presente nei corrispondenti processi elettronici dovuti al decadimento di un singolo pione virtuale emesso dal nucleone. Si calcola per la cattura del mesone μ in idrogeno l'effetto di tale interazione su varie possibili osservazioni e si dimostra che essa raggiunge il 26 %.

(*) *Traduzione a cura della Redazione.*

On Nuclear Magnetic Moment in Meson Field Theory.

S. K. Kundu

Department of Theoretical Physics,
Indian Association for the Cultivation of Science - Calcutta (India)

(ricevuto il 1° Aprile 1958)

Summary. — The nuclear magnetic moment is studied in pseudovector-pseudoscalar charged meson theory with a space-time extended source model and the equivalent energy-momentum cut-off.

1. – Introduction.

It is well known that Chew's [1] model is successful in explaining the low energy meson-nucleon processes in pv-ps theory. But the neglect of nucleon recoil seems to be one of its inherent drawbacks that can not be accounted fully from usual physical processes. In the present paper the effect of nucleon recoil is considered and the magnetic moment of proton and neutron is calculated with the idea that the source-function is extended both in space and time. And this space-time extension of the source, when translated by a Fourier transformation into-energy-momentum space, simply states that there should be an upper limit to the emitted virtual meson energy-momentum four vector. To obtain reasonable values for the meson and nucleon current contributions to the nuclear magnetic moment the value of the cut-off is taken as 2.334 μ, and for the coupling constant the value .015 is used.

---

[1] G. F. Chew: *Phys. Rev.*, **94**, 1748 (1954).

2. – Method of calculation.

The matrix element corresponding to the Feynman diagram I is given by

$$(1)\qquad M_{\mathrm{I}} = \frac{ef^2}{\pi i\mu^2}\int \mathrm{d}^4k\, v^2(|k|)\, U^*_{p_2}\gamma_5 k(p_2-k-m)^{-1}a(q)(p_1-k-m)^{-1}\gamma_5 k\, U_{p_1}(k^2-\mu^2)^{-1}\,,$$

where we we write $\mathrm{d}^4k = (\mathrm{d}k_1\mathrm{d}k_2\mathrm{d}k_3\mathrm{d}k_4)/4\pi^2 i$, $f^2/\pi i$ for one virtual meson and $\gamma_5 k\mu^{-1}v(|k|)$ for one meson vertex in pv-ps theory.

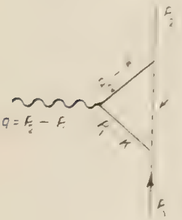

Fig. 1.

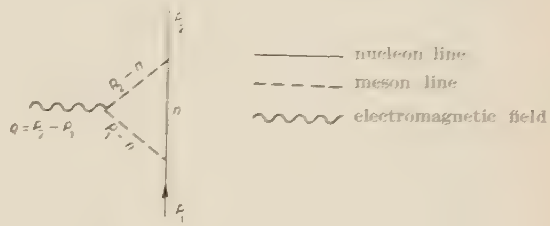

Fig. 2.

Replacing $U^*_{p_2}\gamma_5 k(p_2-k-m)^{-1}$ by $U^*_{p_2}(-\gamma_5)[1+2m/(p_2-k-m)]$ and $\gamma_5 k(p_1-k-m)^{-1}U_{p_1}$ by $[1-2m/(p_1-k-m)]\gamma_5 U_{p_1}$, and neglecting terms that do not contribute to the nuclear magnetic moment, relation (1) reduces to

$$(2)\qquad M_{\mathrm{I}} = -\frac{ef^2}{\pi i\mu^2}(4m^2)\int \mathrm{d}^4k\, v^2(|k|)\, U^*_{p_2}\gamma_5(p_2-k-m)^{-1}\cdot$$
$$\cdot a(q)(p_1-k-m)^{-1}\gamma_5 U_{p_1}(k^2-\mu^2)^{-1}\,.$$

Similarly for diagram II, we find in terms of the average nuclear momentum $\boldsymbol{p}=(\boldsymbol{p}_1+\boldsymbol{p}_2)/2$

$$(3)\qquad M_{\mathrm{II}} = \frac{ef^2}{\pi i\mu^2}(4m^2)\int \mathrm{d}^4n\, v^2(|n|)\, U^*_{p_2}\gamma_5[(\boldsymbol{p}_2-\boldsymbol{n})^2-\mu^2]^{-1}\cdot$$
$$\cdot\frac{2(\boldsymbol{p}-\boldsymbol{n})\cdot\boldsymbol{a}(q)}{n-m}[(\boldsymbol{p}_1-\boldsymbol{n})^2-\mu^2]^{-1}\gamma_5 U_{p_1}\,.$$

The expression for M_{I} and M_{II} is simplified by rationalizing the denominator and bringing the γ_5 factor together. Further the use of the relation $AB+BA=2\boldsymbol{A}\cdot\boldsymbol{B}$, gives

$$M_{\mathrm{I}} \simeq -\frac{f^2}{\pi i}\frac{4m^2}{\mu^2}\int \mathrm{d}^4k\, v^2(|k|)\, U^*_{p_2}\gamma_5 k\, U_{p_1}(k^2-2\boldsymbol{p}_2\cdot\boldsymbol{k})^{-1}(k^2-2\boldsymbol{p}_1\cdot\boldsymbol{k})^{-1}(k^2-\mu^2)^{-1}\,.$$

and

$$M_{\rm II} \frown \frac{f^2}{\pi i}\frac{4m^2}{\mu^2}\int \mathrm{d}^4n v^2(|n|)\, U^*_{p_2} nan\, U_{p_1}(n^2-2\boldsymbol{p}_2\cdot\boldsymbol{n}-\Delta)^{-1}\cdot$$
$$\cdot(n^2-2\boldsymbol{p}_1\cdot\boldsymbol{n}-\Delta)^{-1}(n^2-m^2)^{-1},$$

where $\Delta=\mu^2-m^2$ and the sign $\frown$ signifies contribution only to nuclear magnetic moment.

Thus the evaluation of $M_{\rm I}$ and $M_{\rm II}$ depends upon an integral of the form

$$I=\int_0^1 \mathrm{d}y\int_0^1 2x\,\mathrm{d}x\int(k_\mu k_\nu)v^2(|k|)\,\mathrm{d}^4k(k^2-2\boldsymbol{p}_x\cdot\boldsymbol{k}-\Delta_x)^{-3}, \tag{4}$$

where $\boldsymbol{p}_x=x\boldsymbol{p}_y$ and $\boldsymbol{p}_y=y\boldsymbol{p}_1+(1-y)\boldsymbol{p}_2$.

$$\text{Also}\left|\begin{array}{l}\Delta_x=x\Delta_y+(1-x)\mu^2 \quad \text{with} \quad \Delta_y=0 \quad \text{in the case of } M_{\rm I} \\ \qquad \text{and} \\ \Delta_x=x\Delta_y+(1-x)m^2 \quad \text{with} \quad \Delta_y=\Delta \quad \text{in the case of } M_{\rm II}\,.\end{array}\right. \tag{5}$$

As stated in the introduction we have

$$\int\frac{v^2(|k|)\,\mathrm{d}^4k}{(|k|^2-L)^2}=\frac{1}{4\pi^2 i}\int_0^{m_c}\int_0^{\pi}\int_0^{\pi}\int_0^{2\pi}\frac{|k|^3\sin^2\chi\sin\theta\,\mathrm{d}|k|\,\mathrm{d}\chi\,\mathrm{d}\theta\,\mathrm{d}\varphi}{(|k|^2-L)^2}= \tag{6}$$
$$=\frac{1}{4i}\left[\frac{m_c^2}{L-m_c^2}+\log\frac{L-m_c^2}{L}\right].$$

Substituting $k=k'-p$ in (6) and calling $L-p^2=\Delta$, shows that

$$\int k_\mu v^2(|k|)\,\mathrm{d}^4k(k^2-2\boldsymbol{p}_x\cdot\boldsymbol{k}-\Delta_x)^{-2}=\frac{p_{x\mu}}{4i}\left[\frac{m_c^2}{p_x^2+\Delta_x-m_c^2}+\log\left|\frac{p_x^2+\Delta_x-m_c^2}{p_x^2+\Delta_x}\right|\right]. \tag{7}$$

Differentiating (7) with respect to $p_{x\nu}$ we get

$$\int k_\mu k_\nu v^2(|k|)\,\mathrm{d}^4k(k^2-2\boldsymbol{p}_x\cdot\boldsymbol{k}-\Delta_x)^{-3}=$$
$$=\frac{1}{16i}\,\delta_{\mu\nu}\left[\frac{m_c^2}{p_x^2+\Delta_x-m_c^2}+\log\left|\frac{p_x^2+\Delta_x-m_c^2}{p_x^2+\Delta_x}\right|\right]+$$
$$+\frac{1}{8i}\left[p_{x\mu}p_{x\nu}\left\{\frac{1}{p_x^2+\Delta_x-m_c^2}-\frac{1}{p_x^2+\Delta_x}-\frac{m_c^2}{(p_x^2+\Delta_x-m_c^2)^2}\right\}\right].$$

Thus relation (4) finally reduces to

$$I = \frac{\delta_{\mu\nu}}{8i}\int_0^1 \mathrm{d}y \int_0^1 \mathrm{d}x \left[x\,\frac{m_c^2}{p_x^2 + \Delta_x - m_c^2} + x \log \left| \frac{-m_c^2 + p_x^2 + \Delta_x}{p_x^2 + \Delta_x} \right| - \right.$$

$$\left. + \frac{1}{4i}\int_0^1 p_{\nu\mu} p_{\nu\nu}\,\mathrm{d}y \int_0^1 \mathrm{d}x \left[\frac{x^3}{x^2 p_y^2 + \Delta_x - m_c^2} - \frac{x^3 m_c^2}{(x^2 p_y^2 + \Delta_x - m_c^2)^2} - \frac{x^3}{x^2 p_y^2 + \Delta_x} \right] \right. .$$

The x-integration is easily calculated and for the y-integration we put according to Feynman (²)

$$2y - 1 = \operatorname{tg}\alpha / \operatorname{tg}\theta\,,$$

where α goes from $-\theta$ to θ and θ is defined by $4m^2 \sin^2\theta = q^2$.

Now, using the fact that p_1 operating on the initial state is m, and likewise p_2 when it appears at the left is replaceable by m along with the consistent use of the relation (5) in the respective cases of M_{I} and M_{II}, we finally get

$$M_{\mathrm{I}} = -f^2 \frac{m^2}{\pi\mu^2}\frac{e}{2m}(\mathfrak{a}q - q\mathfrak{a})\frac{1}{\sin 2\theta}\int_{-\theta}^{\theta} I_{\mathrm{I}}\,\mathrm{d}\alpha\,,$$

and

$$M_{\mathrm{II}} = f^2 \frac{m^2}{\pi\mu^2}\frac{e}{2m}(\mathfrak{a}q - q\mathfrak{a})\frac{1}{\sin 2\theta}\int_{-\theta}^{\theta} I_{\mathrm{II}}\,\mathrm{d}\alpha\,,$$

where

$$I_{\mathrm{I}} = \left[\left\{ \left(\frac{\mu^2}{2m^2}\sec^2\theta\cos^2\alpha - \frac{\mu^4}{2m^4}\sec^4\theta\cos^4\alpha \right) \log \left| \frac{m_c^2 - \mu^2}{\mu^2}\,\frac{m^2\sec^2\alpha\cos^2\theta}{m_c^2 - m^2\sec^2\alpha\cos^2\theta} \right\} - \right.$$

$$+ \left\{ \frac{m_c^2(m_c^2 - \mu^2)}{\mu^2} - \frac{4m^2 m_c^2 (m_c^2 - \mu^2)^2}{\mu^2[4m^2(m_c^2 - \mu^2) + \mu^4\sec^2\theta\cos^2\alpha]} - \right.$$

$$\left. + \frac{\mu^2(m_c^2 - 2\mu^2)}{m^2}\sec^2\theta\cos^2\alpha + \frac{\mu^6}{2m^4}\sec^4\theta\cos^4\alpha \right\} \cdot \left\{ \frac{1}{\sqrt{\mu^4 + 4m^2(m_c^2 - \mu^2)\cos^2\theta\sec^2\alpha}} \right. \cdot$$

$$\cdot \log \frac{2m^2\cos^2\theta\sec^2\alpha - \mu^2 - \sqrt{\mu^4 + 4m^2(m_c^2 - \mu^2)\cos^2\theta\sec^2\alpha}}{2m^2\cos^2\theta\sec^2\alpha - \mu^2 + \sqrt{\mu^4 + 4m^2(m_c^2 - \mu^2)\cos^2\theta\sec^2\alpha}} \cdot$$

$$\left. \cdot \frac{-\mu^2 + \sqrt{\mu^4 + 4m^2(m_c^2 - \mu^2)\cos^2\theta\sec^2\alpha}}{-\mu^2 - \sqrt{\mu^4 + 4m^2(m_c^2 - \mu^2)\cos^2\theta\sec^2\alpha}} \right\} -$$

$$+ \left\{ \frac{\mu^2}{2m^4}\sec^4\theta\cos^4\alpha\sqrt{4m^2\mu^2\cos^2\theta\sec^2\alpha - \mu^4}\,\operatorname{tg}^{-1}\frac{\sqrt{4m^2\mu^2\cos^2\theta\sec^2\alpha - \mu^4}}{\mu^2} \right\} -$$

$$- m_c^2 \left\{ -\frac{1}{\mu^2} + \frac{m^2(2m_c^2 - \mu^2)}{\mu^4 + 4m_c^2(m - \mu^2)} \cdot \left(\frac{8(m_c^2 - \mu^2)^2}{\mu^2}\,\frac{1}{\mu^4\cos^2\alpha\sec^2\theta + 4m^2(m_c^2 - \mu^2)} + \right. \right.$$

$$\left. \left. + \frac{1}{m^2 - m_c^2\cos^2\alpha\sec^2\theta} \right) \right\} \right]\,,$$

(²) R. P. Feynman: *Phys. Rev.*, **76**, 749 (1949).

and

$$
\begin{aligned}
I_{\mathrm{II}} = \Bigg[\Bigg\{ & \left(\frac{1}{2} \sec^2\theta \cos^2\alpha - \frac{(\mu^2 - 2m^2)^2}{2m^4} \sec^4\theta \cos^4\alpha \right) \cdot \\
& \cdot \log \left| \frac{m^2 - m_c^2}{m^2} \cdot \frac{m^2 \sec^2\alpha \cos^2\theta + \mu^2 - m^2}{m^2 \sec^2\alpha \cos^2\theta + \mu^2 - m^2 - m_c^2} \right| \Bigg\} + \\
& + \Bigg\{ \frac{(m^2 - m_c^2) m_c^2}{\mu^2 - 2m^2} - \frac{4m^2 m_c^2 (m^2 - m_c^2)^2}{(\mu^2 - 2m^2)[4m^2(m^2 - m_c^2) - (\mu^2 - 2m^2)^2 \sec^2\theta \cos^2\alpha]} + \\
& + \frac{(\mu^2 - 2m^2)(2m^2 - m_c^2)}{m^2} \sec^2\theta \cos^2\alpha - \frac{(\mu^2 - 2m^2)^3}{2m^4} \sec^4\theta \cos^4\alpha \Bigg\} \cdot \\
& \cdot \Bigg\{ \frac{1}{\sqrt{(\mu^2 - 2m^2)^2 - 4m^2(m^2 - m_c^2) \cos^2\theta \sec^2\alpha}} \cdot \\
\cdot \log & \left| \frac{2m^2 \cos^2\theta \sec^2\alpha + \mu^2 - 2m^2 - \sqrt{(\mu^2 - 2m^2)^2 - 4m^2(m^2 - m_c^2) \cos^2\theta \sec^2\alpha}}{2m^2 \cos^2\theta \sec^2\alpha + \mu^2 - 2m^2 + \sqrt{(\mu^2 - 2m^2)^2 - 4m^2(m^2 - m_c^2) \cos^2\theta \sec^2\alpha}} \right. \cdot \\
& \cdot \left. \frac{\mu^2 - 2m^2 + \sqrt{(\mu^2 - 2m^2)^2 - 4m^2(m^2 - m_c^2) \cos^2\theta \sec^2\alpha}}{\mu^2 - 2m^2 - \sqrt{(\mu^2 - 2m^2)^2 - 4m^2(m^2 - m_c^2) \cos^2\theta \sec^2\alpha}} \right| \Bigg\} + \\
& + \Bigg\{ - \frac{\mu^2 - 2m^2}{2m^4} \sec^4\theta \cos^4\alpha \sqrt{4m^4 \sec^2\alpha \cos^2\theta - (\mu^2 - 2m^2)^2} \cdot \\
& \cdot \left(\mathrm{tg}^{-1} \frac{\sqrt{4m^4 \sec^2\alpha \cos^2\theta - (\mu^2 - 2m^2)^2}}{\mu^2} \right) \Bigg\} + \\
& + m_c^2 \Bigg\{ \frac{1}{(\mu^2 - 2m^2)} + \frac{m^2(\mu^2 - 2m^2)}{[(\mu^2 - 2m^2)^2 + 4(m^2 - m_c^2)(\mu^2 - m^2 - m_c^2)]} \cdot \\
& \cdot \left(\frac{8(m^2 - m_c^2)^2}{\mu^2 - 2m^2} \frac{1}{(\mu^2 - 2m^2)^2 \cos^2\alpha \sec^2\theta - 4m^2(m^2 - m_c^2)} - \right. \\
& \left. - \frac{1}{m^2 + (\mu^2 - m^2 - m_c^2) \cos^2\alpha \sec^2\theta} \right) \Bigg\} \Bigg] .
\end{aligned}
$$

Assuming the magnetic field to be very weak and homogeneous the above integral is evaluated numerically. Now, taking the cut-off to be $m_c = 2.334\,\mu$ and the value of the coupling constant as $f^2 = .015$, the meson and nucleon current contributions to the neutron magnetic moment come out to be -1.775 and $-.119$ respectively in nuclear magneton units. Thus for the magnetic moment of the proton and neutron we find

$$\mu_p = 1 + 1.755 + 0 = 2.755$$

and

$$\mu_n = 0 - 1.755 - .119 = -1.874$$

and this values give the anomalous ratio 1.07 against the experimental value 1.06.

3. – Discussion.

The present method of calculating nuclear magnetic moments requires a cut-off limit of $2.334\,\mu$ and a coupling constant of .015 to fit the existing experimental results. But its validity towards other meson-theoretical problems yet requires verification. It is interesting to note that these values of the energy-momentum cut-off and the coupling constant are much smaller than those used by CHEW in his non-relativistic model. Obviously the exact values of these two parameters are finally to be adjusted from the application of the present model to all other meson-nucleon problems.

* * *

The author is indebted to Professor R. E. PEIERLS for kindly going through this paper and for his valuable comments.

RIASSUNTO (*)

Si studia il momento magnetico del nucleone nel quadro della teoria del mesone pseudovettoriale-pseudoscalare carico con un modello di sorgente esteso nello spazio-tempo e l'equivalente taglio energia-impulso.

(*) *Traduzione a cura della Redazione.*

1821

IL NUOVO CIMENTO Vol. VIII, N. 6 16 Giugno 1958

On Weak Interactions of Elementary Particles.

B. D'ESPAGNAT
CERN - Geneva

(ricevuto il 4 Aprile 1958)

Summary. — A transformation similar to the one proposed by Pauli is suggested for the description of 4-vectors rotations in a Euclidian [4] space. Specializing these rotations to rotations in « M » space in the way described by several authors, one is led to a general description of weak interactions which, though rather similar to the one previously studied, nevertheless presents some significant new features, and seems freer from ad hoc assumptions.

The Pauli [1] transformation

$$\begin{pmatrix}\chi\\ \chi^c\end{pmatrix}\to\begin{pmatrix}a & b\gamma_5\\ -b^*\gamma_5 & a^*\end{pmatrix}\begin{pmatrix}\chi\\ \chi^c\end{pmatrix},\tag{1}$$

was shown by GÜRSEY [2] to be appropriate for representing rotations in a [3] isospace. Similarly we would like to point out that the transformation

$$\begin{pmatrix}\varphi^c & \psi\\ \psi^c & -\varphi\end{pmatrix}\to\begin{pmatrix}a & ib\\ ib^* & a^*\end{pmatrix}\begin{pmatrix}\varphi^c & \psi\\ \psi^c & -\varphi\end{pmatrix}\begin{pmatrix}a' & ib'\\ ib'^* & a'^*\end{pmatrix},\tag{2}$$

with $aa^*+bb^*=a'a'^*+b'b'^*=1$ is an adequate mean of representing rotations in a Euclidian [4] space. In fact, (2) describes the most general rotation of the 4-vector

$$A=[A_1, A_2, A_3, A_4]=[(\psi^c+\psi)/\sqrt{2},\ (\psi^c-\psi)/i\sqrt{2},\ (\varphi^c+\varphi)/\sqrt{2},\ (\varphi^c-\varphi)i\sqrt{2}].\tag{3}$$

---

(1) W. PAULI: *Nuovo Cimento*, **6**, 204 (1957).
(2) F. GÜRSEY: *Nuovo Cimento*, **7**, 411 (1958).

If, as suggested by several authors ([3]), there are in Nature some interactions which are 4-dimensionally invariant in isospace and are built up with 4-vectors, then the fields ψ and φ offer a good mean of writing them down. If, for instance, as in the Gell-Mann ([4]) scheme, the $NN\pi$ plus $\Xi\Xi\pi$ interaction is of such a nature, then one should write

$$\text{(4)} \qquad \begin{cases} \psi = \quad \alpha p + \beta \Xi^{-c}\,, \\ \varphi = -\,\alpha n + \beta \Xi^{0c}\,, \end{cases}$$

with

$$\alpha = \tfrac{1}{2}(1+\gamma_5)\,, \qquad \beta = \tfrac{1}{2}(1-\gamma_5)\,,$$

and describe the interaction, as well as the free fields Lagrangian, in terms of ψ and φ. Just, however, as is the case in the GÜRSEY ([2]) work, an interaction containing ψ and φ alone can obviously not conserve P and C separately but only the product PC: a parity and charge conjugation invariant interaction (and also any mass-term) thus requires a doubling of the number of fields (i.e. a return to the original number of independent fields in the usual representation) through the introduction, along with (4), of the fields

$$\text{(5)} \qquad \tilde{\psi} = \beta p + \alpha \Xi^{-c}\,; \qquad \tilde{\varphi} = -\,\beta n + \alpha \Xi^{0c}\,,$$

which here should be assumed to transform in the same way as ψ, φ, *i.e.* according to (2). Any interaction that is separately invariant under P and C is symmetric or antisymmetric with respect to the simultaneous interchanges of ψ with $\tilde{\psi}$ and φ with $\tilde{\varphi}$. It may be pointed out that charge conservation, hypercharge conservation and [3] isospin conservation are particular cases of invariance under (4) ($a' = a^*$, $b = b' = 0$; $a = 1$, $b = b' = 0$; $a' = 1$, $b' = 0$ respectively) while baryonic charge conservation is expressed by invariance under

$$\text{(6)} \qquad \psi \to \exp\,[i\theta\gamma_5]\psi\,; \qquad \varphi \to \exp\,[i\theta\gamma_5]\varphi\,.$$

The fact that interactions involving ψ and φ, but neither $\tilde{\psi}$ or $\tilde{\varphi}$ necessarily violate P and C invariances leads in a natural way to the conjecture that the present formalism may be particularly appropriate for the description of weak interactions. Indeed the assumption can be made that weak interactions involve the four p, n, Ξ^0, Ξ^- fields only through the two independent combinations ψ and φ. Such an idea, which has some similarity with the proposal of FEYNMAN and GELL-MANN ([5]), here receives further support from the fact

([3]) See e.g. J. SCHWINGER: *Phys. Rev.*, **104**, 1164 (1956).
([4]) M. GELL-MANN: *Phys. Rev.*, **106**, 1296 (1957).
([5]) R. P. FEYNMANN and M. GELL-MANN: *Phys. Rev.*, **109**, 193 (1958).

that several authors recently pointed out a mean of describing weak interactions as invariants in some [3] isospace derived from the [4] isospace. If, for instance, as suggested by PRENTKI, SALAM and the author [6] and independently by TAKEDA [7], this [3] space is derived from the [4] space by keeping the direction of the 4-th axis unchanged [8], then the interaction must involve the N and Ξ fields only through the linear combinations that form the vector

$$\boldsymbol{C} = [(\psi^c + \psi)/\sqrt{2},\ (\psi^c - \psi)/i\sqrt{2},\ (\varphi^c + \varphi)/\sqrt{2} = \varphi_3 = \varphi_3^c] \tag{7}$$

and the scalar

$$C_s = (\varphi^c - \varphi)/i\sqrt{2} = \varphi_s = \varphi_s^c\,. \tag{8}$$

In a similar way $\boldsymbol{\Sigma}$ and Λ must only appear through the combinations

$$\boldsymbol{D} = [(\psi'^c + \psi')/\sqrt{2},\ (\psi'^c - \psi')/i\sqrt{2},\ (\varphi'^c + \varphi')/\sqrt{2} = \varphi_3' = \varphi_3'^c]\,, \tag{9}$$

$$D_s = (\varphi'^c - \varphi')/i\sqrt{2} = \varphi_s' = \varphi_s'^c\,, \tag{10}$$

with

$$\begin{cases} \psi' = \alpha\Sigma^+ + \beta\Sigma^{-c} \\ \varphi_3' = \alpha\Sigma^0 + \beta\Sigma^{0c} \\ \varphi_s' = (\alpha\Lambda - \beta\Lambda^c)/i\,, \end{cases} \tag{11}$$

weak interactions of the Fermi type may then be constructed e.g. by first building up a 3-vector involving two such quantities as $\boldsymbol{C}$, C_s, $\boldsymbol{D}$, D_s and by then making the scalar product of this 3-vector with some other 3-vector involving two more fermion fields (two lepton fields or two baryon fields).

Especially remarkable for that purpose is the 3-vector

$$\boldsymbol{V} = \overline{C}_s\gamma_\mu i\gamma_5\boldsymbol{C}\,, \tag{12}$$

---

(6) B. D'ESPAGNAT, J. PRENTKI and A. SALAM: *Nucl. Phys.*, **5**, 447 (1958).

(7) G. TAKEDA: to be published.

(8) Let us rewrite (2) in the more compact notation

$$\Phi \to s\Phi t^T\,,$$

with

$$ss^+ = tt^+ = 1; \qquad \mathrm{Det}\, s = \mathrm{Det}\, t = 1\,,$$

then these particular rotations (rotations in the [3] « M » space) correspond to

$$\Phi \to s\Phi s^{-1}\,.$$

1824

whose components V_1, V_2, V_3 satisfy

$$(13)\quad \begin{cases} (V_1 - iV_2)/\sqrt{2} = V^+ = \bar{\varphi}_s\gamma_\mu i\gamma_5\psi = [\bar{\Xi}^-\gamma_\mu\alpha(\Xi^0 + n) - (\bar{\Xi}^0 + \bar{n})\gamma_\mu\alpha p]/\sqrt{2}\,, \\ (V_1 + iV_2))/\sqrt{2} = V^- = \bar{\varphi}_s\gamma_\mu i\gamma_5\psi^c = \bar{\psi}\gamma_\mu i\gamma_5\varphi_s = \\ \qquad\qquad = [\bar{p}\gamma_\mu\alpha(\Xi^0 + n) - (\bar{\Xi}^0 + \bar{n})\gamma_\mu\alpha\Xi^-]/\sqrt{2}\,, \\ V_3 = \bar{\varphi}_s\gamma_\mu i\gamma_5\varphi_3 = \bar{\varphi}_3\gamma_\mu i\gamma_5\varphi_s = \bar{\Xi}^0\gamma_\mu\alpha n - \bar{n}\gamma_\mu\alpha\Xi^0\,, \end{cases}$$

for, as already pointed out ([9]), if the interaction responsible for β-decay contains $\boldsymbol{V}$ (multiplied by some other vector involving e, ν) this interaction, when associated to a [4] invariant πNN plus πΞΞ strong interaction, cannot, to any order in the latter, induce any $\pi \to e\nu$ decay. The cancellation between matrix elements with $N\bar{N}$ and with $\Xi\bar{\Xi}$ pairs that is responsible for this phenomenon does not take place if, instead of $\boldsymbol{V}$, the vector

$$\boldsymbol{W} = \bar{\boldsymbol{C}}_s\gamma_\mu\boldsymbol{C} \tag{14}$$

is used: then the $N\bar{N}$ and $\Xi\bar{\Xi}$ contributions would add up instead. For this reason we would like to suggest that $\boldsymbol{V}$ should be used in association with the electron-neutrino fields while $\boldsymbol{W}$ should be used in association with the meson-neutrino fields. According to this proposal, possible interaction terms are

$$(\bar{\boldsymbol{C}}_s\gamma_\mu i\gamma_5\boldsymbol{C})(\bar{\boldsymbol{L}}_s\gamma_\mu\Gamma\boldsymbol{L}) \tag{15}$$

for β-decay and $\pi \to e\nu$-decay and

$$(\bar{\boldsymbol{C}}_s\gamma_\mu\boldsymbol{C})(\bar{\boldsymbol{L}}'_s\gamma_\mu\Gamma'\boldsymbol{L}) \tag{16}$$

for μ capture and $\pi \to \mu\nu$-decay, with

$$\Gamma,\ \Gamma' = 1 \quad \text{or} \quad i\gamma_5\,,$$

$$\boldsymbol{L} = [(\beta e^- + \alpha e^+)/\sqrt{2},\ (\beta e^- - \alpha e^+)/i\sqrt{2},\ (\beta\nu^c + \alpha\nu)/\sqrt{2}] \tag{17}$$

$$\boldsymbol{L}_s = (\beta\nu^c - \alpha\nu)/i\sqrt{2} \tag{18}$$

and entirely similar expressions for $\boldsymbol{L}'$ and $\boldsymbol{L}'_s$, e just being replaced by μ. The π branching ratio is then the same as in ref. ([9]) and in no disagreement with experiment, although the assumptions are here somewhat different.

As regards the non-leptonic interactions our new formalism also leads to

([9]) B. D'ESPAGNAT and J. PRENTKI: *Nucl. Phys.*, in the press.

a slight modification of the expressions in ref. (9), namely to such terms as *e.g.*

$$(\overline{C}_s\gamma_\mu \Gamma \boldsymbol{C})(\overline{C}_s\gamma_\mu \Gamma' \boldsymbol{D}) + \text{h. c.} \qquad \Gamma, \Gamma' = 1 \text{ or } i\gamma_5 \tag{19}$$

for the interaction responsible for Σ-decay (and K non-leptonic decays). This interaction does not, however, involve the Λ field. Although Λ decay can be accounted for by (19) through higher order virtual processes such as

$$\Lambda \to \Sigma + \pi \to \mathrm{N} + \mathrm{N}(\Xi) + \overline{\mathrm{N}}(\overline{\Xi}) + \pi \to \mathrm{N} + \pi + \pi \to \mathrm{N} + \pi\,, \tag{20}$$

it may appear somewhat more attractive to introduce directly a weak interaction that involves this particle. For instance one may choose

$$(\overline{D}_s\gamma_\mu \Gamma \boldsymbol{D})(\overline{D}_s\gamma_\mu \Gamma' \boldsymbol{C}) + \text{h. c.} \tag{21}$$

which is obtained from (19) through a full interchange of the symbols C and D. A special feature of (21) is that, according to lemma 1 in ref. (9), it gives a pure $|\Delta \boldsymbol{I}| = \frac{1}{2}$ decay with no $|\Delta \boldsymbol{I}| = \frac{3}{2}$ admixture whatsoever, which is not the case for (19) nor for (20) (thus one might hope to account in a natural way for the fact that the $|\Delta \boldsymbol{I}| = \frac{1}{2}$ rule seems to apply somewhat better to Λ-decay than to K and Σ-decays).

In order to describe the totality of weak interaction phenomena, two more terms should of course be added, one describing the μ, e, ν, ν interaction by means of a product of $\boldsymbol{L}$, L_s, $\boldsymbol{L}'$ and L'_s, one describing a Σ(Λ)N(Ξ)μ(e)ν interaction responsible for K leptonic decays. These can be easily written down according to the same principles as above and in such a way as not to contradict any well established experimental fact (cf. for instance the discussion in ref. (9)). Unfortunately, the problem is still underdetermined so some extent (even the choice of (19) and (21) is far from being unique) a fact which, considering *e.g.* our ignorance of the rare decay modes, should not be surprising. Expressions (15) and (16) on the other hand are compact descriptions for a wide variety of experimental facts.

RIASSUNTO (*)

Per la descrizione delle rotazioni dei 4-vettori nello spazio [4] euclideo si propone una trasformazione simile a quella proposta da Pauli. Limitando queste rotazioni alle rotazioni nello spazio « M » nel modo descritto da diversi autori, si è condotti ad una descrizione generale delle interazioni deboli, la quale, benchè abbastanza simile a quella studiata precedentemente, presenta, nondimeno, alcuni nuovi aspetti di rilievo e appare meno legata ad ipotesi particolari.

(*) *Traduzione a cura della Redazione.*

IL NUOVO CIMENTO Vol. VIII, N. 6 16 Giugno 1958

Properties of Negative K-Mesons (*†).

F. H. Webb (+), E. L. Iloff (×), F. H. Featherston, W. W. Chupp, G. Goldhaber and S. Goldhaber

Department of Physics and Radiation Laboratory
University of California - Berkeley, California

(ricevuto il 5 Aprile 1958)

Summary. — An analysis of interactions of 420 MeV/c K^--mesons incident on a nuclear emulsion stack has been carried out. By following K^--mesons along the track, we obtained information on the interaction of K^--mesons in flight and at rest. The differential scattering cross-section was fitted with diffraction scattering off a black disk with radius $1.32 \cdot A^{\frac{1}{3}}$ fermis in agreement with the total reaction cross-section. A compilation of K^--H elastic scattering and absorption events is presented, giving cross-sections of σ_{KH} (scattering) $= (48.4^{+15}_{-11})$ mb and σ_{KH} (absorption) $= (11.4^{+9}_{-5})$ mb. The inelastic scattering of K^--mesons in complex nuclei has been found to be only 4% of the absorption cross-section. The average energy losses in K^- inelastic scattering events is $\sim 50\%$ of the incident K energy, in contrast to a 25% loss for K^+ inelastic scattering. In the course of this work we have observed a number of decays in flight. Combining these with earlier data, we obtain a mean life of $\tau_{K^-} = (1.3^{+0.4}_{-0.3}) \cdot 10^{-8}$ s. We have identified some of the secondaries from decays in flight, namely $2\, K_{\pi 2}$, $2\, K_{\mu 2}$, and $1\, K_{e3}$. From K^--H absorption events we have obtained a Σ^--Σ^+ mass difference of $(13.9 \pm 1.8)\, m_e$ and a value of the K^- mass of $(966.7 \pm 2.0)\, m_e$. From an analysis of the charged pion spectrum obtained

---

(*) Paper delivered by S. Goldhaber at the International Conference on Mesons and Recently Discovered Particles, Padua-Venice, September 1957. References include only papers published prior to the time of the meeting.

(†) The material presented in this paper is based in part on the Doctors' Dissertations of F. H. Webb, University of California Department of Physics (1957) and E. L. Iloff, University of California Department of Physics (1957), and on the Master's Dissertation of F. H. Featherston, University of California and United States Naval Postgraduate School, Monterey, California. The work was done under the auspices of the U. S. Atomic Energy Commission.

(+) Present address: 3454 Vosberg Street, Pasadena, California.

(×) Present address: Department of Physics, Iowa State College, Ames, Iowa.

from K⁻ interactions at rest, it was possible to calculate the ratio of Λ to Σ hyperons produced in the primary interaction. We find that in the primary K⁻ nucleon absorption reaction, Σ-hyperon formation dominates over Λ-hyperon formation. An energy and strangeness balance shows that 70% of the K⁻ stars at rest emit a Λ-particle. This means that about 60% of the Σ-hyperons that are produced are converted to Λ-hyperons inside the nucleus in which they were formed.

---

1. – Introduction.

From the study of the interactions of negative K-mesons in photographic emulsion, one can obtain information on both the properties of K⁻-mesons and of the Σ and Λ hyperons produced by the interaction of the K⁻-mesons with nuclei.

By following « along the track » of K⁻-mesons with an incident momentum of 420 MeV/c, we have been able to obtain information on the interaction of K⁻-mesons in flight and at rest.

From interactions in flight, we have obtained the elastic differential cross-section, which can be fitted by the diffraction scattering from a black disk of $1.32 \times A^{\frac{1}{3}}$ fermis.

A compilation of the K-H elastic scattering and absorption events in the energy interval $T_{K^-} = 16$ to 150 MeV has been made from which the value of the K⁻-H scattering cross-section of (48.4^{+15}_{-11}) mb and the K⁻-H absorption cross-section of (11.4^{+9}_{-5}) mb were deduced. The inelastic scattering of the K⁻-mesons in complex nuclei has been found to be only 4% of the absorption cross-section.

A number of decays in flight have been observed, which combined with our earlier data yield a mean life of $\tau_{K^-} = (1.3^{+0.4}_{-0.3}) \cdot 10^{-8}$ s.

We have been able to identify several decay modes by analyzing the secondaries from the K⁻ decays in flight. We have found two $K_{\pi 2}$, two $K_{\mu 2}$, and one K_{e3}.

We have reevaluated our earlier K⁻-H absorption events at rest, i.e., $K^- + H \rightarrow \Sigma^{\pm} + \pi^{\mp}$, and have also included an additional event where the resulting Σ decays via the $\Sigma^+ \rightarrow p + \pi^0$ decay mode. From these events we have obtained a Σ^--Σ^+ mass difference of $(13.9 \pm 1.8)\, m_e$ and a value for the K⁻ mass of $(966.7 \pm 2.0)\, m_e$.

From an analysis of the charged-pion spectrum obtained from K⁻ interactions at rest, it was possible to estimate the ratio of Λ to Σ hyperons produced in the primary interaction. We have assumed throughout this analysis that the absorption process of the K⁻ mesons proceeds according to the in-

dependent-particle model, i.e., the K^- is absorbed by a single nucleon. The absorption by two nucleons is estimated to occur in no more than 10% of all interactions. We have assumed two extreme models in order to calculate the modification of the pion spectrum due to the energy dependence of the mean free path of pions in nuclear matter: *a*) Uniform absorption of K^--mesons. and *b*) surface absorption of the K^--mesons. The Λ/Σ ratio is sensitive to the radius at which the absorption occurs. We have fitted the experimental spectrum by an intermediate model, the average between the two above-mentioned cases.

A comparison of the pion spectrum for interactions of K^--mesons in flight with that at rest indicates that absorptions in flight occur most probably at a smaller average absorption radius than those at rest.

From an energy and strangeness balance we find that in approximately 70% of the K^--absorption stars at rest, a Λ^0 particle is emitted. This, when compared with the Λ/Σ production ratio, implies that about 60% of the Σ hyperons that are produced are converted to Λ hyperons on leaving the nucleus in which they were formed.

The experimental data presented in this paper come from our own data (based on 364 K^- stars at rest and 102 K^- stars in flight) and also partly on a compilation prepared by one of us for the Sixth Annual Rochester Conference (1).

2. – Measurements on the primary K^--track.

In all the work reported here, we followed the K^--mesons by « along the track » scanning. In this fashion, both decays in flight and interactions in flight are observed. If the K^--meson does not undergo either of the above processes, it is followed until it comes to rest, and the absorption stars at rest can thus be found in a completely unbiased fashion.

2·1. *Mean life.* – The ratio of the total proper moderation time to the number of decays in flight gives the mean life of the K^--meson. In an earlier compilation for a total moderation time of $12.37\cdot10^{-8}$ s, 13 decays in flight were found, giving a mean life of $\tau_{K^-}=0.95^{+0.36}_{-0.25}\cdot10^{-8}$ s (2). Subsequently we have observed seven additional decays for a total proper moderation time of

(1) S. Goldhaber: *Proceedings of Sixth Annual Rochester Conference on High-Energy Physics*, 1956 (New York, 1956), Sect. 6.1.

(2) E. L. Iloff, G. Goldhaber, S. Goldhaber, J. E. Lannutti, F. C. Gilbert, C. E. Violet, R. S. White, D. M. Fournet, A. Pevsner and D. Ritson: *Phys. Rev.*, **102**, 927 (1955).

$13.85 \cdot 10^{-8}$ s. Combining these two results, we obtain $\tau_{K^-} = (1.3^{+0.4}_{-0.3}) \cdot 10^{-8}$ s. This is to be compared to be value of $\tau_{K^-} = (1.49^{+0.22}_{-0.24}) \cdot 10^{-8}$ s. obtained in a recent counter experiment [3]. The evidence is thus very good that the mean life is the same as that for the K^+-meson [4].

2·2. *Decay modes.* – A study of the decay modes of K^--mesons is possible only by examining decays in flight. A K^--meson when brought to rest is captured into atomic orbits of one of the near-by atoms and is subsequently absorbed by the nucleus. It is therefore more difficult to establish the branching ratio into the various decay modes for K^--mesons than it has been for K^+-mesons, which decay when brought to rest. From a total of 11 secondaries observed we have identified five which constitute all secondaries with a dip angle $\leqslant 15°$. We found in this unbiased sample two $K_{\pi 2}$, two $K_{\mu 2}$, and one K_{e3} decay modes [5]. The decay of the negative τ-mesons has been observed in cloud chamber and bubble chamber experiments [6]. So few secondaries were available for analysis that our only conclusion was that the decay modes of the K^--meson are not inconsistent with those of the K^+-meson [7].

2·3. *The* K^- *interaction cross-section.* – In the 30.6 meters of path length scanned, we have observed 101 inelastic and absorption interactions in complex nuclei and one hydrogen-absorption event ($K^- + H \to \Sigma^\pm + \pi^\mp$) [8]. Table I gives our result on the mean free path for three energy intervals. The mean free path over the entire energy intervals is (30.3 ± 3) cm, excluding the hydrogen events. This mean free path gives an average reaction cross-section in emulsion (Ag, Br and C, O, and N) of (707 ± 70) mb, and the corresponding nuclear radius is $R = (1.32 \pm 0.07) \times A^{\frac{1}{3}}$ fermis.

---

(3) B. Cork, G. R. Lambertson, O. Piccioni and W. Wenzel: *Phys. Rev.*, **106**, 167 (1957).

(4) E. L. Iloff, W. W. Chupp, G. Goldhaber, S. Goldhaber and J. E. Lannutti: *Phys. Rev.*, **99**, 1617 (1955); V. Fitch and R. Motley: *Phys. Rev.*, **101**, 496 (1956); L. W. Alvarez, F. S. Crawford, M. L. Good and M. L. Stevenson: *Phys. Rev.*, **101**, 503 (1956).

(5) Two of these have been published in an ealier communication: G. Ekspong and G. Goldhaber: *Phys. Rev.*, **102**, 1187 (1956).

(6) T. L. Aggson, W. B. Fretter, E. W. Friesen, L. F. Hansen, R. G. Kepler and A. Lagarrigue: *Phys. Rev.*, **102**, 243 (1956); and L. W. Alvarez, H. Bradner, P. Falk-Vairant, J. D. Gow, A. H. Rosenfeld, F. T. Solmitz and R. D. Tripp: *Nuovo Cimento*, **5**, 1026 (1957).

(7) R. W. Birge, D. H. Perkins, J. R. Peterson, D. H. Stork and M. N. Whitehead: *Nuovo Cimento*, **4**, 834 (1956).

(8) One additional K-H scattering event was found in another stack in which 2.4 m of track length was scanned.

TABLE I. – *Energy distribution of the K⁻-meson interactions.*

T_{K^-} (MeV)	Path length (m)	Number of events	Mean free path (cm)
16 to 60	6.73	25	27 ± 5.4
60 to 120	14.49	41	35 ± 5.5
120 to 160	9.39	35	27 ± 4.5
16 to 160 average	30.61	101	30.3 ± 3

2·3.1. *Interaction with complex nuclei.*

a) Inelastic scattering events and absorption events. – The inelastic scattering cross-section of K^--mesons is only a small fraction of the K^- reaction cross-section ($\sim 4\%$). In 30.4 meters scanned along the track, we have seen only four inelastic scattering events with energy loss $\Delta T/T > 10\%$. The measurement technique used to determine energy losses could reliably detect energy changes equal to or greater than 10%. Although the number of inelastic scatters is small, it is interesting to note that in all cases the incident K^--meson loses about one-half its kinetic energy in the collision ($\langle \Delta T/T \rangle = 0.56$ (see Table II). This is of particular interest when compared with K^+-mesons, in which the energy losses are generally smaller ($\langle \Delta T/T \rangle \simeq 0.25$ for K^+-mesons of 20 to 100 MeV). For K^+-mesons the markedly small energy loss, considered to occur in collisions with single bound nucleons, was ascribed to a repulsive nuclear potential. The large energy loss of the K^--meson in collisions with bound nucleons may be an indication of an attractive nuclear potential [9]. The present limited statistics do not permit a detailed analysis of this phenomenon.

The majority of the interaction of the K^--mesons in flight lead to absorption stars giving rise to Σ and Λ hyperons. A detailed discussion of these events is given in Sect. **3**.

TABLE II. – *Characteristics of inelastic K⁻-meson scattering.*

T_{K^-} (MeV)	$\Delta T/T$	θ_K Lab. scattering angle (°)
38	0.58	56
58	0.62	82
103	0.48	59
138	0.55	103

[9] Very similar results were recently observed by the group of Göttingen, who have also drawn the same conclusions independently (M. CECCARELLI: private communication).

b) Charge-exchange scattering events. – Charge-exchange scattering events of K⁻-mesons in complex nuclei such as we deal with in emulsion cannot be distinguished from absorption stars with neutral hyperon emission. It is, however, possible to set an upper limit to the ratio of charge-exchange scattering to non-charge-exchange scattering. Interference between the singlet and triplet isotopic spin states in the K^- scattering interaction leads to an upper limit for the ratio

$$\frac{K^- + p \to \overline{K^0} + n}{(K^- + p \to K^- + p) + (K^- + n \to K^- + n)} \leqslant 2\,.$$

The charge-exchange scattering of K^--mesons can therefore be estimated to be $\lesssim 8\%$ of the reaction cross-section.

2'3.2. *Elastic scattering and total cross-section.* – The experimental procedure used in determining the elastic cross-section consisted of measuring all the space angles of K^- scattering events for which the projected angles are $\geqslant 2°$. The differential cross-section was then computed from these measurements by applying a correction factor, which compensates for the events missed due to the 1.9° cut-off in projected angles. With the K^+-mesons, it was possible to analyze the differential scattering cross-section in terms of an optical-

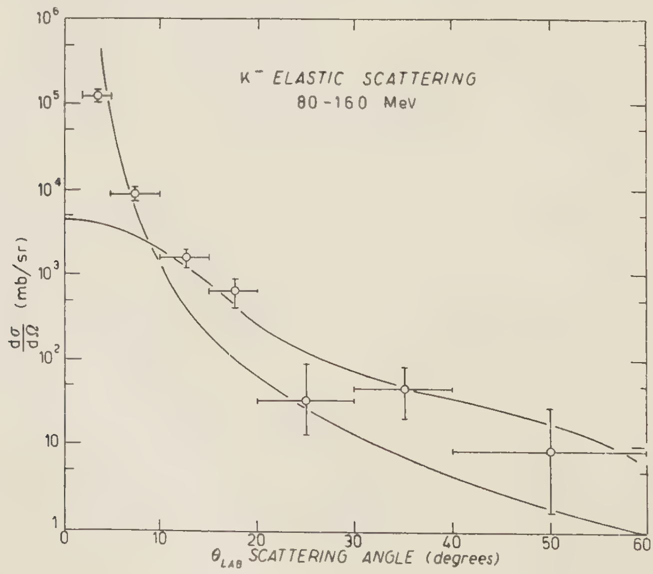

Fig. 1. – K^- nucleon elastic scattering differential cross-section. The experimental cross-section is compared with a point Rutherford scattering and diffraction scattering from a black disk of radius $1.32\,A^{\frac{1}{3}}$ fermis.

1832

model potential [10,11]. For K^--mesons, the large absorption cross-section is evidence for the presence of a large imaginary potential. Conclusions on the sign and magnitude of the real potential are thus more involved in the case discussed here. An exact optical-model calculation similar to the one for K^+-mesons [11] will be carried out shortly [12].

The data can be fitted by a curve calculated for diffraction scattering from a black disk of radius $R = 1.32 \times A^{\frac{1}{3}}$ fermis (see Fig. 1). The total cross-section obtained is about 1400 mb for the mixture C, O, N, and AgBr. This value is twice that for the reaction cross-section. The Rutherford scattering curve from a point nucleus is also shown for comparison. The fact that the observed diffraction cross-section lies above the Rutherford scattering curve for angles greater than 10° is presumably due to interference phenomena including the real and imaginary part of both the Rutherford and diffraction-scattering amplitudes. This result is consistent with constructive interference between Coulomb and K^- nuclear scattering. A definite conclusion on this point must, however, await the completion of a detailed analysis.

2·3.3. *The* K^--H *cross-section*. – In the 33.0 m scanned along the K^- track, we have found only one K^--H scattering event and one K^--H absorption event. To get a reasonable evaluation of the cross-section, we have compiled published results [13,14] which are given in Table III. From these data one obtains a K^--H scattering cross-section of (48.4^{+15}_{-11}) mb, a K^- absorption cross-section of

TABLE III. – *Compilation of* K^-*-hydrogen interaction events.*

Group	Energy interval (MeV)	Number of absorptions in flight	Number of K-H scattering events	Path length (m)
This work	16 to 150	1	1	33
WHITE *et al.* [a]	16 to 150	1	10	30
BARKAS *et al.* [b]	30 to 90	2	6	49.5
Combined	16 to 150	4	17	112.5

(*a*) See reference [13].
(*b*) See reference [14].

(10) See, for example, G. COSTA and G. PATERGNANI: *Nuovo Cimento*, **5**, 448 (1957).

(11) G. IGO, D. G. RAVENHALL, J. J. TIEMAN, W. W. CHUPP, G. GOLDHABER, S. GOLDHABER, J. E. LANNUTTI and R. M. THALER: *Phys. Rev.*, **109**, 2133 (1958).

(12) G. IGO (Stanford University): private communication.

(13) F. C. GILBERT, C. E. VIOLET and R. S. WHITE: *Bull. Amer. Phys. Soc.*, **2**, 222 (1957).

(14) W. H. BARKAS, W. F. DUDZIAK, P. C. GILES, H. H. HECKMAN, F. W. INMAN, C. J. MASON, N. A. NICKOLS and F. M. SMITH: *Phys. Rev.*, **105**, 1417 (1957).

(11.4^{+9}_{-5}) mb, and a total K⁻-H cross-section of (60^{+15}_{-13}) mb. The small number of K⁻-H events found in this work must be attributed to a statistical fluctuation.

3. – K⁻-Hydrogen absorption at rest.

In the course of this work, five events have been observed which we interpret as the absorption of stopped K⁻-mesons in hydrogen [15]. At the 1955 Pisa Conference [1,16] we reported four of these events. At that time we were able to proceed only to the point of stating that *if* the K⁻-mesons involved possessed a *unique* mass value, *then* the Σ^- hyperon is heavier than the Σ^+ hyperon by about 14 m_e.

Recently, BUDDE *et al.* have confirmed our observation by an independent method in which the Q-value of the Σ^- hyperon was measured directly [17]. Further confirmation was also found in emulsions in which the Σ^- decay in flight was observed [18] and the Q-value was measured from the range of the decay pion. In addition, various authors have found other examples of K⁻-H absorption in emulsion [14,19,20]. All these results confirm the observation that the Σ^--Σ^+ mass difference is about 14 m_e.

We have reevaluated our data, based on new and more elaborate measurements, which now allow us to obtain the K⁻ mass in addition to the Σ^--Σ^+ mass difference. The five events that have been identified as the absorption of K⁻-mesons in hydrogen can be classified according to the following two reaction schemes:

$$(a) \qquad K^- + H \to \Sigma^+ + \pi^- + Q_1\,,$$

$$(b) \qquad K^- + H \to \Sigma^- + \pi^+ + Q_2\,.$$

In two events (K_{20} and K_{1003}) of type (a), the Σ^+ hyperons come to rest and decay by the processes $\Sigma^+ \to \pi^+ + n$ and $\Sigma^+ \to p + \pi^0$ respectively. The mea-

(15) Two of these events are due to H. PEVSNER, D. RITSON and M. WIDGOFF: MIT-Harvard private communication.

(16) W. W. CHUPP, G. GOLDHABER, S. GOLDHABER and F. H. WEBB: *Interactions of Negative K Particles at Rest*, UCRL-3044 (June 1955); *Suppl. Nuovo Cimento*, **4**, 382 (1956).

(17) R. BUDDE, M. CHRÉTIEN, J. LEITNER, N. P. SAMIOS, M. SCHWARTZ and J. STEINBERGER: *Phys. Rev.*, **103**, 1827 (1956).

(18) D. F. FALLA, M. W. FRIEDLANDER, F. ANDERSON, W. D. B. GREENING, S. LIMENTANI, B. SECHI-ZORN, C. CERNIGOI, G. IERNETTI and G. POIANI: *Nuovo Cimento*, **5**, 1203 (1957); and B. P. EDWARDS, A. ENGLER, M. W. FRIEDLANDER and A. A. KAMAL: *Nuovo Cimento*, **5**, 1188 (1957).

(19) W. F. FRY, J. SCHNEPS, G. A. SNOW, M. S. SWAMI and O. C. WOLD: *Phys. Rev.*, **104**, 270 (1956).

(20) F. C. GILBERT, C. E. VIOLET and R. S. WHITE: *K-Particle Captures by Bound and Free Protons in Emulsion*, UCRL-4814 (Feb. 1957).

sured ranges of the hyperons are $(806.4 \pm 13)\,\mu$m and $(804.9 \pm 13)\,\mu$m, respectively. In two other events, ($K_{MH\text{-}2}$ and K_2), which we ascribe to reaction (b), the Σ^- hyperons do not give capture stars at the ends of their ranges. Their respective ranges (are $694.1 \pm 22)\,\mu$m and $(687 \pm 10)\,\mu$m.

The errors quoted are all standard errors and include the observational errors, uncertainty in emulsion shrinkage, and Bohr straggling. The fifth event, $K_{MH\text{-}1}$, gives rise to a pion collinear with a Σ hyperon of $574\,\mu$m range, which then decays into a π-meson. The dip angle of the Σ hyperon is 45°, which is too steep to determine whether or not the Σ hyperon came to rest prior to its decay. The most plausible explanation for this event is that it represents a K-H absorption event in which the positive or negative Σ hyperon decays in flight.

3·1. *The Σ^--Σ^+ mass difference.* – The mean Σ^+ range for our events is $(806.0 \pm 11.5)\,\mu$m and the mean Σ^- range is $(689.0 \pm 9.4)\,\mu$m. If we assume a unique K^- mass equal to the K^+ mass (966.17 m_e) then reactions (a) and (b) give $M_{\Sigma^-} - M_{\Sigma^+} = Q_1 - Q_2$. We take $M_{\pi^+} M_{\pi^-}$ according to COHEN, CROWE, DUMONT ([21]). The new range-energy curve of BARKAS *et al.* ([22]) was used to determine the Σ^--Σ^+ mass difference from the hyperon ranges. The result obtained in this way is insensitive to small variations in the stopping power of the emulsion and the value of the K^- mass. The data yield the value $M_{\Sigma^-} - M_{\Sigma^+} = (13.9 \pm 1.8)m_e$.

3·2. *The K^- mass.* – The K^- mass can now be determined from the reactions that yield Σ^+ hyperons, where the accuracy of the K^- mass is limited by the accuracy to which the Σ^+ mass is known ($M_{\Sigma^+} = (2\,327.4 \pm 1.0)\,m_e$ ([23])) and the uncertainty in our Σ^+ range determination. In this case, the uncertainty in emulsion density, resulting in an uncertainty in stopping power, does not cancel out. We determined the emulsion density from the ranges of protons from four Σ^+ decays ($\Sigma^+ \to p + \pi^0$) to an accuracy of $\pm 1\%$.

The proton ranges were:

$$(1637.9 \pm \ \ 3.4)\,\mu\text{m}$$
$$(1630.8 \pm 13.0)\,\mu\text{m}$$
$$(1645.2 \pm 23.2)\,\mu\text{m}$$
$$(1636.8 \pm 22.7)\,\mu\text{m}\,.$$

([21]) E. R. COHEN, K. M. CROWE and J. W. M. DUMONT: *Phys. Rev.*, **104**, 1266 (1956).

([22]) W. H. BARKAS, P. H. BARRETT, P. CÜER, H. H. HECKMAN, F. M. SMITH and H. K. TICHO: *Phys. Rev.*, **102**, 583 (1955); *Range-Energy Relation in Emulsion*, UCRL-3768 and UCRL-3769 (April 9, 1957), to be published.

([23]) W. F. FRY, J. SCHNEPS, G. A. SNOW and M. S. SWAMI: *Phys. Rev.*, **103**, 226 (1956).

This datum and the measured Σ^+ ranges from reaction (1) lead to a value for the K^- mass of $(966.7 \pm 2.0)\, m_e$.

4. – The K^--absorption stars.

As has been shown earlier (24,16), the K^--meson absorption obeys the Gell-Mann selection rule for strong interactions, i.e., $\Delta S = 0$. This selection rule requires the emission of a strange particle. To satisfy the strangeness selection rule and energy conservation, the absorption of negative K-mesons at rest can lead only to emission of hyperons, i.e. Λ^0 or $\Sigma^{\pm,0}$ (25). Through the study of the interaction products of the absorption process at rest, we tried to determine the ratio of Λ^0 to $\Sigma^{\pm,0}$ produced in the primary interaction. In Table IV we summarize the possible K^- reaction with one and two nucleons, respectively (26).

TABLE IV. – *Interactions of K^--mesons with one and two nucleons.*

Interaction	Q (MeV)	Interaction	Q (MeV)
(1) $K^- + p \to \Sigma^+ + \pi^-$	103	(8) $K^- + p + p \to \Sigma^+ + n$	242
(2) $K^- + p \to \Sigma^- + \pi^+$	96	(9) $K^- + p + p \to \Sigma^0 + p$	244
(3) $K^- + p \to \Sigma^0 + \pi^0$	109	(10) $K^- + p + p \to \Lambda^0 + p$	317
(4) $K^- + p \to \Lambda^0 + \pi^0$	182	(11) $K^- + p + n \to \Sigma^0 + n$	244
(5) $K^- + n \to \Sigma^- + \pi^0$	102	(12) $K^- + p + n \to \Lambda^0 + n$	317
(6) $K^- + n \to \Sigma^0 + \pi^-$	105	(13) $K^- + p + n \to \Sigma^- + p$	237
(7) $K^- + n \to \Lambda^0 + \pi^-$	179	(14) $K^- + n + n \to \Sigma^- + n$	237

We have estimated the interactions with two nucleons from the energy spectrum of the hyperons to be no more than 10% of all interactions. In this analysis, we have treated the case of K^- interactions with only a single nucleon, which should thus comprise more than 90% of all interactions.

4·1. *The pion spectrum.* – In nuclear emulsions one cannot, in general, detect the neutral hyperons correlated with a given K^--absorption star. There-

(24) See for instance work by various emulsion groups in the *Proceedings of the Fifth Annual Rochester Conference on High-Energy Physics*, 1955 (New York, 1955); *Proceedings of the Sixth Annual Rochester Conference on High-Energy Physics*, 1956 (New York, 1956) and *Proceedings of the Seventh Annual Rochester Conference on High-Energy Physics*, 1957 (New York, 1957).

(25) We are assuming here that the K^--K^0 mass difference is too small for charge exchange to occur for K^- interactions at rest with bound nucleons.

(26) We have not included interactions leading to the production of two pions.

fore, to arrive at the ratio of Λ^0 to $\Sigma^{\pm,0}$ hyperons at production, one has to utilize indirect information. Such information can be obtained from the charged pions produced in association with Σ and Λ hyperons. Assuming charge independence, we can express the Λ^0 to $\Sigma^{\pm,0}$ production ratio in terms of the charged pions produced in association with the hyperons. Table V summa-

TABLE V. – *Hyperon production from* K^-*-nucleon reactions.*

Reaction	Transition probability
$K^- + p \to \pi^0 + \Lambda^0$	$\frac{1}{2}B_1^2$
$K^- + p \to \pi^+ + \Sigma^-$	$\frac{1}{6}A_0^2 + \frac{1}{4}A_1^2 + 1/\sqrt{6}A_0A_1\cos\varphi$
$K^- + p \to \pi^0 + \Sigma^0$	$\frac{1}{6}A_0^2$
$K^- + p \to \pi^- + \Sigma^+$	$\frac{1}{6}A_0^2 + \frac{1}{4}A_1^2 - 1/\sqrt{6}A_0A_1\cos\varphi$
$K^- + n \to \pi^- + \Lambda^0$	B_1^2
$K^- + n \to \pi^0 + \Sigma^-$	$\frac{1}{2}A_1^2$
$K^- + n \to \pi^- + \Sigma^0$	$\frac{1}{2}A_1^2$

rizes for all K^- reactions with one nucleon the probabilities of hyperon production, for the mixture of isotopic-spin singlet and triplet states. The production amplitudes for the reactions giving Σ and Λ hyperons are designated by A and B, respectively. Subscripts 0 and 1 refer to $T=0$ and $T=1$; φ is the interference angle between the two states.

Let us designate pions produced in association with Σ and Λ hyperons as π_Σ and π_Λ, respectively. Then from the above equations it can easily be seen that for a neutron-to-proton ratio of unity (n/p = 1), we have

$$\pi_\Lambda^-/(\pi^-_{\Sigma^{+,0}} + \pi^+_{\Sigma^-}) = \Lambda^0/\Sigma^{\pm,0} = B_1^2/\tfrac{1}{3}(A_0^2 + A_1^2)\,.$$

Taking into account that the n/p ratio averaged over emulsion nuclei is n/p = 1.2, we obtain

$$0.93\,[\pi_\Lambda^-/(\pi^-_{\Sigma^{+,0}} + \pi^+_{\Sigma^-})] \simeq \Lambda^0/\Sigma^{\pm,0}\,.$$

The charged-pion ratio can be obtained from the pion spectrum. An inspection of Table IV tells us that the Q-values for the reactions producing Λ hyperons is larger by ~ 80 MeV than that for producing Σ hyperons. Therefore the respective pion energies would differ by about 60 MeV. The analysis of the pion spectrum would thus yield direct information on the Λ/Σ ratio at production.

Fig. 2 shows a comparison of the pion spectrum from absorption stars in flight and at rest. Part of this pion spectrum at rest was presented by one

of us at the Sixth Annual Rochester Conference (1). To the spectrum consisting of 124 pions presented at that time, we have added 45 new measurements selected as an unbiased sample from 226 additional K⁻ interactions at rest. The selection consisted of all pions of dip angle less than 20°. The shaded region in Fig. 2 indicates the pions associated with *identified* Σ hyperons. Considering the absorption stars at rest only, we can see that qualitatively there is no appreciable difference (except for a small high-energy tail) between the entire pion spectrum and those pions produced in association with identified Σ hyperons. This indicates that the Σ production is the dominant interaction process in K⁻-absorption events, as was pointed out earlier (1). This result has been observed by ALVAREZ *et al.* (6) to occur also in the absorption of K⁻-mesons in pure hydrogen. In the next section we discuss a quantitative evaluation of the Λ/Σ ratio.

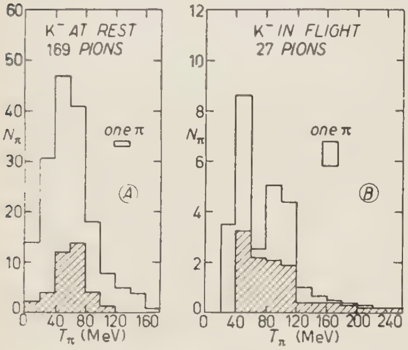

Fig. 2. – The charged-pion spectrum. *a*) A histogram of the observed pion spectrum from K⁻ interactions at rest. *b*) An ideogram of the observed pion spectrum from K⁻ interactions in flight. The shaded region represents the pions produced in association with identified charged hyperons.

4·1.1. *The Λ/Σ ratio.* – In order to analyze the pion spectrum in terms of π_Σ pions and π_Λ pions, we first computed the pion spectrum that would result from reactions (1), (2) and (6) alone and from reaction (7) alone (see Table IV). The pion spectrum has been computed by use of the Serber model. The calculations leading to the comparison with the observed spectra have been arrived at by the following steps (27):

a) A K⁻-meson bound in the atomic orbit around a nucleus interacts with a single nucleon whose momentum is given by a Gaussian momentum distribution. The $1/e$ value has been taken to be 20 MeV.

b) The resulting pion and hyperon are produced inside the nucleus in accordance with conservation of energy and momentum in the center-of-mass system, taking into account the potentials in which these particles find them-

(27) F. H. WEBB JR.: I. *The Interaction of Negative* K-*Mesons at Rest in Complex Nuclei.* - II. *The* K⁻ *Mass,* Σ⁻ *Mass, and* Σ⁻-Σ⁺ *Mass Difference* (*thesis*), UCRL-3785 (May 1957); *A Similar Calculation was performed independently by* R. H. CAPPS; *Optical Model of Sigma-Particle Production Nuclei by Negative* K-*Mesons*, UCRL-3707 (March 1957).

selves. The values we have assumed are:

$$V_\Sigma = V_\Lambda = -15\ \text{MeV}\,,$$
$$V_K = 0\,,$$
$$V_\pi = -40\ \text{MeV}\,,$$
$$V_N = -42\ \text{MeV}\,.$$

c) In order to obtain the pion and hyperon spectrum outside the nucleus, we altered their energies by adding their respective well depths.

d) An additional modification of the pion spectrum is due to the energy dependence of the mean free path of pions in nuclear matter. This has the effect of reducing the high-energy part of the spectrum while enhancing the spectrum around 35 MeV (inelastic scattering). The calculations have been carried out for two extreme models: 1) uniform absorption of the K^--meson, and 2) surface absorption of the K^--meson (see Appendix I for details).

In Table VI we give the resulting Λ/Σ ratios obtained by fitting the experimental pion spectrum with a superposition of the computed π_Λ and π_Σ spectra. The Λ/Σ ratio is given for the two extreme models and also for an intermediate model corresponding to the average between the two. The errors quoted are the statistical errors only.

TABLE VI. – *Fraction of* $\pi_\Lambda^-/\pi_\Sigma^\pm$.

Type of model	At emission	At production	$\Lambda^0/\Sigma^{\pm,0}$
Surface	0.20 ± 0.04	0.23 ± 0.05	0.21 ± 0.07
Homogeneous	0.39 ± 0.10	0.53 ± 0.14	0.50 ± 0.16
Average	0.25 ± 0.06	0.31 ± 0.08	0.28 ± 0.10

As can be seen, the ratio is quite sensitive to the radius R_a at which the absorption occurs.

Fig. 3 shows the experimental pion spectrum

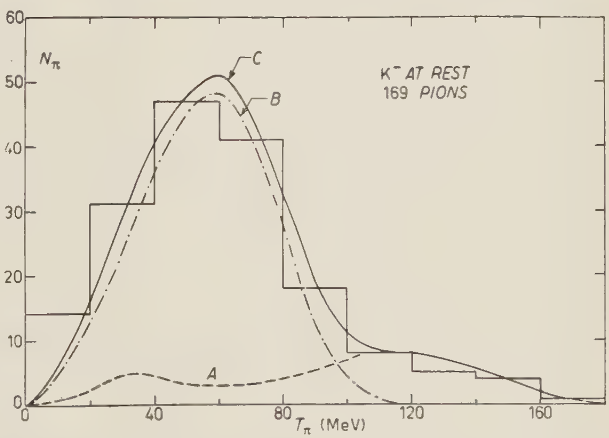

Fig. 3. – Histogram of the charged-pion spectrum. *a*) The calculated spectrum of pions produced in association with Λ hyperons. Intermediate model. *b*) The calculated spectrum of pions produced in association with Σ hyperons. Intermediate model. *c*) Curves *a* and *b* combined.

1839

together with the fit obtained from the theoretical spectrum computed for the intermediate case.

4·2. *Comparison between absorption at rest and in flight.* – In the absorption at rest, the K⁻-meson is captured in K-mesonic Bohr orbits and is finally absorbed into the nucleus. If we define a radius R_a as the average distance from the center of the nucleus at which the absorption takes place, then this radius depends on *a*) the K⁻ nucleon absorption cross-section at the relative energy determined by the K-mesonic orbital energy and the Fermi energy of the nucleon, and *b*) the overlap of the nuclear density distribution and the wave function for the orbit from which the absorption takes place.

The capture mechanism for K⁻ in flight consists of an absorption in a single traversal through the nucleus at impact parameter b. In this case, R_a is equal to the average impact parameter b at which the absorption occurs. Thus, the absorption radius R_a depends on the K⁻-nucleon cross-section at higher energies ($\bar{T}_{K^-} \simeq 105$ MeV) and the nuclear density distribution.

The pion spectrum of interactions in flight is shown in Fig. 2*B*. Although the number of pions observed is small, the following observation can be made:

a) The shape of the total pion spectrum corresponds to the pattern of the pions associated with Σ hyperons in the same way as it does for interactions of K⁻-mesons at rest.

b) The peak in the π_Σ spectrum expected at around 160 MeV (i.e. $\bar{T}_K = 105$ MeV in addition to the peak energy of 60 MeV observed for pions from K⁻ stars at rest) is shifted towards a lower energy and smeared over a large energy interval. The average expected kinetic energy of the pions under discussion here is about the same as that of pions associated with Λ hyperons at rest (~ 150 MeV). By comparing the observed pion spectrum with the calculated π_Λ spectrum for K⁻ absorption at rest, we see that the homogeneous model fits the spectrum better than the surface or average model.

We can use these data to obtain an estimate of the comparative absorption radius for K⁻ interactions in flight and at rest. If we consider the bubble chamber data of ALVAREZ *et al.* [6] and make use of charge independence, we expect the Λ/Σ ratio to be of the order of 0.2. This indicates that the data for the K⁻ interactions at rest are fitted best by a radius not much smaller than indicated by the surface model. We thus conclude that R_a at rest is greater than R_a in flight. This effect is similar to the one found for antiproton annihilation stars at rest and in flight [28].

---

[28] ANTIPROTON COLLABORATION EXPERIMENT: *Phys. Rev.*, **105**, 1037 (1957).

4.3. K^- *absorption stars as a source of Λ^0-hyperons.* – In the preceding section we have obtained from the observed pion spectrum the ratio of Λ^0 to $\Sigma^{\pm,0}$ hyperons *produced.* In this section we estimate the fraction of hyperons *emitted* in the average star formed by K^- interactions with nuclei in nuclear emulsion.

We have obtained this estimate by two methods:

1) energy balance;

2) strangeness balance.

4.3.1. *Energy balance.* – From the observed energy in charged particles emitted in K^- interactions, we have evaluated the energy emitted in neutral particles.

In order to evaluate the average energy per star given to nucleons, we have phenomenologically divided the nucleons into two classes: *a*) those due to the «knock-on» process in which, T_{nucleon} is 30 MeV or more, and *b*) those due to the evaporation process in which, T_{nucleon} is less than 30 MeV. The energy emitted in knock-on neutrons was obtained by using the average knock-on proton energy and a neutron-to-proton ratio $\langle n/p \rangle = \langle (A - Z)/Z \rangle_{\text{emulsion}} = 1.2$. The energy emitted in evaporation neutrons was obtained from the observed frequency of evaporation protons ([29]) and by using an n/p ratio of 4 with an average neutron kinetic energy of 3 MeV ([30]).

The average energy per star given off in pions and hyperons has been obtained from the observed pion and hyperon spectra. A correction factor had to be applied to this average energy to take into account the detection efficiency for these particles. We estimate the detection efficiency for the charged pions as 90%, for Σ^+ hyperons about 95%, and for Σ^- hyperons about 50%. The low detection efficiency for Σ^- hyperons is due to the frequent formation of zero-prong stars in Σ^- absorption.

To estimate the energy in neutral pions and Σ^0 hyperons, we have used charge independence and have assumed the same amount of attenuation for the neutral particles as for their charged counterparts on leaving the nuclei in which they were formed. Table VII summarizes the numerical values obtained. We can now determine the average energy E_0 in neutral particles

([29]) For the evaporation region we have assumed the same α/p ratio and energy spectra for the α's and protons as has been observed in the π^--meson absorption stars; see M. G. K. MENON, H. MUIRHEAD and O. ROCHAT: *Phil. Mag.*, **41**, 583 (1950).

([30]) E. E. GROSS: *The Absolute Yield of Low-Energy Neutrons from* 190 MeV *Proton Bombardment of Gold, Silver, Nickel, Aluminum, and Carbon* (*thesis*), UCRL-3330 (Feb. 1956).

other than in neutrons, neutral pions, and Σ^0 hyperons. We have

$$\begin{aligned}\bar{E}_0 &= M_K - (B_K + B_N) - \bar{U} \\ &= 495 - (8+8) - 331 \text{ MeV} \\ &= 148 \text{ MeV},\end{aligned}$$

where B_K and B_N are the atomic binding energies of the K-meson and the binding energy of the last nucleon in the nucleus, respectively. The 148 MeV carried away by other neutral particles we attribute to Λ hyperons. The Λ hyperons arise from two sources: *a*) the primary process, $K^- + \text{«n»} \to \Lambda^0 + \pi^-$,

TABLE VII. – *Division of energy released in an average* K⁻ *star.*

Particles		Energy (MeV)	Source of data
Evaporation nucleons	$\bar{U}_{ev}$	77	This work
Knock-on nucleons	$U_{k.o.}$	62	This work
Charged pions	$U_{\pi\pm}$	67	1956 Rochester compilation (1)
Charged hyperons	$U_{\Sigma\pm}$	58	1956 Rochester compilation (1)
Hyperfragments	$U_{hyperfr}$	5	This work
Neutral pions	U_{π^0}	33	Inference from charge independence
Neutral hyperons	$\bar{U}_{\Sigma^0}$	29	Inference from charge independence
Energy accounted for	$\bar{U}$	331	

and *b*) the secondary process, interactions of Σ hyperons with nucleons in the same nucleus in which they are produced, i.e. $\Sigma + \text{«n»} \to \Lambda^0 + \text{«n»}$. In both these processes the Λ^0 hyperons are emitted with an average kinetic energy of $\bar{T}_\Lambda \simeq 40$ MeV. The fraction of K⁻ stars in which a Λ^0-particle is emitted as a final product is the given by

$$f_{\Lambda^0} = \frac{\bar{E}_0}{M_\Lambda - M_p + T_\Lambda} = \frac{148}{217} = 0.68,$$

where M_Λ and M_p are the Λ^0 mass and proton mass respectively, in MeV.

4·3.2. *Strangeness balance.* – Conservation of strangeness requires that in each K⁻ interaction either a Σ or Λ hyperon be emitted. From the observed number of Σ hyperons and hyperfragments emitted, we can estimate the amount of missing strange particles. In this evaluation we have taken into account the low detection efficiency for Σ^- ($\sim 50\%$), and have used charge independence to estimate the amount of Σ^0-hyperon production. Table VIII summarizes the observed and inferred percentage of emitted Σ-hyperons.

From Table VIII it can be seen that we can account for strange particles in 35% of the stars. From this figure we deduce that in the remaining 65% of the stars, Λ hyperons must have been emitted. Combining these two results we

TABLE VIII. – *Strangeness balance.*

Type	Percent hyperon emission	Source
$\Sigma^{\pm}$	14	Observed
Σ^{-}	7	Detection efficiency correction
Σ^{0}	10	Charge independence
HF	3	Observed
Trapped Λ^{0}	1	Observed
	35%	

obtain $f_{\Lambda} = 0.66$. The fraction of Λ hyperons emitted in K^- stars and the Λ/Σ ratio at production (Sect. **3**·1) permit an evaluation of the amount of Σ-to-Λ conversion on leaving the parent nucleus. We find 58% of the Σ hyperons are converted into Λ hypreons.

We have thus shown by two independent methods that K^- interactions with bound nucleons in complex nuclei give as their final product mainly Λ hyperons. This effect may thus be utilized as a source for Λ hyperons for the detailed investigation of their properties.

4·3.3. *Prong distribution and visible energy release.* – The average

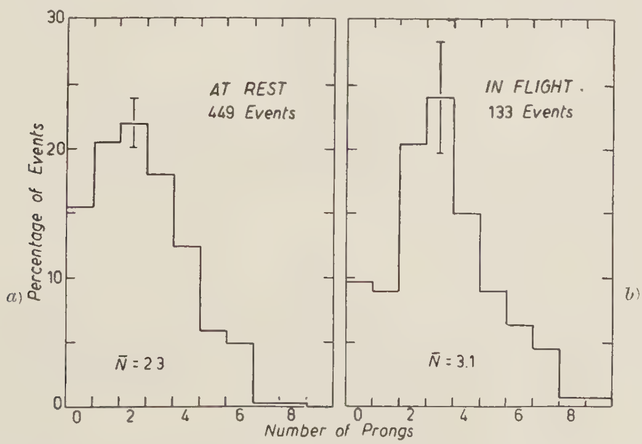

Fig. 4. – Histogram of prong distribution of K^- absorption events. *a*) Absorption at rest. *b*) Absorption in flight.

1843

kinetic energy for the stars in flight is $\bar{T}_K = 105$ MeV. This additional kinetic energy expresses itself in a larger nuclear excitation, as can be observed by comparing Fig. 4 and 5, parts *a* and *b*, which give the prong distribution and visible energy release for the interactions at rest and in flight respectively.

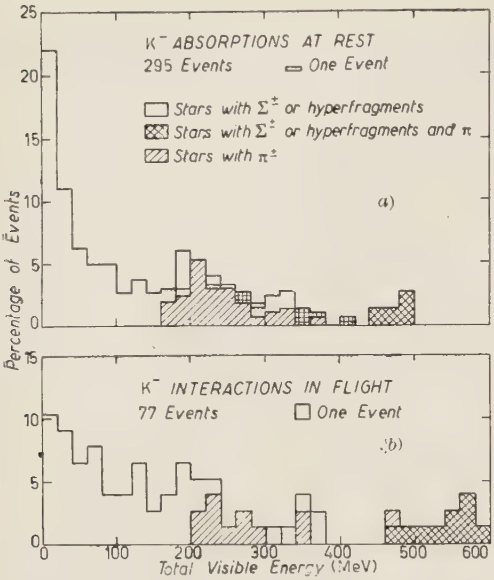

Fig. 5. – Histogram of total visible energy release in K⁻ absorption events. *a*) absorption at rest. *b*) Absorption in flight.

5. – Observations on Σ Hyperons.

In the course of this work we have identified 19 Σ^+, 6 $\Sigma^\pm$, and 16 Σ^- hyperons from K⁻ stars at rest and 5 Σ^+, 6 $\Sigma^\pm$, and 2 Σ^- hyperons from K⁻ stars in flight. In Table IX we list the pertinent information on the Σ^+ and $\Sigma^\pm$ hyperons, and in Table X the information on Σ^- hyperons.

In this work we do not have a sufficiently large sample to attempt a statistical analysis of the properties of the Σ hyperons, viz., lifetimes, Σ^+ mass, and decay asymmetries or asymmetries in the triple scalar product, such as $P_\Sigma \times P_\pi \cdot P_{\pi\Sigma}$, etc. We will thus present our data here only to make them available for inclusion in future compilations.

It is noteworthy that event S_{20} gives a Σ^+ hyperon that we have classified as a $\Sigma^+ \to p + \pi^0$ decay at rest for which the decay proton has an exceptionally long range, $R_p = 1864$ µm. This can have a number of explanations:

a) the Σ^+ was not quite at rest;

b) this is a prong from a Σ^- star;

c) it must be borne in mind that long-lived excited states of Σ hyperons might exist, which could then decay with a higher Q-value. It is thus important to observe the range distribution and watch for possible fine structure. A similar case was reported by Fry *et al.* [31] with $R_p = 1800$ µm.

---

(31) W. F. Fry, G. A. Snow, J. Schneps and M. S. Swami: *Phys. Rev.*, **103**, 226 (1956).

TABLE IX. – *Characteristics of Σ^+ and $\Sigma^\pm$ hyperons from K^- stars.*

Event	Range of Σ (μm)	Kinetic energy of Σ at K^- star	Range of proton if in $p+\pi^0$ mode	Cosine of space angle of decaying pion	Associated π-meson (if present)	Kinetic energy of π-meson ([b]) (MeV)	Time to point of decay ($\cdot 10^{-10}$ s)	Potential time ($\cdot 10^{-10}$ s)
Decay of Σ^+ to $n+\pi^+$ at rest								
K_{114}	11240	64	—	+0.492	—	—	—	1.79
K_{20} ([a])	806.4	13.7	—	+0.158	π^-	~100	—	0.232
S_{11B}	3303	31.2	—	−0.422	$\pi^\pm$	—	—	0.712
S_{23}	4375	36.8	—	−0.175	π^-	178	—	0.867
S_{1003}	1944	22.8	—	+0.911	—	—	—	0.485
K_5	620	11.7	—	+0.517	—	—	—	0.206
K_1	363	8.6	—	−0.919	—	—	—	0.144
K_{14}	950	15.1	—	+0.013	π^-	98	—	0.280
K_{18}	1510	20.0	—	+0.956	π^-	48	—	0.396
K_{21} ([a])	1385	19.6	—	−0.059	$\pi^\pm$	55	—	0.369
K_{28}	475	10.1	—	+0.895	$\pi^\pm$	~125	—	0.173
K_{33}	930	14.8	—	−0.231	π^-	49	—	0.270
K_{44}	1320	18.3	—	+0.218	—	—	—	0.350
K_{50}	1805	21.9	—	−0.187	—	—	—	0.445
K_{1023}	2300	25.3	—	−0.226	π^-	27	—	0.538
Decay of Σ^+ to $p+\pi^0$ at rest								
K_7^-	105	4.1	1631	+0.478	—	—	—	0.96
K_{23}^-	2840	28.5	1638	−0.470	—	—	—	0.63
K_{C31}	960	15.5	1645	−0.558	—	—	—	0.39
K_{1036}	716	12.7	1580	+0.352	$\pi^\pm$	67	—	0.23
K_{4003} ([a])	804.9	13.7	1637	−0.869	$\pi^\pm$	77	—	0.22
K_{10}	356	8.5	1600	+0.943	—	—	—	0.14
K_{52}	1436	19.3	1596	−0.051	π^+	71	—	0.38
S_9	6850	47.8	1669	+0.661	$\pi^\pm$	100	—	1.25
S_{20}	5590	42.3	1864	−0.690	$\pi^\pm$	89	—	1.03
Decay of Σ^+ to $p+\pi^0$ in flight								
K_{Z11}	2560	35.0	2920	−0.788	—	—	0.23	0.80
K_{1049}	1780	52.0	16100	+0.945	$\pi^\pm$	58	0.86	1.30
K_{1002}	19800	122	22400	−0.890	—	—	2.17	3.77
K_{1008}	1250	31.4	18900	−0.930	π (1)	—	0.36	0.70
Decay of $\Sigma^\pm$ to $n+\pi^\pm$ in flight								
K_{6011}	19	13	—	−0.693	$\pi^\pm$	—	0.007	0.242
K_{1038}	13000	95	—	+0.160	—	—	1.25	2.75
S_4	6040	59	—	+0.253	$\pi^\pm$	—	0.72	1.52
S_8	4880	80	—	−0.147	$\pi^\pm$	—	0.42	2.20
S_{138}	23000	137	—	+0.313	$\pi^\pm$	—	1.71	4.31
S_{24}	836	120	—	+0.432	—	—	0.03	3.65
S_{1006}	2010	46	—	−0.930	$\pi^\pm$	—	0.26	1.11
S_{1024}	2035	64	—	+0.769	$\pi^\pm$	—	0.20	1.07

(*a*) K-H absorption events. (*b*) Given only for events in which dip angle was not greater than 20°.

TABLE X. – *Characteristics of Σ^- hyperons from K^- stars.*

Event	Range of Σ (μm)	Kinetic energy (MeV)	No. of prongs of Σ^- star	Range of prongs ([a]) (μm) and comments	Associated π-meson (if present)	Kinetic energy of associated π-meson (MeV)
K_2^-	695	12.6	0	$\Sigma\rho$ from K^-+H absorption. Identified from kinematics	$\pi^\pm$	85
K_{C2}^-	815	13.8	2	168, 87	—	—
K_6^-	254	7.0	1	< 30	$\pi^\pm$	55
K_9^-	4100	35.0	1	< 30	—	—
K_{C10}^-	76	33.0	1	955 and 1 recoil	π^+	57
K_{M13}^-	547	11.0	2	6080, 5760 and 1 recoil	—	—
K_{14}^-	3433	32.0	0	$\Sigma\rho$ with associated electron	—	—
K_{16}^-	1970	23	1	< 30	—	—
K_{19}^-	181	5.1	0	$\Sigma\rho$ with associated electron	—	—
K_{C22}^-	3100	30.0	5	205, 1800, 50, 204, 390 and 1 recoil	—	—
K_{63}^-	222	6.4	1	1195; *d* or α-particle	$\pi^\pm$	82
K_{1001}^-	974	15.4	1	594	π^-	24
K_{1004}^-	827	14.0	1	1730 and 3 recoils	—	—
K_{1060}^-	1068	16.2	1	37	—	—
K_{4001}^-	632	12.2	1	293 and 2 recoils	$\pi^\pm$	84
K_{5018}^-	184	5.7	2	546, 176	$\pi^\pm$	77
S_3^-	2550	27.3	1	695	π^+	54
S_{148}^-	1919	23.1	1	4250	—	—

(*a*) All prongs are consistent with protons unless stated otherwise.

Using the eight $\Sigma^\pm$ hyperons decaying in flight (Table IX) we obtain, from a maximum-likelihood analysis, $\tau_{\Sigma^\pm} = (0.813^{+1.25}_{-0.34})\cdot 10^{-10}$ s [32]. This value is quite consistent with the Σ^+ and Σ^- lifetime and does not give the anomalously low values obtained by FRY *et al.* [33] and GLASSER *et al.* [34].

* * *

We wish to thank Dr. EDWARD J. LOFGREN and the Bevatron crew for their excellent support and co-operation. We are especially grateful to Mr. HUGO BAYONA, Mrs. FRANCES GLENN, Miss GRAYDON HINDLEY, Mr. D. H. KOUNS, Miss SHEILA LIVINGSTON, Miss HELEN PROBST, Mrs. EVELYN ROREM, Mrs. ELISABETH RUSSEL, Mrs. LOUISE SHAW, Mrs. CATHERINE TOCHE and

[32] M. BARTLETT: *Phil. Mag.*, **44**, 249 (1953).

[33] W. F. FRY, J. SCHNEPS, G. A. SNOW, M. S. SWAMI and D. C. WOLD: *Phys. Rev.*, **107**, 257 (1957).

[34] R. G. GLASSER, N. SEEMAN and G. A. SNOW: *Phys. Rev.*, **107**, 277 (1957).

Mr. G. M. Wike for their constant assistance throughout this work. We particularly appreciate the assistance of Miss Susan Klein in the compilation of the data. We are indebted to Dr. Robert Karplus for the many helpful discussions.

This work was done under the auspices of the U.S. Atomic Energy Commission.

Appendix

To evaluate the effect of pion absorption on leaving the nucleus, we have used an optical model. We have applied the pion mean free path as given by Frank, Gammel and Watson (FGW) [35] to two extreme cases. In the first case, we assume that the K^--mesons are absorbed uniformly over the volume of the nucleus (homogeneous model). The fraction of pions leaving the nucleus without interacting is then given by the formula

$$f_T = 3\left[\frac{1}{2x} - \frac{1}{x^3} + \frac{1}{x^3}(1+x)\exp[-x]\right],$$

where $x=2R/\lambda$; λ = mean free path in nuclear matter; and $R=1.4A^{\frac{1}{3}}\cdot 10^{-13}$ cm is the nuclear radius [36]. (The parameter $r_0 = 1.4\cdot 10^{-13}$ cm must be used in this calculation, because the mean free path was computed for this value by FGW).

In the second case we consider the other extreme, in which we assume that all K^--mesons are absorbed on the surface of the nucleus, i.e.; a shell of radius R (surface model). The fraction of pions leaving the nucleus is now given by $f_T = \frac{1}{2}[1+(1-\exp[-x])/x]$. Fig. 6 gives the percentage of pions emitted from the nucleus without interactions, averaged over the emulsion constituents or the two cases. For the

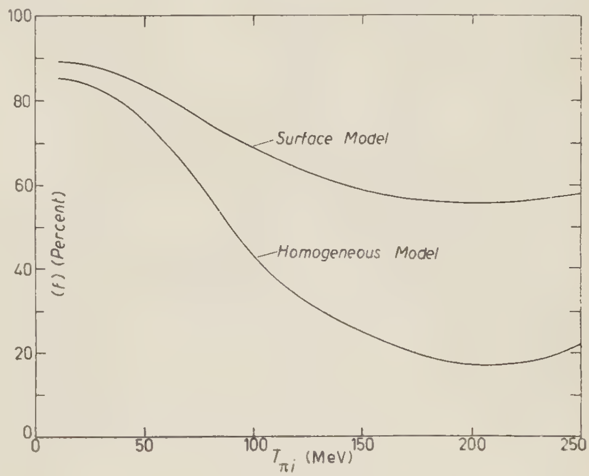

Fig. 6. – Calculated elastic pion emission for the energy interval 0 to 250 MeV inside the nucleus. The upper curve is calculated for the surface model, and the lower curve for the homogeneous model, averaged over the constituents of photographic emulsions.

(35) R. M. Frank, J. L. Gammel and K. M. Watson: *Phys. Rev.*, **101**, 891 (1956).
(36) K. A. Brueckner, R. Serber and K. M. Watson: *Phys. Rev.*, **84**, 258 (1951).

1847

mean free path λ, we have used λ_T, the total mean free path. We thus have $1/\lambda_T = 1/\lambda_a + 1/\lambda_s$, where λ_a = absorption mean free path and λ_s = scattering mean free path.

The fraction of pions emitted, f_T, corresponds thus to those pions that do not undergo any nuclear interaction. The fraction $1 - f_T$ corresponds to those pions that are absorbed or elastically scattered from a nucleon inside the complex nucleus. Those pions that are scattered inside the nucleus can undergo subsequent collisions and are either absorbed or finally emitted at a lower energy. Thus the final pion spectrum consists of the unmodified pions that are a fraction f_T of the pions produced in the K-nucleon absorption process, and superimposed on this is the spectrum of the inelastically scattered pions (pions degraded in energy). To estimate the spectrum of the inelastically scattered pions, we have used the results obtained in studies of pion interactions in nuclear emulsions in the energy range 60 to 150 MeV. In these experiments, it was shown that the inelastic scattering cross-section is about 25% of the pion-reaction cross-section and that the pions are degraded to a final energy centered at about 35 MeV [1,37]. The fraction of inelastically scattered pions has thus been taken as $0.25(1 - f_T)$.

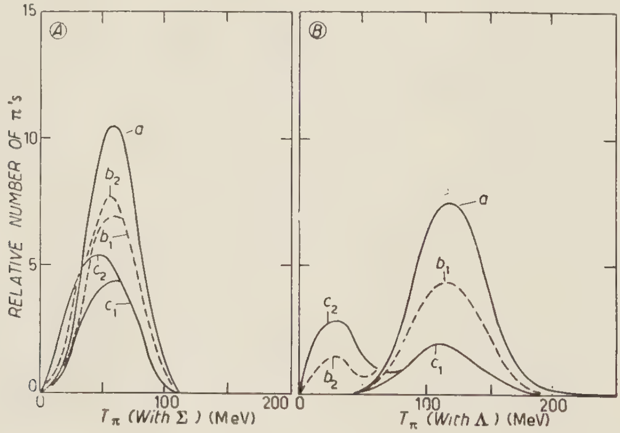

Fig. 7. – The theoretical pion spectra associated with Σ and Λ production. Curves *a* give the original pion distribution at production normalized in each case to the same total intensity. Curves *b* and *c* show modifications due to pion absorption according to the surface and uniform models, respectively. Subscripts 1 and 2 refer to the unmodified and total pion spectrum respectively.

In Fig. 6 we showed the percent pion emission f_T as a function of pion kinetic energy inside the nucleus for the two models under discussion. The

---

([37]) G. Bernardini, E. T. Booth and L. M. Lederman: *Phys. Rev.*, **83**, 1075 (1951); G. Bernardini, E. T. Booth and L. M. Lederman: *Phys. Rev.*, **83**, 1277 (1951); G. Bernardini and F. Levy: *Phys. Rev.*, **84**, 610 (1951); G. Goldhaber and S. Goldhaber: *Phys. Rev.*, **91**, 467 (1953); and A. H. Morrish: *Phys. Rev.*, **90**, 674 (1953).

1848

effect of scattering and absorption for the pions produced in association with Σ and Λ hyperons is shown in Figs. 7*a* and 7*b* respectively, for both the surface and the homogeneous models. For comparison, the original production spectra are also shown. This calculation has been made for equal probabilities of production of Σ and Λ hyperons.

RIASSUNTO (*)

È stata eseguita l'analisi delle interazioni dei mesoni K^- di 420 MeV/c incidenti su un pacco di emulsioni nucleari. Seguendo i mesoni K^- lungo la traccia abbiamo ottenuto informazioni sull'interazione dei mesoni K^- in volo e a riposo. La sezione d'urto differenziale è stata adattata alla sezione d'urto totale della reazione, con uno scattering per diffrazione con raggio $1.32\,A^{\frac{1}{3}}$ fermi in accordo con la sezione d'urto totale della reazione. Si presenta una compilazione di eventi di scattering e di assorbimento K^--H, dando sezioni d'urto di σ_{KH} (scattering) $= (48.4^{+15}_{-11})$ mb e σ_{HK} (assorbimento) $= (11.4^{+9}_{-5})$ mb. Lo scattering inelastico dei mesoni K^- in nuclei complessi è stato trovato essere solo il 4% della sezione d'urto di assorbimento. Le perdite medie di energia negli eventi di scattering K^- anelastici è $\sim 50\%$ dell'energia dei K incidenti in contrasto con la perdita del 25% per gli scattering K^+ anelastici. Nel corso del presente lavoro abbiamo osservato alcuni decadimenti in volo. Combinando questi con dati precedenti otteniamo una vita media $\tau_{K^-} = (1.3^{+0.4}_{-0.3})\cdot 10^{-8}$ s. Abbiamo identificato alcuni dei secondari dei decadimenti in volo: 2 $K_{\pi 2}$, 2 $K_{\mu 2}$ e 1 K_{e3}. Dagli eventi di assorbimento K^--H abbiamo ottenuto una differenza di massa Σ^--Σ^+ di $(13.9 \pm 1.8)\,m_e$ e per la mass del K^- il valore $(966.7 \pm 2.0)\,m_e$. Dall'analisi dello spettro dei pioni carichi ottenuto dalle interazioni K^- a riposo è stato possibile calcolare il rapporto fra gli iperoni Λ e Σ prodotti nell'interazione primaria. Troviamo che nella reazione primaria di assorbimento di un K^-, la formazione di iperoni Σ prevale sulla formazione di iperoni Λ. Il bilancio energetico e della stranezza mostra che il 70 % delle stelle K^- a riposo emettono una particella Λ. Ciò significa che circa il 60 % degli iperoni Σ prodotti si convertono in iperoni Λ all'interno del nucleo in cui si formano.

(*) *Traduzione a cura della Redazione.*

L'hypothèse d'ondes corpuscules et la théorie de la Relativité restreinte.

K. Stiegler
Zagreb

(ricevuto il 15 Aprile 1958)

Résumé. — On montre ici qu'on peut déduire les lois fondamentales de la théorie de la Relativité restreinte partant du système d'axiomes qui au lieu de l'axiome d'Einstein sur la constance de la vitesse de la lumière contient l'axiome d'ondes-corpuscules de M. Louis de Broglie comprenant l'hypothèse de quanta, d'après lequel à chaque corpuscule matériel en mouvement est associée une onde.

1. – Le système d'axiomes proposé.

Supposons que pour la transformation des coordonnées et du temps entre deux systèmes de référence galiléens S et S' existent les relations

$$x = \alpha_{11}x' + \alpha_{12}t' , \tag{1}$$

$$y = y' , \tag{2}$$

$$z = z' , \tag{3}$$

$$t = \alpha_{21}x' + \alpha_{22}t' , \tag{4}$$

α_{11}, α_{12}, α_{21} et α_{22} étant des coefficients que l'on doit déterminer (Ax. 1), que pour les corpuscules matériels qui à l'égard du système S resp. S' parcourent le chemin

$$x_2 - x_1 = \Delta\Lambda , \tag{5}$$

respectivement

$$x_2' - x_1' = -\Delta\lambda\,, \tag{6}$$

dans le temps

$$t_2 - t_1 = \Delta T\,, \tag{7}$$

respectivement

$$t_2' - t_1' = \Delta\tau\,, \tag{8}$$

l'inverse est aussi vrai, c'est à dire les corpuscules matériels qui à l'égard du système S ont parcouru le chemin

$$x_2 - x_1 = \Delta\lambda\,, \tag{9}$$

dans le temps

$$t_2 - t_1 = \Delta\tau\,, \tag{10}$$

doivent à l'égard du système S' parcourir le chemin

$$x_2' - x_1' = -\Delta\Lambda\,, \tag{11}$$

dans le temps

$$t_2' - t_1' = \Delta T\,, \tag{12}$$

(Ax. 2), qu'à chaque corpuscule matériel libre de quantité de mouvement $\mathfrak{p} = m(|\dot{\mathfrak{r}}|)\dot{\mathfrak{r}}$ et d'énergie $E = h\nu$ finie et toujours différente de zéro est associée l'onde

$$\psi = A \exp\left[-\frac{i}{\hbar}\,(Et - \mathfrak{p}\mathfrak{r})\right], \tag{13}$$

où $m(|\dot{\mathfrak{r}}|)$ signifie la masse de corpuscule matériel qui pourrait varier quand on varie la valeur absolue de la vitesse de ce corpuscule, h la constante de Planck, ν la fréquence, A l'amplitude et $\hbar = h/2\pi$ une constante (Ax. 3) et enfin que dans tous les systèmes de référence galiléens les lois physiques ont la même forme analytique (Ax. 4).

2. – Les conséquences de système d'axiomes proposé.

Soit le corpuscule matériel en repos dans S' se mouvant à l'égard de S le long de l'axe X avec la vitesse constante v, tandis que Y et Y' respectivement

Z et Z' sont parallèles. Les observateurs dans S et S' sont muni d'un mètre, et de plusieurs cronomètres qui sont parfaitement identiques et syncronysés par moyens mécaniques.

De l'Ax. 1 et l'Ax. 2, qui sont valables dans la Mécanique classique et aussi dans la Mécanique relativistique il s'ensuit

$$\Delta\Lambda = \alpha_{11}\left(-\Delta\lambda + \frac{\alpha_{12}}{\alpha_{11}}\Delta\tau\right), \tag{14}$$

$$\Delta T = \alpha_{22}\left(-\Delta\lambda\frac{\alpha_{21}}{\alpha_{22}} + \Delta\tau\right), \tag{15}$$

$$-\Delta\Lambda = \frac{\alpha_{22}}{D}\left(\Delta\lambda - \frac{\alpha_{21}}{\alpha_{22}}\Delta\tau\right), \tag{16}$$

$$\Delta T = \frac{\alpha_{11}}{D}\left(-\Delta\lambda\frac{\alpha_{21}}{\alpha_{11}} + \Delta\tau\right), \tag{17}$$

où

$$D = \alpha_{11}\alpha_{22} - \alpha_{12}\alpha_{21} = 1 \tag{18}$$

et par la comparaison de (14) et (16), respectivement (15) et (17)

$$\alpha_{11} = \alpha_{22}\,, \tag{19}$$

$$\alpha_{11}\alpha_{22} - \alpha_{12}\alpha_{21} = 1\,. \tag{20}$$

En désignant la vitesse d'un point se trouvant en repos dans le système S' à l'égard de S par v, à l'aide de (1) et (4) on conclut que la vitesse de l'origine de S' mesurée depuis S est égale et contraire à la vitesse de l'origine de S mesurée depuis S' (conséquence de l'Ax. 2) et par suite

$$\alpha_{12} = \alpha_{11}v\,. \tag{21}$$

A l'égard de S d'après l'Ax. 3 à un corpuscule matériel libre se mouvant le long de l'axe X de S une onde est associée et donnée par

$$\psi_S = A\,\exp\left[-\frac{i}{\hbar}(Et - px)\right], \tag{22}$$

tandis que d'après l'Ax. 3 et l'Ax. 4 à l'égard de S' où le corpuscule matériel est en repos l'onde associée sera donnée par

$$\psi_{S'} = A\exp\left[-\frac{i}{\hbar}E't'\right]. \tag{23}$$

D'après (1), (4), (19) et (21) on obtient de (22)

$$\psi_{S'} = A \exp\left[-\frac{i}{\hbar} E\alpha_{11} \cdot \left(1 - \frac{pv}{E}\right)\left(t' - \frac{(p/E - \alpha_{21}/\alpha_{11})}{1 - (pv/E)} \cdot x'\right)\right] \tag{24}$$

et aussi par comparaison de (23) et (24)

$$E' = E\alpha_{11} \cdot \left(1 - \frac{vp}{E}\right), \tag{25}$$

$$\frac{p}{E} - \frac{\alpha_{21}}{\alpha_{11}} = 0\,. \tag{26}$$

De (19), (20), (21) et (1)–(4) nous obtenons

$$\alpha_{11} = \frac{1}{\sqrt{1 - (v/\sqrt{E/m})^2}} \tag{27}$$

et les transformations de Lorentz et d'Einstein

$$x = \frac{x' + vt'}{\sqrt{1 - (v/\sqrt{E/m})^2}}\,, \quad y = y'\,, \quad z = z'\,, \quad t = \frac{t' + (v/(E/m)) \cdot x'}{\sqrt{1 - (v\sqrt{E/m})^2}}\,. \tag{28}$$

D'après l'Ax. 4 pour la transformation inverse nous avons

$$x' = \frac{x - vt}{\sqrt{1 - (v/\sqrt{E/m})^2}}\,, \quad y' = y\,, \quad z' = z\,, \quad t' = \frac{t - (v/(E'/m')) \cdot x}{\sqrt{1 - (v/\sqrt{E'/m'})^2}}\,. \tag{29}$$

En exprimant des équations (28) les coordonnées de S' au moyen de coordonnées de S et tenant compte que l'énergie E' et la masse m' de corpuscule matériel dans S' est finie, constante et différente de zéro, par comparaison des expressions obtenues et celles de (29) il s'ensuit

$$\frac{E}{m} = \frac{E'}{m'} = C^2\,, \tag{30}$$

relation qui tient pour chaque valeur v de la vitesse relative, C étant une constante universelle.

L'énergie de corpuscule matériel étant d'après l'Ax. 3 toujours finie et différente de zéro, ayant spécialement dans S' une valeur constante bien de-

terminée, de la relation (25) et (27) il en résulte que cette constante universelle C représente pour la vitesse de corpuscule matériel une *limite supérieure* que nous appelerons *la vitesse limite*. Cette constante C ayant d'après (30) pour chaque système de référence galiléen la même valeur, cette relation exprime *le principe de la constance de la vitesse limite.*

RIASSUNTO (*)

Si dimostra qui che si possono dedurre le leggi fondamentali della teoria della relatività ristretta partendo dal sistema d'assiomi che in luogo dell'assioma di Einstein sulla costanza della velocità della luce contiene l'assioma delle onde-corpuscoli di L. De Broglie, comprendente l'ipotesi dei quanti, secondo il quale ad ogni corpuscolo materiale è associata un'onda.

(*) *Traduzione a cura della Redazione.*

The Nature of the Taper Tracks of Heavy Ions in Nuclear Emulsions.

O. SKJEGGESTAD
Institute of Physics, University of Oslo - Blindern, Norway

(ricevuto il 13 Marzo 1958)

Summary. — The thinning down of the tracks of heavy ions as they approach the end of their range in electron sensitive photographic emulsion, can be quantitatively explained on the assumption that the thickness of the developed track is due mainly to δ-rays which no longer have sufficient range at low ion velocities to broaden the track.

1. – Introduction.

The theory of the stopping of charged particles by matter deals with the kinetic energy lost by the moving particle. It is not a theory of the ionization produced in the absorbing medium. The actual number of ion pairs produced by a given transfer of kinetic energy depends in a complicated way upon the nature of the absorber. The total ionization in the medium is the sum of the primary ionization produced by collisions of the primary particle with atomic electrons and the secondary ionization produced by energetic electrons resulting from the primary collisions.

A comprehensive theory of track formation of charged particles in nuclear emulsion has to take into account not only the complicated, and as yet unestablished, relation between energy loss and number of ions effective in producing developable grains, but also the number of developed grains whose blackening is due merely to the process of development or to the proximity of one or more of the activated grains. For multiply charged particles we have to apply these relations both to the primary and to the secondary ionization because of the long δ-rays produced by heavy ions. A theoretical treatment will therefore be extremely complicated, and at present we cannot find any comprehensive theoretical explanation of the process of track formation by heavy ions in nuclear emulsions. Lacking this, we shall try a very simplified model that may also explain quantitatively some features of the track produced by particles with charge $Z > 3$. Tracks from multiply-charged

particles in photographic emulsion are easily detected because of the great number of δ-rays emerging from the solid core of the track, and because of the characteristic tapering of the main core near the end of the range.

It is obvious as first pointed out by HOANG (1), that the δ-rays can also contribute to the width of the solid core of the track. If the density of δ-rays is so great that they cannot be individually resolved in the microscope, such δ-rays cannot be separated from the main core produced by primary ionization of the particle. By examining the δ-ray frequency LONCHAMP (2) determined the « thin-down » length of tracks from multiply-charged particles to be in good agreement with the experimental values.

In the present paper we study how the variation in the mean energy of the δ-rays along the track may explain the variation in thickness of the solid core near the end of the range. In our calculations we assume that:

a) the main contribution to the track width of multiply-charged particles comes from the secondary ionization;

b) the apparent track width varies with the mean energy of those δ-rays whose density is so great that they cannot be individually distinguished.

2. – The δ-ray distribution.

When a heavy particle with charge Ze and velocity $v = \beta c$ passes through the emulsion, the number, $\mathrm{d}n$, of δ-rays with energies in the interval from W to $W + \mathrm{d}W$, produced per unit length of trajectory, is given by the formula of MOTT (3):

$$\mathrm{d}n = \frac{2\pi N Z^2 e^4}{m\beta^2 c^2}\,\frac{\mathrm{d}W}{W^2}\,, \tag{1}$$

where m is the mass of the electron and N the number of electrons per cm³ of the emulsion.

The total number per unit length, n, of δ-rays whose energy is greater than W is given by:

$$n = \frac{2\pi N Z^2 e^4}{m\beta^2 c^2}\left[\frac{1}{W} - \frac{1}{2m\beta^2 c^2}\right], \tag{2}$$

where $2mc^2\beta^2$ is the maximum energy a heavy particle with velocity βc can transfer to en electron.

We want to find the δ-ray energy $W = W_0$ which gives a number of δ-rays (n_0) with energy greater than W_0, where n_0 is the number of δ-rays sufficient to produce clogging. Thus for $n > n_0$ the δ-rays can no longer be individually resolved by means of a microscope, but seem to belong to the solid core of the track.

(1) T. F. HOANG: *Journ. Phys. Rad.*, **12**, 739 (1951).
(2) J. P. LONCHAMP: *Journ. Phys. Rad.*, **14**, 433 (1953).
(3) N. F. MOTT: *Proc. Roy. Soc.*, **124**, 425 (1929).

Replacing n by n_0 and W by W_0 in formula (2) and solving the equation with respect to W_0 we obtain.

$$W_0 = \frac{1021}{(n_0 \cdot 10^3/2.6)\cdot(\beta^2/Z^2) + 1/\beta^2} \text{(keV)}, \tag{3}$$

where the constants e, c, m and N in formula (2) have been replaced by their numerical values (N for an Ilford G-5 emulsion) and where n_0 is in terms of number/100 μm.

From the distribution formula (1) we find that the mean energy W of δ-rays in the interval W_0 to $2mc^2\beta^2$ is given by:

$$\overline{W} = \frac{\ln(2mc^2\beta^2/W_0)}{(1/W_0)-(1/2mc^2\beta^2)}. \tag{4}$$

Equations (3) and (4) now give a relation between the mean energy of the δ-rays and the velocity of the primary particle. By means of a range-energy relation for heavy ions we may in addition find a connection between the mean energy $\overline{W}$ and the particle range R.

3. – Range-energy relation for heavy ions.

For particles of charge $Z > 2$ BARKAS ([4]) gives an empirical range-energy relation for Ilford C-2 emulsion,

$$\frac{Z^2}{M} R = f(\beta) + B_Z, \tag{5}$$

which holds for $\beta > 1.04Z/137$. For particles of charge $Z \leqslant 6$, B_Z varies approximately as $B_Z = 0.12Z^3$, and $f(\beta)$ is given by the ordinary empirical range-energy relation for α-particles.

B_Z for oxygen ions has been found in the following way. In the plates exposed to ^{16}O ions in the heavy ion accelerator in Berkeley (see Sect. 5) we find one small group of ions with range (R_x) appreciably greater than that of the main group with range $R_{^{16}O}$. We measure the ranges to be $R_{^{16}O} = (146.8 \pm 2.7)$ μm and $R_x = (191.8 \pm 4.1)$ μm.

If we neglect the effect of electron pick-up as a first approximation, and put the measured ratio $R_{^{16}O}/R_x$ into the ordinary range-energy relation given by $R = (M/Z^2)f(\beta)$, we obtain $(M/Z^2)_x = 0.326$. If on the other hand we extrapolate Barkas' formula (5) with $B_Z = 0.12Z^3$ to $Z = 8$, we obtain $(M/Z^2) = 0.348$.

In a linear accelerator the ions ^{10}B, ^{12}C, ^{14}N and ^{16}O will all come out with the same velocity, consequently, theoretical values of the quantity (M/Z^2) can be calculated for these ions.

([4]) W. H. BARKAS: *Phys. Rev.*, **89**, 1019 (1953).

TABLE I. – M/Z^2 *values for different elements.*

Element	^{10}B	^{12}C	^{14}N
M/Z^2	0.400	0.333	0.286

From such calculated values shown in Table I it is clear that the only ion with a M/Z^2 value in agreement with the experimental one is ^{12}C. We substitute B_z in formula (5) by the experimental values of Barkas $B_6 = 23.9$ to obtain the equations:

$$\frac{6^2}{12} R_{^{12}\mathrm{C}} = f(\beta) + 23.9\,,$$

$$\frac{8^2}{16} R_{^{16}\mathrm{O}} = f(\beta) + B_8\,,$$

which gives $B_8 = 35.7$ (see Fig. 1).

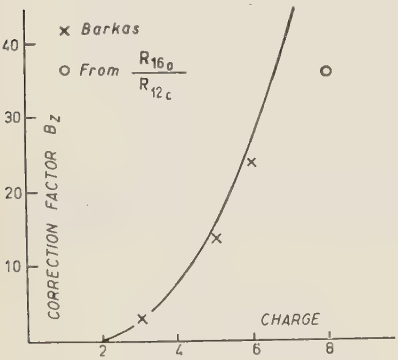

Fig. 1. – Range correction B_Z of heavy ions, due to electron pick-up at the end of the range. The curve shows the function $B_z = 0.12\,Z^3$.

For $\beta < 1.04Z/137$ we have no empirical range-energy relation for heavy ions in nuclear emulsions. In this region, therefore, we use theoretical values which were calculated by LONCHAMP (5) on the assumption that the ions have an effective charge $0.6\,Z$.

4. – Determination of n_0.

By definition n_0 is the number of δ-rays per 100 μm necessary to make the δ-rays individually indistinguishable in the microscope. That is, the density of δ-rays is so large that the ends of the rays form a solid line and cannot be distinguished from the core formed by the primary ionization. The number of δ-rays, n_0, so defined is difficult to determine precisely because of the large scattering of electron tracks.

The plates used in the present investigation have a grain diameter of (0.62 ± 0.08) μm. Within the errors of measurement we have practically the same grain diameter in all the plates.

We suppose the δ-rays to be «evenly» distributed around the main core of the track. But δ-rays going straight up and straight down in the emulsion obviously do not contribute to the track width. It is reasonable to say that just those δ-rays within angles of 90° on each side of the core give significant contribution to the track width. In that case we find $n_0 = 330$ $(100\ \mu\text{m})^{-1}$.

(5) J. P. LONCHAMP: *Journ. Phys. Rad.*, **14**, 89 (1953).

Because of the large scattering of the δ-rays this value represents an upper limit. A brief calculation shows, however, that the value of W_0 in eq. (3) is very insensitive to variations in n_0, so that our approximation appears to be good enough.

5. – Experimental determination of the track width.

The following two sets of plates were used to determine the track widths produced by heavy ions.

1) The A-plates: A stack of Ilford G-5 stripped emulsion, 600 μm thick, exposed to cosmic rays at high altitude.

2) The ^{16}O-plate: An Ilford G-5 plate, 50 μm thick, exposed to ^{16}O-ions in the heavy particle accelerator in Berkeley, California.

The tracks selected in the A-plates were produced by heavy fragments from energetic nuclear disintegrations.

The widths of the tracks were measured by a method described in an earlier paper (6). By means of a projection microscope a drawing of the heavy ion track was made, and the track area measured with a planimeter. The track area per unit length then gives the width of the track as a function of the particle range.

In the planimeter measurement of the track area long δ-rays are also included, provided no gap between the δ-ray and the main core of the track could be seen.

Fig. 2 gives the track width as a function of residual range for different particles. In the A-plates we have no heavy fragments from nuclear disintegrations with charge greater than that of boron ($Z = 5$); this makes a direct comparison with the track width from the ^{16}O-plate impossible.

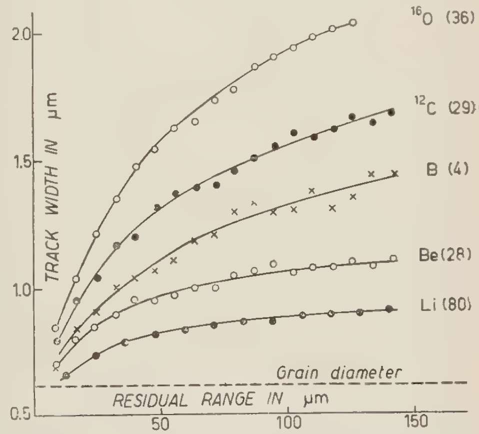

Fig. 2. – Experimental values of mean track width versus residual range for different charge values. The numbers in brackets indicate the number of each sort of particle that is measured.

Measurements of mean grain diameter, and track width produced by α-particles from Thorium stars may, however, give some information about the specific ionization for the two types of plates.

The data given in Table II show that the mean grain diameter, and the mean track width of α-particles from Thorium stars are the same in the

(6) O. SKJEGGESTAD: *Arch. Math. Naturvidenskab*, B **54**, no. 1 (1956).

TABLE II.

Plate	Grain diameter in μm	Track width of α-particles from Th-stars in μm
A-plates	0.60 ± 0.08	0.78 ± 0.07
^{16}O-plate	0.64 ± 0.07	0.75 ± 0.08

A-plates and the ^{16}O plate. From this fact we may conclude that the ionization within the errors of measurements is the same in both types of plates, thus making a comparison between the track width of ions from different plates possible.

6. – Comparison between the experimental and calculated track widths.

Equations (3), (4) and (5) give the mean δ-ray energy $\overline{W}$ as a function of the heavy particle range R for different values of Z. For small ranges the particle charge Z in formula (3) should be replaced by the effective charge, Z_{eff}, because of the electron pick-up by particles of small velocities. The relation between the effective charge and the velocity of the particle in photographic emulsion is very uncertain, but we find, however, that the maximum error in the value of W_0 that results from using Z in (3) instead of Z_{eff}, is less than 4% for ranges greater than 15 μm. Such an error is negligible compared with errors arising from rather uncertain assumptions made in our calculations.

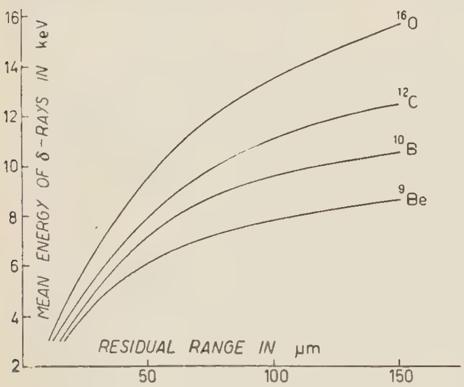

Fig. 3. – Theoretical curves of the mean energy of δ-rays from different heavy ions as a function of the range of the particle.

Fig. 3 shows the theoretical curves calculated for $n_0 = 330$. The form of these curves shows the same general tendency as the curves of Fig. 2 where the track width (as defined in this paper to be track area per unit length) increases with increasing range for the first 150 μm.

In order to compare the theoretical values given by equations (3), (4)

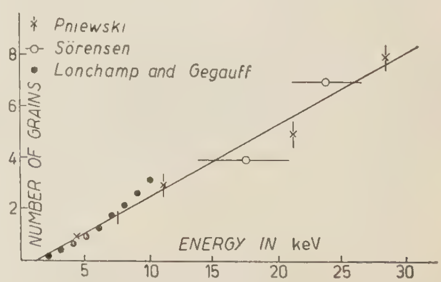

Fig. 4. – The relation between the mean number of grains in an electron track and the corresponding energy.

and (5) with the *absolute* values of the track width, given by the curves in Fig. 2, a relation between energy and range of low energy electrons is necessary. Fig. 4 shows the mean number of grains, q, in a δ-ray track as a function of the δ-ray energy as given by several authors [7-9].

For δ-rays of energy $W < 30$ keV the number of grains, q, is approximately given by:

$$q = 0.3(\overline{W} - 1) .$$

If the mean range of δ-rays is set proportional to the mean number of grains, we get for the track width, a_μ, expressed in μm,

$$a_\mu = K(\overline{W} - 1) + Q(Z, R) , \tag{6}$$

where K is a constant, and Q is a function certainly of the charge and possibly of the range that gives the contribution of the primary ionization to the track width.

In order to investigate possible variation of the function Q with the particle range, the widths of tracks of ^{16}O and ^{12}C ions from an *electron non-sensitive* emulsion Ilford D-1 have been measured. Data shown in Fig. 5 demonstrate that the track width is practically independent of range in this emulsion. The same result is found by LOZHKIN [10] in an insensitive emulsion for particles with charge $Z = 7$. In the very insensitive emulsion used by LOZHKIN the ^{14}N ions formed tracks consisting of separate grains, the entire track width thus characterized the total specific ionization loss dE/dx of the nitrogen ions.

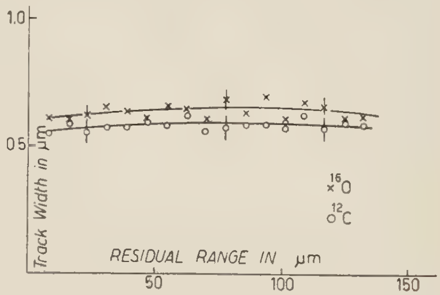

Fig. 5. – The mean track width versus residual range of ^{16}O and ^{12}C ions in a *electron non-sensitive* photographic emulsion.

That the rate of energy loss is nearly constant over the region of thin-down for ions with masses near that of nitrogen, has also been found by REYNOLDS *et al.* [11].

In accordance with this we therefore assume that the track width due to the primary ionization of the particle is independent of the range, and that it varies with the charge of the particle according to a simple power law. Equation (6) is therefore replaced by

$$a_\mu = K(\overline{W} - 1) + CZ^x , \tag{7}$$

---

[7] S. O. SÖRENSEN: *Thesis* (Oslo, 1951).
[8] J. PNIEWSKI: *Acta Phys. Polonica*, **11**, 215 (1952).
[9] J. P. LONGCHAMP and C. GEGAUFF: *Journ. Phys. Rad.*, **17**, 132 (1956).
[10] O. V. LOZHKIN: *Žu. Èksper. Teor. Fiz.*, **32**, 208 (1957).
[11] H. L. REYNOLDS, D. W. SCOTT and A. ZUCKER: *Phys. Rev.*, **95**, 671 (1954).

where K, C and x are numerical constants which can be determined by combining experimental values of a_μ for three different ions with the corresponding theoretical values of $\overline{W}$.

At a range of about 100 μm the effective charge Z_{eff}, is practically identical with the charge number Z for all ions included in the present investigation. At the same range a variation in grain number counts of less than two is found for δ-rays with energy in the interval W_0 to $2mc^2\beta^2$. At this range, therefore, one may expect to have the most trustworthy values of both the calculated energy $\overline{W}$ and the measured track width a_μ.

In order to determine the numerical values of the constants K, C and x n equation (7), we have, therefore, at a range of 100 μm, combined the experimental track widths, a_μ, with the calculated values, $\overline{W}$, for the ^{16}O, ^{12}C and ^{10}B ions.

We thus get 3 equations, from which the constants can be obtained, the result is

$$a_\mu = 0.09(\overline{W}-1) + 0.20Z^{0.68}\,. \tag{8}$$

The curves in Fig. 6 give the relation between the track width a_μ and the particle range R as calculated from equations (3), (4), (5) and (8). We see from the figure that the theoretical curves for the track width lie within the errors of measurement for the experimental values in the whole range up to 140 μm. We should expect less agreement between the measured and the calculated values for particles of lower charge.

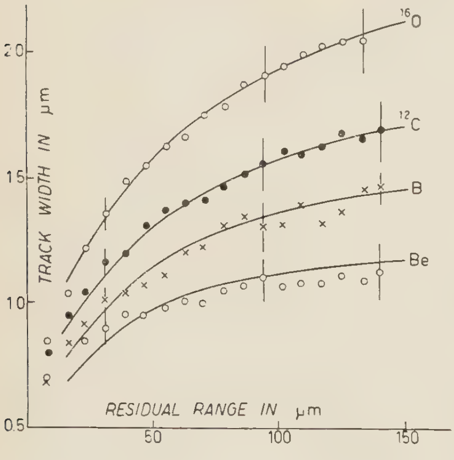

Fig. 6. – Variation of the theoretical mean track width with range, compared with the experimental values given in Fig. 2.

From Fig. 3 we see that the mean δ-ray energy, $\overline{W}$, is less than 9 keV for Be-ions of range less that 150 μm. If a comparison be made with Fig. 4, where we find that a minimum energy of 5 keV is required to produce one grain, it is obvious that our simple hypothesis in which the track width for heavy ions results mainly from the action of δ-rays, can hardly be applied to ions with charge as low as that of Be. That our hypothesis cannot be applied to Li either, is clear from the fact that tracks from Li-particles show a significant number of gaps.

* * *

The author wishes to thank Dr. S. O. Sörensen for helpful discussions, and Professor R. Tangen and Professor J. Holtsmark for providing laboratory facilities. This work was supported by The Royal Norwegian Council for Scientific and Industrial Research.

RIASSUNTO (*)

L'assottigliamento delle tracce degli ioni pesanti verso la fine del loro range in emulsioni fotografiche sensibili agli elettroni si può spiegare quantitativamente nell'ipotesi che lo spessore della traccia sviluppata sia dovuto principalmente ai raggi δ che alle basse velocità degli ioni non hanno più range sufficiente per dilatare la traccia.

(*) *Traduzione a cura della Redazione.*

1863

IL NUOVO CIMENTO Vol. VIII, N. 6 16 Giugno 1958

Semiautomatic Scattering Measurements in Nuclear Emulsions.

C. Castagnoli, M. Ferro-Luzzi and M. Muchnik

Istituto di Fisica dell'Università - Roma
Istituto Nazionale di Fisica Nucleare - Sezione di Roma

(ricevuto il 7 Aprile 1958)

Summary. — A simple device is described to semiautomatize scattering measurements and computations, in nuclear emulsion work. Advantages of the system achieved in this laboratory are its low cost and a minimum time gain of 4 or more depending on the type of measurements.

1. – Introduction.

Various solutions to the problem of automatizing multiple scattering measurements in nuclear emulsions have been proposed in the last few years ([1-5]).

These solutions involve, as a rule, the suppression of one or other of the several operations performed during and after the measurement. These operations are: *a*) alignement of a filar micrometer with the track; *b*) reading of the corresponding y-co-ordinate; *c*) displacement of the microscope stage over a fixed distance along the x-axis (cell); *d*) computing the second differences $(\Delta_2 y)_n = y_{n+2} - 2y_{n+1} + y_n$ and the sum total of the absolute values, $\sum_n |\Delta_2 y|_n$.

A method has been developed in this laboratory whose main advantages are simplicity and economy; furthermore, the method tackles the semiautomatization of the whole process rather than of one of its parts, altering to the least extent the standardized procedure of measurement as it is usually done today.

(1) M. Blau, R. Rudin and S. Lindenbaum: *Rev. Sci. Instr.*, **21**, 978 (1950).
(2) A. G. Ekspong: *Ark. Fys.*, **9**, 49 (1954).
(3) B. Stiller and F. I. Louckes jr.: *Nuovo Cimento*, **4**, 642 (1956).
(4) V. Brisson-Fouché: *Compt. Rend. Acad. Sci.*, **245**, 1800 (1957).
(5) G. Giumelli: *Suppl. Nuovo Cimento*, **2**, 454 (1956).

It consists essentially of two mechanisms: *a*) a mechanism for the semi-automatic movement of the filar micrometer of the eyepiece and for the subsequent transcription and arithmetical manipulation of the y-co-ordinate so as to obtain the sum total of the absolute values of the second differences (« automatic reader »); *b*) a mechanism for the automatic resetting of the x-stage of the microscope, capable of performing constant or variable cell schemes (« cell-setter »).

2. – General description.

A block diagram of the complete device is shown in Fig. 1. The measurement of a single co-ordinate implies the following operations, in order: the observer manipulates the three-position switch which governs the motion of a synchronous 1 rps motor attached to the usual filar eye-piece micrometer drum and to an analogue-to-decimal converter. Once the hairline is aligned with the track, the observer presses switch T to start the reading of the analogue-to-decimal converter and the computing operations on a calculating machine (Olivetti Tetractys). This is done by means of a uniselector circuit. Simultaneously switch T starts the automatic cell-setting. By means of the memory provided by a commercial tape recorder, two successive cell-defining pulses drive an electromagnetic clutch and motor attached to the x-stage of the microscope (Koristka M S 2). Thus the track is translated over a given cell, and the observer is ready to carry out the next measurement of the y-co-ordinate. Indeed, he can start the alignment operation while the track

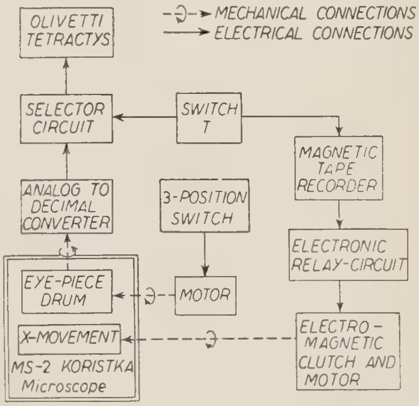

Fig. 1.

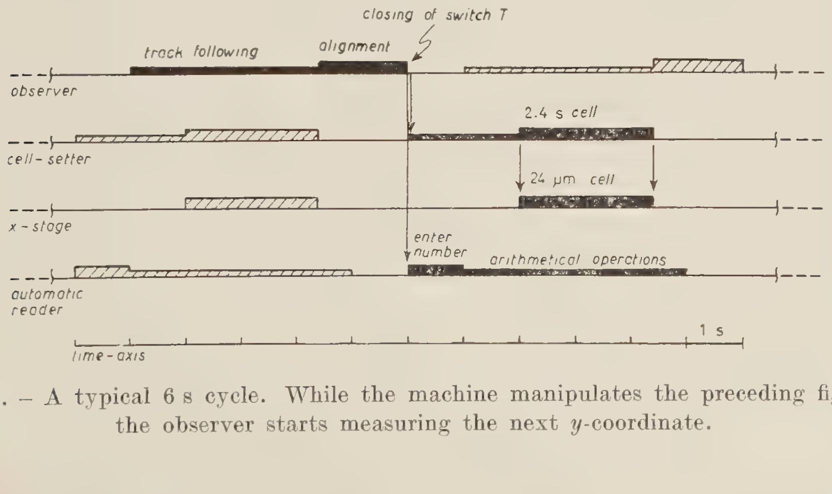

Fig. 2. – A typical 6 s cycle. While the machine manipulates the preceding figures the observer starts measuring the next y-coordinate.

1865

is still moving. How these operations develop in time for the case of a 24 μm cell as performed in our particular experimental conditions, is shown in Fig. 2.

Fig. 3 is a photograph of the apparatus.

Some details of the automatic reader and the automatic cell-setter follow.

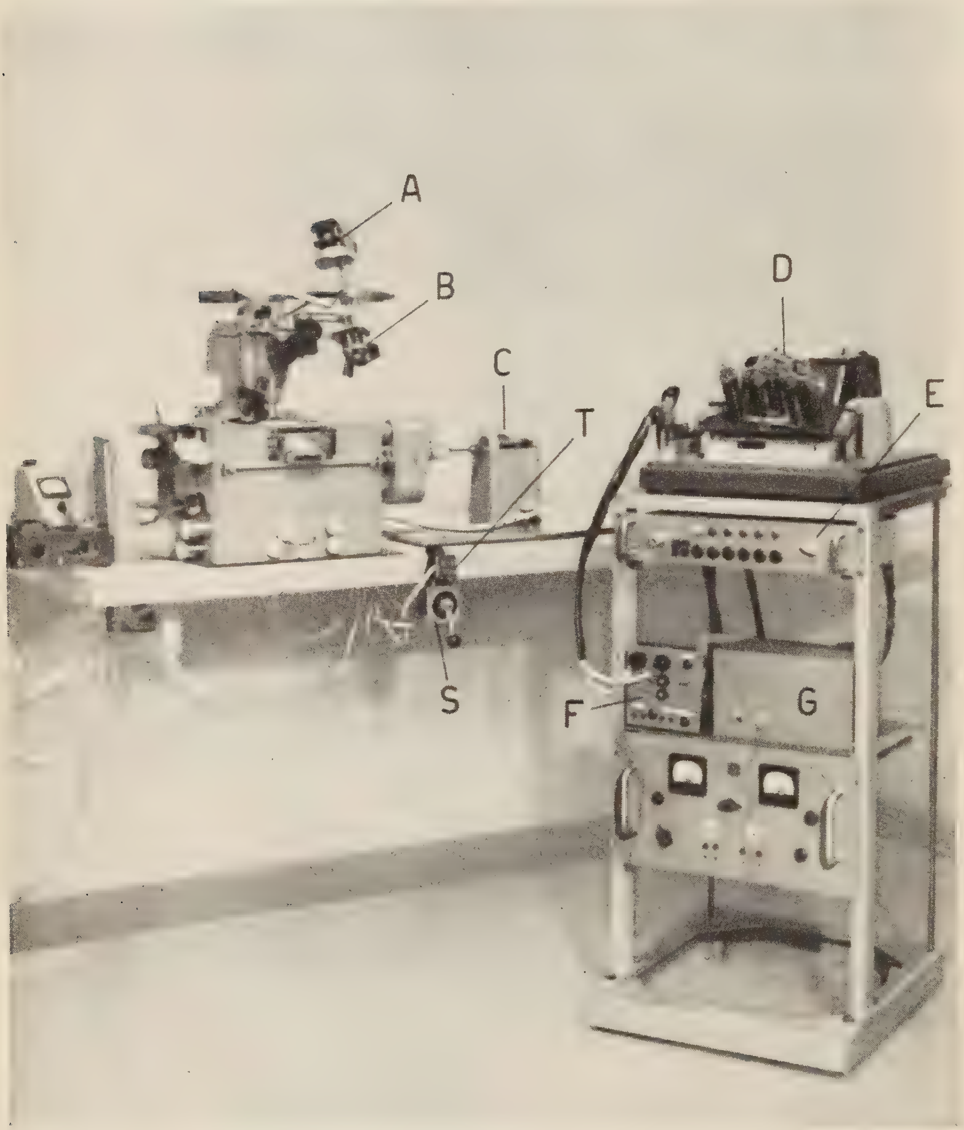

Fig. 3. – *A*) motor; *B*) analogue-to-decimal converter; *C*) electromagnetic clutch and motor; *D*) calculating machine; *E*) electronic-relay circuit; *F*) selector circuit; *G*) magnetic tape recorder; *T*) switch; *S*) three-position switch.

1866

3. – The automatic reader.

The converter consists of three brush-contacts which rotate in the ratios 1:10:100, each one closing successively ten independent circuits in each revolution (Fig. 4). The circuits are respectively connected in parallel and lead each one to a solenoid whose iron core slides down to press a key on the calculating machine keyboard. As previously said, once the alignment is satis-

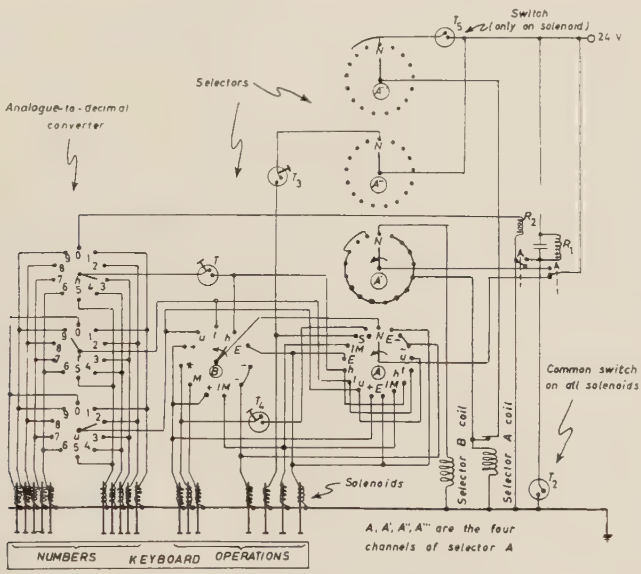

Fig. 4.

factory, the closing of switch T will start the reading and computing operations. A telephone-selector circuit sends in succession the hundreds, tens, and units recorded by the analogue-to-decimal converter, into the calculating-printing machine. The machine—Olivetti Tetractys—has a memory, a repeater usable as an additional memory, and two totalizers; it can thus perform second differences in succession and sum their absolute values. To do this it is not necessary to send the number into the keyboard more than once. The set of operations being cyclic, it is stored permanently in the telephone selector. The last order is to wait still for the next pressing of switch T, whence it repeats the set of operations. Thus the selector circuit scheme of operations runs as follows:

a) Close switch T; the current circulates in the circuit of the hundreds in the converter (« h » in Fig. 4), energizing—through the selector—the corresponding solenoid on the keyboard. Thus the hundreds enter the calculating machine.

b) Simultaneously the iron core of the solenoid closes a side contact T_2 which, by means of a relay R_1 switches off the solenoid and energizes briefly the selector B coil, which advances by one step.

c) One step ahead the selector closes the tens' circuit (« t ») in the converter, and the previous operations take place once more.

d) The units enter the calculating machine. Now the whole number is in the keyboard. The selector keeps moving, sending the set of eight orders contained in B to the keys of the calculating machine, so that the y-co-ordinate is printed and memorized and the second difference with respect to the previous co-ordinates is formed, printed and its absolute value accumulated. The last step of the selector leaves it in the circuit of switch T, which is open; so it stops.

e) At the end of the measurement, upon closing switch T_3 the machine prints out $\sum_n |\Delta_2 y|_n$.

The standard cut-off at four times the mean second difference may be performed now by hand in order to obtain the true Δ_2. Then the $p\beta$ is obtained in the usual manner.

Switch T_4 serves to clear the machine of the residual numbers remaining from any previous measurement. The described cycle of operations is valid only from the third cell on; for the first two cells the cycle differs, and is carried out by selector A.

4. – The automatic cell-setting.

The cell-scheme is recorded as a succession of properly spaced pulses on magnetic tape. A pulse drives, by means of an electronic-relay circuit, an electromagnetic clutch which connects mechanically a permanently functioning motor to the x-knob of the microscope stage. The next pulse de-energizes the clutch, simultaneously stopping the tape recorder. The latter will not start if switch T is not pressed again. Thus switch T serves both to start the automatic reader and the cell setter. A mechanical counter gives at each time the number of cells already measured. The pulses are recorded in the tape by means of the electromagnetic induction from the solenoid of an electric timer. Thus distances are recorded to the nearest 1/10 of a second, the precision of the watch. Fig. 5 shows the reproducibility of the cell-scheme,

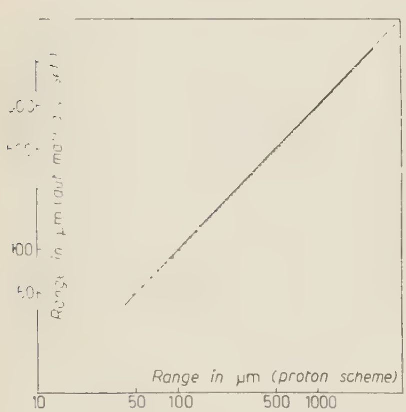

Fig. 5. – Comparison between expected and actual ranges. The abscissa of each point corresponds to the integral range required by the half-cell scheme for protons at rest. The ordinate of each point corresponds to the range as read on the automatically set micrometer drum.

by comparing the theoretical first hundred half proton cells according to the Dilworth scheme with the settings obtained automatically, as read on the x-stage micrometric drum.

Our motor moves the stage at the rate of 10 μm per second, a speed well suited for the short cells of the constant sagitta method or for the constant cell method when the cells are short and not among the pre-established cell-lengths provided by the escapement movement of the microscope. Naturally the velocity of the motor may be increased to suit long cells.

5. – Discussion of the method.

In our laboratory we usually perform scattering measurements having one observer who manipulates the microscope and reads out the values of the y-co-ordinates, and another who writes out these values, computes first and second differences, and reads out—in constant sagitta measurements—the next value of the x-co-ordinate to be set.

To analyze the *time gains* obtained by the semiautomatization, let us examine first the constant cell scheme. If the length of the constant cell is included as one of the choices of the escapement movement of the microscope, (the Koritska MS 2 allows the possibility of 25, 50, 100, 500 μm cells), it takes about 15 minutes of two persons to measure 100 cells and to obtain the mean second difference. With our semiautomatic method, the process requires 10 minutes of one person with a time gain of about 3. It is obvious that the automatic cell-setter does not offer any advantage in this case, and that the time gain is entirely due to the automatic computation. If, on the other hand, the required constant cell is short and not one of the possibilities of the escapement movement of the microscope, the usual measurement takes about 20 minutes of two observers; the machine still requires 10 minutes with only one person. Thus, in this case the time gain is 4.

Let us examine the variable cell scheme. One hundred constant sagitta half-proton cells are measured by our two men in 20 minutes; the automatic system does it in 10 minutes with one person. Thus we have also in this case a factor of 4.

It is to be noticed furthermore: *a*) that the automatic movement of the hairline does not introduce any time-gain with respect to its normal operation by hand; but that it reduces the observer's fatigue and eliminates vibrations and displacements which are otherwise unavoidable; *b*) that the semiautomatization permits a higher efficiency on the part of the observer, reducing his strain, dispensing him of reading the cell-length on the x-stage micrometric drum and of continually refocusing his eyes from the eye-piece drum to the x-stage drum and to the microscopic field of view: he need only position the movable hairline.

We believe that all these factors increase the efficiency in such manner that the time-gain may certainly be considered greater than the factor 4 previously mentioned.

We notice further that the automatization eliminates mistakes: the machine cannot « jump » a cell, nor can it register a mistaken y-co-ordinate or second difference.

It remains to investigate how the semiautomatization affects the actual scattering measurements. To do this we selected a 700 MeV/c negative pion in a 600 μm G5 emulsion. According to the usual multiple scattering rules, such a track should be measured with 200 μm cells. We used 25 μm cells in order to eliminate multiple and spurious scattering, thus to record only the over-all microscope, observer and semiautomatization-device noise. The same track was afterwards measured in the ordinary manner, to obtain the microscope and observer noise. The results, over 500 cells, are:

$$\text{Semiautomatically:} \qquad \Delta_2 = (0.190 \pm 0.009)\ \mu\text{m}\,,$$

$$\text{Manually:} \qquad \Delta_2 = (0.192 \pm 0.009)\ \mu\text{m}\,.$$

Thus we can say that no new noise is introduced by the semiautomatization.

A further advantage is the low cost of the apparatus. Aside from the calculating machine, which may be used for the usual laboratory routine work, the whole equipment consists of simple and cheap parts.

RIASSUNTO

Viene descritto un semplice apparato per rendere semiautomatiche le misure ed i calcoli dello scattering in emulsioni nucleari. I vantaggi del sistema realizzato sono il basso costo ed un guadagno minimo in tempo di un fattore 4 o più a seconda dei vari tipi di misura.

On a Minimum Property of Free Energies.

T. D. SCHULTZ (*)

Department of Mathematical Physics, University of Birmingham, England

(ricevuto il 27 Marzo 1958)

PEIERLS [1] has proved a theorem a special case of which gives a lower bound to the partition sum (hence an upper bound to the free energy) of a quantum mechanical system:

$$(1)\qquad \sum_k \exp[-\beta E_k] \geqslant \sum_n \exp[-\beta H_{nn}] .$$

The E_k are the eigenvalues of H and the H_{nn} are the diagonal matrix elements of H in an arbitrary orthonormal representation. As $\beta \to \infty$ the theorem is obvious, reducing to the fundamental inequality $E_0 \leqslant H_{nn}$ for all n. However for finite β it is not so obvious since higher eigenvalues of H do not necessarily lie lower than corresponding diagonal matrix elements H_{nn}. In fact, the inequality (1) does not depend on the fact that $\exp[-\beta E]$ is a monotonically decreasing function of E, as might be concluded from the original proof. It depends only on the fact that the exponential function is concave upward. We give a very simple proof of the theorem under this somewhat more general condition.

(*) National Science Foundation Postdoctoral Fellow.

(1) R. E. PEIERLS: *Phys. Rev.*, **54**, 918 (1938).

Let $\{\varphi_n\}$ be a complete orthonormal set of state vectors, and let $\boldsymbol{O}$ be an Hermitean operator which for convenience is assumed to have a pure point spectrum with eigenvalues O_k and eigenstates ψ_k. Let $f(x)$ be a real valued function such that

$$(2)\qquad \mathrm{d}^2 f/\mathrm{d}x^2 > 0$$

in an interval including the whole spectrum of O_k. Then, if $\operatorname{Tr} f(\boldsymbol{O})$ exists we prove the

Theorem:

$$(3)\qquad \operatorname{Tr} f(\boldsymbol{O}) \geqslant \sum_n f(O_{nn}) ,$$

where

$$O_{nn} = \langle n|\boldsymbol{O}|n\rangle .$$

The equality holds if and only if the φ_n's are the eigenstates of $\boldsymbol{O}$.

Since

$$\operatorname{Tr} f(\boldsymbol{O}) = \sum_n \langle n|f(\boldsymbol{O})|n\rangle$$

it is sufficient for the proof to point out that (3) follows from

$$(4)\qquad \langle n|f(\boldsymbol{O})|n\rangle \geqslant f(O_{nn}) ,$$

which is valid for all n. The inequalities (4) are derived (2) from

$$f(O_k) \geqslant f(O_{nn}) + (O_k - O_{nn})\, f'(O_{nn}) \,, \tag{5}$$

which is a consequence of (2), the right hand side for fixed n being the line tangent to $f(O_k)$ at O_{nn}. Multiplying (5) by $|\langle n|k\rangle|^2$ and summing on k, we obtain (4). We observe further that the equality in (4) holds if and only if $|\langle n|k\rangle|^2 = 0$ unless $O_k = O_{nn}$, *i.e.* if and only if φ_n is an eigenstate of $\boldsymbol{O}$.

If $f(\boldsymbol{O})$ is positive definite, then the set φ_n need not be complete, since the theorem is true even more strongly if positive terms are omitted from the sum $\sum_n f(O_{nn})$.

With the choice $f(\boldsymbol{O}) = \exp[-\boldsymbol{O}]$ and $\boldsymbol{O} = \boldsymbol{H}/kT$, we have the original theorem of Peierls giving an upper bound to the free energy. With $\boldsymbol{O} = (\boldsymbol{H} - \mu \boldsymbol{N})/kT$ we have an analogous theorem for the grand potential. The theorem as just proved is a generalization in that it no longer requires $f(x)$ to be monotonic; it requires only that $\mathrm{Tr}\, f(\boldsymbol{O})$ be finite which can occur even if $f(x)$ is not monotonic provided $\boldsymbol{O}$ is bounded.

(2) The inequality (4) has been used for the probability density of a classical variable by R. P. FEYNMAN: *Phys. Rev.*, **97**, 660 (1955). The particular proof given here was communicated to me by M. COHEN.

The Selection Rules on the Hyperon Decays.

K. Nakagawa and H. Umezawa

Department of Physics, University of Tokyo - Tokyo, Japan

(ricevuto il 18 Aprile 1958)

In studying the selection rules in the Σ-decay processes (1), use has been made of the observed branching ratio (2)

$$R_\Sigma = \frac{w(\Sigma^+ \to p + \pi^0)}{w(\Sigma^+ \to n + \pi^+)} \simeq 1 \tag{1}$$

and the ratio of the life times (2,3)

$$R'_\Sigma = \frac{\tau(\Sigma^+)}{\tau(\Sigma^-)} \simeq \frac{1}{2} . \tag{2}$$

It is aimed here to note that the anisotropy coefficients concerning the two channels of the Σ-decay have much importance in analysing the interactions for the processes under consideration. We have now strong evidence for the non-conservation of the parity in the Σ-decay processes. The angular distribution of the pions produced in the processes have been known to be of the form $[1 + P\alpha \cos\theta]$. Here, θ is the angle of the pion momentum relative to the polarization of Σ in the rest system of the Σ-particle, α denotes the anisotropy coefficient and P is the magnitude of the polarization. *The ratio*

$$\frac{\overline{P}\alpha_0(\text{for } \Sigma^+ \to p + \pi^0)}{P\alpha_+(\text{for } \Sigma^+ \to n + \pi^+)} = \frac{\alpha_0}{\alpha_+} \tag{3}$$

depends only on the interactions for the Σ-decay processes. This is because the ratio (3) is independent of the quantity P. The latter quantity depends on the strong interactions. Experiments (4) have shown that

$$\begin{cases} \overline{P}\alpha_0 = -0.37 \pm 0.19 \, , \\ \overline{P}\alpha_+ = -0.36 \pm 0.21 \end{cases} \tag{4}$$

---

(1) R. Gatto and R. D. Tripp: *Nuovo Cimento*, **6**, 367 (1957); B. T. Feld: *Nuovo Cimento*, **6**, 650 (1957); C. Ceolin: *Nuovo Cimento*, **6**, 1006 (1957).

(2) G. A. Snow: *Proceedings of the Rochester Conference* (1957), Sect. **8**, p. 14.

(3) A. Rosenfeld: *Proceedings of the Rochester Conference* (1957), Sect. **8**, p. 16.

(4) F. S. Crawford jr., M. Cresti, M. L. Good, K. Gottstein, E. M. Lyman, F. T. Solmitz, M. L. Stevenson and H. K. Ticho: *Phys. Rev.*, **108**, 1102 (1957).

and therefore that

$$\frac{\alpha_0}{\alpha_-} \simeq 1 . \tag{5}$$

We shall see later that *the interactions invariant under time reversal lead to the result* $\alpha_0/\alpha_+ = 1$ *when we assume the one to one law* saying that the coupling constants for the parity conserving and non-conserving terms are of a same magnitude. In this case the experimental results (4) exclude the scalar and pseudoscalar interactions [5].

Let us assume the interaction of the (V, A)-types for the Σ-decay processes:

$$H = g_1 \overline{\psi}_p (a_1 + b_1\gamma_5)\gamma_\mu \psi_{\Sigma^+} \partial_\mu \varphi_{\pi^0} + g_2 \overline{\psi}_n (a_2 + b_2\gamma_5)\gamma_\mu \psi_{\Sigma^0} \partial_\mu \varphi_{\pi^+} + \\ + g_3 \overline{\psi}_n (a_3 + b_3\gamma_5)\gamma_\mu \psi_{\Sigma^-} \partial_\mu \varphi_{\pi^-} + \text{h. c.} . \tag{6}$$

Here the spin of the Σ-particle is assumed to be $\frac{1}{2}$. Tye constants a_i and b_i $i = 1, 2, 3$) are in general complex. Without any loss of generality we can introduce the following normalization condition:

$$\gamma^2 |a_i|^2 + |b_i|^2 = 1 . \tag{7}$$

Here the constant

$$\gamma^2 = \frac{(s\text{-wave part of the transition probability})/|g_i a_i|^2}{(p\text{-wave part of the transition probability})/|g_i b_i|^2}$$

is calculated to be 1.4 in the lowest order approximation of the perturbational calculation. The ratio α_0/α_+ is obtained to be

$$\frac{\alpha_0}{\alpha_+} = \frac{\text{Re}\,(a_1^* b_1)}{\text{Re}\,(a_2^* b_2)} . \tag{8}$$

Here the mass difference of the nucleons and that of the pions are out of consideration. We see from (5) that

$$\text{Re}\,(a_1^* b_1) \approx \text{Re}\,(a_2^* b_2) . \tag{9}$$

This leads to the condition

$$a_1 b_1 \approx a_2 b_2 \tag{10}$$

when the interaction is invariant under time reversal. The condition (10) together with (7) gives us the following result:

$$\begin{cases} a_1^2 \approx a_2^2 , \\ b_1^2 \approx b_2^2 , \end{cases} \qquad \text{or} \qquad \begin{cases} b_1^2 \approx \gamma^2 a_2^2 . \\ b_2^2 \approx \gamma^1 a_1^2 , \end{cases} \tag{11}$$

The one-to-one law ($|a_i| = |b_i|$) is consistent with (11).

---

[5] H. UMEZAWA, M. KONUMA and K. NAKAGAWA: *Nucl. Phys.*, **6** (in press).

Experiments on the Σ^--decay [4,6] tell us nothing about a_3 and b_3, as no measurable anisotropy has been observed. It may probably be the case that the produced Σ^--hyperon is unpolarized for some reason.

The relations (1) and (2) lead us to the result

$$|g_1|^2 = |g_2|^2 = |g_3|^2 . \tag{12}$$

We now come to a problem on the selection rules concerning the isotopic spin. Our problem is to ask if the conditions (11) and (12) could be consistent with the selection rule $|\Delta I| = \frac{1}{2}$ for the isotopic spin. The interaction consistent with this selection rule should be an isotopic spinor:,

$$H_{|\Delta I| = \frac{1}{2}} = \bar{\psi}_N (A + B\gamma_5)\gamma_\mu \psi_{\Sigma i}\partial_\mu \varphi_{\pi i} + (\bar{\psi}_N \tau_i)(A' + B'\gamma_5)\gamma_\mu \psi_\Sigma t_i \partial_\mu \varphi_\pi + \text{h. c.} \tag{13}$$

$$= \sqrt{2}\,\bar{\psi}_p (A' + B'\gamma_5)\gamma_\mu \psi_{\Sigma^+}\partial_\mu \varphi_{\pi^0} + \bar{\psi}_n\big\{(A + A') + (B + B')\gamma_5\big\}\gamma_\mu \psi_{\Sigma^+}\partial_\mu \varphi_{\pi^+} + \\ + \bar{\psi}_n\big\{(A - A') + (B - B')\gamma_5\big\}\gamma_\mu \psi_{\Sigma^-}\partial_\mu \varphi_{\pi^-} + \text{h. c.} . \tag{13'}$$

Notations here are as follows,

$$\psi_\Sigma = \begin{pmatrix} \psi_{\Sigma 1} \\ \psi_{\Sigma 2} \\ \psi_{\Sigma 3} \end{pmatrix}, \qquad \varphi_\pi = \begin{pmatrix} \varphi_{\pi 1} \\ \varphi_{\pi 2} \\ \varphi_{\pi 3} \end{pmatrix}, \qquad \psi_N = \begin{pmatrix} \psi_p \\ \psi_n \end{pmatrix},$$

$$\begin{cases} \psi_{\Sigma^\pm} = \dfrac{1}{\sqrt{2}}(\psi_{\Sigma 1} \pm i\psi_{\Sigma 2}) , \\ \psi_{\Sigma^0} = \psi_{\Sigma 3} , \end{cases} \qquad \begin{cases} \varphi_{\pi^\pm} = \dfrac{1}{\sqrt{2}}(\varphi_{\pi 1} \pm i\varphi_{\pi 2}) , \\ \varphi_{\pi^0} = \varphi_{\pi 3} , \end{cases}$$

$$t_1 = \begin{pmatrix} 0 & 0 & 0 \\ 0 & 0 & -i \\ 0 & i & 0 \end{pmatrix}, \qquad t_2 = \begin{pmatrix} 0 & 0 & i \\ 0 & 0 & 0 \\ -i & 0 & 0 \end{pmatrix}, \qquad t_3 = \begin{pmatrix} 0 & -i & 0 \\ i & 0 & 0 \\ 0 & 0 & 0 \end{pmatrix},$$

$$\tau_1 = \begin{pmatrix} 0 & 1 \\ 1 & 0 \end{pmatrix}, \qquad \tau_2 = \begin{pmatrix} 0 & i \\ -i & 0 \end{pmatrix}, \qquad \tau_3 = \begin{pmatrix} 1 & 0 \\ 0 & -1 \end{pmatrix}.$$

Here the constants A, B, A' and B' are in general complex. They have a same phase in the case where the interaction is invariant under time reversal. It can be shown (*) that no interaction of the form (13) is consistent with the conditions (1), (2) and (5) as far as the invariance of the theory under time reversal and the one-to-one law (+) are assumed. This is true even when the experimental errors and the final state interactions are taken into account.

---

(6) F. EISLER, R. PLANO, A. PRODELL, N. SAMIOS, M. SCHWARTZ, J. STEINBERGER, P. BASSI, V. BORELLI, G. PUPPI, H. TANAKA, P. WALOSCHEK, V. ZOBOLI, M. CONVERSI, P. FRANZINI, I. MANNELLI, R. SANTANGELO, V. SILVESTRINI, D. A. GLASER, C. GRAVES, and M. L. PERL: *Phys. Rev.*, **108**, 1353 (1957).

(*) Detailed discussions will be published elsewhere.

(+) It sometimes happens that the one-to-one law leads to results depending on the expression for the interaction; it depends on the definition of the coupling constants. Our results in this paper are, however, independent of the expressions [*i.e.* (13) and (13')[for the interaction. It should be noted that the one-to-one law for (13) is just that for (13') when B/A and B'/A' are of the same sign. This may be only a reasonable case, because the one-to-one law should be uniquely determined by the properties of the particles concerned.

No experiment has shown any violation of the invariance under time reversal. This is so for the one-to-one law too [5]. On the other hand we have had some experimental results which are inconsistent with the selection rule $|\Delta I| = \frac{1}{2}$: the observed branching ratio $R_\theta = w(\theta_1^0 \to \pi^0 + \pi^0)/w(\theta_1^0) = 0.14 \pm 0.06$ [7] cannot be explained without assuming considerably large transition with $|\Delta I| = \frac{3}{2}$. Contrary to this, the $\theta^\pm$-decay processes need only a small amount of transitions with $|\Delta I| = \frac{3}{2}$ because the life time of $\theta^\pm$ is longer than that of θ_1^0 by a factor 500. The only experiment, which is consistent with the $|\Delta I| = \frac{1}{2}$ rule, is the branching ratio $R_\Lambda = w(\Lambda^0 \to p + \pi^-)/w(\Lambda^0)$; the experimental value 0.65 ± 0.05 [7] agrees quite well with $R_\Lambda = \frac{2}{3}$ predicted by the $|\Delta I| = \frac{1}{2}$ rule. Thus the necessity for the selection rule $|\Delta I| = \frac{1}{2}$ is very poor.

Let us now remember the discussions [5] which seem to suggest that the weak interactions may play an important role in an extremely small domain ($r \lesssim 10^{-20}$ cm). Assuming this to be true, we feel that the isotopic spin does not have much importance in the small domain concerning the weak interactions.

* * *

We are grateful to Professor S. MACHIDA and Dr. M. KONUMA for their inspiring discussions. We are also indebted to Dr. S. SATO and Dr. J. OTOKOZAWA for their excellent co-operations.

---

(7) F. EISLER, N. SAMIOS, M. SCHWARTZ and J. STEINBERGER: *Nuovo Cimento*, **5**, 1700 (1957).

A Simple Formulation of the Elementary Particle Scheme of Gell-Mann and Nishijima.

M. KRETZSCHMAR

Institut für Theoretische Physik der Universität Göttingen - Göttingen

(ricevuto il 6 Maggio 1958)

As it is usually written down (*) the elementary particle scheme of Gell-Mann and Nishijima does on first sight not exhibit much intrinsic symmetry. Some symmetry, however, becomes obvious, if one characterises each particle, that occurs in the scheme, by the three quantum numbers N (baryon number), Q (electrical charge) and U (hypercharge (×)) and then interprets N, Q, U as co-ordinates in a formal 3-dimensional space. In this space each elementary particle corresponds to a lattice point in the neighbourhood of the origin. One obtains the following array:

$N = -1$

	$U=-1$	$U=0$	$U=+1$
$Q=+1$		$\overline{\Sigma^{-}}$	$\overline{\Xi^{-}}$
$Q=0$	n	$\overline{\Sigma^0}$ $\overline{\Lambda^0}$	$\overline{\Xi^0}$
$Q=-1$	$\bar{\text{p}}$	$\overline{\Sigma^{+}}$	

$N = 0$

	$U=-1$	$U=0$	$U=+1$
$Q=+1$		π^+	K^+
$Q=0$	$\overline{K^0}$	π^0	K^0
$Q=-1$	K	π	

$N = +1$

	$U=-1$	$U=0$	$U=+1$
$Q=+1$		Σ^+	p
$Q=0$	Ξ^0	Σ^0 Λ^0	n
$Q=-1$	Ξ^-	Σ^-	

For all elementary particles, which are known today, the quantum numbers N, Q, U fulfill the condition

$$|N| \leqslant 1\,, \qquad |Q| \leqslant 1\,, \qquad |U| \leqslant 1\,. \tag{1}$$

Considering all possible sets of quantum numbers (N, Q, U) consistent with (1) one observes:

(*) For example cf. R. G. SACHS: *Phys. Rev.*, **99**, 1573 (1955), Fig. 1 or C. FRANZINETTI and G. MORPURGO: *Suppl. Nuovo Cimento*, **6**, 608 (1957).

(×) This expression has been used by J. SCHWINGER: *Phys. Rev.*, **104**, 1164 (1956). U is defined as $U = N + S$, where S means strangeness.

a) Elementary particles correspond only to those sets (N, Q, U), which are consistent with

$$Q \cdot U \geqslant 0 \,. \tag{2}$$

All other sets describe no particle. It is easily seen, that (2) is a consequence of (1) and the well known equation

$$Q = T_3 + (U/2) \,, \tag{3}$$

where T means isobaric spin.

b) The Gell-Mann Nishijima scheme shows—safe from mass differences between different particles—complete symmetry with regard to Q and U.

c) To a given particle one finds its antiparticle by reflection at the origin of the (N, Q, U)-co-ordinate system.

d_1) A particle is a fermion or a boson, if $N = \pm 1$ or $N = 0$.

d_2) A particle is an isofermion or an isoboson, if $U = \pm 1$ or $U = 0$.

e) If Λ^0 and its antiparticle $\overline{\Lambda^0}$ are considered separately, then we have a one-to-one correspondence between elementary particles, that occur in nature, and those sets $(N, Q\ U)$, which satisfy (1) and (2).

If Λ^0 and $\overline{\Lambda^0}$ are taken out of the scheme, charge multiplets can be defined by the conditions $N = \text{const}$, $U = \text{const}$, the multiplicity being the total isobaric spin. With this definition of isobaric spin d_2) follows from *e*).

The main point of this note is to show, that—provided a separate consideration of Λ^0 and $\overline{\Lambda^0}$—the statements d_1) and *e*) together contain all information, that the Gell-Mann-Nishijima scheme gives us about those combinations of baryon number, electrical charge, strangeness, spin and isobaric spin, which are realized in nature.

IL NUOVO CIMENTO Vol. VIII, N. 6 16 Giugno 1958

On the Unitarity of the S-Matrix in Quantum Field Theories with Indefinite Metric.

R. Ascoli

Istituto di Fisica dell'Università - Torino
Istituto Nazionale di Fisica Nucleare - Sezione di Torino

E. Minardi

Società Nazionale Cogne - Aosta
Istituto Nazionale di Fisica Nucleare - Sezione di Torino

(ricevuto il 12 Maggio 1958)

Recently Heisenberg (1) has shown in a particular case of the Lee model how a quantum field theory with indefinite metric may give rise to a unitary S matrix which may be interpreted probabilistically in the usual way, so that there is conservation of probability in scattering problems. The problem studied by Heisenberg (1) is the scattering of two θ particles on one N particle, in the particular case in which the eigenvalue equation for the energy of one V particle has two coinciding roots (dipole ghost case).

Now we have investigated very generally the possibility of getting a unitary S matrix and of having conservation of scattering probability in a theory with indefinite metric. In this preliminary account we report only a theorem in consequence of which the results of Heisenberg and of Pauli and Källén (2) may be considered as particular cases: moreover other interesting conclusions may be drawn. The theorem is the following:

Let us consider a quantum theory with arbitrary metric where the state vector φ satisfies (at least formally) a Schrödinger equation with a self-conjugate Hamiltonian H ($H^+=H$). Then if the eigenstates of H which belong to real positive eigenvalues and are permitted from eventual supplementary conditions have never negative norm (3), a unitary S matrix may always be definite and there is conservation of probability in scattering problems.

The proof of this theorem, although it is not complicated, requires some care in the definition of the concepts used

(1) W. Heisenberg: *Nucl. Phys.*, **4**, 532 (1957).

(2) G. Källén and W. Pauli: *Dan. Mat. Fys. Medd.*, **30**, no. 7 (1955).

(3) Naturally if the metric is indefinite, there are certainly also non-orthogonal eigenvectors of H of zero norm which belong to complex conjugate eigenvalues, or there are eigenstates of negative norm which are not permitted from the eventual supplementary conditions, or finally it may happen that the eigenvectors of H do not form a complete system; moreover any one of these cases does not exclude the other.

in it. So we give here only the main lines of such a proof.

The state vector in Schrödinger picture $\varphi(t)$ satisfies:

$$i\,\frac{\mathrm{d}\varphi(t)}{\mathrm{d}t} = H\varphi(t)\,. \tag{1}$$

Now we remark that all the calculation rules referring to vectors and operators are postulated independently from the metric [4]. So the formal solution gives as usually:

$$\varphi(+\infty) = S\varphi(-\infty)\,, \tag{2}$$

with

$$S = \exp\left[-i\int H\,\mathrm{d}t\right]. \tag{3}$$

From $H^+ = H$ and (3) it follows

$$S^+S = 1\,. \tag{4}$$

Now it must be possible to measure the energy of any physical state, so any physical state must be a superposition of eigenstates of H which are permitted from the eventual supplementary conditions and belong to real and positive eigenvalues.

Let us call h_I the Hilbert space of these eigenstates. Now let φ belong to h_I. Then it follows that $H\varphi$ belongs also to h_I, because it is again a superposition of the eigenstates of H which belong to h_I. Then from (3) it follows that also $S\varphi$ belongs to h_I. So S transforms any vector of h_I into another vector of h_I.

In general with the assumptions of the theorem the Hilbert space h_I will have semidefinite metric. Let us consider a subspace of it $h_{I'}$ with positive definite metric having the highest possible dimension. Let us call P the operation of projecting any vector of h_I into $h_{I'}$. One sees immediately that such an operation does not modify any scalar product. It follows that

$$P^+P = 1 \tag{5}$$

and that the physical interpretation for the vectors φ in h_I is the same as for their projections φ' on $h_{I'}$ because any probability is given by a scalar product.

Then from (2) it follows for the projections φ' of vectors φ of h_I:

$$\varphi'(+\infty) = S_{I'}\varphi'(-\infty)\,, \tag{6}$$

where

$$S_{I'} = PSP^+\,. \tag{7}$$

Then from (4) and (5) it follows

$$S_{I'}^+S_{I'} = 1 \tag{8}$$

so that a unitary S matrix in the Hilbert space h_I, of positive definite metric may be definite. So the theory may be interpreted probabilistically in the usual way and there is conservation of scattering probability [5].

Let us discuss some consequences of the theorem. Firstly let us consider the problem of the scattering of two θ on one N in the Lee model. Then the theorem guarantees immediately that a unitary S matrix may be defined and that the theory may be physically interpreted in the case in which a dipole ghost occurs. Indeed in this case there are only energy eigenstates of positive or zero norm.

Moreover the theorem proves that the same consequences may be drawn in the same scattering problem even when there are two discrete non-orthogonal energy eigenstates of a V particle, which have a zero norm and belong to complex conjugate eigenvalues. Indeed in this case all the energy eigenstates belonging to real eigenvalues have positive norm.

---

(4) We refer to Dirac's book (P. A. M. DIRAC: *The principles of quantum mechanics*, Cambridge, 1947), where such calculation rules are defined abstractly, without using any assumption about metric: indeed formula (8) p. 21 ($\langle A\,|\,A\rangle > 0$ except when $|\,A\rangle = 0$) is not used up to Sect. 8 (p. 28).

So the occurrence of the dipole ghost is not necessary for the possibility of having conservation of scattering probability: the case of the dipole ghost and of the complex energy eigenvalues are equivalent from the point of view of the possibility of giving a physical interpretation of a theory.

On the contrary if there is an energy eigenstate of negative norm for the V particle, as in the case studied by KÄLLÉN and PAULI, the relation $S^+S=1$ still holds, but it may be shown that it is impossible generally to give a physical probabilistic interpretation to the theory, because negative scattering probabilities appear ([5]). From this remark it follows that the occurrence of the dipole ghost or of the complex energy eigenvalues for the V particle does not prove that it is possible to give a probabilistic interpretation to the theory in problems different from the scattering of two θ with one N particle: if in some problem an energy eigenstate of negative norm occurs, the theory cannot be interpreted. For instance if an eigenstate of negative norm occurs in the subspace $(\mathrm{N}+2\theta,\ \mathrm{V}+\theta)$ (this question has not yet been answered), negative probabilities appear in the scattering of three θ on one N particle ([6]).

Finally we remark that evidently the theorem guarantees also that the treatment of GUPTA and BLEULER of quantum electrodynamics leads to a unitary S matrix and that the theory so obtained may be interpreted probabilistically.

([5]) Let the relation $S^+S=1$ hold, but let the metric of the Hilbert space on which S operates have indefinite metric. Then it may be shown that it is not possible to give a probabilistic interpretation to the theory, because negative scattering probabilities appear.

([6]) Therefore we do not agree with the arguments given by HEISENBERG ([1]) (Sect. 5·2) to prove that even if such an eigenstate occurs, the theory may be probabilistically interpreted.

On the Optical Absorption of Ferric Alum at Low Temperatures.

R. Pappalardo

H. H. Wills Physical Laboratory - Bristol (*)

(ricevuto il 14 Maggio 1958)

The optical absorption of crystals of $Fe(NH_4)_2(SO_4)_2 \cdot 12H_2O$ was investigated to check the prediction of the crystal field theory for $3d^5$-systems and to see if the same satisfactory agreement found in the case of Mn^{2+} is also verified for Fe^{3+} [1-3].

For this purpose ferric alum was chosen, since it possesses cubic symmetry and the interpretation of the spectrum is made easier. We were in particular interested in the optical absorption in the region from 23 000 cm^{-1} upwards, where the prediction is for the absorption to be in the form of sharp lines. No lines were observed, even cooling the crystals down to 20 °K. We should take notice of the fact that the observation of the absorption spectrum in the interesting region is strongly disturbed by the presence of a very intense band with threshold at 27 300 cm^{-1} and extending throughout the ultraviolet (electron - transfer band); this absorption masks almost completely the predicted weak transitions taking place inside the $3d^5$-system.

For details of the experimental apparatus see ref. [3]. The crystalline samples had thickness from 3 to 4 mm; a large Hilger quartz spectrograph was used and the absorption was studied at room temperature, at 90 °K, 78 °K and 20 °K.

The features of the absorption are the following: at room temperature we observe a flat weak absorption, centered at 24 600 cm^{-1} and ranging from 23 850 to 25 600 cm^{-1} (Fig. 1); its structure consists of three narrow bands A, B, C with peaks at 24 250, 24 650 and 24 850 cm^{-1}, the latter showing very fine structure. In the 27 000 cm^{-1} region, though the strong electron-transfer band is now predominant, with a threshold at 27 300 cm^{-1} which is fairly temperature independent, there is evidence of a very weak absorption at 26 300 cm^{-1} and of a weak broad line at 27 550.

No remarkable difference is observed in the absorption at 90 °K, 78 °K and 20 °K: we shall only mention what happens at 20 °K. In the 25 000 cm^{-1} region we have a weak absorption ranging

(*) Present address: *Radiation Laboratory - Pittsburgh University, Pittsburgh Pa.*

(1) Y. Tanabe and S. Sugano: *Journn. Phys. Soc. Japan*, **9**, 753(1954).

(2) J. Gielessen: *Ann. der Phys.*, **22**, 537 (1935).

(3) R. Pappalardo: *Phil. Mag.*, **2**, 1397 (1957).

from 24400 to 25700 cm^{-1} with a fourfold structure (A, B, C, D); a weaker absorption (E) (Fig. 2), a broad line at 27650 similar in all respects to the corresponding line at room temperature, finally another broad line at 28050 cm^{-1}.

As for the intensities of the observed absorptions, we estimate the extinction coefficient for the 25000 cm^{-1} absorption peaks as ~ 0.5 cm^{-1} with no appreciable change with temperature. The oscillator strength of the whole absorption of Fig. 1 is estimated as $\sim 6\cdot10^{-7}$ and for the analogous absorption at 20 °K as $\sim 7.5\cdot10^{-7}$. All these values compare reasonably with typical oscillator strengths and extinction coefficients in manganous hydrated salts (³).

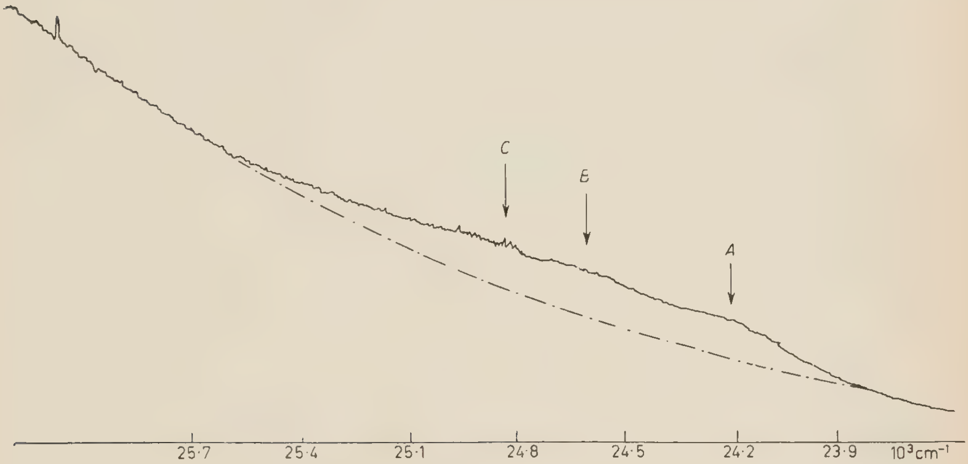

Fig. 1.

The excited levels of the $3d^5$-system can be predicted by means of the ligand field theory (« strong field » formalism) as a function of the empirical parameter

TABLE I.

Transitions	Predicted energy (*)	Experimental (SCHLÄFER)
${}^6A_1(d\varepsilon^3\,d\gamma^2) \to {}^4T_1(d\varepsilon^4\,d\gamma)$	$18.8\cdot10^3$ cm^{-1}	$19\ \cdot10^3$ cm^{-1}
$\to {}^4T_2(d\varepsilon^4\,d\gamma)$	22.3	23
$\to {}^4E\,(d\varepsilon^3\,d\gamma^2)$	24.4	24.5
$\to {}^4A_1(d\varepsilon^3\,d\gamma^2)$	24.5	
$\to {}^4T_2(d\varepsilon^3\,d\gamma^2)$	27.8	27.5
$\to {}^4_bE\,(d\varepsilon^3\,d\gamma^2)$	29.6	29
$\to {}^4T_1(d\varepsilon^3\,d\gamma^2)$	33.6	31.5
$\to {}^4A_2(d\varepsilon^3\,d\gamma^2)$	40	40
$\to {}^4T_1(d\varepsilon^2\,d\gamma^3)$	41	42
$\to {}^4T_2(d\varepsilon^2\,d\gamma^3)$	44	
		electron-transfer band

(*) Inclusive of configuration interaction.

1883

Fig. 2.

Dq (ligand field strength) and of B^* and C^*, Racah's parameters of electrostatic interaction of the $3d^5$-electrons in the complex ion.

As we mentioned above, there is a good agreement in the predicted and experimental data for Mn^{2+}. We report here for instance the values of the absorption bands observed by SCHLÄFER (4) in $MnCl_2(H_2O)_4$ crystals at room temperature—using a spectrophotometric method—and the position of the predicted levels, that we evaluated using the energy matrices gives by TANABE and SUGANO (1) (Table I).

We assumed $C^* = 4.5\,B^*$ and $B^* = 750\ \text{cm}^{-1}$ (the latter from the assignment ${}^6A_1 \to {}^4A_1 : 22\ B^* + 7\ C^* = 24\,500\ \text{cm}^{-1}$): the value of $Dq = 800\ \text{cm}^{-1}$ was chosen as the one giving the best fit. The agreement is really quite good. We applied the cubic field formalism to a tetrahedral complex, since in the « strong field » formalism the treatment of tetrahedral symmetry is equivalent to that of cubic symmetry applied to positive holes.

The corresponding room temperature spectrum reported by SCHLÄFER in ferric alum is in equally fair agreement with the predictions (Table II), provided one assumes the same values of B^* and C^* and the value $Dq = 1\,400\ \text{cm}^{-1}$. This increase in the value of Dq is reasonable since trivalent ions have higher values of Dq than divalent ions.

A good agreement is also found in the predicted intensities of the absorptions and the experimental values (3) for Mn^{2+} and Fe^{3+}.

The simple cubic field treatment does not allow more than two peaks in the $24\,500\ \text{cm}^{-1}$ region: the supplementary peaks we observed (C, D) can only be explained introducing effects connected with spin-dependent forces and complex-ion vibrations, and this is in fact also required for manganous complexes (3).

TABLE II.

Transitions	Predicted energy	Experimental (SCHLÄFER)
${}^6A_1(d\varepsilon^3\,d\gamma^2) \to {}^4T_1(d\varepsilon^4 d\gamma)$	$13.1 \cdot 10^3\ \text{cm}^{-1}$	$12.5 \cdot 10^3\ \text{cm}^{-1}$
$\to {}^4T_2(d\varepsilon^4\,d\gamma)$	17.8	19
$\to {}^4E\ (d\varepsilon^3\,d\gamma^2)$	24.4	24.5
$\to {}^4A_1(d\varepsilon^3\,d\gamma^2)$	24.5	
$\to {}^4T_1(d\varepsilon^3\,d\gamma^2)$	27.1	27.5
		electron-transfer band

One important remark is that levels such as ${}^4E$ and ${}^4A_1$ are not dependent on Dq, hence the corresponding transitions are expected to show no frequency shift on cooling the sample; besides the transitions ought to be in form of sharp lines at low temperatures. Both predictions are actually verified in Mn^{2+} but not in the ferric alum, as can be seen from Fig. 1 and Fig. 2: there are no lines even at 20 °K, and an appreciable shift in frequency ($\sim 300\ \text{cm}^{-1}$) is observed at low temperatures.

Yet we think that these failures are not due to a serious shortcoming of the theory; the new fact in $Fe(H_2O)_6^{3+}$ is the presence of the electron-transfer band at the relatively low energy of $27\,300\ \text{cm}^{-1}$ in comparison with the much

(4) H. L. SCHLÄFER: *Zeit. f. Phys. Chem.*, **4**, 116 (1955).

higher value 43 000 cm^{-1} for $Mn(H_2O)_4^{2+}$. These intense absorptions involve the transfer of an electron from the co-ordinated water molecules to the central paramagnetic ion: since these transitions produce a strong admixture of $3d^5$ and $3d^6$-states, it is no wonder that in $Fe(H_2O)_6^{3+}$ the sharply defined levels $^4A_1$ and ^4E are considerably broadened and show a temperature shift.

In conclusion the observation at low temperature of the spectrum of $Fe(H_2O)_6^{3+}$ does not allow a very good check on the theoretical predictions. The situation will be undoubtedly better for Fe^{3+} complex-ions with ligands different from water and such to require higher energies for the electron-transfer process.

* * *

The writer is very grateful to Prof. M. H. L. Pryce and Dr. L. C. Jackson for their interest in this research and for making available the facilities of the H. H. Wills Physical Laboratory; and to the Collegio Borromeo in Pavia for granting a scholarship.

LIBRI RICEVUTI E RECENSIONI

SAMUEL GLASSTONE – *Ingegneria dei reattori nucleari* – Trad. Italiana di *Principles of nuclear reactor engineering* a cura di Mario Maraghini e Bruno Rumi, (Edizioni Italiane Roma 1957; pag. XVI – 1132 £ 12.000).

Nella realizzazione di un reattore nucleare devono essere affrontati, insieme a quelli puramente fisici, innumerevoli altri problemi di carattere tecnologico: l'importanza che questi ultimi sono venuti assumendo man mano che il reattore è passato da strumento da laboratorio ad apparecchiatura industriale è anzi tale che gli sviluppi nella produzione ed utilizzazione dell'energia di fissione di elementi pesanti sono sempre più vincolati a quelli possibili in campo tecnologico. Non sempre si tratta di problemi nuovi, connessi, solo o quasi, al particolare processo che si svolge nel reattore; molti di essi si presentano sia in apparenza che nella sostanza non dissimili da altri già risolti per impianti industriali più o meno comuni. In ogni caso è però indispensabile che i tecnici li considerino sempre, fin dall'inizio, da un punto di vista sotto molti aspetti diverso da quello usuale: per averne una visione realmente chiara e completa devono infatti essere tenute sempre ben presenti esigenze, di varia natura ed entità, imposte sia dalle proprietà fisiche e dal comportamento dei combustibili nucleari sia dalle caratteristiche operative del reattore, determinate cioè da fenomeni che, fino a tempi recentissimi, non avevano mai interessato la tecnica industriale.

Principles of nuclear reactor engineering è valido aiuto e preziosa guida per il tecnico che intende avviarsi a raggiungere questo punto di vista, sia per la scelta degli argomenti che per il modo in cui questi sono svolti.

Vi sono descritti, in forma sempre chiara e piana, i fondamenti per la progettazione, la costruzione e l'esercizio dei reattori nucleari.

La trattazione degli argomenti non va, in generale, oltre una buona impostazione, ridotta, per quanto possibile, ai suoi termini essenziali. In tal modo il lettore è messo in grado di approfondire quanto più gli interessa sulla letteratura specializzata, ma nello stesso tempo è avvantaggiato dalla maggior snellezza dell'opera nell'ottenere una visione d'assieme dei problemi. Quest'ultima sarebbe altrimenti difficilmente raggiungibile anche per la grande varietà di essi ed è invece utilissima, soprattutto per il futuro lavoro in gruppo che la realizzazione degli impianti nucleari richiede in ogni caso a tecnici delle specializzazioni più diverse, dal fisico all'ingegnere al chimico.

L'aver evitato di scendere in dettagli, inoltre, non solo diminuisce il pericolo d'indurre nel lettore ancora poco esperto della materia, false impressioni su tecniche di valore ancora molto provvisorio oltre che spesso limitato a casi singoli; ma conferisce all'opera una validità indipendente, entro larghi limiti, dai mutamenti delle varie tecnologie,

1887

pur essendone in essa fissati i principi che determinano queste ultime.

La materia è divisa in tredici capitoli, in ognuno dei quali sono raggruppati argomenti affini, riguardanti rispettivamente generalità sugli scopi dell'ingegneria dei reattori, le reazioni e le radiazioni nucleari, la teoria dello stato stazionario e del regime variabile dei reattori, gli apparecchi di controllo dei reattori, il controllo dei reattori, il trattamento dei combustibili dei reattori, i materiali per i reattori, la protezione dalle radiazioni, la schermatura dei reattori, gli aspetti termici nei reattori, la scelta delle caratteristiche costruttive dei reattori, la descrizione di alcuni tipi di reattori.

La traduzione italiana, ben aderente nella sostanza e curata nella forma, costituisce un ulteriore pregio dell'opera per il lettore Italiano.

G. C. BELISARIO

Reports on Progress in Physics, volume XX (1957), a cura di A. C. STICKLAND. Ed. The Physical Society, London, pagg. 568.

Le monografie del ventesimo volume dei *Reports on Progress in Physics* spaziano, come è d'uso, in campi assai vari della Fisica, sia sperimentale che teorica, e, per la maggior parte almeno, mettono a punto con cura e precisione, lo stato presente di problemi di viva attualità.

Mesoni K ed iperoni non potevano quindi mancare: le loro interazioni forti e deboli ed i processi di produzione e di decadimento sono passati in rassegna da R. H. DALITZ in un articolo di 140 pagine, corredato da vastissima bibliografia. Questo lavoro è basato sulla documentazione disponibile alla fine del 1956, ma in una appendice sono discusse alcune osservazioni più recenti sulla violazione di principi di invarianza, come la conservazione della parità. Queste osservazioni portano naturalmente a modificare le precedenti conclusioni.

A. E. TAYLOR analizza invece i risultati di esperimenti recenti sullo « scattering » di protoni di alta energia: interazioni protone-protone, sia per il campo tra 100 e 400 MeV (fra cui osservazioni con fasci polarizzati), sia per energie superiori, sino al limite ottenibile dal Bevatrone di Berkeley, con produzione di mesoni e di antiprotoni; interazioni protone-nucleo dalle quali si conclude in favore di modelli più dettagliati di quelli basati sulla trasparenza nucleare, che pure hanno servito a spiegare molti dei fatti osservati.

Le teorie del comportamento collettivo dei sistemi di molte particelle, esposte in forma generale e riassuntiva da D. TER HAAR in uno degli articoli, trovano ampliamento e applicazione nel lavoro sulla teoria dell'elio liquido (^{4}He) di J. WILKS ed in quello sulla teoria delle oscillazioni del plasma nei metalli, dovuta a S. RAIMES.

Altri due scritti riguardano le proprietà dei solidi: quello di D. M. S. BAGGULEY e J. OWEN sul comportamento rispetto alle microonde (risonanza magnetica degli elettroni, risonanza ciclotronica e alcuni fenomeni di assorbimento senza risonanza) e quello di E. R. DOBBS e G. O. JONES sulle proprietà dell'argon solido, poste a confronto con la teoria.

Ricordiamo finalmente due articoli che riguardano un campo ricco di importanti applicazioni pratiche, quello della fotografia, nel quale i problemi, sia teorici che applicativi, sono tutt'altro che esauriti. Lo scritto di J. W. MITCHELL, partendo dallo studio delle imperfezioni nei cristalli e giungendo sino ad impostare questioni applicative, tratta della sensibilità fotografica. Quello di J. S. COURTNEY-PRATT, di carattere più decisamente tecnico, passa in rivista i metodi della fotografia ad alta velocità, illustrati ampiamente da immagini e da schemi.

Il volume ha la solita, dignitosissima presentazione editoriale; esso si chiude con gli indici dei volumi dal 16 al 20, per autori e per materia, che sono però ridotti nella forma più schematica ed offrono perciò scarso ausilio al lettore.

FRANCO A. LEVI

A. R. EDMONDS – *Angular Momentum in Quantum Mechanics*, Princeton University Press, Princeton, New Jersey, 1957, pag. VIII-196.

In questi ultimi anni sono apparsi vari libri di diversi autori sulla teoria dei momenti angolari e sulle proprietà del gruppo di rotazione. Questo volume di EDMONDS è senz'altro uno dei più completi sull'argomento. Vi sono raccolti la gran parte degli sviluppi formali più recenti e gli argomenti matematici vi si trovano svolti con cura ed in dettaglio.

Il capitolo primo contiene cenni sulla teoria dei gruppi e della loro rappresentazione. Nel resto del volume viene fatto poco uso di argomenti gruppali; pertanto questa introduzione alla teoria dei gruppi è limitata alle nozioni essenziali. Nel capitolo secondo viene esposta la quantizzazione del momento angolare e la rappresentazione degli operatori. Da notare una discussione sul significato fisico delle regole di commutazione per i momenti angolari in relazione al processo di misura, ed ancora la rappresentazione degli operatori mediante operatori differenziali nello spazio degli spin. Questa rappresentazione viene utilizzata in seguito per costruire una espressione esplicita per gli elementi di matrice degli operatori D associati alle rotazioni. Il capitolo terzo tratta estesamente dei coefficienti di addizione, che vengono espressi nella combinazione simmetrica di Wigner sotto forma di simboli $3j$. Notevole in questo capitolo l'introduzione delle quantità contragradienti, che si trova utile nel seguito per la definizione dei simboli $6j$ e $9j$. Il problema della rappresentazione delle rotazioni finite e delle proprietà degli operatori D è trattato nel capitolo quarto. Nel capitolo quinto l'autore introduce la nozione di tensori sferici secondo Racah ed espone il fondamentale teorema di Wigner-Eckart insieme ad alcune sue applicazioni.

Il capitolo sesto discute la costruzione di invarianti a partire dai coefficienti di addizione, e tratta in dettaglio le proprietà dei simboli $6j$ e $9j$, con breve cenno sui simboli $12j$. Nel capitolo settimo infine vengono svolti alcuni esempi particolari, come il calcolo degli elementi di matrice per forze centrali, la struttura iperfina della molecole simmetriche ed il calcolo delle relative intensità di transizione. Vi sono infine due appendici e delle tavole dei coefficienti $3j$, $6j$ e delle D. Da lodare l'iniziativa dell'autore di confrontare alla fine di ogni capitolo le varie numerosissime notazioni usate dai diversi autori per grandezze più o meno equivalenti. Diciamo più o meno perchè ogni autore dotato di originalità curerà di cambiare qua e là qualche fase, col risultato che, chi lavora su problemi di correlazioni e cose simili, a meno di non stare molto attento, come è noto, può vedersi spuntare alla fine qualche sezione d'urto negativa o immaginaria pura.

In conclusione riteniamo che il libro sarà molto utile a quanti lavorano su problemi in cui sono essenziali simmetrie rispetto al gruppo di rotazione; e sappiamo tutti che l'attuale crisi della teoria dei campi ha certamente contribuito a fare crescere il numero di fisici che hanno trovato nello studio delle proprietà di simmetria l'unico modo per fornire qualche risultato preciso anche se spesso incompleto. Purtroppo, pure nella estrema ricchezza degli argomenti trattati, questo libro è ancora ben lontano dal comprendere i moltissimi sviluppi e le applicazioni della teoria dei gruppi di rotazione. In particolare non ci sentiamo di conclu-

dere che la lettura del volume sia sufficiente da sola ad insegnare come usare i tensori sferici e come trarre vantaggio dal poderoso formalismo sviluppato. Occorre dire che manca tuttora un libro che presenti una trattazione completa delle proprietà del gruppo delle rotazioni, discusse sotto i vari aspetti e secondo i diversi metodi, e che nello stesso tempo dia una sufficiente illustrazione della applicazione dei metodi a problemi fisici. La opportunità di un tale lavoro ci era già apparsa tempo addietro ma in verità eravamo rimasti sbigottiti di fronte alla considerazione dell'enorme mole di lavoro e del molto spazio necessari per una trattazione completa dell' argomento. Questa conclusione risulta evidente anche dalla lettura di questo volume di EDMONDS, che pure essendo sufficientemente ampio e dettagliato negli argomenti trattati tuttavia, compatibilmente con la sua mole modesta, lascia intatte moltissime questioni ed è soprattutto povero di esempi e di illustrazioni a carattere fisico.

R. GATTO

P. GRIVET – *Optique Electronique - Microscopes, diffractographes, spectrographes de masse, oscillographes cathodiques;* pag. 339, fig. 197, Bordas, Paris, 1958.

Questo libro fa parte di un'opera più vasta che il Prof. GRIVET intende compiere in tre volumi tutti dedicati ai problemi dell'ottica elettronica. Il primo volume, edito nel 1955 ed ormai molto noto, svolge lo studio teorico delle lenti elettroniche; il secondo, che esce adesso dalle stampe, è dedicato agli strumenti dell'ottica elettronica mentre il terzo, in preparazione, tratterà gli acceleratori di particelle e gli spettrometri β.

Riassumiamo in breve la materia trattata nel volume che segnaliamo: il primo capitolo è dedicato ai tubi a raggi catodici, il secondo descrive i convertitori e gli amplificatori d'immagine. In altri sette capitoli sono trattati i diversi tipi di microscopi elettronici con uno studio accurato sulla loro struttura meccanica, sui limiti nel potere risolutivo e sulle tecniche di preparazione degli oggetti. Degli ultimi tre capitoli uno è dedicato ai difrattografi per elettroni e due ai prismi elettronici, alle sorgenti di ioni e agli spettrometri di massa.

L'autore si è soffermato soprattutto a discutere le parti propriamente « ottiche » delle apparecchiature. Ciascuno strumento è visto come una particolare applicazione pratica della teoria delle lenti già esposta nel primo volume. L'impostazione generale dell'opera ha quindi un carattere unitario che giova molto sia alla chiarezza dell'esposizione sia alla completezza degli argomenti svolti.

Per altro ciò comporta che tutti i circuiti elettronici, costituenti la necessaria apparecchiatura ausiliare, siano passati in rassegna molto brevemente. Inoltre, ad eccezione dello spettrometro di massa tutti gli altri strumenti presentati sono solamente quelli che hanno un analogo corrispondente nell'ottica luminosa. Non si fa quindi alcun cenno di tutte le numerose applicazioni che l'ottica elettronica ha avuto nella tecnica radar e televisiva come pure nei tubi per microonde.

Tutto questo, se da una parte toglie all'opera il carattere di un trattato completo sull'ottica elettronica, dall'altro la rende molto più utile a tutti coloro che sono interessati allo studio delle lenti elettroniche ed in particolare alla loro applicazione nei microscopi elettronici.

U. PELLEGRINI